

Antagonism of Cellular Antiviral Systems by Flaviviruses

by

Shangmei Hou

A thesis submitted in partial fulfillment of the requirements for the degree of

Doctor of Philosophy

Department of Cell Biology

University of Alberta

© Shangmei Hou, 2017

Abstract

Flaviviruses are important human pathogens that have an enormous impact on global health. Examples that have been studied in my research include dengue virus (DENV), West Nile virus (WNV) and most recently, Zika virus (ZIKV). Currently, there are very few vaccines against or therapeutic treatments for flavivirus infections, and our understanding of how these viruses causes diseases is rather limited. Accumulating evidence from our laboratory and others has demonstrated that flaviviruses target specific host cell proteins to counteract the innate immune systems during infection. In this thesis, I investigated the mechanisms by which DENV, WNV and ZIKV interfere with cellular antiviral pathways, including the peroxisome-mediated antiviral response, the Type-I interferon response, and the host stress response.

A major finding was that flavivirus infection impairs biogenesis of peroxisomes, organelles that are important signaling platforms for early antiviral response including interferon production. This phenomenon is due in part to sequestration of the essential peroxisome biogenesis factor PEX19 by the viral capsid proteins. Analyses of ZIKV-infected cells revealed that this emerging pathogen interferes with the interferon production and signaling through multiple mechanisms. Specifically, the viral non-structural proteins NS1, NS4A and NS5 were identified as suppressors of interferon induction. NS5 was shown to target the antiviral transcription factor STAT2 for proteasomal degradation. Lastly, ZIKV infection was shown to modulate the cellular stress response and inhibit stress granule formation. The virus utilizes multiple viral components to hijack key stress granule proteins likely to facilitate viral replication.

Together, this thesis work describes novel host-virus interactions that occur during flavivirus infection and provides mechanistic insights into these processes, which in turn may provide new avenues for therapeutic development.

Preface

Many findings in this thesis are the results of collaborative work.

Chapter 3 of this thesis has been published as You, J., Hou, S., Malik-Soni, N., Xu, Z., Kumar, A., Rachubinski, R.A., Frappier, L. and Hobman, T.C. “Flavivirus Infection Impairs Peroxisome Biogenesis and Early Antiviral Signaling” *J Virol.* 2015 Dec;89(24):12349-61. J. You and I contributed equally to hypotheses development, experimental design and performance, data collection and analyses, as well as manuscript editing. N. Malik-Soni and L. Frappier performed and provided the data for mass spectrometry. Z. Xu performed the co-immunoprecipitation assays. A. Kumar and R.A. Rachubinski offered intellectual inputs. R. A. Rachubinski also provided the rabbit anti-SKL antibody. T.C. Hobman was the supervisory author and contributed to concept formation and manuscript composition.

Chapter 4 of this thesis has been published as Kumar, A., Hou, S., Airo, A.M., Limonta, D., Mancinelli, V., Branton, W., Power, C. and Hobman, T.C. “Zika virus inhibits Type-I interferon production and downstream signaling” *EMBO Rep* 2016 17:1766–1775. A. Kumar and I contributed equally to hypotheses development, experimental design and performance, data collection and analyses, as well as manuscript composition and revision. A.M. Airo performed and provided data for one of the qRT-PCR assays. V. Mancinelli provided technical support for RNA isolation and immunoblot analyses. W. Branton and C. Power prepared and provided primary human fetal astrocytes. D. Limonta helped with primary cell cultures. T.C. Hobman was the supervisory author and contributed to concept formation and manuscript composition.

Chapter 5 of this thesis has been submitted for publication as Hou, S., Kumar, A., Xu, Z., Airo, A.M., Stryapunina, I., Wong, C. P., Branton, W., Tchesnokov, E., Götte, M., Power, C., Hobman, T.C. 2017. “Zika virus hijacks stress granule proteins and modulates the host stress

response” *J Virol.* doi:10.1128/JVI.00474-17. A. Kumar and I contributed equally to hypotheses development, experimental design and performance, data collection and analyses, as well as manuscript composition and revision. Z. Xu performed the co-immunoprecipitation assays. A.M. Airo performed and provided data for one of the RNAi assays. I. Stryapunina constructed the viral protein expression plasmids. C. P. Wong helped with immunoblot analyses during paper revision. W. Branton and C. Power prepared and provided primary human fetal astrocytes. E. Tchesnokov and M. Götte designed and performed the Zika virus NS5 protein purification protocol required for antibody generation. T.C. Hobman was the supervisory author and contributed to concept formation and manuscript composition.

Acknowledgements

To my supervisor Dr. Tom Hobman, for taking me in to be part of his wonderful research team. It has been a rewarding experience learning about flaviviruses and cell biology in one of the finest research institutes across Canada. I feel truly grateful for the scientific opportunities and environment Tom has offered throughout my doctoral studies. Thank you for being always sincere about my performance, for challenging me to think more critically and for helping me complete my graduate program.

To my supervisory committee members Dr. Richard Rachubinski and Dr. Luis Schang, who have provided valuable insights and advice regarding my doctoral projects. Thank you for sitting in every committee meetings and guiding me through my graduate studies.

To my amazing colleagues Dr. Anil Kumar, Dr. Zaikun Xu, Dr. Justin Pare, Dr. Jae Hwan You, Dr. Joaquin Lopez, Dr. Daniel Limonta, Adriana Airo and Cheung Pang Wong, who have made my everyday research much more colorful and enjoyable. I cherish the scientific conversations we exchanged and those hard-working hours we shared. Without their presence, my progress would not have been possible.

To Valeria Mancinelli and Eileen Reklow, who have provided crucial technical support for the many experiments we collaborated on. Thank you for giving me encouragements and comfort whenever I needed them.

To my PhD defense examiners Dr. Bruce Banfield and Dr. David Marchant, who have taken their time to read my thesis and offer insightful comments.

To my partner Pejman Alanjari, who has walked along side throughout my PhD journey and elevated me with his kindness, personal strength and perseverance. He has been a true example of hard work and success and has shown me how to turn adversities into opportunities.

To my twin sister Nicole (Shangming) Hou, one of the most gifted individuals I have ever known. She has never failed to amaze me with her courage and energy. Through her, I have learnt to think outside of the box and try out new ideas and experiences.

Most importantly, to my beloved parents, who instilled scientific curiosity and passion in me; who has paved the way for my higher education aboard; who share my ups-and-downs regardless of our distance, and continue to inspire me and believe in me. They have made everything possible and immensely delightful. For that, I am forever grateful.

Dedication

In memory of my grandparents

Table of Contents

Chapter 1 Introduction	1
1.1 Flaviviruses	2
1.1.1 Overview	2
1.1.2 Classification of flaviviruses.....	2
1.1.3 Epidemiology and clinical importance	5
1.1.3.1 WNV	5
1.1.3.2 DENV	7
1.1.3.3 ZIKV	9
1.1.3.4 Other pathogenic flaviviruses	11
1.1.4 Pathogenesis of severe flavivirus diseases.....	12
1.1.4.1 WNV neuroinvasive diseases: crossing the blood-brain barrier (BBB) and neuropathogenesis.....	12
1.1.4.2 Severe dengue: immunopathogenesis mediated by the adaptive immune system.	14
1.1.4.3 Zika congenital disease: crossing the placental barrier and fetal neuropathogenesis	16
1.1.5 Flavivirus genome and proteins	19
1.1.6 Flavivirus replication cycle.....	24
1.2 Interactions between flaviviruses and cellular antiviral systems	28
1.2.1 The IFN system.....	29
1.2.1.1 Types of IFNs	29
1.2.1.2 IFN response pathways	32
1.2.1.3 Antagonism of the IFN system by flaviviruses.....	37
1.2.2 The peroxisome: a new antiviral signaling platform	41
1.2.2.1 Peroxisome metabolic functions	41
1.2.2.2 Peroxisome biogenesis.....	43
1.2.2.3 Peroxisomal protein import.....	46
1.2.2.4 Peroxisomes and viruses	49
1.2.3 The cellular stress response	50
1.2.3.1 Induction of the stress response	51
1.2.3.2 Formation of stress granules (SGs).....	54

1.2.3.3 Modulation of the stress response by flaviviruses	57
1.3 Objectives of thesis	60
Chapter 2 Materials and Methods	62
2.1 Materials	63
2.1.1 Reagents	63
2.1.2 Commonly used buffers and solutions.....	68
2.1.3 Oligonucleotides	70
2.1.4 Antibodies	77
2.1.5 Detection systems	81
2.1.6 Cell lines and viruses	82
2.1.6.1 Cell lines	82
2.1.6.2 Viruses	82
2.2 Methods.....	83
2.2.1 Molecular biology	83
2.2.1.1 Isolation of plasmid DNA from <i>Eschericia coli</i> (<i>E. coli</i>)	83
2.2.1.2 Polymerase chain reaction (PCR)	83
2.2.1.3 Restriction endonuclease digestion.....	83
2.2.1.4 Agarose gel electrophoresis	84
2.2.1.5 Purification of DNA fragments.....	84
2.2.1.6 Ligation of DNA	85
2.2.1.7 Transformation of <i>E. coli</i>	85
2.2.1.8 Construction of recombinant plasmids	85
2.2.2 Cell culture and transfection	88
2.2.2.1 Cell culture maintenance.....	88
2.2.2.2 Transient transfection of cell lines.....	88
2.2.2.3 RNA interference	89
2.2.3 Virology techniques	89
2.2.3.1 Virus infection	89
2.2.3.2 WNV, DENV-2, ZIKV and RV plaque assays.....	90
2.2.3.3 Production and use of lentiviruses	91
2.2.4 Microscopy	92
2.2.4.1 Indirect Immunofluorescence	92

2.2.4.2	Quantification of peroxisome numbers and sizes	93
2.2.4.3	Quantification of stress granule (SG) numbers.....	93
2.2.5	Flow cytometry	94
2.2.6	Protein gel electrophoresis and detection	94
2.2.6.1	Sodium dodecyl-sulphate polyacrylamide gel electrophoresis (SDS-PAGE).....	94
2.2.6.2	Immunoblot analysis.....	95
2.2.6.3	Detection of fluorophore-conjugated secondary antibodies	95
2.2.7	Biochemical analysis of protein-protein interactions	96
2.2.7.1	Co-immunoprecipitation	96
2.2.8	RNA techniques	97
2.2.8.1	RNA isolation	97
2.2.8.2	cDNA synthesis	98
2.2.8.3	Quantitative real-time PCR (qRT-PCR)	98
2.2.8.4	Protein-RNA interaction by RNA-IP.....	99
2.2.9	Luciferase reporter assays.....	99
2.2.10	Cell viability assay.....	100
Chapter 3 Flavivirus infection impairs peroxisome biogenesis and antiviral signaling... 102		
3.1	Rationale	103
3.2	Results.....	107
3.2.1	DENV and WNV capsid proteins interact with PEX19	107
3.2.2	Flavivirus infection leads to PEX19 degradation	111
3.2.3	Flavivirus infection alters peroxisome distribution	115
3.2.4	Flavivirus infection leads to reduction in peroxisome numbers	119
3.2.5	Capsid protein expression leads to reduction in peroxisome numbers	123
3.2.6	Flaviviruses suppress Type- III IFN induction	125
3.2.7	The peroxisome biogenesis factor PEX19 plays a role in the IFN response	127
3.2.8	ZIKV infection leads to reduction in peroxisome abundance	130
3.2.9	Different peroxisome biogenesis factors play different roles in IFN induction	133
3.3	Summary.....	135
Chapter 4 Zika virus inhibits the induction and downstream signaling of Type- I interferon response		136
4.1	Rationale	137

4.2 Results.....	138
4.2.1 ZIKV inhibits the host cell IFN response	138
4.2.2 ZIKV inhibits the induction of Type- I IFN expression	143
4.2.3 ZIKV blocks Type- I and -III IFN signaling	147
4.2.4 ZIKV infection induces proteasomal degradation of human STAT2	151
4.2.5 ZIKV infection does not induce degradation of mouse STAT2	155
4.2.6 ZIKV NS5 protein induces degradation of human STAT2	157
4.2.7 ZIKV NS5 interacts with human STAT2 through its MTase domain	162
4.3 Summary	164
Chapter 5 Zika virus hijacks stress granule proteins and modulates the host stress response.....	165
5.1 Rationale	166
5.2 Results.....	167
5.2.1 ZIKV infection does not induce robust SG formation.....	167
5.2.2 ZIKV inhibits SG formation induced by various stress stimuli.....	172
5.2.3 ZIKV inhibits SG formation induced by hippuristanol	176
5.2.4 ZIKV infection activates the host stress response through PKR and the unfolded protein response (UPR).....	178
5.2.5 ZIKV infection leads to protein translation arrest	183
5.2.6 ZIKV proteins NS3 and NS4A promote protein translation arrest.....	186
5.2.7 ZIKV infection does not alter expression of SG proteins.....	189
5.2.8 ZIKV infection does not disrupt the microtubule network.....	191
5.2.9 Inhibition of SG formation is mediated by the viral capsid protein, NS3, NS2B-3 and NS4A.....	193
5.2.10 The SG proteins G3BP1, TIAR and Caprin-1 are important for ZIKV replication	196
5.2.11 ZIKV capsid protein interacts with G3BP1 and Caprin-1	198
5.2.12 Capsid proteins of MVEV and YFV inhibit SG formation	202
5.3 Summary	205
Chapter 6 Discussion and Perspectives.....	206
6.1 Synopsis	207
6.2 Interaction between flaviviruses and peroxisomes	207
6.2.1 Peroxisomes as signaling platforms.....	208

6.2.2 Peroxisome-mediated antiviral signaling.....	209
6.2.3 Modulation of peroxisome biogenesis and antiviral signaling by flaviviruses.....	212
6.2.4 Perspective: the role of peroxisomes in flavivirus replication and pathogenesis	216
6.3 The immune evasion strategies of ZIKV	217
6.3.1 Interference with IFN induction.....	217
6.3.2 Interference with IFN signaling	223
6.3.3 Perspective: targeting NS5-STAT2 interaction as a novel antiviral strategy	226
6.4 How ZIKV modulates the host cell stress response.....	227
6.4.1 Activation of PKR and UPR signaling	227
6.4.2 Induction of protein translation arrest.....	229
6.4.3 Inhibition of SG formation.....	231
6.4.4 Perspective: physiological consequences of stress response modulation	234
6.5 Concluding remarks	235
Reference	236

List of Tables

Table 1.1 Molecular antagonisms of the IFN system by flaviviruses	39
Table 1.2 Modulation of the stress response pathways by flaviviruses	59
Table 2.1 Commercial sources of materials, chemicals, and reagents	63
Table 2.2 Molecular markers	67
Table 2.3 DNA/RNA modifying enzymes	67
Table 2.4 Multi-component systems	67
Table 2.5 Buffers and solutions	68
Table 2.6 Primers	70
Table 2.7 siRNA sequences	75
Table 2.8 Primary antibodies	77
Table 2.9 Secondary antibodies	80
Table 2.10 Detection systems	81
Table 3.1 Non-structural functions of flavivirus capsids in modulating cellular pathways	104

List of Figures

Figure 1.1 The classification of <i>Flavivirus</i> subgenera	4
Figure 1.2 The schematic representation of flavivirus genome organization and polyprotein processing	21
Figure 1.3 The replication cycle of flaviviruses	26
Figure 1.4 The Type-I, -II, and -III IFN signaling pathways	31
Figure 1.5 Induction of the IFN response during flavivirus infections	33
Figure 1.6 The pathways of peroxisome formation in mammalian cells	44
Figure 1.7 Biogenesis factors for peroxisome membrane assembly, matrix protein import and peroxisome division	48
Figure 1.8 The unfolded protein response (UPR)	53
Figure 1.9 The stress granule assembly pathway	56
Figure 3.1 Flavivirus capsid proteins interact with endogenous PEX19	108
Figure 3.2 PEX19 co-localized with capsid proteins during flavivirus infection	110
Figure 3.3 Flavivirus infection reduces levels of PEX19 protein	112
Figure 3.4 The effect of proteasomal and lysosomal inhibitors on virus-induced degradation of PEX19	114
Figure 3.5 Flavivirus infection alters peroxisome distribution	117
Figure 3.6 Flavivirus infection reduces peroxisome numbers	120
Figure 3.7 Flavivirus infection does not alter peroxisome size significantly	122
Figure 3.8 Expression of capsid proteins leads to reduction in peroxisome numbers	124
Figure 3.9 Flavivirus infection inhibits type-III IFN (IFN- λ) production	126
Figure 3.10 <i>PEX19</i> -silencing reduces <i>ifn-λ</i> expression	128
Figure 3.11 <i>PEX19</i> -silencing reduces DENV and WNV production	129
Figure 3.12 ZIKV infection reduces peroxisome numbers	131
Figure 3.13 Transient silencing of <i>PEX</i> genes differentially affect the induction of Type-I and type-III IFNs	134
Figure 4.1 ZIKV inhibits the host IFN response	140
Figure 4.2 Multiple ZIKV proteins inhibit IFIT1 promoter activity	142
Figure 4.3 ZIKV blocks the induction of Type-I IFN response	144

Figure 4.4 ZIKV NS1, NS4A and NS5 block TBK1-mediated IFN induction	146
Figure 4.5 ZIKV suppresses Type-I and –III IFN signaling	148
Figure 4.6 ZIKV NS5 blocks Type-I and -III IFN signaling	150
Figure 4.7 ZIKV NS5 induces STAT2 degradation in human cells	152
Figure 4.8 ZIKV-induced degradation of STAT2 requires the proteasome	154
Figure 4.9 ZIKV does not induce degradation of murine STAT2	156
Figure 4.10 Expression of ZIKV NS5 induces STAT2 degradation in human cells	158
Figure 4.11 Neither the MTase or the RdRP domain of ZIKV NS5 is sufficient to induce efficient degradation of STAT2	160
Figure 4.12 ZIKV NS5 interacts with human STAT2	163
Figure 5.1 ZIKV infection does not induce robust SG formation	169
Figure 5.2 ZIKV infection does not alter P-body abundance	171
Figure 5.3 ZIKV inhibits SG formation induced by arsenite and poly(I:C)	173
Figure 5.4 ZIKV inhibits SG formation in primary human fetal astrocytes (HFAs)	175
Figure 5.5 ZIKV inhibits SG formation induced by hippuristanol	177
Figure 5.6 ZIKV infection activates the stress response pathways	179
Figure 5.7 ZIKV infection does not block the induction of host stress response	181
Figure 5.8 ZIKV infection inhibits host cell protein synthesis	184
Figure 5.9 Expression of NS3 or NS4A inhibits protein translation	187
Figure 5.10 ZIKV infection does not affect steady state levels of SG-associated proteins	190
Figure 5.11 ZIKV infection does not disrupt the microtubule network	192
Figure 5.12 Expression of ZIKV capsid, NS3/NS2B-3 or NS4A blocks SG formation	194
Figure 5.13 The SG components G3BP1, TIAR and Caprin-1 are important for ZIKV replication	197
Figure 5.14 ZIKV capsid protein interacts with G3BP1 and Caprin-1	199
Figure 5.15 ZIKV RNA binds G3BP1	201
Figure 5.16 Expression of flavivirus capsid proteins have differential effects on SG formation	203
Figure 6.1 Model to account for how flaviviruses interfere with peroxisome biogenesis	213
Figure 6.2 Sequence alignment of the NS4A-B region within the polyprotein of ZIKV strains Z1106033 and PF13/251013-18	220

Figure 6.3 How ZIKV non-structural proteins inhibit interferon (IFN) induction and signaling	222
Figure 6.4 Sequence alignment of the amino terminal ends of DENV-2 and ZIKV NS5 proteins	224
Figure 6.5 Model to account for how ZIKV NS5 protein affects Type-I/III interferon (IFN) signaling.	225
Figure 6.6 Modulation of the stress response by ZIKV	233

List of Nomenclature and Abbreviations

°C	degrees Celsius
17 β -HSD	17- β hydroxysteroid dehydrogenase
3D-SIM	three-dimensional structured illumination microscopy
A	ampere
AcGFP	ammonium Persulfate GFP
ADE	antibody-dependent enhancement
ADP	adenosine diphosphate
APS	ammonium persulfate
ATF	activating transcription factor
ATP	adenosine triphosphate
ATPase	adenosine triphosphatase
BAAT	bile acid
BBB	blood-brain barrier
BiP	immunoglobulin heavy-chain binding protein
BSA	bovine serum albumin
C	capsid
CARD	caspase activation and recruitment domain
cDNA	complementary deoxyribonucleic acid
cGAS	cyclic GMP-AMP synthase
CNS	central nervous system
CT	threshold cycle
DAPI	4',6-diamidino-2-phenylindole
DC-SIGN	dendritic-cell-specific ICAM-grabbing non-integrin
DENV	Dengue virus
DHF	Dengue hemorrhagic fever
DMEM	Dulbecco's modified Eagle's medium

DMSO	dimethyl sulphoxide
DNA	deoxyribonucleic acid
DNase	deoxyribonuclease
dNTP	deoxyribonucleotide triphosphate
DRP	dynamain-related protein
dsRNA	double-stranded ribonucleic acid
DSS	Dengue shock syndrome
DTT	dithiothreitol
E	envelope
EDTA	ethylenediaminetetraacetic acid
eGFP	enhanced green fluorescent protein
eIF	eukaryotic initiation factor
ER	endoplasmic reticulum
ERAD	ER-associated degradation
FBS	fetal bovine serum
Fis1	Fission protein 1
<i>g</i>	gravitational force
G3BP	Ras-GAP SH3 domain-binding protein
GADD34	Growth arrest and DNA damage-inducible protein
GAS	IFN-gamma-activated sequence
GBS	Guillain-Barré syndrome
GCN2	general control nonderepressible-2
GTPases	guanosine triphosphate hydrolase
h.p.i	hour-post infection
HCMV	human cytomegalovirus
HCV	hepatitis C virus
HEK293T	human embryonic kidney 293T cells
HEPES	4-(2-hydroxyethyl)-1-piperazineethanesulphonic acid

HFA	human fetal astrocyte
HIPP	hippuristanol
HIV-1	human immunodeficiency virus-1
hr	hour
HRI	heme-regulated inhibitor
HRP	horseradish peroxidase
HSP	heat shock protein
HuR	Hu antigen R
IAV	influenza A virus
IF	Immunofluorescence
IFIT	IFN-induced protein with tetratricopeptide repeats
IFITM	IFN-inducible transmembrane
IFN	Interferon
IFNAR	IFN-alpha receptor
IFNGR	IFN-gamma receptor
IFNLR	IFN-lambda receptor
IgG	immunoglobulin G
IKK	inhibitor of κ B kinase
IL	interleukin
IP	immunoprecipitation
IRE1 α	inositol-requiring protein-1
IRES	internal ribosome entry site
IRF	interferon regulatory factor
ISRE	IFN-stimulated response element
JAK	Janus kinase
JEV	Japanese encephalitis virus
kb	kilo ($\times 10^3$) base-pairs
kDa	kilo Daltons

L	liter
m	milli ($\times 10^{-3}$)
M	moles per liter
MAM	mitochondrion-associated-endoplasmic reticulum membranes
MAVS	mitochondrial antiviral signalling
MDA5	differentiation-antigen 5
MEF	mouse embryonic fibroblast
MEM	minimal essential media
Mff	mitochondria fission factor
Mfn	mitofusion
min	minute
MOI	multiplicity of infection
mRNA	messenger RNA
mRNP	mRNA ribonucleoprotein
MTase	methyltransferase
mTORC	mammalian target of rapamycin complex
MVEV	Murray Valley encephalitis virus
MYD88	myeloid differentiation factor 88
n	nano (10^{-9})
NA	numerical aperture
NEMO	NF- κ B essential modulator
NF κ B	nuclear factor- κ B
NP40	nonidet-P40
NS	non-structural
nt	nucleotide
OAS	2'-5'-oligoadenylates
OHFV	Omsk hemorrhagic fever virus
p	pico (1×10^{-12})

PAMP	pathogen-associated molecular pattern
P-body	processing body
PBS	phosphate buffered saline
PBS-T	phosphate buffered saline, tween 20
PCC	Pearson correlation coefficient
PCR	polymerase chain reaction
PERK	PKR-like ER kinase
PEX	peroxin
pH	power hydrogenii
PKR	dsRNA-binding kinase R
PMP	peroxisome membrane protein
poly(I:C)	polyinosinic-polycytidylic acid
PPAR α	peroxisome proliferative activated-receptor α
prM	precursor membrane
PRR	pattern recognition receptor
PVDF	polyvinylidene difluoride
RACK	receptors for activated C-kinase
RdRP	RNA-dependent RNA polymerase
RIG-I	retinoic acid inducible gene-1
RING	really interesting new gene
RLR	RIG-I-like receptor
RNAi	RNA interference
RNase	ribonuclease
RNF125	ring-finger protein 125
RNP	ribonucleoprotein
RV	Rubella virus
SAPK	stress-activated p38 and JNK MAPK
SDS	sodium dodecyl-sulphate

SDS-PAGE	SDS-polyacrylamide gel electrophoresis
sec	second
sfRNA	subgenomic flavivirus RNA
SG	stress granule
SIM	Structure illumination microscopy
siRNA	short interfering RNA
Smurf	Smad ubiquitin regulatory factor
ssRNA	single-stranded RNA
STAT	signal transducers and activators of transcription
STING	stimulator of interferon genes
SVP	Subviral partical
TAK1	transforming growth factor- β -activated kinase 1
TAM	TYRO3, AXL and MER
TBEV	Tickborne encephalitis virus
TBK1	TANK-binding kinase 1
TEMED	N,N,N',N'-tetramethylenediamine
TIA-1	T-cell-restricted intracellular antigen 1
TIAR	TIA-1-related protein
TIM	T-cell Immunoglobulin and Mucin domain
TLR	Toll-like repter
TNF	tumor neurosis factor
TRIF	TIR-domain-containing adaptor inducing interferon
TRIM25	tripartite motif-containing protein 25
tRNA	transfer RNA
TSC	tuberous sclerosis complex
TYK	tyrosine kinase
U	enzymatic units
UPR	unfolded protein response

USP10	ubiquitin-specific protease 10
V	volt
v/v	volume per volume
VLFA	very long chain fatty acid
VSV	vesicular stomatitis virus
w/v	weight per volume
WB	western blot
WHO	World Health Organization
WNV	West Nile virus
XBP1	X-box binding protein 1
YFV	yellow fever virus
ZIKV	Zika virus
μ	micro ($\times 10^{-6}$)

Chapter 1 Introduction

1.1 Flaviviruses

1.1.1 Overview

Flaviviruses are arboviruses belonging to the large RNA virus family *Flaviviridae*. Many members of this group are significant human pathogens that impose an enormous impact on global health. For example, the mosquito-borne flavivirus, Dengue virus (DENV) alone, is estimated to cause almost 400 million infections per year in over 100 countries in the world (Bhatt et al., 2013). Although vaccines are available for a few flaviviruses including yellow fever virus (YFV) and Japanese encephalitis virus (JEV), therapeutic and prevention options for other members of the family are limited. With rapid urbanization, climate change, increased international travelling and unprecedented spread of vectors, the global burdens of flaviviruses continue to expand, putting hundreds of millions of people at risk. To provide a general understanding of flaviviruses and the associated diseases, this chapter discusses viral epidemiology and clinical significance (Section *1.1.3*), viral pathogenesis (Section *1.1.4*) as well as viral biology (Sections *1.1.5* and *1.1.6*). Based on the main research interest of this thesis work, the discussion will be focused on West Nile virus (WNV), DENV and Zika virus (ZIKV).

1.1.2 Classification of flaviviruses

Flaviviridae is a large family of viruses with positive-sense, single-stranded RNA (ssRNA) genomes. It is divided into three genera: *Pestivirus*, *Hepacivirus* and *Flavivirus*, with *Flavivirus* being the largest genus (Gould and Solomon, 2008). *Flavivirus* is derived from the Latin word “*flavi*”, meaning “yellow”, due to the condition jaundice caused by YFV. The term “flaviviruses” traditionally refers to members of the *Flavivirus* genus which can be further categorized into subgenera based on their host ranges and transmissibility. Thus far, four subgenera of flaviviruses have been identified: mosquito-borne, tick-borne, insect-specific, and those with

unknown vectors (Figure 1.1). Many of the medically important flaviviruses are mosquito-borne, including JEV, YFV, WNV, DENV and ZIKV (reviewed in (Villordo et al., 2016)). These viruses can be further classified into groups depending on their serocomplex specificity (Figure 1.1). For example, the JEV group contains several encephalitic viruses including JEV, WNV, Murray Valley encephalitis virus (MVEV) and St. Louis encephalitis virus. The DENV group includes DENV serotypes 1, 2, 3 and 4. The YFV group is composed of YFV and Spondweni virus, while the Spondweni virus group contains Spondweni virus and ZIKV (Gould and Solomon, 2008).

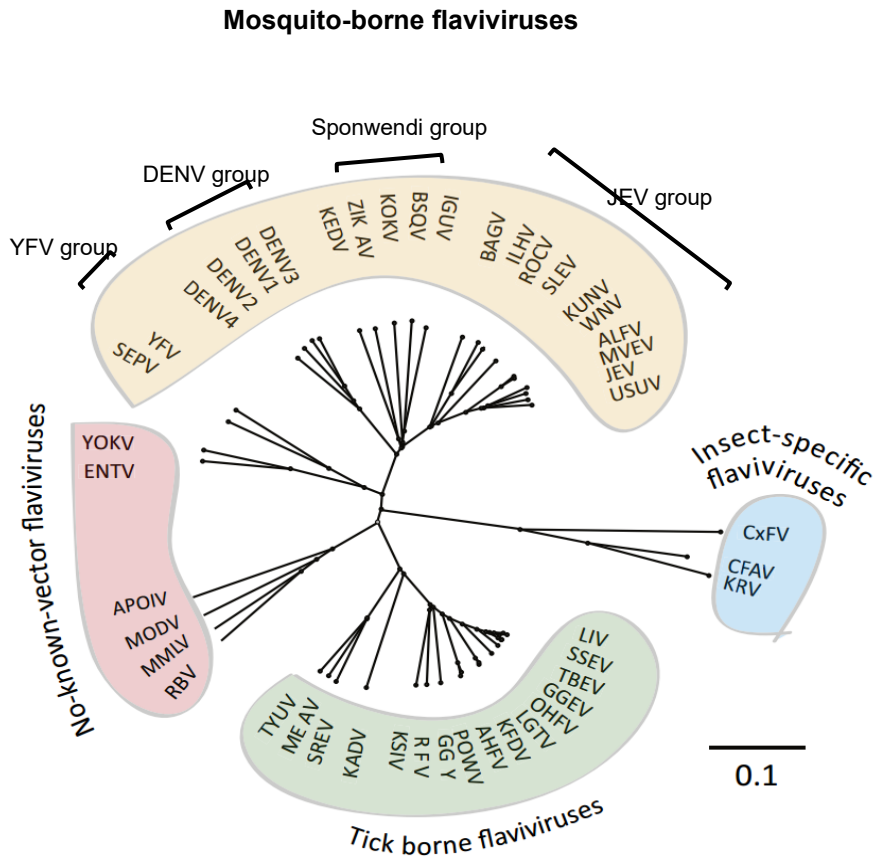


Figure 1.1 The classification of *Flavivirus* subgenera. A phylogenetic tree representing the evolutionary relationships among the 4 groups of flaviviruses based on the viral genomic sequences (modified from Villordo, et al 2016).

1.1.3 Epidemiology and clinical importance

For the past few decades, notable advances have been achieved in the prevention and control of several mosquito-borne flaviviruses. A good example is YFV, the causative agent of yellow fever, a hemorrhagic illness that can develop in some patients infected with the virus. This virus is thought to cause 30,000 deaths per year, primarily in Africa (Jentes et al., 2011). Since 2006, extensive vaccination campaigns led by the World Health Organization (WHO) have significantly reduced YFV incidence (WHO, 2013). The yellow fever vaccine was shown to induce long-lasting (up to 20 years) neutralizing antibodies in > 90% vaccine recipients (Gotuzzo et al., 2013) and it remains to be one of the most successful vaccine developments for arboviruses. Similarly, several safe and effective vaccines are now available for Japanese encephalitis (reviewed in (Ishikawa et al., 2014)), a serious neurological illness caused by JEV. Although the risk of outbreaks remains in endemic regions (Campbell et al., 2011; Jentes et al., 2011), continuous reinforcement, evaluation and improvement of vaccination programs have helped lessen the burden of disease caused by YFV and JEV. More importantly, valuable knowledge derived from these prevention strategies will hopefully advance vaccine development and deployment for other flaviviruses such as WNV and ZIKV.

1.1.3.1 WNV

WNV was first isolated in 1937 from the blood of a woman with febrile illness during surveillance of YFV in the West Nile region of Uganda (Smithburn et al., 1940). In the late 1990s, an outbreak of neuroinvasive disease was found associated with a WNV epidemic in Romania (Tsai et al., 1998) and later in Russia as well as New York City of the U.S.A (Nash et al., 2001). WNV is now endemic in many parts of the Americas, Asia, Africa and Europe, where it causes illnesses in horses and in humans (as reviewed in (Troupin and Colpitts, 2016)). In 2012, a public

health emergency of WNV outbreak was declared in the Dallas county of Texas, U.S.A., where ~663 human cases and 18 deaths were reported in the region (CDC, 2016). This was marked as one of the largest WNV outbreaks in the Americas since 2003. Currently, WNV remains as the most common cause of mosquito-borne encephalitis in humans in North America.

WNV circulates in various bird species through *Culex* mosquitoes, although it can also be transmitted through other routes among the avian hosts (Gyure, 2009). Depending on the virus and host species, infection outcomes in birds can range from non-pathogenic to lethal. In the latter case, reporting and testing of dead birds can be a useful means for surveillance of WNV (Public Health Agency of Canada, 2015). Apart from birds, some studies suggest that alligators may also serve as a natural reservoir for WNV, particularly in the southeastern U.S.A. (Jacobson et al., 2005; Klenk et al., 2004). Although it can cause sickness in alligators, the epidemiological importance of WNV infection in the reptile host remains unclear. Infection of WNV in mammals including horses and humans is primarily through mosquito bites (Gyure, 2009). Due to the inability of the virus to produce high titre in the circulation, most mammals are considered dead-end hosts, in which the vector-mediated transmission cycle terminates. Although extremely rare, human-to-human transmission has been reported through blood-transfusion (Mezochow et al., 2015; Betsem et al., 2017), organ transplants (Iwamoto et al., 2003; Mezochow et al., 2015; Winston et al., 2014) and from mother to baby during pregnancy, delivery, or breastfeeding (Ceccaldi et al., 2007).

Infection by WNV in adult humans is mostly asymptomatic (70-80%). About 20% of patients develop a febrile syndrome characterized by fever, headache, vomiting and fatigue, but most recover completely (as reviewed in (Hayes et al., 2005)). However, approximately 1% of infected individuals develop severe neurological illnesses including acute flaccid paralysis, meningitis and encephalitis. There is a greater risk associated with the elderly,

immunocompromised patients, individuals with other medical conditions (such as diabetes) and certain genetic predispositions (reviewed in (Brinton, 2002) and (Suthar et al., 2013)). Recovery in these patients usually takes longer (from weeks to months) and some of the neurological conditions become permanent (Hayes et al., 2005). In less than 10% of those who develop serious illnesses, mortality can ensue due to paralysis of respiratory muscles. At the moment, several veterinary vaccines are available for horses (reviewed in (Ishikawa et al., 2014)), but no licensed vaccine or specific treatments are available for humans. However, several WNV vaccine candidates have showed promise in the developmental phases. For instance, the ChimeriVAX-WN02, a chimeric vaccine consisting of the WNV precursor membrane (prM) and envelope (E) genes in the YFV vaccine 17D backbone, was shown to confer > 96% seroconversion rates in a Phase-II clinical trial (Biedenbender et al., 2011). Currently, supportive care is the only treatment for patients with severe WNV symptoms.

1.1.3.2 DENV

Due to uncontrolled urbanization, substandard water treatment systems, increased international travelling, as well as increased vector spread (Guzman and Harris, 2015; Kraemer et al., 2015), the global dengue burden has increased dramatically over the past 50 years, with the affected regions having expanded from originally Latin America, South-East Asia, Western Pacific and Africa, to more recently, the U.S.A. and several European nations (Guzman et al., 2010). According to the most recent global estimate, ~390 million dengue infections occur annually, affecting more than 100 countries, while causing ~96 million dengue clinical manifestations (Bhatt et al., 2013). Today, severe dengue disease remains as a leading cause of hospitalization and death among children in many Latin American and Asian countries.

In contrast to WNV, DENV is transmitted between humans and non-human primates primarily through mosquito-bites. The vector for this virus belongs to the *Aedes* genus, with *Ae. aegypti* as the principle and *Ae. albopictus* as the less common vector (Guzman et al., 2010). Accordingly, the prevalence of DENV infection closely correlates with the presence of *Aedes spp.* both geographically and seasonally. Although the primary transmission is mediated by mosquitoes, incidences of DENV infection through blood transfusion and from mother to newborns have also been documented (Janjindamai and Pruekprasert, 2003; Schmidt et al., 2014).

In healthy adults, DENV infection is often asymptomatic or limited to flu-like symptoms. However, in ~20% of cases, individuals develop dengue fever (4-10 days after mosquito bite), which is characterized by high fever, rash, severe pain behind the eyes, muscle and joint pain and mild bleeding (e.g., nose or gums) (WHO, 2009). Dengue hemorrhagic fever (DHF) and dengue shock syndrome (DSS) can also occur in a small proportion of patients (1-2%). In these cases, symptoms include severe plasma leakage, organ impairment and bleeding (WHO, 2009). Without prompt and proper medical care, death can ensue within 24-48 hours of this critical stage (WHO, 2009). Several factors have been implicated in severe dengue diseases, including secondary infection with a different virus serotype, weakened immunity, age and certain clinical predispositions (as reviewed in (Martina et al., 2009)). Unfortunately, no specific treatment is available for severe dengue and prevention of disease progression relies on supportive medical care.

Thus far, surveillance and control of mosquito vectors are the primary means to prevent dengue infection. In late 2015 and early 2016, the first dengue vaccine, Dengvaxia® (CYD-TDV) from Sanofi Pasteur, was licensed for use in several Asian and Latin American countries. According to WHO guidelines, this vaccine is intended for individuals between 9 and 45 years-

old who are currently living in endemic areas (WHO, 2016). The CYD-TDV is a tetravalent live-attenuated virus encoding the prM and E proteins from the 4 DENV serotypes using the YFV vaccine strain 17D as backbone. Although results from the efficacy trials showed some promise in protection against severe dengue diseases, the overall vaccine efficacy was suboptimal (~55-60% in participants ≥ 9 years-old), providing the least protection against DENV-2 (~40%) (Capeding et al., 2014; Villar et al., 2015). It was also suggested to enhanced risk in seronegative children < 9 years of age (Hadinegoro et al., 2015). Clearly, there remains a pressing need to improve existing vaccine candidates and develop successful therapeutic strategies for dengue.

1.1.3.3 ZIKV

Closely related to DENV, ZIKV has emerged/re-emerged as an important human pathogen since the latest outbreak in Brazil in 2015. ZIKV was first isolated from an infected monkey in Uganda in 1947 and later from *Aedes* mosquitoes in 1949 during a research designed for YFV studies (Dick et al., 1952). Sporadic outbreaks of Zika occurred in several continents since its discovery, where the virus caused mostly mild illnesses. The first large Zika outbreak occurred in the Pacific Island of Yap in 2007, where 73% of Yap residents became infected; but no severe cases of disease were reported (Duffy et al., 2009). The second large outbreak occurred in French Polynesia in 2014, where the first evidence of ZIKV perinatal transmission was identified (Besnard et al., 2014). The clinical significance of ZIKV was underappreciated until 2015, when the Zika endemic in South America was linked to significant increases in Guillain-Barré syndrome (GBS) and microcephaly (Araujo et al., 2016; Rubin et al., 2016). Thus far, ZIKV has spread across the Americas and has reached as far North as Florida and potentially Texas in the U.S.A. (CDC, 2016). According to the WHO Zika Situation Report, possible endemic transmissions of ZIKV have also been reported in several Southeast Asian countries including Singapore, Thailand, Maldives,

Philippines and Vietnam (WHO, 2017). It is still unclear how the virus spread so rapidly during the outbreaks in South America, but one theory is that a spontaneous mutation acquired in the viral non-structural protein 1 (NS1) enhances its antigenemia in the mammalian hosts and therefore promotes ZIKV infectivity and prevalence in mosquitoes (Y. Liu et al., 2017).

ZIKV shares the same mosquito host with DENV, species of the *Aedes* genus. Not surprisingly, the spread of Zika also correlates strongly with the prevalence of vectors. Different from DENV however, ZIKV can be transmitted across the placenta (Besnard et al., 2014; Calvet et al., 2016; Driggers et al., 2016; Oliveira Melo et al., 2016) as well as through sex (Moreira et al., 2017). Although potential Zika transmission through blood transfusion has been reported, these cases are still under investigation.

The majority of ZIKV infections are asymptomatic, but ~25% of infected individuals develop fever, headache, conjunctivitis, muscle and joint pain, rash, and vomiting. In some adults, ZIKV infection may trigger GBS (Cao-Lormeau et al., 2016), a neurological condition that is characterized by numbness in muscles and in more severe cases, paralysis (Goodfellow and Willison, 2016). GBS can progress to near-total paralysis and death in some patients but fortunately, this is relatively rare. Due to the ability of ZIKV to cross the placenta, it can also cause congenital defects including microcephaly in newborns when infection occurs during pregnancy (Brasil et al., 2016; Calvet et al., 2016; de Araújo et al., 2016; Driggers et al., 2016; Oliveira Melo et al., 2016). A recent report from Brazil suggests that ZIKV infection during the first, second and third trimester can lead to adverse birth outcomes in ~55%, ~52% and ~29% cases respectively (Brasil et al., 2016).

Since its resurgence, increasing international effort has been made to understand ZIKV pathogenesis and advance the development of vaccine and therapeutics. For example, several vaccine strategies are now undergoing Phase-I clinical trials to evaluate their safety and immunogenicity (as reviewed in (Barouch et al., 2017)). Until a vaccine is developed and implemented, surveillance and control of mosquito vectors, practice of safe sex as well as thorough medical monitoring of women and newborns prior, during and after pregnancy will remain as the key methods to prevent and control Zika diseases.

1.1.3.4 Other pathogenic flaviviruses

Apart from the mosquito-borne viruses described above, other flavivirus members can also cause serious disease in humans and animals (as reviewed in (Gould and Solomon, 2008)). For instance, several mammalian tick-transmitted flaviviruses, such as tickborne encephalitis virus (TBEV) and Omsk hemorrhagic fever virus (OHFV), can cause encephalitis and hemorrhagic fever in humans. TBEV is most common in Central and Eastern Europe as well as Northern Asia; while the Powassan virus strain of TBEV is also endemic in North America (as reviewed in (Dobler et al., 2012)); while OHFV infections are confined mainly to Western Siberia (CDC, 2013). Both viruses circulate within specific tick populations but they can also infect humans through tick-bites, consumption of raw milk from infected animals or contact with infected rodents (in the case of OHFV) (Gould and Solomon, 2008). For TBEV, 20-30% of human infections can lead to neurological disorders including meningitis, encephalitis and meningoencephalitis, while 1-20% of TBEV infections can be fatal in hospitalized patients (Hubálek and Rudolf, 2012). For OHFV infections, a subset of individuals develop high fever and encephalitis, but the fatality rate is typically below 3% (CDC, 2013). A vaccine for TBEV is available in some endemic areas, but prophylactic options do not currently exist for OHFV (as reviewed in (Ishikawa et al., 2014)).

Similar to the WNV, DENV and ZIKV, supportive treatment is the only currently available option for patients with severe illnesses.

In summary, although there has been notable success in limiting infection by some flaviviruses, overall members of *Flaviviridae* remain a significant global concern due to the lack of vaccines and therapeutics. As well as unexpected clinical manifestations, routes of transmission and viral persistence (as demonstrated by ZIKV), better characterization of flavivirus biology is still needed to lessen the impact of pathogenesis by these viruses.

1.1.4 Pathogenesis of severe flavivirus diseases

Given their impact on global health, a great deal of effort has focused on understanding how flaviviruses cause disease. Data suggest that a combination of viral determinants and dysregulated host immune responses both contribute to the development of severe clinical outcomes associated with flavivirus infections.

1.1.4.1 WNV neuroinvasive diseases: crossing the blood-brain barrier (BBB) and neuropathogenesis

One of the most dangerous complications associated with WNV infection is severe neuroinvasive diseases such as encephalitis. Studies in animal models (e.g., mice, hamsters and monkeys) have revealed the importance of viral neuroinvasion and immunopathogenesis in determining WNV disease development (as reviewed in (Lim et al., 2011)). Neuroinvasion of WNV usually coincides with, or occurs shortly after, the peak of viremia, which follows dissemination of the virus throughout the lymphatic system and into the peripheral tissues (Suthar et al., 2013). Neuroinvasiveness of WNV is linked to its ability to enter the central nervous system (CNS) and propagate efficiently in different brain cell types. For entry into the CNS, disruption of

the BBB, either directly by the virus or by virus-induced inflammatory response, is proposed to be a major factor in WNV neuroinvasion.

The BBB is mainly composed of endothelial cells that are bridged by tight junction complexes. This highly selective barrier separates the circulating blood from the brain and provides vital protection for the CNS (Goasdoué et al., 2016). Pathogenesis studies in mice revealed that a key N-linked glycan on domain I of the envelope protein enhances WNV neuroinvasiveness, possibly by allowing the virus to bind endothelial cells and therefore cross the BBB (Chambers et al., 1998; Beasley et al., 2005). Moreover, following infection of endothelial cells by WNV, significant degradation of tight junction proteins occurs, a mechanism that could contribute to breakdown of the BBB (Xu et al., 2012). WNV infection can also induce production of vasoactive cytokines such as tumor necrosis factor α (TNF- α), which increases permeability of the endothelial layer (Wang et al., 2004). Finally, WNV may breach the BBB by increasing the levels of matrix metalloproteinases, which induce turnover of BBB basement membrane and promote degradation of tight junction proteins (Wang et al., 2008; Verma et al., 2010; Roe et al., 2012). Other modes of CNS entry have been proposed for WNV, including infecting immune cells and hijacking them as “Trojan horses” to cross the BBB (Bai et al., 2010); infecting olfactory neurons to enter the brain through the olfactory bulb (Getts et al., 2008; Yamada et al., 2009); and infecting peripheral neurons to reach the CNS through axonal retrograde transport (Samuel et al., 2007).

Once inside the CNS, WNV can replicate efficiently in astrocytes, microglia and neurons (reviewed in (Lim et al., 2011)) and in doing so, inflict direct damage to the cells by inducing production of reactive oxygen species and apoptosis of neurons, resulting in neurocytotoxicity (Parquet et al., 2001; Raung et al., 2001; Samuel et al., 2007).

Apart from virus-mediated cytopathology, immunopathogenesis also contributes to WNV neurological disease. Studies in mouse models and *ex vivo* human brain cells showed that inflammatory cytokines and chemokines such as TNF- α and IL-1 β that are released from infected neurons, enhance caspase-dependent apoptosis (Marle et al., 2007). As well as neurons, other cell types also play a role in WNV-induced immunopathology. For instance, viral infection of the CNS can lead to reactive gliosis, a condition that is characterized by activation of glia cells (e.g., astrocytes and microglia) and increased recruitment of leukocytes into the CNS (Ghoshal et al., 2007; Marle et al., 2007). These processes are accompanied by augmented production of pro-inflammatory molecules that contribute to neuroinflammation. Similarly, a report using macrophages from young and elderly cohorts suggests that upregulation of pro-inflammatory cytokines due to a dysregulated TLR3-signaling can lead to an exaggerated innate immune response and thus virus-associated neuropathology (Kong et al., 2008). To what extent the immune system contributes to WNV neuropathology is still being unravelled, but elucidating the role of immunopathogenesis would allow us to better understand why certain individuals are more prone to severe WNV disease.

1.1.4.2 Severe dengue: immunopathogenesis mediated by the adaptive immune system

The development of severe dengue disease, namely DHF and DSS, is influenced by viral and host factors. For example, the secreted DENV NS1 protein has been shown to increase capillary permeability by inducing production of pro-inflammatory cytokines as well as by destroying endothelial glycocalyx layer through direct binding (Beatty et al., 2015; Chen et al., 2015; Modhiran et al., 2015). As for host factors, increasing evidence points to the involvement of the adaptive immune system in severe dengue pathogenesis. Currently, two theories dominate the

field of dengue immunopathogenesis: a) antibody-dependent enhancement (ADE) and b) skewed T cell-mediated immune response.

ADE refers to antibody Fc receptor-mediated uptake of DENV particles during secondary infection by a different DENV serotype (Halstead, 2007). The idea is that antibodies generated from the previous infection, primarily those against the prM and E proteins, bind to the different DENV serotype virions with low avidity and instead of neutralizing the virus, these cross-reactive antibodies facilitate the entry of the virus into Fc receptor-bearing cells (e.g., dendritic cells, monocytes and macrophages). Thus far, several lines of evidence from *in vitro* and *in vivo* studies support the ADE theory (reviewed in (Diamond and Pierson, 2015)). For example, intravenous administration of DENV-reactive antibodies increases viral burden in an immune-compromised mouse model (Zellweger et al., 2010) as well as in non-human primates (Goncalvez et al., 2007). This may explain why severe dengue disease usually occurs in patients during secondary infection (Halstead, 2007). This is further supported by the observation that infants born to mothers previously infected with DENV are at risk for increased disease severity during primary DENV infection. This is likely due to ADE of DENV in infants mediated by the non-neutralizing antibodies passively transferred from their mothers during pregnancy (Diamond and Pierson, 2015). While the validity of the ADE theory continues to be tested, it has provided a vital perspective for designing effective DENV vaccines.

Besides the humoral response, the T cell-mediated immune response contributes to dengue immunopathology. A skewed T-cell response is thought to drive disease development by enhancing production of pro-inflammatory cytokines and through reduced clearance of pathogens (Diamond and Pierson, 2015). Studies of T-cell responses in dengue cohorts suggest that during secondary infection, there is an expansion of cross-reactive memory T cells that are specific for

the primary-infection serotype but poorly recognize the secondary-infection serotype (Mongkolsapaya et al., 2003, 2006). Consequently, clearance of the virus is impaired. Moreover, these cross-reactive T cells display altered functionalities in that they fail to undergo normal degranulation and eliminate infected cells. Instead, they increase release of pro-inflammatory cytokines such as TNF- α and IFN- γ that may contribute to the eventual cytokine storm and vascular leak observed in DHF patients. Certainly, like ADE, skewed T-cell responses do not explain how severe cases of dengue disease occur during primary infections. Despite the immunopathology associated with severe dengue, the protective role of the adaptive immune system is essential in controlling DENV infection as well as disease progression (reviewed in (Diamond and Pierson, 2015)). Hopefully, recent successes in the development of severe dengue animal models (Tang et al., 2015) will shed more light onto the immunopathogenesis of this flavivirus.

1.1.4.3 Zika congenital disease: crossing the placental barrier and fetal neuropathogenesis

ZIKV is a recently emerged human pathogen. Unlike other flaviviruses, ZIKV is distinct in that it can be transmitted sexually and cause congenital defects in newborns. Supported by evidence from clinical and animal studies, ZIKV can replicate efficiently within immune-privileged sites such as the eyes and testes (de Oliveira Dias et al., 2017; Govero et al., 2016; Mansuy et al., 2016; Miner et al., 2016), suggesting that the virus has evolved ways to cross different physical/anatomical barriers and replicate in diverse specialized cell types. Given the significance of ZIKV-associated congenital syndromes, several mechanisms have been proposed to explain how the virus crosses the placenta and impedes fetal neurodevelopment.

Initial evidence of ZIKV as a neuro-teratogenic agent stems from the fact that the virus was isolated from brain tissue of an aborted fetus from a mother infected with ZIKV during pregnancy

(Driggers et al., 2016). This suggests that the virus can cross the placental barrier and persist in the fetal brain. The placenta is a highly complex organ that separates the maternal and fetal circulations and provides protection and nutrients for the fetus (Goasdoué et al., 2016). Upon conception, the placenta undergoes dramatic changes through cell/tissue differentiation and proliferation; and due to this changing nature, pathogens have to circumvent multiple cell/tissue layers in order to reach the embryo/fetus (Kim and Shresta, 2016). Accordingly, the routes of viral crossing and its success in breaching this barrier may vary depending on gestation periods. Consistent with this idea, statistical analyses of Zika outbreaks in Brazil and French Polynesia suggest that exposure to ZIKV early during pregnancy, especially in the first trimester, is associated with a greater risk of fetal microcephaly (Cauchemez et al., 2016; de Araújo et al., 2016). Similarly, studies using placental explants have demonstrated a stronger resistance to ZIKV infection nearer to term of pregnancy (Bayer et al., 2016; Quicke et al., 2016).

Based on studies *ex vivo*, *in vitro* and *in vivo*, one major mechanism of ZIKV transplacental transmission is through direct infection of placental cells, which may serve as an initial platform for viral amplification and dispersal (Kim and Shresta, 2016). Thus far, several placental cell types have been shown to support ZIKV replication, including decidual fibroblasts, decidual macrophages, umbilical cord fibroblasts, mesenchymal stem cells as well as Hofbauer cells, although the level of viral production varies depending on the cell type and gestation period (Bhatnagar et al., 2017; Costa et al., 2016; Miner et al., 2016; Noronha et al., 2016; Quicke et al., 2016; Tabata et al., 2016). In addition, virus-induced damage to placental integrity was also observed in some studies (Miner et al., 2016; Noronha et al., 2016), a phenomenon that may aid in further spread of the virus. However, studies of other congenital viruses and a recent report of ZIKV based on *in vitro* infection experiments suggest that trophoblasts are relatively resistant to

ZIKV (Bayer et al., 2016; Kim and Shresta, 2016). This may indicate that the virus gains access to the fetal compartment through alternative pathway(s) at least during late pregnancy.

The study of human cytomegalovirus (HCMV), a virus that causes congenital infections, indicates that multiple modes of transplacental transmission are possible. For example, virus-induced production of inflammatory cytokines or chemokines can promote disruption of the trophoblast barrier thereby facilitating virus entry through the placenta (Kim and Shresta, 2016; Quicke et al., 2016). Moreover, based on studies of HCMV (Maidji et al., 2006), it is possible that ZIKV complexed to maternal immunoglobulins bind to the neonatal Fc receptors on trophoblasts and cross this barrier via transcytosis. Similarly, given that DENV-specific antibodies can cross-react with ZIKV and allow for ADE of ZIKV (Priyamvada et al., 2016), it is tempting to speculate that pre-existing DENV antibodies in the maternal system may facilitate transcytosis (i.e., transport of macromolecules across the interior of a cell) of ZIKV through the trophoblast layer, particularly in patients that reside in areas endemic for both viruses.

Once inside the fetal circulation, ZIKV may cross the BBB and replicate in the fetal brain, thereby causing neuropathology. The fetal BBB is still undergoing development particularly during early gestation (Kim and Shresta, 2016). This means that there could be a window when the BBB is somewhat leaky in which case the virus can gain access to the fetal brain relatively easily. To the contrary, others argue that the BBB matures as early as 12-18 weeks post-conception as evidenced by the appearance of hallmark tight junction proteins (Goasdoué et al., 2016), inferring that ZIKV must disrupt this barrier in order to reach the fetal brain during pregnancy. Possible mechanisms of breaching the BBB may involve pro-inflammatory cytokines and/or virus-induced degradation of tight junction proteins (as discussed in Section *1.1.4.1*).

Once inside the fetal CNS, ZIKV can replicate efficiently in various brain cell types including astrocytes, microglia, neuroprogenitor cells as well as neuroprogenitor-derived neurons (Bayless et al., 2016; Hamel et al., 2017; Li et al., 2016; Nowakowski et al., 2016; Retallack et al., 2016; Xu et al., 2016), some of which may support viral persistence as proposed by previous animal and *ex vivo* studies (Bhatnagar et al., 2017; Hirsch et al., 2017). The eventual fetal neuropathology is probably influenced by a combination of factors including virus-induced apoptosis, dysregulation of cell-cycle pathways and prolonged activation of innate immune responses (Bayless et al., 2016; Li et al., 2016; Miner et al., 2016; Noronha et al., 2016), all of which could impede fetal development.

As depicted above, due to the unique tropism and pathogenesis of ZIKV, potential prevention strategies must be proven effective for both mothers and fetuses (Pierson and Graham, 2016). Despite such challenges, the momentum of Zika vaccine development has been quite impressive. Within the first two years upon recognition of Zika emergence, several Phase-I clinical trials were already underway based on various vaccine platforms (reviewed in (Barouch et al., 2017)). Hopefully, effective prevention and treatment strategies will become available in the near future.

1.1.5 Flavivirus genome and proteins

Flaviviruses have a positive-sense RNA ([+]RNA) genome with an average size of 11 kb. The viral RNA contains a type-I cap (7-methylguanylate cap; m⁷G) at its 5' end but it lacks a polyadenylated tail (Wengler et al., 1978). As well as the protein-coding region, sequence elements and secondary structures within the untranslated regions (UTRs) at both ends of the genomic RNA play crucial roles in genome translation and replication (as reviewed in (Villordo et al., 2016)). For instance, the Y shaped stem-loop A at the 5' UTR and the small hairpin stem-loop in the 3'

UTR, the two most conserved RNA structures across flavivirus genomes, are required for synthesis of viral RNAs (Mohan and Padmanabhan, 1991; Filomatori et al., 2006). The genomic RNA which encodes three structural and 7 non-structural proteins, is translated into a single polypeptide at the ER membrane, (Figure 1.2). Most if not all of the viral proteins have multiple functions.

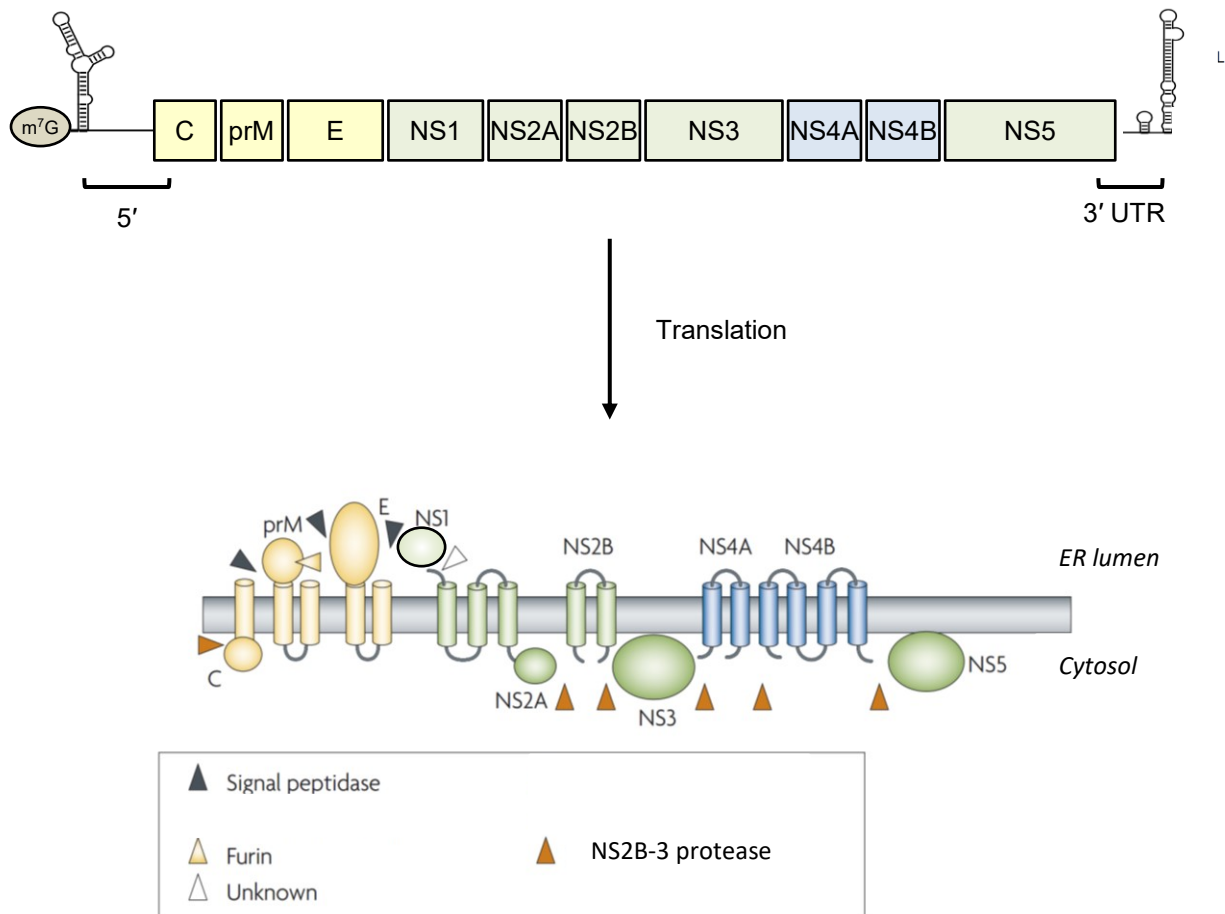


Figure 1.2 Schematic representation of flavivirus genome organization and polyprotein processing. The flavivirus genome which contains a 7-methylguanylate cap (m⁷G) at the 5' end, is ~11 kb in length and contains an open reading frame encoding three structural proteins (capsid (C), precursor membrane (prM) and envelope (E)) and 7 non-structural proteins (NS1, NS2A, NS2B, NS3, NS4A, NS4B and NS5). The genome also contains 5' and 3' untranslated regions (UTR) that help regulate genome translation and replication. The proposed topologies of viral proteins with respect to the ER membrane are presented. The host and viral proteases involved in the polypeptide processing are also indicated (colored triangles). Structural proteins are shown in yellow and non-structural proteins are shown in green or blue. (Modified from Murray, et al 2008).

The structural components include the capsid, membrane (M) and envelope (E) protein, which later become part of the virion. Capsid proteins are small proteins (~13 kDa) that associate with the viral genome to form the nucleocapsid (Khromykh and Westaway, 1996). The M protein (~26 kDa) and its precursor prM are glycoproteins that facilitate budding of immature virion as well as maintain the proper folding and arrangement of E proteins prior to and during virion maturation (Guirakhoo et al., 1991; Lorenz et al., 2002; Yu et al., 2009). Closely associated with prM/M, the E protein (~53 kDa) is glycosylated and is an important surface component required for virus attachment, entry and fusion of viral and cellular membranes during initiation of the viral life cycle (Hung et al., 1999; Mandl et al., 2000; Allison et al., 2001). These structural proteins are also involved in the modulation of host cell signaling processes (reviewed in (Urbanowski et al., 2008); (Arjona et al., 2007)).

The non-structural proteins are not integrated into the virion but instead they participate in viral replication, virion assembly, modulation of cellular pathways and evasion of immune responses. Although discussed separately below, it is important to keep in mind that these viral proteins interact and/or coordinate with each other to perform their diverse functions (Yon et al., 2005; Roosendaal et al., 2006; Klema et al., 2015; Zou et al., 2015). NS3 and NS5 are both large multifunctional proteins and the only two viral proteins with enzymatic activities. Using NS2B as a cofactor, NS3 (~70 kDa) serves as a serine protease that cleaves specific junctions within the viral polypeptide to produce mature structural and non-structural proteins (Chambers et al., 1990). In addition, it contains nucleoside 5'-triphosphatase, RNA helicase, and 5' RNA triphosphatase activities, which are important for ATP hydrolysis, RNA duplex unwinding and dephosphorylation of the viral RNA prior to 5'-RNA cap addition respectively (Takegami et al., 1995; Yon et al., 2005; Wang et al., 2009). In addition to genome synthesis, NS3 is thought to function in virion

assembly (Patkar and Kuhn, 2008), further highlighting the significance of this viral protein in the flavivirus life cycle. NS5 (~100 kDa) is the largest viral protein and is comprised of two enzymatic domains: the RNA-dependent RNA polymerase (RdRP) and the methyltransferase (MTase) domain. While the RdRP domain is required for viral RNA synthesis, the MTase domain enables 5'-RNA capping of nascent viral genomes (Ray et al., 2006; Steffens et al., 1999). Both NS3 (NS3/2B) and NS5 are also involved in antagonizing host innate immunity (see Sections *1.2.1.3* and *1.2.3.3* for more details). Due to their essential roles in viral replication, NS3 and NS5 are popular targets for antiviral drug design.

NS1 (~50 kDa) is a glycoprotein that exists in multiple oligomeric forms. In the ER, it is produced as a soluble monomer that dimerizes and becomes associated with the luminal face of the ER to assist in replication complex formation (Winkler et al., 1989; Westaway et al., 1997; Scaturro et al., 2015). In mammalian cells, NS1 can also be secreted as hexamers (Flamand et al., 1999), which later associate with certain polysaccharides such as heparan sulfate on the host cell surface (Alcon-LePoder et al., 2005; Avirutnan et al., 2007). Detection of circulating NS1 can be used as a diagnostic marker for dengue infection (Young et al., 2000; Zainah et al., 2009). NS1 is important for genome replication as well as evasion of complement-mediated immune response. Exactly how NS1 facilitates viral RNA synthesis is unclear, but it may act as a scaffold that anchors the replication machineries to the ER from the luminal side by interacting with other non-structural proteins that are inserted at the ER membrane (Scaturro et al., 2015; Youn et al., 2012). To evade the complement-based defense system, secreted NS1 binds multiple complement factors in the circulation and interferes with complement-mediated neutralization of infected cells (Avirutnan et al., 2010; 2011). In addition, NS1 is a pathogenic determinant that modulates cellular immune systems such as the IFN and pro-inflammatory responses (further described in Section *1.2.1.3*).

Finally, increasing effort has been directed into developing NS1-based avenues for vaccines and therapeutics.

The remaining four non-structural proteins, NS2A, NS2B, NS4A and NS4B, are relatively small membrane proteins with no known enzymatic functions. Although little is known about their precise modes of action, all of them are required for viral replication. NS2A is important for viral genome synthesis and packaging (Kümmerer and Rice, 2002; Xie et al., 2015), it may also facilitate transport of genomic RNA to assembly sites thereby regulating the switch from genome replication to packaging (Apte-Sengupta et al., 2014). NS2B, as mentioned earlier, is a cofactor for the viral protease NS3; disruption of the NS2B-NS3 interaction destroys the proteolytic activity of NS3 (Jan et al., 1995; Yusof et al., 2000). A recent report of JEV suggests that NS2B may also influence viral RNA production and particle assembly through interaction with NS2A (Li et al., 2016). NS4A and NS4B induce membrane rearrangements that are crucial for biogenesis of replication complexes (Miller et al., 2007; Roosendaal et al., 2006), but their modes of action remain unknown. Finally, mutagenesis studies of DENV and WNV implicate NS4B in cell culture adaptation and pathogenicity in animal models (Zmurko et al., 2015), suggesting a more direct role of this protein in viral replication. These non-structural proteins also interact with multiple cellular factors to mediate evasion of innate immunity (as discussed in Sections *1.2.1.3*, *1.2.2.4* and *1.2.3.3*).

1.1.6 Flavivirus replication cycle

As with all viruses, flavivirus replication relies on host cell resources and machineries. The flavivirus life cycle is composed of four stages: viral entry, genome translation and replication, virion assembly and virus exit. Although categorized into “stages”, most of these phases overlap significantly, making transitions between them rather indistinctive. For instance, viral genome

replication and assembly are thought to occur as coupled events both spatially and temporally (Khromykh et al., 2001; Apte-Sengupta et al., 2014). As such, isolation of replication and assembly sites has been technically challenging. However, recent advances in 3D-electron tomography and membrane protein crystallography have made it possible to visualize unique viral factories and protein structures, which in turn have provided substantial insights into flavivirus biology.

The viral life cycle (Figure 1.3) starts when virions attach to the surface of a host cell and enter it by receptor-mediated endocytosis (Gollins and Porterfield, 1985; Chu and Ng, 2004). Several primary receptors have been identified that facilitate flavivirus entry into different types of mammalian cells, including heparan sulfate (a type of glycoaminoglycan), DC-SIGN (dendritic-cell-specific ICAM-grabbing non-integrin), Hsp70/90 (heat-shock protein 70/90), mannose 6-phosphate receptors and members of the TIM (*T*-cell Immunoglobulin and Mucin domain) and TAM (TYRO3, AXL and MER) receptor families (reviewed in (Perera-Lecoin et al., 2013)). The acidic endosomal environment triggers conformational changes in the virion, primarily the E protein, leading to fusion between the viral and cellular membranes and release of nucleocapsid into the cytoplasm (Gollins and Porterfield, 1986). How exactly capsids dissociate from the genomic RNA is unclear, but several models have been proposed. For instance, as proposed for certain alphaviruses, pH-dependent conformational changes in capsids within the late endosome may drive nucleocapsid disassembly (Mauracher et al., 1991). Some studies also suggest that elongating polysomes promote dissociation of capsids from the genomic RNA in the cytosol (Garcia-Blanco et al., 2016). A recent study revealed a non-degradative ubiquitination step required for genome uncoating in DENV-infected cells (Byk et al., 2016).

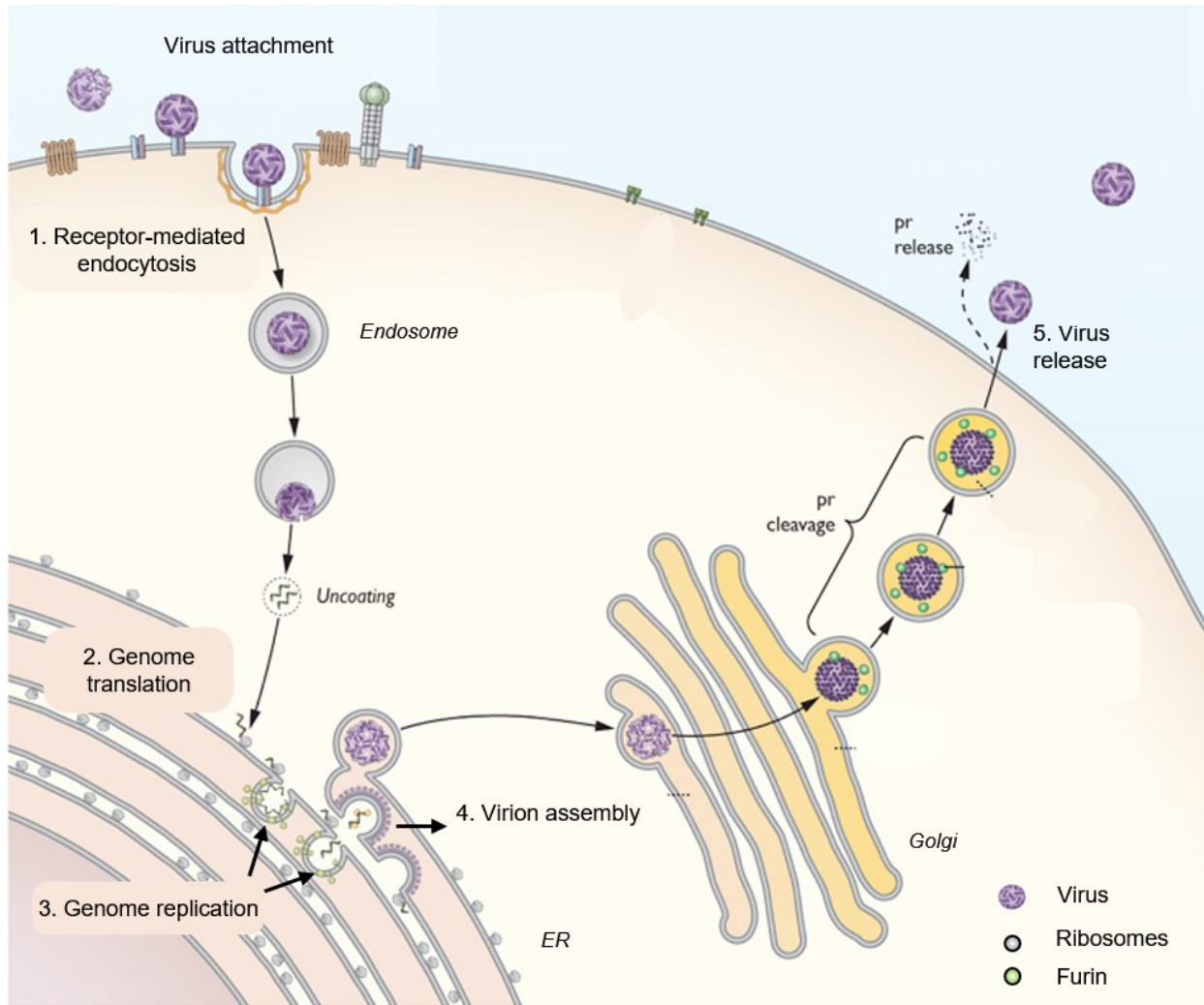


Figure 1.3 The replication cycle of flaviviruses. The flavivirus replication cycle begins when a virion attaches to a host cell receptor and subsequently enters the cell by receptor-mediated endocytosis (step 1). Acidification of the endosomes triggers conformational changes in the virion, resulting in fusion between the viral and the endosomal membranes and release of nucleocapsid into the cytoplasm. The viral genomic RNA is targeted to the rough endoplasmic reticulum (ER), where it is translated into a single polyprotein (step 2). Subsequently, the polypeptide is processed by viral and host proteases, leading to generation of individual viral proteins. Viral replication complexes are formed at the ER membrane where genome synthesis takes place (step 3). The newly synthesized RNA is packaged into the nucleocapsid, and the virion is assembled as the nucleocapsid buds into the ER lumen (step 4). This results in production of non-infectious, immature viral particles that are transported through the Golgi to the *trans*-Golgi network. Here, the host protease furin cleaves between pr and M proteins, leaving the former associated with the virion until it exits the host cell (step 5). Release of pr in the extracellular milieu allows the virion to become fully infectious, which is ready to initiate a new round of infection in the neighbouring cells. (Modified from Pierson and Diamond, 2012)

The uncoated 5'-capped (+)RNA genome is translated into a single polyprotein in a cap-dependent manner (Holden and Harris, 2004; Ray et al., 2006); however, it can also occur through a cap-independent pathway if cap-mediated translation is suppressed (Edgil et al., 2006). Genome translation is closely associated with the ER and the resulting polyprotein is proposed to maintain a unique topology across the ER membrane, likely due the presence of specific signal and transmembrane sequences (Clum et al., 1997; Hsieh et al., 2010; Roosendaal et al., 2006). This viral polyprotein is processed co- and post-translationally by viral and host proteases, resulting in the production of structural and non-structural proteins.

The transition from genome translation to genome synthesis is not well understood, but several mechanisms have been proposed. In one scenario, buildup of genome replication proteins such as NS5 on genomic RNA blocks the access of cellular translation initiation factors and thus promotes transition into RNA replication (Garcia-Blanco et al., 2016). Production of viral RNAs occurs within an extensive ER-derived membranous network whose formation is mediated by the non-structural proteins NS4A and NS4B (Roosendaal et al., 2006; Welsch et al., 2009; Gillespie et al., 2010). Genome replication is composed of two steps: a) generation of (-)RNA templates and b) synthesis of (+)RNA using the (-)RNA templates (as reviewed in (Lindenbach and Rice, 2003)). In general, the production of (+)RNA is favored over (-)RNA (Khromykh et al., 2001; Filomatori et al., 2006) and this process requires non-covalent circularization of the viral genome, likely mediated by specific elements at both ends of the viral RNA (Alvarez et al., 2005). Genome replication is also dependent on the functions of multiple viral proteins and secondary structures within the viral RNAs.

Relatively little is known about the underlying mechanisms of flavivirus assembly. One major puzzle is how specificity of genome packaging is maintained when there appears to be an

absence of unique packaging sequences. Nevertheless, viral genomes are somehow packaged into virions specifically, excluding cellular mRNAs. One model proposes that coordinated budding of structural components (i.e., capsid, prM and E) and newly synthesized RNAs at the ER allows for incorporation of a single viral genome into the maturing virion (Lobigs and Lee, 2004; Welsch et al., 2009). Another puzzling aspect of the assembly process is the formation of subviral particles (SVPs) that lack nucleocapsids. This phenomenon can be recapitulated by expression of prM and E proteins in the absence of other viral proteins (Schalich et al., 1996) and therefore, it appears that viral particle assembly, at least for SVPs, is independent of nucleocapsids. Tangible evidence of capsid-prM/E protein interaction is still lacking and it remains unclear how nucleocapsid is incorporated into the virion. Some studies suggest that temporal proteolytic processing of capsid proteins as well as capsid-E protein interaction may mediate the integration of nucleocapsids into the budding membranes containing prM and E (Lee et al., 2000; Lobigs and Lee, 2004; Blazevic et al., 2016).

Nascent virus particles that have budded into the ER are non-infectious because they cannot induce host-cell membrane fusion (Elshuber et al., 2003; Yu et al., 2008). These immature virions are transported through Golgi apparatus after which the E protein undergoes acidic pH-induced conformational rearrangement in the *trans*-Golgi network. In parallel, prM undergoes proteolytic processing by the host protease furin in the same intracellular compartment after which mature virions are released from the cell by exocytosis (Ishak et al., 1988; Stadler et al., 1997).

1.2 Interactions between flaviviruses and cellular antiviral systems

To control and defend against viruses, host cells are equipped with an elaborate network of antiviral pathways. Not surprisingly, flaviviruses have evolved ways to evade and modulate these cellular defenses. The following sections discuss three anti-flavivirus responses, the Type-I

interferon (IFN) response (Section *1.2.1*), the peroxisome-mediated antiviral response (Section *1.2.2*) and the host stress response (Section *1.2.3*). In addition, the molecular mechanisms by which flaviviruses counteract these defense programs are reviewed.

1.2.1 The IFN system

The IFN system consists of a family of autocrine and paracrine proteins that stimulate a network of signaling cascades that confer crucial protection for infected cells. Thus far, the immunological functions of IFNs are not only implicated in regulation of innate antiviral defenses, but also regulation of adaptive immunity as well as cancer progression (reviewed in (Borden et al., 2007)).

1.2.1.1 Types of IFNs

Thus far, three types of IFNs have been identified: Type-I, -II, and -III (Figure 1.4). In humans, Type-I IFNs include IFN- α , - β , - ϵ , - κ , and - ω , which interact with IFN receptor 1 (IFNAR1) and IFNAR2; Type-II IFN only consists of IFN- γ , which binds to IFN- γ receptor 1 (IFNGR1) and IFNGR2; and Type III IFNs are the four isoforms of IFN- λ , whose cognate receptors are IFN- λ receptor 1 (IFNLR1) and interleukin 10 receptor 2 (IL10R2) (Borden et al., 2007).

Despite sharing similar signaling molecules, different IFNs play distinctive roles in regulating resistance to infections. For instance, Type-I IFNs are produced by diverse cell types including immune cells, fibroblasts, endothelial cells and epithelial cells and they are thought to provide the first line of defense against a wide range of viral infections by activating the production of antiviral molecules (Borden et al., 2007). In contrast, Type-II IFNs are secreted from a subset of immune cells including T lymphocytes, macrophages and natural killer cells (Saha et al., 2010). Their main function is to activate and recruit leukocytes to sites of infection and promote clearance

of intracellular pathogens such as viruses (Saha et al., 2010). More recently, Type-III IFNs and their cognate receptors were discovered. The receptors for Type-III IFNs are largely confined to cells of the epithelial origin including respiratory, intestinal and reproductive tract epithelial cells (Bayer et al., 2016; Sommereyns et al., 2008), suggesting that the Type-III IFN response is important for limiting viral infections in anatomical compartments lined with mucosal barriers.

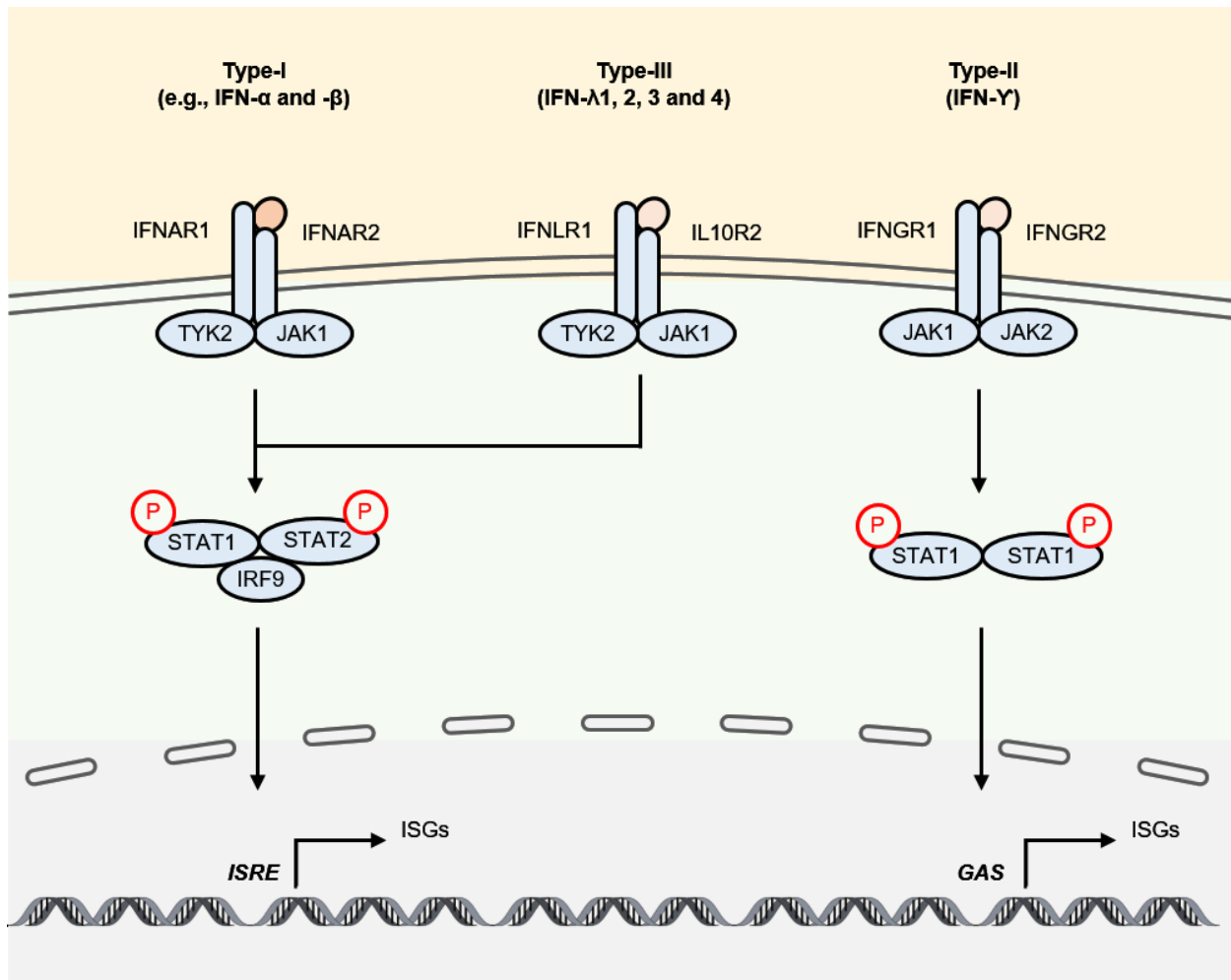


Figure 1.4 The Type-I, -II, and -III interferon (IFN) signaling pathways. The IFN system includes three types of IFN: Type-I (e.g., IFN- α and - β), Type-II (IFN- γ and - ω) and Type-III (IFN- λ 1, 2, 3 and 4) (in humans). IFN signaling is initiated upon binding of IFNs to their cognate receptors. Specifically, Type-I IFNs bind to IFN- α receptor 1 (IFNAR1) and IFNAR2; Type-II IFNs bind to IFN- γ receptor 1 (IFNGR1) and IFNGR2; and Type III IFNs bind to IFN- λ receptor 1 (IFNLR1) and interleukin 10 receptor 2 (IL10R2). This leads to activating phosphorylation of the JAK kinase family (JAK1 and TYK2), which phosphorylate the downstream transcription factors STAT1 (signal transducer and activator of transcription protein 1) and STAT2. During Type-I and -III IFN response, activated STAT1 and STAT2 dimerize and form a complex with the transcriptional activator IRF9 (IFN-regulatory factor 9), with which they stimulate the expression of IFN-stimulated genes (ISGs) through the *ISRE* (IFN-stimulated response element) promoter. During Type-II IFN response, phospho-STAT1 form a homodimer, which translocates into the nucleus to promote transcription of ISGs through the *GAS* (IFN-gamma-activated sequence) promoter. Production of diverse ISGs confers protection and resistance to viral infections through their specific functions in limiting viral entry, replication as well as spread.

1.2.1.2 IFN response pathways

The IFN response is composed of two phases: an initial induction stage where detection of pathogens activates the expression and release of IFNs; and a downstream signaling stage where binding of IFNs to their cognate receptors triggers the production of a wide range of antiviral molecules (Figure 1.5). Consequently, through the release of IFNs, an infected cell can “signal” its neighbours to generate an effective antiviral state against a wide range of pathogens.

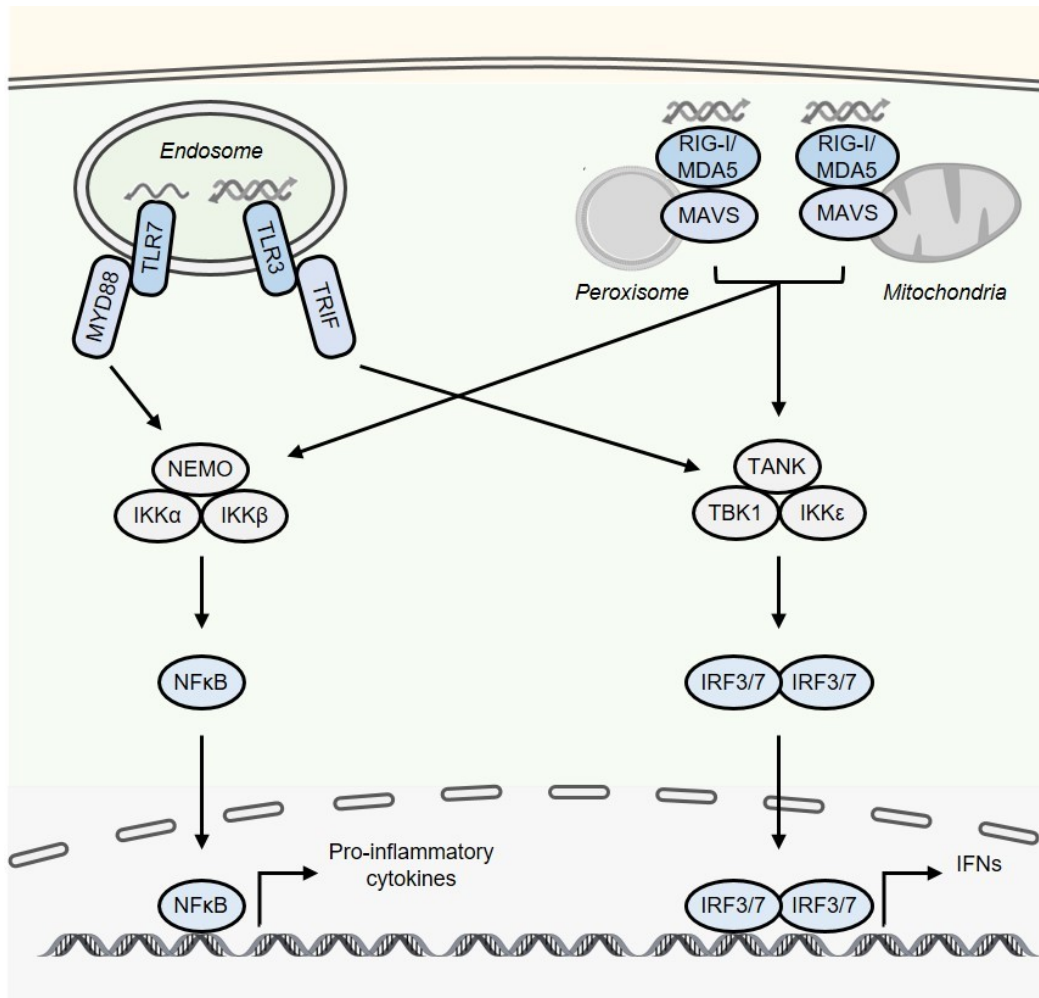


Figure 1.5 Induction of IFN response during flavivirus infection. During viral infection, the endosomal RNA sensors Toll-like receptors (TLR) 3 and 7, as well as the cytoplasmic RNA helicases RIG-I (retinoic-acid inducible gene) and MDA5 (melanoma differentiation-antigen 5) detect viral double-stranded RNA (dsRNA) and ssRNA. This leads to their activation and subsequent recruitment of adaptor molecules. In case of TLRs, the adaptors TRIF (TIR domain-containing adaptor protein inducing IFN β) and MyD88 (myeloid differentiation primary-response gene 88) interact with TLR3 and TLR7 respectively, leading to the activation of two kinase complexes. One kinase complex contains TAK1 (transforming growth factor- β -activated kinase 1), TBK1 (TANK-binding kinase 1) and IKK ϵ (inhibitor of κ B kinase epsilon), and the other contains NEMO (NF- κ B essential modulator), IKK α and IKK β . RIG-I and MDA5 interact with the adaptor molecule MAVS (mitochondrial anti-viral signalling), which is localized to mitochondria, peroxisomes as well as the mitochondrion-associated-endoplasmic reticulum membranes (not shown). Interaction between the helicases and MAVS also activate similar kinase complexes, which mediate signaling that eventually leads to the activation of the interferon regulatory factors (IRF) 3 and 7 and the canonical nuclear factor- κ B (NF- κ B), respectively. These activated transcriptional factors translocate into the nucleus and induce the expression of IFNs as well as pro-inflammatory chemokines and cytokines. Although not shown in this diagram, viral dsRNAs can also be detected by the dsRNA-activated protein kinase PKR. In addition, the IFN response can be triggered by the cytosolic DNA sensor cGAS (cyclic GMP-AMP synthase).

Several pathogen pattern recognition receptors (PRRs) have been identified in detecting flavivirus-specific pathogen-associated molecular patterns (PAMPs), although their effectiveness in inducing an antiviral response varies depending on the cell type and virus. Three types of RNA sensors recognize distinct non-self RNA structures of flaviviruses: the Toll-like receptor (TLR) family (TLR3 and TLR7), the retinoic acid inducible gene (RIG-I)-like receptor (RLR) family (RIG-I and melanoma differentiation-antigen 5 (MDA5)) and the dsRNA-activated protein kinase PKR (Diamond and Gale Jr., 2012; Ye et al., 2013). TLR3 and TLR7, which are present mainly in endosomes, detect double-stranded (dsRNA) and single-stranded RNA (ssRNA) of viral origin respectively (Kato et al., 2011). RIG-I and MDA5 are cytosolic RNA helicases (Kato et al., 2011). RIG-I recognizes structures within the 5' triphosphate termini of dsRNA, as well as short dsRNA and uridine (U)- or adenosine (A)-rich viral RNA motifs (Anchisi et al., 2015; Kato et al., 2011; Schuberth-Wagner et al., 2015). Similarly, MDA5 binds long dsRNA and AU-rich viral RNAs (Kato et al., 2011; Runge et al., 2014). PKR is both a cytosolic PRR that detects viral dsRNA and an ISG capable of controlling viral replication by blocking translation of viral genome (Diamond and Gale Jr., 2012). The PRR function of PKR is activated upon binding to viral dsRNA, which leads to its dimerization and subsequent autophosphorylation. Precisely how PKR mediates IFN induction is unclear, but it has been proposed to facilitate activation of IRF3 by interacting and possibly facilitating RLR-signaling (Pham et al., 2016). However, the role of PKR in IFN induction during flavivirus infection remains controversial. While activation of this kinase induces production of IFNs against WNV infection (Diamond and Gale Jr., 2012), studies of DENV suggest that it is dispensable for IFN-mediated inhibition of viral replication (Diamond and Harris, 2001).

Paradoxically, a cytoplasmic DNA sensor, cyclic GMP-AMP synthase (cGAS) (Cai et al., 2014) has been reported to stimulate the IFN response during flavivirus infection (Schoggins et al., 2014). How exactly cGAS senses RNA viruses is still unclear, but recent evidence suggests that it detects PAMPs associated with these viruses through crosstalk with the RIG-I/MDA5 pathway (Zevini et al., 2017). Interestingly, binding of mitochondrial DNAs that are released due to mitochondrial damage may also facilitate cGAS activation during flavivirus infection (Chatel-Chaix et al., 2016).

Upon binding to viral RNAs, the RNA sensors undergo conformational changes, leading to recruitment and activation of specific adaptor molecules that trigger downstream signaling cascades. In case of TLRs, the adaptors TRIF (TIR-domain-containing adaptor inducing interferon) and MyD88 (myeloid differentiation factor 88) interact with TLR3 and TLR7, respectively, leading to activation of the kinases TAK1 (transforming growth factor- β -activated kinase 1), TBK1 (TANK-binding kinase 1) and IKK- ϵ (inhibitor of κ B kinase epsilon), which in turn activate the transcriptional factors NF- κ B and IRF-3 and/or IRF-7 respectively (Diamond and Gale Jr., 2012). RIG-I and MDA5 interact with the adaptor molecule MAVS, which is localized on mitochondria, peroxisomes, and mitochondria-associated-endoplasmic reticulum membranes (MAM) (Kawai et al., 2005; Seth et al., 2005; Dixit et al., 2010; Horner et al., 2011). Subsequent oligomerization of MAVS triggers the activation of the kinase complexes TBK1/IKK ϵ and NEMO (NF- κ B essential modulator) (Kawai et al., 2005; Seth et al., 2005; Tang and Wang, 2009; Hou et al., 2011), leading to nuclear translocation of the IFN-regulatory factors (IRFs) (e.g., IRF3 and IRF7) and NF- κ B, respectively (as reviewed in (Belgnaoui et al., 2011)). Together, these transcriptional activators promote expression of IFNs and pro-inflammatory chemokines such as TNF- α and IL-6. During flavivirus infection, signal transduction from cGAS was shown to be

dependent on the adaptor molecule STING, an ER transmembrane protein, which also induces Type-I IFNs through the TBK1-IRF3 signaling axis (Zevini et al., 2017).

Secreted IFNs can act in autocrine or paracrine fashion through binding to cognate receptors on the same or neighbouring cells respectively (Figure 1.4). Binding of IFNs to their receptors leads to recruitment, activation and tyrosine phosphorylation of the JAK family kinases, JAK1 and TYK2, which then phosphorylate the downstream transcription factors STAT1 and STAT2 (Borden et al., 2007). When activated, STAT1 and STAT2 dimerize and form a complex with IRF9 in Type-I and -III IFN signaling pathways. In the Type-II IFN signaling pathway, phospho-STAT1 forms a homodimer. STATs then translocate into the nucleus where they induce transcription of many different and diverse IFN-stimulated genes (ISGs) through the *ISRE* (IFN-stimulated response element) and *GAS* (IFN-gamma-activated sequence) promoter sequences respectively. Thus far, *in vitro* and animal studies have revealed specific antiviral functions of ISGs in limiting viral entry (e.g., IFITMs), replication (e.g., OAS, IFITs and RNAs L) as well as pathogen recognition (e.g., RIG-I, MDA5 and TLR3) (reviewed in (Schoggins et al., 2011, 2014; Diamond and Gale Jr., 2012)). Other ISGs are implicated in immune-modulation and cell-death promoting functions. Altogether, the collective activities of ISGs ensure effective elimination of pathogens.

The IFN response must be tightly regulated, and over the past few decades a growing spectrum of signaling mediators has been identified as integral regulators of this antiviral system. Components of the ubiquitination machinery, the autophagy process and the MAP kinase signaling networks have all been implicated in regulating IFN production and downstream signaling (reviewed in (Chan and Gack, 2015; Ivashkiv and Donlin, 2014)).

1.2.1.3 Antagonism of the IFN system by flaviviruses

Studies in knockout mice have established the importance of the IFN system in controlling flavivirus replication and pathogenesis. Moreover, flaviviruses have evolved multiple mechanisms to counteract both the induction as well as the downstream signaling in IFN pathways (Table 1.1).

To suppress induction of the IFN response, flaviviruses evade or delay detection by PRRs (Table 1.1). For instance, as revealed by electron microscopy analyses, flavivirus genome synthesis takes place within an almost completely enclosed membranous web (Överby et al., 2010; Welsch et al., 2009). This membrane architecture is thought to provide spatial separation for genome replication and virion assembly (Welsch et al., 2009), but it may also protect the viral factories from detection by the cellular RNA sensors RLRs and PKR, thereby delaying activation of the antiviral response (Boon and Ahlquist, 2010; Överby et al., 2010). In addition, as demonstrated by WNV, flavivirus NS5 methylates the viral genome 5'-cap at the ribose-2'-*O* position, a conserved structure present in cellular mRNAs. This mimicry of host mRNA avoids recognition by MDA5 and therefore prevents the induction of MDA5-mediated antiviral signaling (Szretter et al., 2012; Züst et al., 2011).

Flaviviruses can also directly interfere with signal transduction initiated from PRRs to suppress transcription of IFNs (Table 1.1). For example, WNV NS1 blocks TLR3-induced transcription of IFN- β and IL-6 (Wilson et al., 2008) while expression of the viral protein NS2A attenuates production of IFN- α/β through a yet unknown mechanism (Liu et al., 2004). NS4B of both DENV and WNV inhibits TBK1/IKK ϵ -mediated activation of IRF3 and thereby reduces the expression of IFN- β (Dalrymple et al., 2015). In human cells, the PRR-signaling adaptor molecule STING is cleaved by DENV protease NS2B-3, thus disrupting IFN production in a species-specific manner (Aguirre et al., 2012; Rodriguez-Madoz et al., 2010; Yu et al., 2012). In addition, DENV

NS4A interacts with the RLR-signaling adaptor protein MAVS and prevents it from interacting with RIG-I (He et al., 2016). Viral RNA can also antagonize IFN responses as well. Recently, the subgenomic RNA (sfRNA) of DENV was shown to blunt RIG-I-mediated IFN induction by binding to and destabilizing TRIM25 (Tripartite motif-containing protein 25), a positive regulator of RIG-I (Manokaran et al., 2015). However, it remains uncertain whether sfRNA-mediated targeting of TRIM25 is a common strategy deployed by other flaviviruses.

Apart from blocking the expression of IFNs, flaviviruses can also hinder the IFNR-initiated signaling pathways (Table 1.1). For example, WNV infection results in depletion of IFAR1 through a non-canonical protein degradation pathway that may be mediated by viral non-structural proteins (Evans et al., 2011). Since STAT1 and STAT2 are essential for the production of ISGs, a common scheme employed by flaviviruses is to interfere with their activation. For example, the non-structural proteins have been shown to prevent phosphorylation of STAT1 and/or STAT2 during infection of WNV (Guo et al., 2005; Liu et al., 2005; Muñoz-Jordán et al., 2005), DENV (Muñoz-Jordán et al., 2003), JEV (Lin et al., 2006), YFV (Muñoz-Jordán et al., 2005) and TBEV (Best et al., 2005; Werme et al., 2008). In addition, DENV NS5 targets STAT2 for proteasomal degradation by co-opting the ubiquitin E3 ligase UBR4 (Ashour et al., 2009; Morrison et al., 2013). Although many of these findings require further validation in more physiologically relevant systems (such as primary immune cells, the major sites for flavivirus replication), they have revealed several attractive candidates for novel antiviral therapeutics.

Even when IFN-signaling occurs, flaviviruses can impair the functions of multiple downstream ISGs (Table 1.1). For instance, NS5 of WNV modifies the viral 5'-cap with a 2'-*O*-methylation, thus evading the restriction of viral replication imposed by IFIT1, a potent executioner molecule strongly induced during flavivirus infections (Dong et al., 2012). How

flaviviruses interact with other ISGs remains largely unknown; nonetheless, better characterizations of the antiviral functions of ISGs will provide further mechanistic insights into how flaviviruses counteract the IFN system.

Table 1.1 Viral antagonism of the IFN system by flaviviruses

Virus	Viral determinant	Cellular target	Mode of action	Reference
<i>Antagonisms of IFN induction</i>				
DENV	NS4A	MAVS	Binds MAVS and prevents its interaction with RIG-I	(He et al., 2016)
DENV	NS2B-3	STING	Cleaves human STING	(Aguirre et al., 2012)
DENV	NS2A, NS4B and NS4A (for DENV-1)	TBK1	Inhibits phosphorylation of TBK1	(Dalrymple et al., 2015)
DENV, WNV	NS3	14-3-3 ϵ	Binds 14-3-3 ϵ and blocks RIG-I translocation to mitochondria	(Chan and Gack, 2016)
WNV and other members	NS5	5'-cap structure	Modifies the viral RNA 5'-cap with a 2'-O-methylation and thus evades MDA5 detection	(Dong et al., 2012; Züst et al., 2011)
WNV	E	RIP1	Blocks dsRNA-induced poly-ubiquitination activation of RIP1 and thus Type-I IFN induction	(Arjona et al., 2007)
WNV	NS4B	TBK1	Inhibits phosphorylation of TBK1	(Dalrymple et al., 2015)
WNV	sfRNA	unknown	Suppresses IRF3/IRF7-mediated Type-I IFN production	(Schuessler et al., 2012)
WNV	NS1	unknown	Inhibits TLR3 signaling	(Wilson et al., 2008b)
WNV	NS2A	unknown	Suppresses IFN- β promoter activity	(Liu et al., 2004)

Table 1.1 (continued)

ZIKV	NS1, NS4B	TBK1	Binds TBK1 and inhibits its phosphorylation	(Wu et al., 2017)
<i>Antagonisms of IFN-signaling</i>				
DENV	NS5	STAT2	Directs human STAT2 for proteasomal degradation	(Agrawal et al., 2011; Ashour et al., 2009; Morrison et al., 2013)
DENV	sfRNA	G3BP1, G3BP2, Caprin-1	Sequesters these cellular factors to block ISG translation	(Bidet et al., 2014)
DEVN, WNV, JEV	NS5	STAT1/2	Blocks STAT1 and STAT2 phosphorylation	(Best et al., 2005; Laurent-Rolle et al., 2010; Lin et al., 2006; Liu et al., 2005)
TBEV	NS5	hScrib	Binds hScribble and blocks STAT1 phosphorylation activation	(Werme et al., 2008)
WNV	NS4B	JAK1, TYK2	Blocks JAK1 and TYK2 phosphorylation	(Evans and Seeger, 2007; Guo et al., 2005)
WNV	unknown	IFNAR1	Infection induces IFNAR1 depletion	(Evans et al., 2011)
WNV, TBEV	unknown	SOC1, JAK1	Infection upregulates SOCS1 which suppresses JAK1 activity	(Mansfield et al., 2010)
WNV, YFV, DENV	NS4B (or NS4A in DENV)	STAT1	Blocks STAT1 phosphorylation activation	(Muñoz-Jordán et al., 2005)
ZIKV	NS2B-3	JAK1	Targets JAK1 for degradation	(Wu et al., 2017)
ZIKV	NS5	STAT2	Targets STAT2 for proteasomal degradation	(Grant et al., 2016; Kumar et al., 2016)

Antagonisms of ISG functions

Table 1.1 (continued)

WNV (and other members)	NS5	5'-cap structure	Modifies the viral RNA 5'-cap with a 2'- <i>O</i> -methylation and thus evades IFIT1 detection	(Dong et al., 2012; Szretter et al., 2012)
-------------------------	-----	------------------	--	--

1.2.2 The peroxisome: a new antiviral signaling platform

Studies by Dixit and colleagues revealed the exciting but unexpected finding that peroxisomes serve as important signaling platforms in the IFN system (Dixit et al., 2010; Odendall et al., 2014). Since then, the role of peroxisomes during viral infections of mammalian cells has been investigated by a number of groups revealing novel interactions between specific peroxisomal factors and viral components. To provide a background context for my studies in this area, the sections below review some of the key metabolic functions, biogenesis pathways and documented interactions between viruses and peroxisomes.

1.2.2.1 Peroxisome metabolic functions

Peroxisomes are membrane bound organelles that are found in almost all eukaryotic cells (reviewed in (Smith and Aitchison, 2013)). They are important for fatty acid catabolism, biosynthesis of bile acids and ether phospholipids, as well as regulation of oxidative homeostasis in mammalian cells (reviewed in (Waterham et al., 2016)). In humans, the significance of peroxisomal metabolic functions is illustrated by the severe developmental disorder, Zellweger syndrome. Patients with this disease have genetic mutations in one or more of the genes essential for peroxisome biogenesis. Due to reduced or lack of peroxisomal functions, infants born with Zellweger syndrome have severe developmental defects particularly in their CNS and other vital organs such as kidneys and lungs (Wilson et al., 1986). Unfortunately, these patients usually do not survive childhood. Over the past few decades, identification and characterization of different

genetic peroxisomal disorders have revealed the underlying functions of peroxisomes in human metabolism and health.

When peroxisomes were initially discovered, they were defined by their ability to produce hydrogen peroxide (H_2O_2) from organic substrates and to remove H_2O_2 by the hallmark peroxisomal enzyme, catalase (Duve and Baudhuin, 1966). H_2O_2 is a byproduct generated through fatty acid β -oxidation, a major function of peroxisomes. Although they share some catalytic reactions with mitochondria, human peroxisomes catalyze distinct substrate species using oxidase enzymes. In general, the peroxisomal β -oxidation pathway uses very long chain fatty acids (C22 and higher), branched-chain fatty acids, bile acid intermediates, and long chain dicarboxylic acids as substrates, whereas mitochondria oxidize long chain, medium chain, and short chain fatty acids (C18 and shorter) (reviewed in (Waterham et al., 2016)). The resultant high energy-products are transferred to mitochondria for cellular energy production. Genetic deficiencies in the peroxisomal β -oxidation pathway are associated with a variety of metabolic diseases such as X-linked adrenoleukodystrophy, acyl-coA oxidase deficiency and D-bifunctional protein deficiency.

Peroxisomes also produce ether phospholipids such as plasmalogens and bile acids. Both membrane-associated and matrix enzymes are responsible for generation of plasmalogens, an essential biomolecule with links to neurodegenerative disorders such as Alzheimer disease (Lizard et al., 2012). Interestingly, the process of plasmalogen production is anti-oxidant in nature and is important for maintaining redox balance in the host cell (Marmer et al., 1986). Synthesis of bile acids from cholesterol is carried out by liver-specific peroxisomal enzymes. Genetic disorders such as bile acid synthetic (BAAT) defects have been linked to mutations in the *BAAT* gene (Fujiki et al., 2012).

1.2.2.2 Peroxisome biogenesis

The origin of peroxisomes has been debated for many years. Currently, two models of peroxisome biogenesis have been proposed based on studies from yeast and mammalian systems: a) fission and division of pre-existing peroxisomes; and b) *de novo* biogenesis from the ER (Figure 1.6). Although these pathways are distinct, they are not mutually exclusive as they share common molecular factors and may coordinate with each other to regulate peroxisome abundance depending on the state of cell cycle and environmental cues (reviewed in (Titorenko and Rachubinski, 2001; Smith and Aitchison, 2013)).

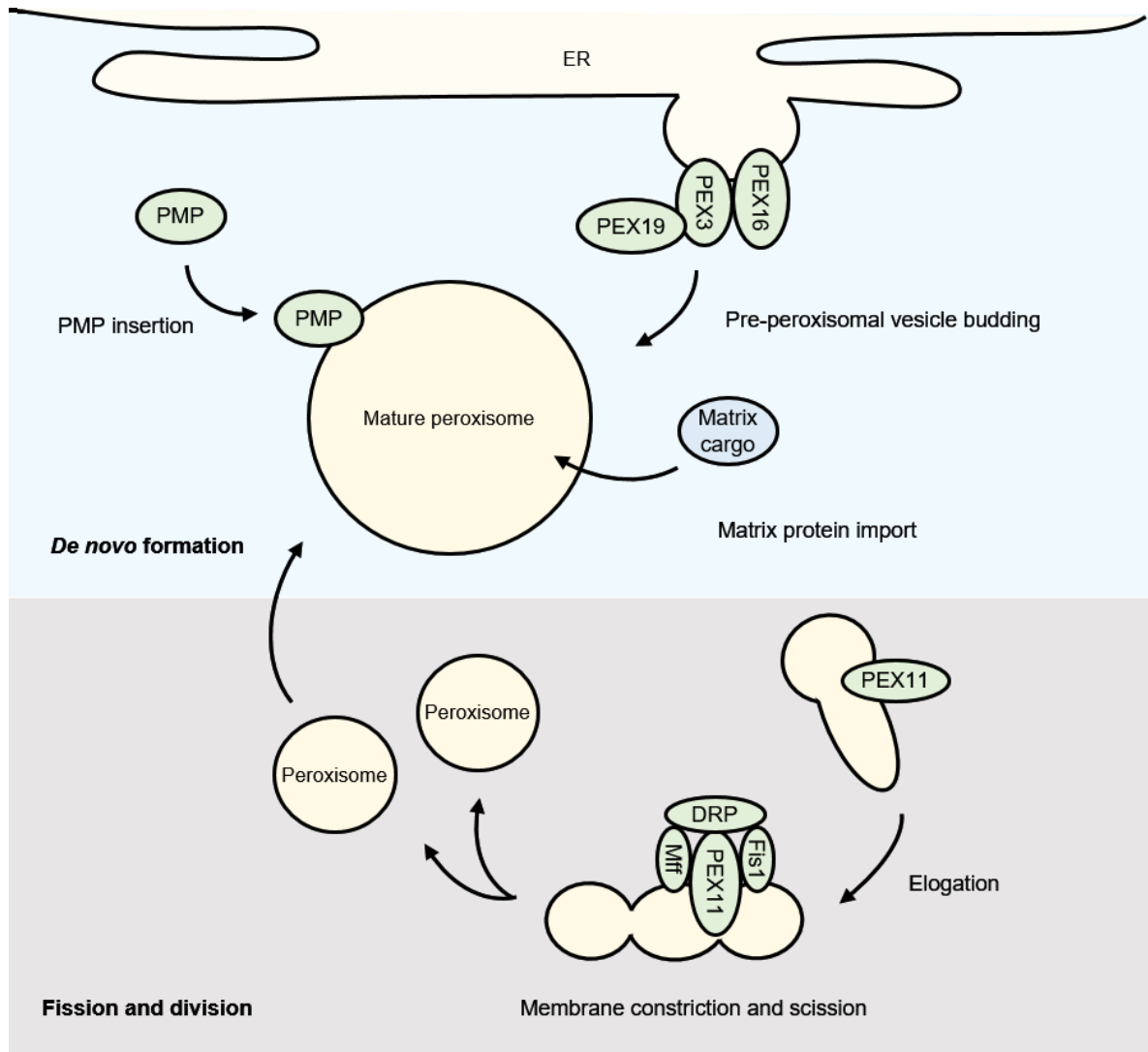


Figure 1.6 Peroxisome biogenesis pathways in mammalian cells. Two predominant mechanisms have been proposed to account for peroxisome formation: 1) *de novo* formation of peroxisomes from the endoplasmic reticulum (ER) (top pane); and 2) peroxisome proliferation through division and fission (bottom pane). During *de novo* formation, biogenesis factors such as PEX16 are targeted to the ER in order to recruit cellular factors that can induce membrane curvature. Subsequently, PEX16 recruits other peroxisomal membrane proteins (PMPs) such as PEX3 and PEX11 to the ER membrane to promote formation of pre-peroxisomal vesicles. The process of pre-peroxisomal vesicle budding is still unclear, but it may be mediated by PEX19. Import of PMPs and matrix proteins is facilitated by the membrane import machinery and the matrix protein importer, respectively. Consequently, immature peroxisomes acquire full functionality. The division and fission pathway is dependent on pre-existing peroxisomes. Initially, PEX11 β induces peroxisome elongation. Interactions between PEX11 and the membrane-anchored fission factors Fis1 (fission protein 1) and Mff (mitochondrial fission factor) coordinate the subsequent recruitment of dynamin-regulated proteins (DRPs) to the elongated organelle. Lastly, DRPs facilitate the constriction and scission of peroxisomal membranes and thus production of organelle progenies.

Peroxisome division is a well-established, multi-step process similar to that of mitochondria. The key players involved in this pathway belong to the PEX11 protein family and the dynamin-related protein (DRP or DLP) family. In mammals, three isoforms of PEX11 have been described, PEX11- α , - β and - γ , with PEX11 β as the best known inducer of peroxisome proliferation when overexpressed (Li and Gould, 2002; Delille et al., 2010). DRPs are large GTPases that possess mechanochemical properties to constrict and tubulate membranes, and their role in mediating peroxisome fission was reported more than a decade ago (Koch et al., 2003). As well as PEX11 and DRPs, mitochondrial fission factors Fis1 and Mff are implicated in proliferation and morphogenesis of peroxisomes (Gandre-Babbe and Blik, 2008; Kobayashi et al., 2007).

In general, nascent peroxisomes are derived from pre-existing peroxisomes and the molecular mechanism is composed of two main steps (Figure 1.6). First, PEX11 β induces peroxisome elongation through the conserved amphipathic helix at its N-terminus (Li and Gould, 2002; Kobayashi et al., 2007; Opaliński et al., 2011). How exactly PEX11 β becomes activated in mammalian systems is still unclear, but in yeasts, phosphorylation events have been shown to be important in regulating PEX11 β functions (Joshi et al., 2012; Knoblauch and Rachubinski, 2010). Interactions between PEX11 and the membrane-anchored Fis1 and Mff coordinate the subsequent recruitment of DRPs to the elongated organelle (Kobayashi et al., 2007; Li and Gould, 2002). Next, DRPs are recruited through interaction with Fis1 and Mff, and together they facilitate the constriction and scission of peroxisomal membranes to form nascent peroxisomes (Kobayashi et al., 2007; Koch et al., 2003). A recent study revealed that PEX11 also serves as a GTPase-activating protein (GAP) of DRPs during peroxisome fission (Williams et al., 2015), further highlighting the indispensable role of PEX11 in the peroxisome proliferation pathway.

De novo formation of peroxisomes is dependent on the ER (Smith and Aitchison, 2013b). In yeast, the pathway involves generation and fusion of distinct classes of ER-derived pre-peroxisomal vesicles, resulting in formation of functionally mature peroxisomes (Titorenko et al., 2000; van der Zand et al., 2012; Mast et al., 2016). More recently, the ER-dependent mode of peroxisome biogenesis has also been observed in mammalian cells, where the roles of several essential biogenesis factors including PEX16 and PEX3 are described (Jones et al., 2004; Kim et al., 2006; Toro et al., 2009; Yonekawa et al., 2011; Aranovich et al., 2014; Hua et al., 2015).

In the proposed model (Figure 1.6), the initial assembly of pre-peroxisomal vesicles at the ER requires recruitment of membrane modulating factors to induce membrane curvature (Hua and Kim, 2016). PEX16 is proposed to be a plausible candidate to mediate this process as it has been shown to be inserted co-translationally into the ER membrane and recruit other peroxisomal membrane proteins (PMPs) such as PEX3 and PEX11 to the ER (Kim et al., 2006; Toro et al., 2009; Agrawal et al., 2011; Aranovich et al., 2014; Hua et al., 2015). How precisely these peroxisome precursors bud from the ER is unknown, but a study using complementation in *PEX3*-null human fibroblasts indicates the importance of PEX3-PEX19 interaction in mediating this budding process (Schmidt et al., 2012). Reports in yeasts also support an essential role of PEX19 in the formation of pre-peroxisomal vesicles (Agrawal et al., 2011; 2016).

1.2.2.3 Peroxisomal protein import

Following their release from the ER, maturation of the pre-peroxisomal vesicles requires import of PMPs and matrix proteins, which allows the organelle to acquire full functionality (Figure 1.7). Insertion of PMPs are dependent on PEX19, PEX3 and PEX16 (reviewed in (Hua and Kim, 2016). PEX19 acts as a general cytosolic chaperone that binds newly synthesized PMPs, while PEX3 and PEX16 form a docking complex that receives PEX19-cargos and facilitates PMP-

membrane insertion (Jones et al., 2004; Matsuzaki and Fujiki, 2008; Fujiki et al., 2006; Schmidt et al., 2012). Of note, integrations of many PMPs to the organelle membrane are shown to be mediated through the ER route particularly in yeasts (Hoepfner et al., 2005; Kim et al., 2006; van der Zand et al., 2010; Agrawal et al., 2016); however, to what extent the ER-dependent pathway contributes to PMP-trafficking in mammalian cells remains to be elucidated.

Matrix protein import relies on four groups of biogenesis factors, which consists of the soluble receptors (PEX5/PEX7), the docking complex (PEX13/PEX14), the RING-ubiquitination complex (PEX2/PEX10/PEX12), and the AAA-type ATPase complex (PEX1/PEX6/PEX26) (Figure 1.7). Cargo receptors bind to matrix proteins, many of which contain a peroxisomal targeting signal (Gould et al., 1989; Petriv et al., 2004), and guide them to the docking complex at the organelle membrane (Albertini et al., 1997; Elgersma et al., 1996; Nair et al., 2004; Stanley et al., 2006). Subsequently, ubiquitination- and ATP-dependent extraction of receptors allows for release of matrix cargo and their transport through the “transient translocation pore” into the peroxisome lumen (Dammai and Subramani, 2001; Nair et al., 2004; Erdmann and Schliebs, 2005; Meinecke et al., 2010). Ubiquitination and ATP-hydrolysis are mediated by the RING complex and AAA-type ATPase complex respectively (Platta et al., 2005; El Magraoui et al., 2012). Peroxisomal protein import is a highly regulated process that involves intricate signaling networks in response to specific environmental cues. As such, studies on this dynamic process are important for understanding the many functions of peroxisomes including its role in cellular defense programs.

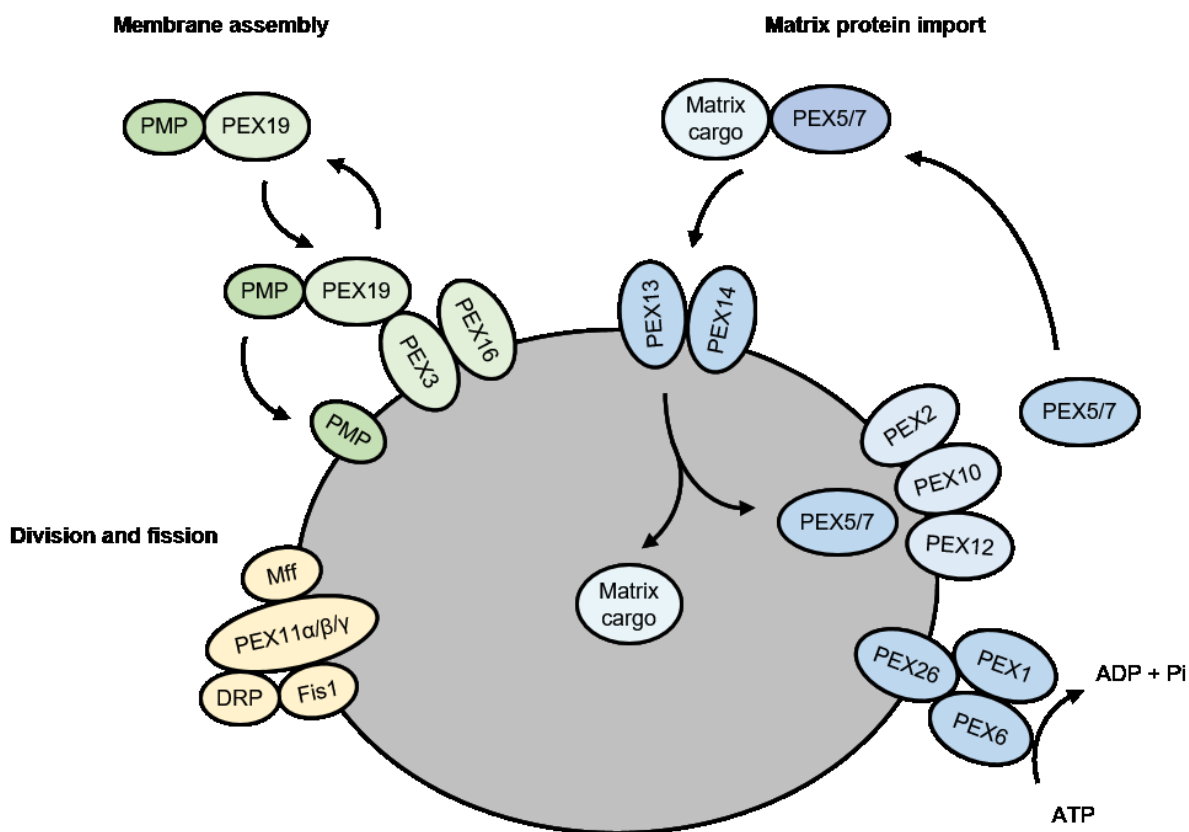


Figure 1.7 Peroxisome biogenesis factors for membrane assembly, matrix protein import and organelle division. In mammalian cells, peroxisome biogenesis involves three groups of host factors: the membrane assembly complex (PEX19, PEX3 and PEX16; green), the matrix protein importer (PEX13, PEX14 and PEX5/7; blue) and the division and fission machinery (PEX11, DRPs, Fis1 and Mff; yellow). The import of peroxisomal membrane proteins (PMPs) requires the cytoplasmic chaperone PEX19, which binds newly synthesized PMPs and transports them to the organelle membrane. Subsequently, through interaction with the docking complex PEX3 and PEX16, PMP cargoes are inserted into the peroxisomal membrane. PEX19 is then recycled to the cytosol to perform new rounds of chaperone function. For import of matrix cargoes, the soluble receptors PEX5 and PEX7 bind to matrix proteins and guide them to the docking complex PEX13 and PEX14. Subsequently, ubiquitination and ATP-dependent extraction of receptors allows for the release of matrix cargoes and their transport through the docking complex channel into the peroxisomal lumen. Ubiquitination and ATP-hydrolysis are mediated by the RING-ubiquitination complex (PEX2/PEX10/PEX12) and the AAA-type ATPase complex (PEX1/PEX6/PEX26), respectively. The division and fission machinery is comprised of PEX11 proteins (PEX11- α , - β and - γ), dynamin-related proteins (DRPs) as well as the fission protein 1 (Fis1) and mitochondria fission factor (Mff). While PEX11 induces elongation of peroxisomes, DRPs, Fis1 and Mff coordinate membrane constriction and scission.

1.2.2.4 Peroxisomes and viruses

As mentioned above, peroxisomes function as signaling platforms that regulate the innate immune response against a diverse group of pathogens (Dixit et al., 2010; Odendall et al., 2014). Dixit et al reported that a pool of MAVS, a mitochondrial adaptor protein that mediates the RLR-induced IFN production, is localized to peroxisomes. How MAVS is targeted to peroxisomes is not clear, but it may require the PMP-import machinery composed of PEX19, PEX3 and PEX16. Subsequent studies revealed that peroxisomal MAVS regulates both Type-I and –III IFN induction (Bender et al., 2015; Odendall et al., 2014) but very little is known about the molecular players and the signaling events involved. To this end, over-expression of PEX16 was shown to enhance the transcription activity mediated by IRF1 and NFκB following treatment with IFN-λ and Sendai virus respectively (Zhou et al., 2015).

Given the multi-functionality of peroxisomes, it is not surprising that viruses target this organelle for their benefit. Members of the plant virus family *Tombusviridae* remodel peroxisomal membranes to facilitate viral RNA synthesis, a process that may be linked to an impaired peroxisomal function in H₂O₂ removal and thus pathologies observed in infected plant leaves (Panavas et al., 2005; Rochon et al., 2014; Russo et al., 1983). The VP4 protein of rotavirus, a virus that infects mammalian cells, is targeted to peroxisomes, but the significance of this phenomenon is unclear (Mohan et al., 2002). It has been speculated that the virus may exploit the activities of specific peroxisomal enzymes to alter host lipid metabolism and/or modify VP4 itself for virion assembly (Lazarow, 2011).

One of the earliest clues that implicated peroxisomes in viral biology came from the observation that the NS1 protein of influenza virus forms a complex with the peroxisomal enzyme 17-β hydroxysteroid dehydrogenase (17β-HSD) (Wolff et al., 1996). The role of 17β-HSD in the

virus life cycle is not known, but based on the observation that over-expression of 17 β -HSD reduces production of viral proteins, influenza virus may modulate this cellular enzyme to benefit viral replication. Around the same time, another virus-peroxisome interaction was identified. In this case, the Nef protein of human immunodeficiency virus 1 (HIV-1) was shown to bind peroxisomal acyl-CoA thioesterase. The resulting augmented lipid metabolic activity was postulated to facilitate Nef-mediated down-regulation of the essential T-cell signaling receptor CD4 (Cohen et al., 2000; Liu et al., 1997; Watanabe et al., 1997).

Recent studies have provided more evidence that peroxisomes perform important antiviral functions. The vMIA of HCMV was shown to bind PEX19 and hijack the PMP-importer complex for its peroxisomal trafficking (Magalhães et al., 2016). Notably, this process is linked to the ability of vMIA to subvert peroxisome-mediated antiviral signaling, implying that vMIA-peroxisomal targeting is a novel countermeasure deployed by HCMV. Similarly, the NS3-4A protease of HCV cleaves both mitochondrial and peroxisomal forms of MAVS, leading to release of this adaptor molecule into the cytosol and thereby blocking the RLR-induced IFN expression (Bender et al., 2015; Ferreira et al., 2016). Although the contribution of peroxisomes in the IFN system is still unclear, these virus-peroxisome interactions, in association with the altered antiviral response, posit a more general role of this organelle in regulating innate immune defenses.

1.2.3 The cellular stress response

The cellular stress response is an indispensable defense mechanism against viral infections. A hallmark of the stress response is global translation arrest as well as formation of stress granules (SGs), both of which regulate cell survival and homeostasis during stress conditions. To favor viral production, viruses including flaviviruses have evolved ways to modulate stress response pathways.

1.2.3.1 Induction of the stress response

During flavivirus infection, the stress response can be triggered through activation of PKR as well as through the unfolded protein response (UPR). PKR is a cytosolic PRR and an ISG, which recognizes viral genome replication intermediate dsRNA and activates itself through dimerization and subsequent auto-phosphorylation (Dey et al., 2005). Besides promoting RLR-mediated induction of IFNs (Pham et al., 2016), PKR is one of the key cellular kinases that target the essential translation initiation factor eIF2 α and induce translation arrest. Infection of cells with flaviviruses such as JEV, WNV and DENV induces phosphorylation of PKR (Gilfoy and Mason, 2007; Roth et al., 2017; Tu et al., 2012) and its downstream target eIF2 α (Umareddy et al., 2007; Tu et al., 2012). However, PRK-mediated phosphorylation of eIF2 α appears to be cell type-dependent, as some reports indicate that flaviviruses do not significantly activate this host kinase (Elbahesh et al., 2011) or increase the level of phospho-eIF2 α in certain *in vitro* systems (Roth et al., 2017).

The UPR is a type of stress response triggered by accumulation of unfolded or misfolded proteins in the ER lumen. The main function of UPR is to restore ER homeostasis through increased production of protein chaperones, enhanced activity of the ER-associated protein degradation (ERAD) machinery, and transient attenuation of nascent protein synthesis (Ron and Walter, 2007). When the ER protein burden becomes too severe, the UPR activates signaling pathways to promote cell death.

The UPR can be triggered through three parallel ER stress sensors, IRE1 (inositol-requiring protein-1), ATF6 (activating transcription factor)-6 and PERK (PKR-like ER kinase), all of which are ER transmembrane residents that detect disturbances in the ER lumen (reviewed in (Ron and Walter, 2007)) (Figure 1.8). In the absence of stress, these sensors are sequestered by the

immunoglobulin heavy-chain binding protein (BiP) and kept in an inactive state. During ER stress, binding of unfolded or misfolded proteins to BiP allows for the release and subsequent activation of these stress sensors. Consequently, IRE1 and ATF6 increase the expression of ER chaperones and components of the ERAD machinery, while PERK phosphorylates eIF2 α and promotes repression of cap-dependent mRNA translation as well as activation of pro-survival programs.

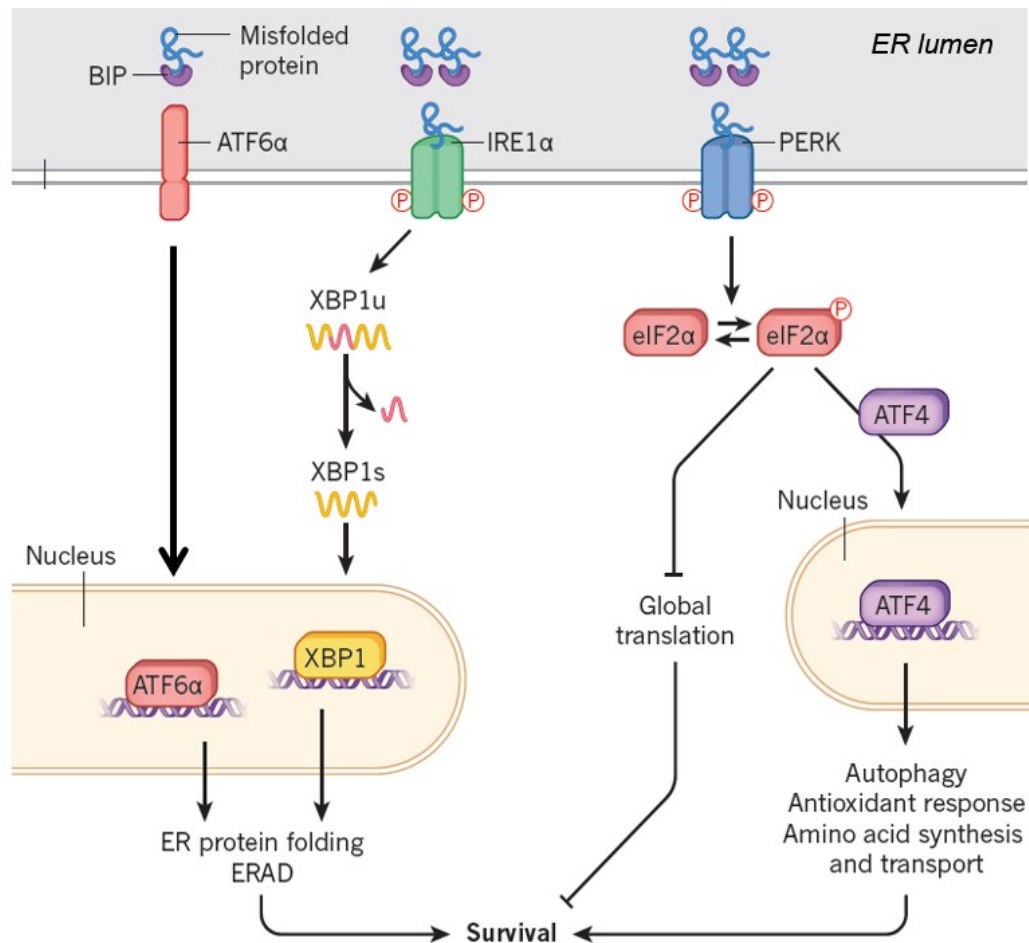


Figure 1.8 The unfolded protein response (UPR). During endoplasmic reticulum (ER) stress, unfolded and misfolded proteins interact with the immunoglobulin heavy-chain binding protein (BiP), which sequesters ATF6 α (activating transcription factor 6 α), IRE1 α (inositol-requiring protein 1 α) and PKR-like ER kinase (PERK) in an inactive form. Consequently, three parallel arms of UPR signaling are triggered through activated ATF6 α , IRE1 α and PERK. ATF6 is a transcriptional activator that promotes expression of genes involved in ER protein folding and the ER-associated protein degradation (ERAD) pathway. IRE1 α homodimerizes and autophosphorylates to cleave the X-box binding protein 1 (XBP1), leading to its nuclear translocation and subsequent expression of genes involved in resolving ER stress. PERK also dimerizes and undergoes autophosphorylation, after which it can phosphorylate the eukaryotic translation initiation factor 2 α (eIF2 α), leading to cellular translation arrest. In addition, PERK activates ATF4 (activating transcription factor 4), which stimulates transcription of genes implicated in several pro-survival pathways. The overall outcome of the UPR is to increase ER-protein processing capacity and cell survival, and if the ER stress persists, apoptosis can ensue (Modified from Wang and Kaufman, 2016).

Activation of the UPR during flavivirus infection has been well documented. DENV induces all three arms of UPR signaling, leading to upregulation of *XBPI* splicing (X-box binding protein 1), a transcription factor downstream of IRE1, ATF6-dependent gene expression, as well as phosphorylation of PERK and eIF2 α (Umareddy et al., 2007; Yu et al., 2006). Other flaviviruses such as WNV and JEV can also trigger IRE1- and ATF6-mediated UPR signaling (Ambrose and Mackenzie, 2011; Yu et al., 2006); however, it is not clear if they activate PERK.

1.2.3.2 Formation of stress granules (SGs)

Under stress conditions, SG formation can be induced by phosphorylation of eIF2 α . Phosphorylated eIF2 α binds to the GTP exchange factor eIF2B with high affinity and inhibits the exchange of GDP with GTP, leading to reduced availability of ternary complexes and therefore suppressed translation initiation (Sudhakar et al., 2000). Consequently, pre-initiation complexes (primarily composed of eIF3, eIF4A, B, E and G, eIF5, PABP and the 40S ribosomal subunit) are “stalled” on mRNAs, which can undergo condensation and form SGs in the cytoplasm. SGs are dynamic ribonucleoprotein (mRNP) aggregates that are induced in response to various stress stimuli. They are essential for maintaining cellular RNA homeostasis as they store translationally silenced mRNPs until stress is resolved. During recovery from stress, SG contents are released to allow resumption of translation through a process that is not well understood (as reviewed in (Buchan and Parker, 2009)). However, if stress persists, they are processed for RNA degradation through processing bodies (P-bodies), another crucial RNA granule that regulates RNA metabolism in the host cell (Sheth and Parker, 2003). Transient and dynamic interactions have been observed between SGs and P-bodies in stressed cells, but little is known about the mechanisms of this process apart from the observation that over-expression of certain mRNA decay factors such as TTP (Tristetraprolin) can promote SG-P-bodies interaction (Kedersha et al.,

2005). In addition to mediating translation arrest, SGs are linked to cellular innate immunity during viral infections (Ng et al., 2013; Oh et al., 2016; Yoo et al., 2014; Onomoto et al., 2014).

SG aggregation is induced by translation arrest mostly through stress-induced phosphorylation of eIF2 α . Besides PKR and PERK, two other kinases, HR1 (heme-regulated inhibitor) and GCN2 (general control nonderepressible-2), target eIF2 α in response to oxidative or heat shock stress and nutrient starvation, respectively (Chong et al., 1992; Dever et al., 1993; Harding et al., 1999; McEwen et al., 2005). SG formation can also be triggered through an eIF2 α -independent process. For instance, hippuristanol, an inhibitor of the RNA-helicase eIF4A that is required for initiation of cap-dependent translation, induces SG assembly by blocking translation initiation without phosphorylation of eIF2 α (Cencic and Pelletier, 2016; Mazroui et al., 2006). Therefore, it seems that blocking translation initiation *per se*, can lead to SG formation.

SG assembly is a rapid process that consists of multiple steps (Figure 1.9). The initial step is mediated by key RNA-binding proteins (RBPs) that possess self-aggregating properties and thus promote nucleation of mRNPs. Some of the better characterized nucleating factors include Ras-GAP SH3 domain-binding protein (G3BP), T-cell-restricted intracellular antigen 1 (TIA-1) and the TIA-1-related protein (TIAR) (Kedersha et al., 1999; Gilks et al., 2004; Matsuki et al., 2013). The next step involves post-translational modifications (e.g., acetylation, methylation, phosphorylation/dephosphorylation, ubiquitination, etc) of SG proteins (Tourrière et al., 2003; Dolzhanskaya et al., 2006; Kwon et al., 2007; Tsai et al., 2008) leading to further condensation of mRNPs whereas the last step involves the transport of mRNPs on microtubules (Ivanov et al., 2003; Loschi et al., 2009). The last step facilitates the growth of these RNA granules. Other host factors have also been shown to be recruited to SGs but exactly how they aid in granule condensation is not clear.

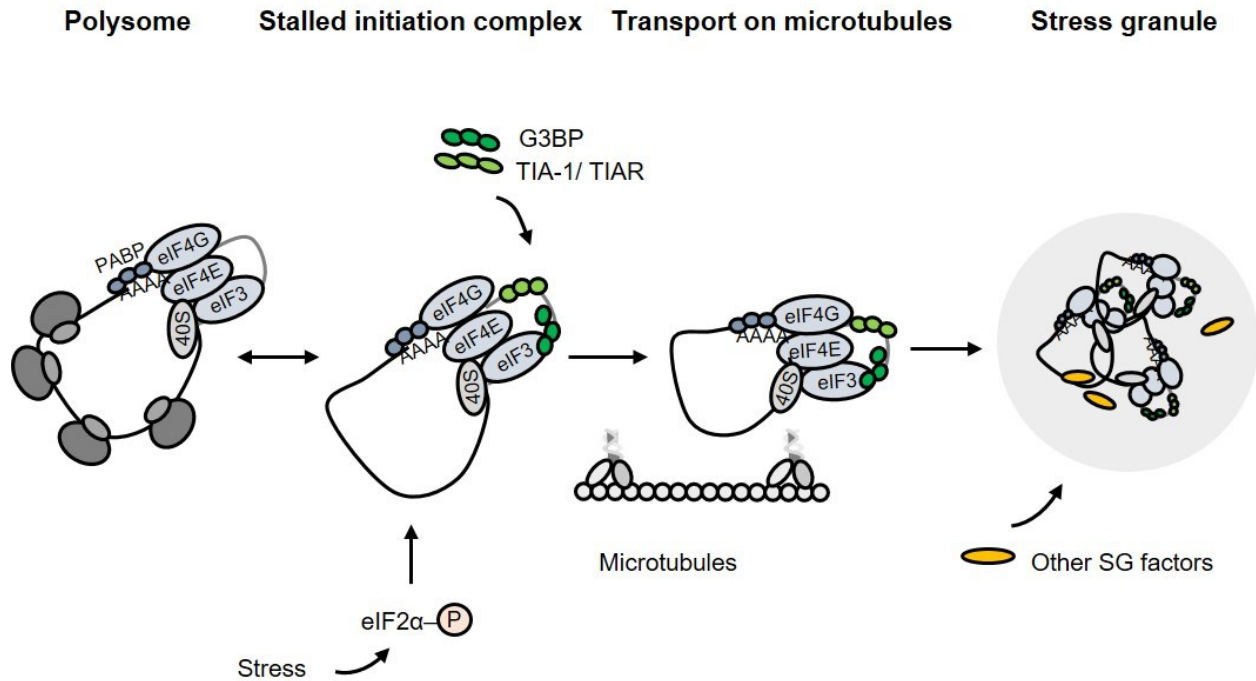


Figure 1.9 The stress granule (SG) assembly pathway. SG formation can be induced through translational arrest. For example, repression of translation initiation can be triggered by phosphorylation of the eukaryotic translation initiation factor 2 α (eIF2 α) under stress conditions. The phosphorylated eIF2 α reduces the GTP-exchange activity of eIF2B, leading to a decline in ternary complex formation and therefore decreased translation initiation. The stalled translation initiation complexes can be bound by key RNA-binding proteins such as the Ras-GAP SH3 domain-binding protein (G3BP), T-cell-restricted intracellular antigen 1 (TIA-1) and the TIA-1-related protein (TIAR), which promote the nucleation of these ribonucleoproteins. Further condensation of the ribonucleoprotein complexes is mediated by post-translational modification of SG proteins (process not shown). These complexes are then transported on the microtubule network to the growing granules, leading to formation of larger SGs.

The composition of SGs can vary considerably depending on the type of stress and intracellular environment (reviewed in (Onomoto et al., 2014)). Canonical SGs are defined by the presence of key translation initiation factors (e.g., eIF4E, eIF4G, eIF3), mRNA transcripts and the 40S small ribosomal subunit (Kedersha et al., 2002). Additional markers include other proteins with RNA-binding ability and/or self-aggregative capacity (e.g., G3BP, TIA-1, TIAR, Caprin-1) (Kedersha et al., 1999; Solomon et al., 2007; Matsuki et al., 2013). However, other factors are only found in a specific type of SG. For example, Hsp27 (heat shock protein 27) is found only in SGs that form as a result of stress from heat shock (N. L. Kedersha et al., 1999), while Sam68 (Src-associated protein in mitosis of 68 kDa) is present in SGs following infection with poliovirus but absent in those triggered by heat-shock stress (Piotrowska et al., 2010).

Due to the lack of a compartmentalizing membrane and their dynamic nature, biochemical isolation of SGs has been technically challenging. However, recent studies on the interactions between SGs and viruses have revealed novel SG-associated factors and their modes of action, thus advancing our knowledge of SG functions.

1.2.3.3 Modulation of the stress response by flaviviruses

Activation of stress response pathways can have antiviral or proviral effects. Infection-induced translation shut-off and SG formation can restrict viral translation and potentially lead to cell death. On the other hand, upregulation of stress-coping proteins (such as ER chaperons) can alleviate ER stress and therefore benefit viral protein translation. Not surprisingly, to establish productive infections, flaviviruses deploy diverse strategies to tailor this host response in favor of viral replication (Table 1.2).

A key observation that supports the antiviral effect of the stress response is that some flaviviruses suppress specific signaling steps in the stress response pathways. For instance, a study of WNV infection in rodent cells showed that the virus avoids activation of PKR and thus downstream eIF2 α phosphorylation possibly by “hiding” viral dsRNA in the membranous replication compartments (Elbahesh et al., 2011). Similarly, DENV, WNV and ZIKV all repress eIF2 α phosphorylation in a human hepatocyte cell line through an as yet undefined mechanism (Roth et al., 2017). Since eIF2 α inactivation can lead to translation arrest, it is tempting to speculate that flaviviruses interfere with this early signaling event to inhibit cellular translation shut-off.

The NS2B-3 and NS4A/NS4B proteins of DENV and WNV are implicated in IRE1- and ATF6-mediated UPR-signaling respectively, although the impact of infection on phospho-PEKR and phospho-eIF2 α is negligible (Ambrose and Mackenzie, 2011; Umareddy et al., 2007). Moreover, knockdown of XBP1, the effector downstream of IRE1, exacerbates the cytotoxic effect during DENV and JEV infection (Yu et al., 2006), suggesting that UPR signaling promotes cell survival and benefits viral replication. While some of these findings do not specify whether translation repression occurred or not, a recent report by Roth, et al. indicates that flavivirus infections generally lead to translation attenuation (Roth et al., 2017). Current evidence seems to indicate that these viruses selectively activate a subset of stress response pathways in order to create an optimal intracellular milieu to the advantage of the virus.

While a number of RNA viruses induce SG formation (Lindquist et al., 2010; Garaigorta et al., 2012), this does not generally occur in cells infected with flaviviruses. In fact, a common strategy deployed by these pathogens to block SG formation is by sequestration of SG-associated proteins by viral components. For example, the capsid protein of JEV interacts with Caprin-1 (Kato et al., 2013), a conserved cytoplasmic protein that facilitates SG formation (Solomon et al.,

2007). As well as preventing SG formation, capsid redirects Caprin-1 for viral genome synthesis. Similarly, DENV and WNV hijack TIA-1 and TIAR for genome replication and thus inhibit SG formation using viral RNA (Emara and Brinton, 2007). Other SG factors such as USP10, G3BP1 and Caprin-1 were also found to associate with the UTR regions of DENV genome and with viral replication complexes, suggesting a role of these host proteins in viral genome production.

SGs appear to have a proviral effect on HCV, a member of the *Flaviviridae*. Specifically, HCV infection induces SG or SG-like foci, which contains the viral core protein and several SG assembly factors including G3BP1, TIA-1, TIAR, PABP, and USP10, in an oscillating fashion (Garaigorta et al., 2012; Ruggieri et al., 2012). Further analyses suggest that these cellular factors positively regulate replication at different stages of the viral life cycle (Ariumi et al., 2011; Garaigorta et al., 2012). Nonetheless, SG formation is generally viewed as an antiviral strategy against flaviviruses, which have evolved successful means to circumvent this cellular stress response.

Table 1.2 Modulation of the stress response pathways by flaviviruses

Virus	Viral determinant	Cellular pathway/target	Mode of action	Reference
<i>Modulation of stress response induction</i>				
DENV	NS2B-3	IRE1- and ATF6-mediated UPR	Induces UPR	(Umareddy et al., 2007)
DENV, WNV, ZIKV	unknown	eIF2 α	Suppresses phosphorylation of eIF2 α	(Roth et al., 2017)

Table 1.2 (continued)

WNV	unknown	PKR	Prevents PKR phosphorylation activation	(Elbahesh et al., 2011)
WNV	NS4A/4B	IRE1- and ATF6-mediated UPR	Induces UPR	(Ambrose and Mackenzie, 2011)

Interference with SG formation

JEV	capsid	Caprin-1	Hijacks Caprin-1 for viral replication	(Kato et al., 2013)
TBEV	viral RNA	TIA-1	TIA-1 modulates viral translation independent of the formation of G3BP1/eIF3/eIF4B-positive granules	(Albornoz et al., 2014)
DENV, WNV	viral RNA	TIA-1/TIAR	Hijacks TIA-1/TIAR for genome replication	(Emara and Brinton, 2007)
WNV	unknown	PRK?	Suppresses early RNA replication and thus prevents PKR-induced SG formation	(Courtney et al., 2012)
ZIKV	Capsid, NS3, NS2B-3, NS4A		Inhibits SG formation possibly by capsid-mediated sequestration of G3BP1 and Caprin-1	(Hou et al., 2017)

1.3 Objectives of thesis

Flaviviruses are relatively slow-replicating RNA viruses, and to ensure their efficient production and spread, they must encode multifunctional proteins to evade host defense mechanisms. As such, elucidating how flavivirus infections modulate cellular pathways could reveal novel targets for antiviral therapies. In this thesis, I focused on the molecular mechanisms

by which DENV, WNV and ZIKV interfere with three important antiviral programs: the IFN response, the peroxisome-mediated antiviral response and the cellular stress response.

As detailed in Chapter 3, we report that DENV and WNV interfere with the biogenesis of peroxisomes, a subcellular organelle that is crucial for host cell metabolism and early antiviral signaling. This novel countermeasure is mediated by the capsid protein, which sequesters the essential peroxisome biogenesis factor PEX19 and may facilitate its degradation during viral infection. Importantly, this process strongly correlates with virus-induced suppression of Type-III IFN expression, an integral antiviral pathway partially mediated through PEX19 and peroxisomes.

In Chapter 4, we report that, like other flaviviruses, ZIKV subverts the IFN system through multiple mechanisms. Specifically, ZIKV was found to inhibit the induction of Type-I IFNs as well as suppress downstream IFN-signaling using the viral proteins NS1, NS4A and NS5. Moreover, the viral polymerase NS5 was shown to target the essential IFN-signaling molecule STAT2 for proteasomal degradation, a process that occurs in a species-specific manner.

Finally, in Chapter 5 we report how ZIKV manipulates the cellular stress response pathways, an integral host antiviral system. Our findings indicate that ZIKV activates the UPR as well as triggers translation arrest, a process that is uncoupled from SG formation. Further analyses revealed roles for capsid, NS3 and NS4A in suppressing SG assembly, possibly by re-directing the SG nucleating factors G3BP1 and Caprin-1 for viral replication. Altogether, by addressing the three aims of my doctoral thesis, we have provided novel insights into host-virus interactions during flavivirus infections, which in turn, may reveal opportunities for antiviral developments.

Chapter 2 Materials and Methods

2.1 Materials

2.1.1 Reagents

The following reagents were purchased from the indicated suppliers and utilized according to the manufacturers' recommendations unless otherwise stated.

Table 2.1 Commercial sources of materials, chemicals, and reagents

Reagent	Source
1-Bromo 3-chloropropane	Sigma-Aldrich
4', 6-diamidino-2-phenylindole (DAPI)	Sigma-Aldrich
7.5% BSA solution in DPBS	Sigma Adrich
Acetone (Certified ACS)	Thermo Fisher Scientific
Acid washed glass beads (425-600 micron)	Sigma-Aldrich
Acrylamide/Bis-acrylamide solution 40% (29:1)	Bio-Rad
Adenine hemisulfate salt	Sigma-Aldrich
Agar	Difco
Agarose ultrapure electrophoresis grade	Invitrogen
Ammonium acetate	Invitrogen
Ammonium chloride	Sigma-Aldrich
Ammonium persulphate (APS)	Sigma-Aldrich
Ammonium sulfate	Thermo Fisher Scientific
Ampicillin	Sigma-Aldrich
Bacto-tryptone	Difco
Bacto-yeast extract	Difco
Bafilomycin A	Sigma-Aldrich
Bovine serum albumin (BSA)	Sigma-Aldrich
Bromophenol blue	Sigma-Aldrich
Chloroform	Thermo Fisher Scientific

Table 2.1 (continued)

Reagent	Source
Coelenterazine	Gold Biotechnology USA
Complete TM EDTA-free protease inhibitors	Roche
Crystal violet	Sigma-Aldrich
Dimethyl sulphoxide (DMSO)	Sigma-Aldrich
Dithiothreitol (DTT)	Sigma-Aldrich
D-luciferin	Gold Biotechnology USA
Dulbecco's modified Eagle's medium (DMEM)	Invitrogen
Ethanol	Commercial Alcohols
Ethidium bromide solution	Sigma-Aldrich
Ethylenediaminetetraacetic acid (EDTA)	EMD Chemicals
Expoxomicin	Sigma-Aldrich
Fetal bovine serum (FBS)	Invitrogen
Formaldehyde 40% (v/v)	Sigma-Aldrich
Glacial acetic acid	Thermo Fisher
Glucose	Thermo Fisher Scientific
Glutathione sepharose 4 fast flow	GE Healthcare
Glycerol	Thermo Fisher Scientific
Glycine	EM Science
Glycylglycine	Sigma Aldrich
Guanidine hydrochloride	Thermo Fisher Scientific
Hydrochloric acid	Thermo Fisher Scientific
Isopropanol	Commercial Alcohols
Isopropanol molecular biology grade	Sigma-Aldrich
Kanamycin	Sigma-Aldrich
Latrunculin B	Sigma-Aldrich
Luria broth base	Invitrogen

Table 2.1 (continued)

Reagent	Source
LB agar	Invitrogen
Leptomycin B	Sigma-Aldrich
L-Glutamine	Invitrogen
L-Histidine	Sigma-Aldrich
L-Leucine	Sigma-Aldrich
Magnesium chloride (MgCl ₂)	EMD Chemicals
Magnesium phosphate (MgSO ₄)	BDH Inc.
Methanol	Thermo Fisher Scientific
Methylcellulose	Sigma-Aldrich
MG132	Sigma-Aldrich
Minimal essential media (MEM)	Sigma-Aldrich
N, N, N', N'-tetramethylenediamine (TEMED)	Sigma-Aldrich
Nocodazole	Sigma-Aldrich
Non-essential amino acids (NEAA)	Gibco
Nonidet P-40 (NP-40)/IGEPAL	Sigma-Aldrich
Nuclease-free water	Thermo Fisher
OptiMEM	Invitrogen
Paraformaldehyde EM-grade (16%)	Electron microscopy sciences
Penicillin-streptomycin solution (100X)	Invitrogen
Polyinosinic-polycytidylic acid (poly(I:C))	Sigma Aldrich
Poly-L-lysine	Sigma-Aldrich
Halt phosphatase inhibitor cocktail (100x)	Thermofisher
Potassium acetate	Anachemia
Potassium chloride (KCl)	Becton Dickinson & Company
Potassium phosphate (K ₂ PO ₄)	BDH Inc.
ProLong Gold Antifade reagent without DAPI	Life Technologies

Table 2.1 (continued)

Reagent	Source
Protein A-sepharose	GE Healthcare
Protein G-sepharose	GE Healthcare
Puromycin	Sigma-Aldrich
Random oligonucleotide primers	Invitrogen
Restore™ Western Blot Stripping Buffer	Pierce
RNaseOUT	Invitrogen
SlowFade® mounting reagent without DAPI	Invitrogen
Sodium arsenite	Sigma Aldrich
Sodium azide	Sigma-Aldrich
Sodium chloride (NaCl)	Sigma-Aldrich
Sodium dodecyl sulphate (SDS)	Bio-Rad
Sodium fluoride (NaF)	Sigma Aldrich
Sodium hydroxide	Sigma-Aldrich
Sucrose	EMD Chemicals
Thapsigargin	Sigma Aldrich
TPCK trypsin	Sigma Aldrich
Tris base	VWR
Triton X-100	Invitrogen
Trypsin-EDTA (0.25%)	Invitrogen
Tween 20 (polyoxyethylenesorbitan monolaureate)	Thermo Fisher Scientific
UltraPure distilled water	Invitrogen
β-Mercaptoethanol	Thermo Fisher Scientific

Table 2.2 Molecular markers

Marker	Source
GeneRuler 1 kb DNA Ladder	Fermentas
PageRuler Pre-stained Protein Ladder (10-170 kDa)	Fermentas

Table 2.3 DNA/RNA modifying enzymes

Enzyme	Source
Benzonase	Millipore
Calf intestinal alkaline phosphatase	Antarctica/ Invitrogen
DNase I amplification grade	Invitrogen
Restriction endonucleases	New England BioLabs/ Invitrogen
RNase A	Invitrogen
T4 DNA ligase	Invitrogen

Table 2.4 Multi-component systems

System	Source
CellTiter-Glo [®] Luminescent Cell Viability Assay	Promega
Improm-II Reverse Transcriptase system	Promega
Lipofectamine 2000 Transfection reagent	Invitrogen
Lipofectamine RNAiMAX Transfection reagent	Invitrogen
NucleoBond [®] Xtra Maxi	Macherey-Nagel
NucleoBond [®] Xtra Mini	Macherey-Nagel
NucleoSpin [®] RNA isolation kit	Macherey-Nagel
PerfeCTa SYBR Green SuperMix Low Rox	Quanta Biosciences
Pierce BCA Protein Assay kit	Thermo Scientific
Platinum High Fidelity Taq PCR System	Invitrogen
QIAEX II gel extraction kit	QIAGEN

Table 2.4 (continued)

System	Source
QIAGEN plasmid maxi kit	QIAGEN
QIAprep spin miniprep kit	QIAGEN
QIAquick PCR Purification kit	QIAGEN
RNeasy mini kit	QIAGEN
SuperScript II Reverse Transcriptase system	Invitrogen
TransIT-LT1 Transfection reagent	Invitrogen

2.1.2 Commonly used buffers and solutions

Table 2.5 Buffers and solutions

Name	Ingredients
Alkaline lysis buffer	200 mM NaOH, 1% (w/v) SDS
Bacteria resuspension buffer	50 mM Tris-HCl (pH 8.0), 10 mM EDTA, 100 µg/mL RNase A
IP buffer (<i>for detecting G3BP1/Caprin-1-ZIKV capsid interaction</i>)	150 mM NaCl, 2 mM EDTA, 1% NP-40, 50 mM Tris-HCl (pH 7.2), 1mM fresh DTT and 1x protease inhibitor cocktail
IP buffer (<i>for detecting STAT2-ZIKV NS5 interaction</i>)	137 mM NaCl, 50 mM Tris pH 7.5, 1% (v/v) NP-40, 1 mM NaF, 1 mM DTT
Cracking buffer	8 M Urea 5% (w/v) SDS, 40 mM Tris-HCl (pH 6.8), 0.1 mM EDTA, 0.4 mg/ml bromophenol blue
HEPES-buffered saline (HEBS)	137 mM NaCl, 5 mM KCl, 6 mM dextrose, 0.7 mM Na ₂ HPO ₄ , 20 mM Hepes pH 7.0
LB growth media	1% (w/v) Bacto-tryptone, 0.5% (w/v) Bacto-yeast extract, 0.5% (w/v) NaCl, 0.1% (v/v) 1 M NaOH
Luciferase lysis buffer	0.1% (v/v) Triton-X-100, 25 mM glycylglycine (pH 7.8), 15 mM MgSO ₄ ; 4 mM EGTA and 1 mM fresh DTT
Luciferase assay buffer	25 mM glycylglycine (pH 7.8), 15 mM K ₂ PO ₄ , (pH 7.8), 15 mM MgSO ₄ , 4 mM EGTA, 1 mM fresh DTT and 2 mM fresh ATP
Neutralization buffer	3.0 M Potassium acetate (pH 5.5)

Table 2.5 (continued)

Name	Ingredients
NP-40 lysis buffer	50 mM Tris-HCl (pH 7.2), 150 mM NaCl, 2 mM EDTA, 1% (v/v) NP-40, 1 mM fresh DTT
PBS-T	137 mM NaCl, 2.7 mM KCl, 8 mM Na ₂ HPO ₄ (pH 7.4), 0.05% (v/v) Tween-20
Phosphate buffered saline (PBS)	137 mM NaCl, 2.7 mM KCl, 8 mM Na ₂ HPO ₄ (pH 7.4)
Protein loading buffer (1X)	50 mM Tris-HCl pH 6.8, 2% (w/v) SDS, 10% (v/v) glycerol, 5 mM EDTA, 0.02 % (w/v) bromophenol blue
RIPA buffer	50 mM Tris-HCl (pH 7.5), 150 mM NaCl, 0.1% (w/v) SDS, 1% (v/v) Triton X-100 1% (w/v) sodium deoxycholate, 5 mM EDTA
RNA-IP buffer	137 mM NaCl, 50 mM Tris (pH 7.5), 1% (v/v) NP40, 1mM NaF, 1 mM DTT
SDS-PAGE resolving gel buffer	0.1% SDS, 374 mM Tris-HCl (pH 8.8)
SDS-PAGE running buffer	250 mM glycine, 0.1% SDS, 100 mM Tris Base (pH 8.3)
SDS-PAGE stacking gel buffer	0.1% SDS, 250 mM Tris-HCl (pH 6.8)
TAE	40 mM Tris acetate, 1 mM EDTA (pH 8.0)
TBS-T	137 mM NaCl, 2.7 mM KCl, 24 mM Tris-HCl (pH 7.4), 0.05% (v/v) Tween-20
TE	1 mM EDTA, 10 mM Tris-HCl pH 7.5
Transfer buffer	200 mM glycine, 25 mM Tris base (pH 8.3), 20% (v/v) methanol, 0.1% (w/v) SDS
Tris-buffered saline (TBS)	137 mM NaCl, 2.7 mM KCl, 24 mM Tris-HCl (pH 7.4)

2.1.3 Oligonucleotides

Table 2.6 Primers

Primer name	Sequence (5'-3')	Engineered sites*	Usage
CMV3F-WNV C Forward	<u>GAATTC</u> ATGTCTAAGAAACCAGGAGGGC	EcoRI	Cloning
CMV3F-DENV C Forward	<u>GAATTC</u> ATGAATGACCAACGGAAAAAG	EcoRI	Cloning
PEX11- β -myc forward	TAGC <u>ACTAGT</u> ATG GGGAAACTG	SalI	Cloning
PEX11- β -myc reverse	GTACG <u>TCGACTT</u> ACAGATCCTCTTCTGAG ATGAGTTTTTGTTCGGGCTTGAGTCG	SpeI	Cloning
Myc-DENV C forward	ATTAGCGCTAGCATGGAACAAAAACTCAT CTCAGAAGAGGATCTGAATGACCAACGG AAAAAGGC	NheI	Cloning
Myc-DENV C reverse	GTACG <u>GATCCTT</u> ATCTGCGTCTCCTATTCA AGA	BamHI	Cloning
Myc-JEV C forward	ATTAGCGCTAGCATGGAACAAAAACTCAT CTCAGAAGAGGATCTGACTAAAAAACCA GGAGGGC	NheI	Cloning
Myc-JEV C reverse	GTACG <u>GATCCTT</u> ATCTTTTGTTCCTTTC TGCC	BamHI	Cloning
Myc-MVEV C forward	ATTAGCGCTAGCATGGAACAAAAACTCAT CTCAGAAGAGGATCTGTCTAAAAAACCA GGAGGAC	NheI	Cloning
Myc-MVEV C reverse	GTACG <u>GATCCTT</u> ATCTTTTCTTTTGTTCCTTTC GCC	BamHI	Cloning
Myc-WNV C forward	ATTAGCGCTAGCATGGAACAAAAACTCAT CTCAGAAGAGGATCTGTCTAAGAAACCA GGAGGGCC	NheI	Cloning
Myc-WNV C reverse	GATC <u>GATCCTT</u> ATCTTTTCTTTTGTTCCTTTC AGC	BamHI	Cloning

Table 2.6 (continued)

Primer name	Sequence (5'→3')	Engineer site*	Usage
Myc-YFV C forward	ATTAG <u>CGCTAG</u> CATGGAACAAAAACTCAT CTCAGAAGAGGATCTGTCTGGTCGTAAAG CTCAGGG	NheI	Cloning
Myc-YFV C reverse	GTAC <u>GGATCCT</u> TATTAACGGCGTTTCCTT GAG	BamHI	Cloning
Triple-Flag epitope reverse	GGCGGGAGCGGCGGGGACTACAAAGACC ATGACGGTGATTATAAAGATCATGACATC GACTACAAGGATGACGATGACAAGTAGG GCGCGCC <u>CTCGAG</u> ATATAT	XhoI	Cloning
ZIKV Capsid Forward	ATATAT <u>GCTAGC</u> GTTTAAACGCCACCATG AAAAACCCAAAAAAGAAATCC	NheI	Cloning
ZIKV Capsid Reverse	ATATAT <u>CTCGAG</u> GGCGCGCCTCATTTGTC ATCGTCATCCTTGTAGTCCCCGCCGCTCCC GCCTCGTCTCTTCTTCCTTCCTAGC	XhoI	Cloning
ZIKV Envelope Forward	ATATAT <u>GCTAGC</u> GTTTAAACGCCACCATG GGAAGCTCAACGAGCCAAAAAGTC	NheI	Cloning
ZIKV Envelope Reverse	ATATAT <u>CTCGAG</u> GGCGCGCCTCATTTGTC ATCGTCATCCTTGTAGTCCCCGCCGCTCCC GCCAGCAGAGACAGCTGTGGATAAGAA	XhoI	Cloning
ZIKV NS2A Forward	ATATAT <u>GCTAGC</u> GTTTAAACGCCACCATG GGAAGCTCAACGAGCCAAAAAGTCATAT ACTTGGTCATGATACTGCTGATTGCCCCG GCATACAGCATCAGGTGC	NheI	Cloning
ZIKV NS2A Reverse	ATATAT <u>CTCGAG</u> GGCGCGCCTCATTTGTC ATCGTCATCCTTGTAGTCCCCGCCGCTCCC GCCCGCTTCCCACTCCTTGTGAGCAA	XhoI	Cloning
ZIKV NS2B Forward	ATATAT <u>GCTAGC</u> GTTTAAACGCCACCATG AGCTGGCCCCCTAGCGAAGTACTC	NheI	Cloning
ZIKV NS2B Reverse	ATATAT <u>CTCGAG</u> GGCGCGCCTCATTTGTC ATCGTCATCCTTGTAGTCCCCGCCGCTCCC GCCCTTTTTCCAGTCTTCACGTATAC	XhoI	Cloning

Table 2.6 (continued)

Primer name	Sequence (5'→3')	Engineer site*	Usage
ZIKV NS2B-3 Forward	ATATAT <u>GCTAGC</u> GTTTAAACGCCACCATG AGCTGGCCCCCTAGCGAAGTACTC	NheI	Cloning
ZIKV NS2B-3 Reverse	ATATAT <u>CTCGAG</u> GGGCGCGCCTCATTTGTC ATCGTCATCCTTGTAGTCCCCGCCGCTCCC GCCTCTTTTCCCAGCGGCAAACCTCCTT	XhoI	Cloning
ZIKV NS3 Forward	ATATAT <u>GCTAGC</u> GTTTAAACGCCACCATG AGTGGTGCTCTATGGGATGTGCCT	NheI	Cloning
ZIKV NS3 Reverse	ATATAT <u>CTCGAG</u> GGGCGCGCCTCATTTGTC ATCGTCATCCTTGTAGTCCCCGCCGCTCCC GCCTCTTTTCCCAGCGGCAAACCTCCTT	XhoI	Cloning
ZIKV NS3 triple-FLAG forward	ATGCCACCTTCACTTCACGTCTAC		Cloning
ZIKV NS4A Forward	ATATAT <u>GCTAGC</u> GTTTAAACGCCACCATG GGAGCGGCTTTTGGAGTGATGGAA	NheI	Cloning
ZIKV NS4A Reverse	ATATAT <u>CTCGAG</u> GGGCGCGCCTCATTTGTC ATCGTCATCCTTGTAGTCCCCGCCGCTCCC GCCTCTTTGCTTTTCTGGCTCAGGTAT	XhoI	Cloning
ZIKV NS4A-B Forward	ATATAT <u>GCTAGC</u> GTTTAAACGCCACCATG GGAGCGGCTTTTGGAGTGATGGAA	NheI	Cloning
ZIKV NS4A-B Reverse	ATATAT <u>CTCGAG</u> GGGCGCGCCTCATTTGTC ATCGTCATCCTTGTAGTCCCCGCCGCTCCC GCCTCTTTGACCAAGCCAGCGTTTCT	XhoI	Cloning
ZIKV NS4B Forward	ATATAT <u>GCTAGC</u> GTTTAAACGCCACCATG TCTCCCCAGGACAACCAAATGGCA	NheI	Cloning
ZIKV NS4B Reverse	ATATAT <u>CTCGAG</u> GGGCGCGCCTCATTTGTC ATCGTCATCCTTGTAGTCCCCGCCGCTCCC GCCTCTTTGACCAAGCCAGCGTTTCT	XhoI	Cloning
ZIKV NS5 Forward	ATATAT <u>GCTAGC</u> GTTTAAACGCCACCATG CGTGGGGGTGGAACAGGAGAGACC	NheI	Cloning
ZIKV NS5 MTase Forward	ATATAT <u>GCTAGC</u> GTTTAAACGCCACCATG CGTGGGGGTGGAACAGGAGAGACC	NheI	Cloning

Table 2.6 (continued)

Primer name	Sequence (5'→3')	Engineer site*	Usage
ZIKV NS5 MTase Reverse	ATATAT <u>CTCGAG</u> GGCGCGCCTCATTTGTC ATCGTCATCCTTGTAGTCCCCGCCGCTCCC GCCCTCGTCAAAGAACCACGTTTCCGC	XhoI	Cloning
ZIKV NS5 RdRP Forward	ATATAT <u>GCTAGC</u> GTTTAAACGCCACCATG AACCACCCATATAGGACATGGGCT A	NheI	Cloning
ZIKV NS5 RdRP Reverse	TATAT <u>CTCGAG</u> GGCGCGCCTCATTTGTCA TCGTCATCCTTGTAGTCCCCGCCGCTCCCCG CCCAGCACTCCAGGTGTAGACCCTTC	XhoI	Cloning
ZIKV NS5 Reverse	ATATAT <u>CTCGAG</u> GGCGCGCCTCATTTGTC ATCGTCATCCTTGTAGTCCCCGCCGCTCCC GCCCAGCACTCCAGGTGTAGACCCTTC	XhoI	Cloning
ZIKV NS5 S56A Flanking Forward	ATATAT <u>GCTAGC</u> GTTTAAACGCCACCATG CGTGGGGGTGGAACAGGAGAGACC	NheI	Cloning
ZIKV NS5 S56A Flanking Reverse	CCCATCATGTT <u>TGTACACACA</u> ACTCTGGCA C	BsrGI	Cloning
ZIKV NS5 S56A Fusion Forward	GGCCATGCTGTGGCCCGAGGAAGTGCAA AG		Cloning
ZIKV NS5 S56A Fusion Reverse	CTTTGCACTTCCTCGGGCCACAGCATGGC C		Cloning
ZIKV NS5 triple-FLAG forward	GAGGAGAGTGCCAGAGTTGTGTGT		Cloning
ZIKV NS5 Δ10 Forward	ATATAT <u>GCTAGC</u> GTTTAAACGCCACCATG AAATGGAAGGCCCGCTTGAACCAG	NheI	Cloning
ZIKV NS5 Δ10 Reverse	CCCATCATGTT <u>TGTACACACA</u> ACTCTGGCA C	BsrGI	Cloning
ZIKV prM Forward	ATATAT <u>GCTAGC</u> GTTTAAACGCCACCATG GGCGCAGATACTAGTGTCGGAATT	NheI	Cloning

Table 2.6 (continued)

Primer name	Sequence (5'→3')	Engineer site*	Usage
ZIKV prM Reverse	ATATATCTCGAGGGCGCGCCTCATTTGTC ATCGTCATCCTTGTAGTCCCCGCCGCTCCC GCCGCTGTATGCCGGGGCAATCAGCAG	XhoI	Cloning
IFIT1 Reverse	CTGAAACCGACCATAGTGGAAAT		qRT-PCR
IFIT1 Forward	AGAAGCAGGCAATCACAGAAAA		qRT-PCR
IFN-β Forward	TAGCACTGGCTGGAATGAGA		qRT-PCR
IFN-β Reverse	TCCTTGGCCTTCAGGTAATG		qRT-PCR
IFN-λ1 Forward	CGCCTTGGAAGAGTCACTCA		qRT-PCR
IFN-λ1 Reverse	GAAGCCTCAGGTCCCAATTC		qRT-PCR
IFN-λ2 Forward	AGTTCCGGGCCTGTATCCAG		qRT-PCR
IFN-λ2 Reverse	GAACCGGTACAGCCAATGGT		qRT-PCR
IFN-λ3 Forward	TAAGAGGGCCAAAGATGCCTT		qRT-PCR
IFN-λ3 Reverse	CTGGTCCAAGACATCCCCC		qRT-PCR
mGAPDH Forward	TGGCAAAGTGGAGATTGTTGCC		qRT-PCR
mGAPDH Reverse	AAGATGGTGATGGGCTTCCCCG		qRT-PCR
PEX16 Forward	GCCTCCTGAGTGACAGAAAG		qRT-PCR
PEX16 Reverse	GAAGCGGTCATAGAAAGGAGAG		qRT-PCR
PEX3 Forward	ACATGTTGGAAAGCCCAGAT		qRT-PCR
PEX3 Reverse	GTCCTGTTCAGTAGGTCGAAAG		qRT-PCR
Zika virus Forward	CCTTGGATTCTTGAACGAGGA		qRT-PCR
Zika virus Reverse	AGAGCTTCATTCTCCAGATCAA		qRT-PCR
β-actin Forward	CCTGGCACCCAGCACAAT		qRT-PCR

Table 2.6 (continued)

Primer name	Sequence (5'→3')	Engineer site*	Usage
β-actin Reverse	GCCGATCCACACGGAGTACT		qRT-PCR

* *Restriction sites are underlined*

Table 2.7 siRNA sequences

siRNA	Strand	Sequence (5'-3')	Source
siControl	Antisense	rArUrArCrGrCrGrUrArUrUrArUrArCrGrCrGrArUrUrArA rCrGrArC	IDT
	Sense	rCrGrUrUrArArUrCrGrCrGrUrArUrArArUrArCrGrCrGrU AT	IDT
siPEX19 #1	Antisense	rGrGrGrUrUrCrUrUrCrCrUrCrArGrCrCrArArCrUrCrCrUr UrCrArU	IDT
	Sense	rGrArArGrGrArGrUrUrGrGrCrUrGrArGrGrArArGrArAr CCC	IDT
siPEX19 #2	Antisense	rGrUrCrArGrCrUrCrUrUrCrUrUrCrCrGrArCrArUrGrCrU rGrGrArG	IDT
	Sense	rCrCrArGrCrArUrGrUrCrGrGrArArGrArArGrArGrCrUrG AC	IDT
simSTAT2 #1	Antisense	rArArArGrArUrGrUrCrUrGrArUrArArArCrCrUrUrCrArA rGrGrUrU	IDT
	Sense	rCrCrUrUrGrArArGrGrUrUrUrArUrCrArGrArCrArUrCrU TT	IDT
simSTAT2 #2	Antisense	rCrUrGrGrArUrUrCrGrArUrUrUrUrCrArArUrCrUrCrArA rGrCrUrG	IDT
	Sense	rGrCrUrUrGrArGrArUrUrGrArArArArUrCrGrArArUrCrC AG	IDT
siPEX3 #1	Antisense	rGrArCrUrGrCrUrUrCrArCrCrArGrGrArArArCrUrGrUrU rUrCrUrU	IDT
	Sense	rGrArArArCrArGrUrUrUrCrCrUrGrGrUrGrArArGrCrArG TC	IDT

Table 2.7 (continued)

siRNA	Strand	Sequence (5'-3')	Source
siPEX3 #2	Antisense	rCrUrGrGrArArArGrArCrUrArUrUrCrArUrArGrArGrUrU rArCrCrA	IDT
	Sense	rGrUrArArCrUrCrUrArUrGrArArUrArGrUrCrUrUrUrCrC AG	IDT
siPEX7	Antisense	rArUrCrArGrGrCrUrUrArArCrGrArGrUrCrArGTT	Bioneer
	Sense	rCrUrGrArCrUrCrGrUrUrArArGrCrCrUrGrArUTT	Bioneer
siPEX13	Antisense	rArUrCrArCrUrUrUrGrUrGrCrUrGrUrArCrUrCTT	Bioneer
	Sense	rGrArGrUrArCrArGrCrArCrArArArGrUrGrArUTT	Bioneer
siG3BP1	Antisense	rUrArGrUrCrArUrGrArCrUrCrUrCrArArArGrArArGrArA rArCrArA	IDT
	Sense	rGrUrUrUrCrUrUrCrUrUrUrGrArGrArGrUrCrArUrGrArC TA	IDT
siTIA-1#1	Antisense	rArCrArArCrArUrGrArCrCrUrUrCrArArUrGrGrUrArGrU rArCrCrA	IDT
	Sense	rGrUrArCrUrArCrCrArUrUrGrArArGrGrUrCrArUrGrUrU GT	IDT
siTIA-1 #2	Antisense	rUrUrGrGrArCrUrArGrArCrUrGrArUrUrUrArCrArArCrC rUrCrArU	IDT
	Sense	rGrArGrGrUrUrGrUrArArArUrCrArGrUrCrUrArGrUrCrC AA	IDT
siTIAR #1	Antisense	rUrArGrUrCrArUrArUrCrArGrGrArGrArUrUrCrUrUrUrA rCrCrCrC	IDT
	Sense	rGrGrUrArArArGrArArUrCrUrCrCrUrGrArUrArUrGrArC TA	IDT
siTIAR #2	Antisense	rArArCrArUrUrCrCrUrCrArArArGrArUrArCrUrArUrArA rArCrArA	IDT
	Sense	rGrUrUrUrArUrArGrUrArUrCrUrUrUrGrArGrGrArArUr GTT	IDT

Table 2.7 (continued)

siRNA	Strand	Sequence (5'-3')	Source
siControl	siRNA pool	(Catalog number: D-001810-10-05)	Dharmacon
siCAPRIN-1	siRNA pool	(Catalog number: L-012099-00-0005)	Dharmacon
siG3BP1	siRNA pool	(Catalog number: M-016057-01-0005)	Dharmacon

2.1.4 Antibodies

Table 2.8 Primary antibodies

Antibody	Catalog number	Dilution	Application*	Source
Goat anti-GFP	ab5450	1: 2000	WB	Abcam
Goat anti-TIA-1	sc-1751	1: 500, 1: 250	WB, IF	Santa-Cruz Biotechnology
Goat anti-TIAR	sc-1749	1: 500, 1:250	WB, IF	Santa-Cruz Biotechnology
Goat anti-ZIKV NS5		1:500, 1:1000	IF, WB	ProSci Inc.
Guinea pig anti-DENV2 capsid	GP2455/2456	1:1000, 1:1000	WB, IF	Pocono Rabbit Farm & Laboratory
Guinea pig anti-WNV capsid	2356	1:1000, 1:1000	WB, IF	Pocono Rabbit Farm & Laboratory
Human anti-DENV2		1:2500	IF	Dr. Robert Anderson, Dalhousie University
Mouse anti-dsRNA J2	10010200	1:1000	IF	Scicons, Hungary
Mouse anti-FLAG epitope (M2)	F3165	1:2000, 1:1000, 1:20		Sigma Aldrich
Mouse anti-Hsp60	611563	1:1000	IF	BD Sciences

Table 2.8 (continued)

Antibody	Catalog number	Dilution	Application*	Source
Mouse anti-myc (4A6)	05-724	1:1000, 1:1000	IF/WB	Millipore
Mouse anti-myc (9E10)	CRL-17 29	1: 20	IP	ATCC
Mouse anti-pan-flavivirus Envelope (E) protein (4G2)	MAB10 216	1: 1000, 1: 1000	WB, IF	Millipore
Mouse anti-PMP70	SAB420 0181	1:1000, 1:1000	WB, IF	Sigma Aldrich
Mouse anti-WNV NS3/2B	MAB29 071	1:1000	IF	R&D systems
Mouse anti- β -actin	a3853	1:2000	WB	Sigma Adrich
Mouse anti-ZIKV E protein	BF- 1176-56	1:5000	WB	Biofront Technologies
Rabbit anti-Caprin-1	SAB110 1135	1:500	WB	Sigma Aldrich
Rabbit anti-Catalase	ab1877	1:1000	WB	Abcam
Rabbit anti-eIF2 α	9722S	1: 500	WB	Cell Signaling
Rabbit anti-G3BP1	07-1801	1: 2000, 1: 1000, 1: 30	WB, IF, IP	Millipore
Rabbit anti-G3BP1 (phospho- S149)	G8046	1:500	WB	Sigma Aldrich
Rabbit anti-GAPDH	ab9485	1:2000	WB	Abcam
Rabbit anti-IRF3 (D6I4C)	11904	1:1000, 1:250	WB, IF	Cell Signaling
Rabbit anti-Phospho IRF3 (Ser 396)	4947	1:500	WB	Cell Signaling
Rabbit anti-human STAT2	sc-476	1: 500, 1:250	WB, IF	Santa-Cruz Biotechnology
Rabbit anti-mouse STAT2	sc-950	1:250	IF	Santa-Cruz Biotechnology
Rabbit anti-LC3B	ab51520	1:500	WB	Abcam
Rabbit anti-PEX11 β	ab74507	1: 500	WB	Abcam

Table 2.8 (continued)

Antibody	Catalog number	Dilution	Application*	Source
Rabbit anti-PEX13	ab19021 3	1: 500	WB	Abcam
Rabbit anti-PEX14	nbp1- 71841	1: 500	WB, IF	Millipore
Rabbit anti-PEX19	ab13707 2	1:1000, 1:5000 1:20	WB, IF, IP	Epitomic and Abcam
Rabbit anti-PEX2	ab11000 4	1: 500	WB	Abcam
Rabbit anti-PEX5	ab94533	1: 500	WB	Abcam
Rabbit anti-PEX7	ab13375 4	1: 500	WB	Abcam
Rabbit anti-phospho-PKR (T451)	ab81303	1: 500	WB	Abcam
Rabbit anti-phospho-eIF2 α (S51)	9721S	1: 500	WB	Cell Signaling
Rabbit anti-PKR	ab32506	1: 1000	WB	Abcam
Rabbit anti-SKL		1:1000	IF	Dr. Rachubinski, University of Alberta
Rabbit anti-STAT1	SC-346	1:500, 1: 250	WB, IF	Santa-Cruz Biotechnology
Rabbit anti-TBK1	3504	1:500	WB	Cell Signaling
Rabbit anti-phospho-TBK1 (S172)	5483	1:500	WB	Cell Signaling

* *WB*: western blot; *IF*: immunofluorescence; *IP*: immunoprecipitation

Table 2.9 Secondary antibodies

Antibody::Conjugate	Catalog Number	Dilution	Application*	Source
Chicken anti-goat::Alexa488	A21467	1: 1000	IF	Invitrogen
Chicken anti-goat::Alexa647	A21469	1: 1000	IF	Invitrogen
Donkey anti-goat::Alexa680	A21084	1:10000	WB	Invitrogen
Donkey anti-mouse::Alexa488	A10038	1: 1000	IF	Invitrogen
Donkey anti-mouse::Alexa546	A21202	1: 1000	IF	Invitrogen
Donkey anti-mouse::Alexa568	A10036	1: 1000	IF	Invitrogen
Donkey anti-mouse::Alexa647	A21463	1: 1000	IF	Invitrogen
Donkey anti-mouse::Alexa680	A10038	1:10000	WB	Invitrogen
Donkey anti-rabbit::Alexa488	A21206	1: 1000	IF	Invitrogen
Donkey anti-rabbit::Alexa546	A10040	1: 1000	IF	Invitrogen
Donkey anti-rabbit::Alexa568	A10042	1: 1000	IF	Invitrogen
Donkey anti-rabbit::Alexa647	A31573	1: 1000	IF	Invitrogen
Donkey anti-rabbit::Alexa800	926-32213	1:10000	WB	Li-COR
Donkey anti-guinea pig::Alexa488	706-546-148	1: 1000	IF	Invitrogen
Goat anti-guinea pig::Alexa647	A21450	1: 1000	IF	Invitrogen
Donkey anti-guinea pig::AlexaIRDye800	926-32411	1:10000	WB	Li-COR

Table 2.9 (continued)

Antibody::Conjugate	Catalog Number	Dilution	Application*	Source
Donkey anti-mouse::HRP	713-035-150	1:4000	WB	Jackson ImmunoResearch Laboratories
Goat anti-rabbit::HRP	111-035-045	1:4000	WB	Jackson ImmunoResearch Laboratories

* *WB*: western blot; *IF*: immunofluorescence

2.1.5 Detection systems

Table 2.10 Detection systems

System	Source
T100 Thermal cycler	BIO-RAD
DeltaVision OMX V4 structured illumination microscope	Applied Precision, GE
Illuminator plate reader	BioTek
IX-81 spinning-disk confocal microscope	Olympus
LSRFortessa digital benchtop flow cytometer	BD Biosciences
Molecular Imager GelDoc™ XR+ imaging system	BIO-RAD
MX3005P	Stratagene
NanoDrop ND-1000 Spectrophotometer	Thermo Scientific
Odyssey Infrared Imaging System	LiCor
Rx film	Fuji
Ultraviolet Transilluminator	Thermo Fisher Scientific
XO-MAT Developer	Kodak

2.1.6 Cell lines and viruses

2.1.6.1 Cell lines

A549 (human alveolar basal epithelial), HEK293T (human embryonic kidney), Vero (Green monkey kidney) cells, MEFs (mouse embryonic fibroblasts), RK-13 (rabbit kidney) and C6/36 cells (*Aedes albopictus* mosquito cell line) were purchased from the American Type Culture Collection (Manassas, VA). Primary human fetal astrocytes (HFAs) were prepared as previously described from 15–19 week aborted fetuses (Vivithanaporn et al., 2016) with written consent approved under the protocol 1420 by the University of Alberta Human Research Ethics Board (Biomedical).

2.1.6.2 Viruses

WNV strain NY99 and DENV-2 (New Guinea strain) were provided by Dr. Mike Drebot (Public Health Agency of Canada, Winnipeg, MB). The Zika virus (strain PLCal_ZIKV) was kindly provided by Dr. David Safronetz at the Public Health Agency of Canada. The M33 strain of Rubella virus (RV) was obtained from Dr. S. Gillam (University of British Columbia, Vancouver, BC). WNV, DENV-2 and RV stocks were generated using Vero cells while ZIKV stock was generated using C6/36 cells. All virus stocks were titered by plaque assay (as described in Section 2.2.6.2). Influenza virus A (IAV; strain PR8) was obtained from Dr. Katherine Magor (University of Alberta).

2.2 Methods

2.2.1 Molecular biology

2.2.1.1 Isolation of plasmid DNA from Eschericia coli (E. coli)

E. coli cultures harboring specific plasmids were grown overnight at 37 °C on a shaker at 220 rpm. Small-scale and large-scale DNA isolations were performed using QIAprep spin mini prep or NucleoBond® Xtra Mini kit, and QIAGEN plasmid maxi or NucleoBond® Xtra Maxi kit (Table 2.4) respectively. The concentrations of plasmid DNAs were determined using a NanoDrop ND-1000 Spectrophotometer (Table 2.10). DNA samples were kept at 4 °C for short-term storage and at -20 °C for long-term storage.

2.2.1.2 Polymerase chain reaction (PCR)

To reduce incidence of polymerase-introduced mutations, cDNAs were amplified using Platinum High fidelity Taq (Table 2.4). Typically, reactions (50 µL) contained ~100 ng of DNA template, 1 mM MgSO₄, 200 nM of forward and reverse primers, 200 nM of each dNTP and 2.5-5 U of DNA polymerase. Annealing temperatures were set according to the melting temperatures of primers, while the extension times were based on the lengths of cDNAs. Reactions were performed for 30 to 35 cycles in a TC-312 thermocycler (Techne). When trouble-shooting failed PCR reactions, a gradient thermocycler, T100 Thermal cycler (Bio-Rad; Table 2.10) was used to obtain optimal annealing temperatures.

2.2.1.3 Restriction endonuclease digestion

For digestion of PCR products, reactions were usually performed in 50 µL volumes containing the majority of the purified PCR products together with 2-10 U of restriction enzymes

(Table 2.3). For digestion of plasmids, reactions were carried out in 20 μ L volumes containing 2 μ g of DNA and 2-10 U of enzymes in the appropriate digestion buffer. Where indicated, vector DNA was dephosphorylated using calf intestinal alkaline phosphatase (Table 2.3) according to manufacturer's recommendations. If digestion products were not processed immediately for gel purification, the restriction enzymes were inactivated at 70-85 $^{\circ}$ C followed by cooling on ice for 2 min. The digested DNAs were kept at -20 $^{\circ}$ C until use.

2.2.1.4 Agarose gel electrophoresis

Electrophoresis grade agarose (0.8%-2.5% [w/v]; Table 2.1) was dissolved in TAE buffer by heating (Table 2.5). To visualize DNA, ethidium bromide (Table 2.1) was added to the agarose solution at a final concentration of 0.5 μ g/mL. Following solidification at room temperature, the agarose gels were immersed in TAE, after which the DNA samples were mixed with 10x DNA gel loading dye (Table 2.1), loaded into the wells and separated by running at \sim 100 volts (V). DNA fragments were visualized using a Molecular Imager GelDoc XR+ imaging system (Table 2.10). For excision of DNA fragments, an Ultraviolet transilluminator (Table 2.10) was used to visualize the DNA fragments.

2.2.1.5 Purification of DNA fragments

When used for plasmid construction, PCR products were purified using a QIAquick PCR purification kit (Table 2.4) prior to restriction endonuclease digestion. Following digestion and separation by agarose gel electrophoresis, the DNA fragments were excised with a clean razor blade and subsequently extracted from the gel using a QIAEX gel extraction kit (Table 2.4). To maximize DNA concentration for subsequent ligation, 30 μ L of ddH₂O was used to elute the DNAs.

2.2.1.6 Ligation of DNA

To avoid degradation of the adhesive ends, DNA ligations were performed immediately following gel extraction. Inserts and vectors were combined in molar ratios ranging from 3:1-6:1, using no more than 150 ng of DNA in total with a minimum of 1–5 U of T4 DNA ligase (Table 2.3). A negative control containing only the vector but no insert was also used. Reactions were performed in a 20 µL volume overnight at 16 °C in a Thermocycler.

2.2.1.7 Transformation of *E. coli*.

SubCloning Efficiency chemically-competent DH5α *E. coli* (Invitrogen) and MAX Efficiency DH5α *E. coli* (Invitrogen) were used for plasmid DNA transformation. The bacterial cells were transformed by heat-shock at 42 °C for 45 sec and cooled on ice for 2 min. To avoid cytotoxicity, a maximum of 10% of the ligation mixture was added to cells, which were recovered at 37 °C in SOC media (Invitrogen) for a minimum of 30 min. Transformed cells were cultured in the appropriate antibiotics following the manufacturer's recommendations. Sixteen-hours later, individual colonies were selected and cultured for plasmid isolation the next day.

2.2.1.8 Construction of recombinant plasmids

Construction of recombinant plasmids was performed using PCR and standard subcloning techniques. All primers used for cloning are listed in Table 2.7. The authenticity of each plasmid construct was verified by DNA sequencing at The Applied Genomics Centre (University of Alberta).

DENV-2/WNV capsid expression plasmids: DENV-2 and WNV capsid inserts were amplified by PCR using cDNAs generated from total RNA extracted from infected A549 cells.

The PCR primer pairs are listed in Table 2.7. Prior to ligation, the inserts and vector (pCMV 3.1) were digested with EcoRI and BamHI.

FLAG-tagged ZIKV protein expression plasmids: To produce C-terminal FLAG-tagged ZIKV prM, NS2A, NS2B, NS3, NS2B-3, NS4A, NS4B, NS4A-B and NS5, a partial genomic clone of strain H/PF/2013 ZIKV (unpublished data) was used as the PCR template. The resultant PCR products were subcloned into a pCDNA-3.1(-) plasmid between the NheI and XhoI restriction sites. To produce FLAG-tagged ZIKV capsid and E, PCR templates were first generated through reverse-transcription of total RNAs isolated from A549 cells infected with ZIKV (strain PLCal_ZIKV) using the primers listed in Table 2.7. The cDNAs were then subcloned into the pCDNA-3.1(-) plasmid using the NheI and XhoI restriction sites. All of the reverse primers used in PCR reactions contained a FLAG-epitope (Table 2.7). The pCDNA-3.1(-) prM-E and NS1-FLAG constructs were synthesized by Thermofisher scientific based on the sequence from ZIKV (strain H/PF/2013). The prM-E construct contains the membrane anchor region from the ZIKV capsid protein. Similarly, the E-FLAG construct contains the carboxyl-terminal transmembrane region of prM, while NS1-FLAG contains the analogous region from the E protein. Lastly, the NS4B insert contains the 2K fragment from NS4A, which was shown to be required for ER membrane localization and subsequent proteolytic processing of NS4A-B (Lin et al., 1993; Miller et al., 2007).

FLAG-tagged ZIKV NS5 mutant expression constructs: To generate NS5 mutants, the pcDNA-3.1(-) plasmid encoding a wild-type FLAG-tagged ZIKV NS5 was used as the PCR template and the primer pairs used are listed in Table 2.7. Following PCR, the NS5 MTase-FLAG and the NS5 RdRP-FLAG inserts were cloned into the pcDNA-3.1(-) plasmid between the restriction sites NheI and XhoI. The NS5 deletion mutant $\Delta 10$ PCR insert was cloned back into

the plasmid containing a FLAG-tagged wildtype NS5 between the restriction sites NheI and BsrGI. The NS5 mutant S56A was generated by a two-step PCR procedure. First, two over-lapping fragments containing the single point mutation S56A were generated using the fusion primers listed in Table 2.7. These fragments were then combined and used as templates for the second-round of PCR using the flanking primers (Table 2.7). The resultant PCR insert containing the introduced point mutation was cloned back into the plasmid containing the FLAG-tagged wildtype NS5 between the restriction sites NheI and BsrGI.

Triple FLAG-tagged ZIKV protein expression constructs: The triple FLAG-tagged ZIKV capsid, prM, E, NS1, NS2A, NS2B, NS4A and NS4B cDNAs were generated by PCR from the corresponding plasmids encoding single FLAG-tagged versions of the viral proteins (Kumar et al., 2016) as templates. The PCR products were then cloned into pcDNA-3.1(-) plasmid using the restriction sites NheI and XhoI. To generate triple FLAG-tagged NS3 and NS5, the single FLAG-tagged NS3 and NS5 constructs (Kumar et al., 2016) were used as templates for PCR. The resultant PCR products were cloned into the same single FLAG-tagged NS3 and NS5 plasmids using the restriction sites AfeI and XhoI (for NS3) as well as BsrGI and XhoI (for NS5). All reverse primers used for the above PCRs contained a double-FLAG epitope (Table 2.7).

Myc-tagged flavivirus capsid protein expression plasmids: cDNAs encoding Myc-tagged capsid proteins were generated by PCR using the pTRIP-AcGFP lentivirus vector (Urbanowski and Hobman, 2013) encoding the corresponding flavivirus capsid proteins as templates. The PCR inserts were subcloned into a pcDNA-3.1 plasmid between the restriction sites NheI and BamHI. All forward primers used contained a Myc epitope (Table 2.7).

2.2.2 Cell culture and transfection

2.2.2.1 Cell culture maintenance

A549, HEK293T, Vero and MEF cells were cultured in Dulbecco's modified Eagle's medium (DMEM; Table 2.1) containing 10% (v/v) heat-inactivated FBS (Table 2.1), 4.5 g/L D-glucose (Table 2.1), 2 mM glutamine (Table 2.1), 25 mM HEPES (pH 7.4; Table 2.1), 110 mg/L sodium pyruvate (Table 2.1), 100 units/mL penicillin and 100 µg/mL streptomycin (Table 2.1). C6/36 and RK-13 cells were cultured in MEM containing 10% (v/v) FBS, 2 mM glutamine, 25 mM HEPES (pH 7.4), 110 mg/L sodium pyruvate, 1x non-essential amino acids (Table 2.1), 100 units/mL penicillin and 100 µg/mL streptomycin. Mammalian cells were incubated at 37 °C while C6/36 cells were grown at 25 °C. All cells were maintained in a humidified atmosphere with 5% CO₂.

2.2.2.2 Transient transfection of cell lines

HEK293T, A549, Vero and MEF cells were transiently transfected with plasmids using Lipofectamine 2000 or TransIT-LT1 transfection reagent (Table 2.4) as described by the manufacturers. Twenty-four hours prior to transfection, HEK293T (3×10^5 per well), A549 cells (1×10^5 per well), Vero cells (1×10^5 per well) or MEFs (3×10^4 per well) were seeded into 12-well plates. Cells were then transfected with 1-2 µg of plasmid DNAs using 3 µL of Lipofectamine 2000 or TransIT-LT1 in OptiMEM media (Table 2.1). When cells were to be used for indirect immunofluorescence microscopy, TransIT-LT1, which has lower cytotoxicity, was used for the transfections. For introduction of poly(I:C) (Table 2.1) into cells, 2-8 µg of the dsRNA were transfected using 3-6 µL of Lipofectamine 2000 or TransIT-LT1. Cells were incubated with the transfection mixtures for 12-24 hrs, after which the transfection inoculum was replaced with fresh

culture medium. When other culture dish formats were used, the amount of cells, DNA plasmids and transfection reagents were scaled up or down according to the surface area of the dish/well. Transfected cells were processed for experimental analysis 24-48 hrs post-transfection as indicated.

2.2.2.3 RNA interference

Small interfering RNAs (siRNAs) were used to transiently reduce/knockdown expression of proteins in transfected cells (Table 2.1). A549 cells (1×10^5 per well) or MEFs (3×10^4 per well) were seeded into 12-well plates 24 hrs before transfection. Cells were then transfected with 15-20 pmol of control siRNA (siControl) or gene-specific siRNAs together with 4 μ L of Lipofectamine RNAiMAX reagent (Table 2.4) according to manufacturer's recommendations in OptiMEM media. One-day later, transfection inoculum was replaced with fresh media and cells were incubated at 37 °C for another 24 hrs before processed for further experimental treatments or analyses.

2.2.3 Virology techniques

2.2.3.1 Virus infection

WNV, DENV-2 and ZIKV infection: Experiments with WNV (strain NY99) were performed in CL-3 facilities (University of Alberta) while DENV-2 and ZIKV were handled under CL-2 conditions. Virus stocks were diluted in DMEM lacking FBS to achieve a multiplicity of infection (MOI) of 0.5-10, depending on the experimental objectives. Cells were then incubated with diluted virus for 2-4 hrs at 37 °C, after which the inoculum was replaced with normal growth media. Infected cultures were maintained at 37 °C until experimental analysis.

Rubella virus (RV) infection: RV infection was performed under CL-2 conditions. RV stocks were diluted in DMEM which were then used to infect cells at an MOI of 1-5 for 4 hrs at 35 °C. Subsequently, the inoculum was replaced with normal growth media and the infected cultures were maintained at 35 °C until experimental analyses.

Influenza A virus (IAV) infection: A549 cells (1×10^5 per well) grown on 12-well plates the day before were washed three times with PBS. Cells were then infected with IAV strain PR8 that had been diluted in DMEM containing 0.5% (w/v) BSA and 0.1 µg/mL TPCK trypsin (Table 2.1). Infection with the virus was done at 37 °C with gentle rocking every 10 min for 1 hr. Subsequently, virus inoculum was removed and cells were washed with PBS once before replacing with growth media containing 0.1 µg/mL TPCK trypsin. Samples were collected 24-48 hrs post-infection for analyses.

2.2.3.2 WNV, DENV-2, ZIKV and RV plaque assays

The day before infection, Vero cells (1.5×10^5 per well) were seeded into 24-well plates. Culture supernatants from WNV-, DENV-2-, ZIKV- or RV-infected cells were 10-fold serially diluted in serum-free DMEM. To each well, 100 µL of DMEM was added, after which 100 µL of virus-containing dilution was added. Plates were placed in a 37 °C with 5% CO₂ incubator with occasional rocking. One-hour later, 1 mL of DMEM containing 0.5% methylcellulose (Table 2.1), and 100 units/mL penicillin and 100 µg/mL streptomycin was added to each well. After 3, 4 and 6 days (for WNV, ZIKV and DENV-2 respectively), cells were fixed with 10% (v/v) formaldehyde, and then stained with 1% (w/v) crystal violet in 20% (v/v) methanol (Table 2.1) for 30 min. After drying the plates, the numbers of plaques in each well were counted. For plaque assay of RV, titrations were performed using a similar protocol as described above except that

infection was done in a 35 °C with 5% CO₂ incubator. Seven-days later, RV plaques were fixed and quantified using the same method.

2.2.3.3 Production and use of lentiviruses

Lentiviruses encoding DENV-2 or WNV capsid proteins: To produce infectious lentiviral pseudoparticles, HEK293T cells (3×10^6) grown in 100 mm-diameter dishes were co-transfected with 5.6 µg of pTRIP-IRES-AcGFP-DENV-2/WNV-capsid (Urbanowski and Hobman, 2013) or pTRIP-IRES-AcGFP, 5.6 µg of pGag-Pol and 1.6 µg of pHCMV-VSV G (Schoggins *et al.*, 2011) using 48 µL of TransIT-LT1 transfection reagent. Transfection mixtures were added to cells incubated with DMEM containing 3% (v/v) FBS, 4 µg/mL polybrene (Table 2.1) and 20 mM HEPES (pH 7.4). Forty-eight and 72 hrs later, supernatants were collected and centrifuged at 1000xg to remove cell debris. Lentiviruses were aliquoted into cryo-vials and stored at -80 °C.

For titering, lentivirus stocks were 2-fold serially diluted in DMEM containing 3% (v/v) FBS, polybrene (4 µg/mL) and HEPES (20mM, pH7.4) and then added to A549 cells (2×10^5 per/well) in 6-well plates. The cells were spinoculated at 1000xg in an Eppendorf A-4-62 rotor for 1 hr at 37 °C. Subsequently, inoculum was replaced with fresh growth media and cells were incubated at 37 °C for 48 hrs. Samples were fixed with 2% (v/v) paraformaldehyde (Table 2.1) for 15 min and then processed by flow cytometry (Section 2.2.5). The percentage of cells expressing AcGFP was determined and the corresponding lentivirus titre was calculated using the following formulas:

$$\text{Lentivirus titre} = \% \text{ of (AcGFP-positive cells} \times \text{number of cells)} / \text{volume of lentivirus added}$$

To transduce A549 (4×10^5 per well), Vero (4×10^5 per well) or HEK293T (8×10^5) cells, lentivirus stocks were diluted in DMEM containing 3% (v/v) FBS, polybrene (4 µg/mL polybrene)

and HEPES (20mM, pH7.4) and then spinoculated for 1 hr at 37°C. The lentivirus inoculum was replaced with fresh growth media and transduced cells were incubated at 37 °C for 48 hr before processing for additional experimental treatments.

2.2.4 Microscopy

2.2.4.1 Indirect Immunofluorescence

A549 (1×10^5 per well), HFA (2×10^5 per well) and MEFs (3×10^4 per well) were cultured in 12-well plates with coverslips 24 hr prior to experimental manipulation. After experimental treatments, cells were washed once with PBS and fixed with 4% (v/v) PFA for 15 min at room temperature. After washing three times with PBS, cells were permeabilized with Blocking Buffer containing 3% (w/v) BSA and 0.2% (v/v) Triton X-100 (Table 2.1) for 1 hr at room temperature. Primary antibodies (Table 2.8) diluted in the same Blocking Buffer were added to cells, followed by incubation at 4 °C overnight. The next day, cells were washed three times with Wash Buffer containing 0.3% (w/v) BSA and 0.02% (v/v) Triton X-100 for 15 min each wash. Incubation with secondary antibodies (Table 2.9) and 1 μ g/mL DAPI (Table 2.1) was performed in Blocking Buffer at room temperature for 1 hr. After three washes with PBS, coverslips were mounted onto slides with Prolong Gold anti-fade reagent without DAPI or SlowFade® mounting reagent without DAPI (Table 2.1). When the latter mounting reagent was used, the coverslips were sealed with nail polish.

Where indicated, images (Z-stacks using 200 nm optical sectioning) were acquired on an Olympus IX-81 spinning-disk confocal microscope equipped with 40X and 60X/1.42-numerical-aperture oil PlanApo N objectives (Table 2.10). For super-resolution microscopy, images (Z-stacks using 125 nm optical sectioning) were acquired on a DeltaVision OMX V4 structured

illumination (SIM) microscope (Applied Precision, GE) equipped with a 60X/1.42 oil PSF (PlauApo N) objective and immersion oil $N=1.514\sim 1.516$ (Table 2.10). The number of Z-stacks was determined (automatically) by setting the highest and lowest focal plan position of selected cells prior to acquisition. 3D-SIM images were processed post-acquisition using SoftWorx 6.5.2 software (GE Healthcare Life Sciences). All images were analyzed using Volocity 6.2.1 software (PerkinElmer).

2.2.4.2 Quantification of peroxisome numbers and sizes

The numbers and sizes of peroxisomes were quantified using Volocity 6.2.1 software. Images of individual cells (from confocal or 3D-SIM microscopy) were cropped and used as single images for analyses. Peroxisomes (identified by staining with antibodies to SKL or PEX14) were selected using the corresponding channel with pixel intensity higher than 10,000-20,000 depending on the primary antibody used. The selected objects were further filtered using the following analysis parameters: separating touching objects, excluding objects smaller than $0.0005\ \mu\text{m}^3$ and objects larger than $5\ \mu\text{m}^3$. The data regarding numbers and sizes of selected objects were copied into Microsoft Office Excel for statistical analyses.

2.2.4.3 Quantification of stress granule (SG) numbers

The numbers of SGs were quantified using Volocity 6.2.1 software. Images of individual cells taken on a confocal microscope were cropped and used as single images for analyses. SGs were selected using the G3BP1 channel with pixel intensity greater than 10,000. The selected objects were further filtered using the following analysis parameters: separating touching objects, excluding objects smaller than $0.0005\text{-}0.001\ \mu\text{m}^3$ and objects larger than $4\text{-}6\ \mu\text{m}^3$. The numbers of selected objects were copied into Microsoft Office Excel for statistical analyses.

2.2.5 Flow cytometry

A549 cells ($2-4 \times 10^5$) in 12-well or 6-well plates were transduced with lentiviruses encoding the capsid protein of DENV-2 or WNV using various virus-to-media ratios as described in Section 2.2.3.3. Forty-eight hours post-transduction, cells were fixed with 2% PFA for 15 min and then washed with PBS twice before re-suspending in a final volume of 200-500 μ L in PBS. Samples were subjected to flow cytometry using an LSRFortessa bench-top cytometer (Table 2.10) equipped with three lasers. Data were then analyzed using BD FACSDiva™ Software v6.1.

2.2.6 Protein gel electrophoresis and detection

2.2.6.1 Sodium dodecyl-sulphate polyacrylamide gel electrophoresis (SDS-PAGE)

Cells were lysed with Protein Loading Buffer (Table 2.5) containing 2-5% (v/v) β -mercaptoethanol and 0.2 μ L/sample Benzonase and then heated at 95 °C for 5 min. For analysis of phospho-proteins, 20 mM of NaF (Table 2.1) and 2X Halt phosphatase inhibitor cocktail (Table 2.1) were included in the lysis buffer in order to block phosphatases. Proteins were separated by discontinuous gel electrophoresis (5% stacking gel and 10%, 12% or 15% resolving gels). Stacking gels were prepared by adding 5% acrylamide/bis-acrylamide to Stacking gel buffer (Table 2.5) with 0.1% (w/v) ammonium persulphate and 0.1% (v/v) TEMED. Resolving gels were prepared by combining appropriate amounts of acrylamide/bisacrylamide with Resolving gel buffer (Table 2.5), 0.1% (w/v) APS and 0.1% (v/v) TEMED. After loading protein samples, electrophoresis was performed in SDS-PAGE running buffer (Table 2.5) at 80–130 V in a Bio-Rad Mini-Protean III system. After electrophoresis, gels were processed for immunoblot analysis as described below.

2.2.6.2 Immunoblot analysis

Following SDS-PAGE, proteins were transferred from gels to 0.45 μm PVDF membranes. Prior to transfer, PVDF membranes were activated in methanol and then incubated in Transfer Buffer (Table 2.5). Transfer was carried out using Western Blot Transfer Buffer (Table 2.5) and a Mini Trans-Blot Electrophoresis transfer cell apparatus (Bio-Rad) at a constant current of 320 mA for 2 hr in an ice-filled bucket or at 40 mA overnight at room temperature. Subsequently, the PVDF membranes were incubated with Blocking Buffer containing 5% (w/v) BSA in PBS-T (Table 2.5) for at least 1 hr at room temperature or overnight at 4 °C on a rocking device.

After blocking, membranes were incubated with primary antibodies (diluted in Blocking Buffer containing 0.04% (w/v) sodium azide for 2 hrs at room temperature or at 4 °C overnight on a rocking device. After three washes (15 min each) with PBS-T at room temperature, membranes were incubated with secondary antibodies (diluted in Blocking Buffer) for a minimum of 1 hr. Finally, membranes were washed three times with PBS-T (15 min each) and processed for protein detection as described below.

2.2.6.3 Detection of fluorophore-conjugated secondary antibodies

After incubation with primary and secondary antibodies followed by washes, membranes were subjected to a final wash with PBS (minimum of 5 min at room temperature) to remove any residual Tween-20. Membranes were placed face-down on the scanner bed of an Odyssey Infrared Imaging system and then scanned at 84- μm resolution (quality setting of “Medium” or “High”). Quantification of proteins was performed using Odyssey Image Studio Lite software Version 5.2.

2.2.7 Biochemical analysis of protein-protein interactions

2.2.7.1 Co-immunoprecipitation

Co-immunoprecipitation of PEX19 and WNV/DENV-2 capsid protein: HEK293T cells (3×10^6) were seeded into p100 dishes and on the next day, were infected with WNV or DENV-2 (MOI=5) for 48 hr. Cells were washed once with ice-cold PBS and then lysed with NP-40 Lysis Buffer (Table 2.5) containing Complete protease inhibitors (Table 2.1) on ice for 30 min. The lysates were clarified at 14,000 rpm for 20 min in a microcentrifuge at 4 °C and then pre-cleared with protein G or protein A Sepharose beads (Table 2.1) for 10 min at 4 °C with rotation. Subsequently, lysates were incubated with anti-PEX19 or anti-capsid antibodies for 1-2 hours at 4 °C with rotation. Twenty-microliters of protein A-Sepharose or protein G-Sepharose beads (50% suspension) were then added to samples which were incubated for 2 hr at 4 °C with rotation. After centrifugation (500xg), the beads were washed three times with lysis buffer containing protease inhibitors, and the bound proteins were eluted by heating at 95 °C for 10 min in Protein Sample Buffer containing 2% β -ME. Proteins were separated by SDS-PAGE and transferred to PVDF membranes for immunoblot analysis.

Co-immunoprecipitation of STAT2 and ZIKV NS5-FLAG (wild type or mutants): A549 cells were transfected with pCDNA-3.1 NS5-FLAG, NS5 mutants or empty vector (pCDNA3.1-FLAG) with Lipofectamine 2000 for 48 hr. Because ZIKV-NS5 induces degradation of human STAT2 (Kumar et al., 2016), infected cells were treated with 200 nM epoxomicin (Table 2.1) for 12-24 hrs before collection. Cells were washed once with ice-cold PBS, harvested with a cell scraper, pelleted by spinning in a microcentrifuge at 500xg for 5 min at 4 °C and then resuspended in IP buffer (Table 2.5) with a cocktail of freshly added protease inhibitors. The supernatants were

clarified by centrifugation at 16,000g for 15 min and then divided into aliquots that were incubated overnight with anti-FLAG, anti-human STAT2 or anti-myc antibodies at 4 °C with rotation. The next day, protein G sepharose was added and samples were incubated for 2 hrs at 4 °C with rotation. After five washes with IP buffer, SDS Sample Buffer containing 2% β -ME was added to the beads and proteins were eluted by heating at 95 °C for 10 min. Proteins were resolved by SDS-PAGE followed by immunoblot analysis.

Co-immunoprecipitation of G3BP1 or Caprin-1 and triple FLAG-tagged ZIKV proteins:

HEK293T cells (3×10^6) were seeded into p100 dishes the day before transfection. On the next day, cells were transfected with plasmids encoding triple-FLAG-tagged ZIKV proteins using Lipofectamine 2000 for 48 hr. The transfected cells were pelleted and resuspended in IP buffer (Table 2.5) containing $\sim 2 \mu\text{L}$ of Benzonase. The supernatants were clarified by centrifugation at 16,000xg for 15 min and then precleared with Protein G-sepharose beads for 1 hr at 4 °C to remove proteins that non-specifically bind to the beads. Aliquots of the pre-cleared cell lysates were incubated overnight with anti-FLAG or anti-myc antibodies at 4 °C. The next day, antibody/lysate mixtures were incubated with Protein G-sepharose beads for 2 hr after which the beads were subjected to three washes with IP buffer (without benzonase). Bound proteins were eluted by heating at 95 °C for 10 min and then resolved by SDS-PAGE followed by immunoblot analysis.

2.2.8 RNA techniques

2.2.8.1 RNA isolation

Total RNA from cell lysates was isolated using the RNeasy mini Kit (QIAGEN) or Nucleospin RNA isolation kit (Macherey-Nagel) according to manufacturers' recommendations. Samples were stored at -80 °C until further use.

2.2.8.2 cDNA synthesis

To reverse transcribe the isolated RNA into cDNAs, the Superscript II Reverse Transcriptase system (Invitrogen) or Improm-II Reverse Transcriptase systems (Promega) were utilized. In a typical reaction (20 μ L), 4 μ L of RNA and 1 μ L of random primers (200 ng/ μ L) were added. cDNA synthesis reactions were carried out at 42 °C for 2 hrs in a T100 Thermal cycler (Bio-Rad). Reactions were terminated by incubation at 75 °C for 10 min after which the cDNAs were diluted (1:3) in nuclease-free water and then stored at -20 °C until use.

2.2.8.3 Quantitative real-time PCR (qRT-PCR)

To quantify the relative level of RNA, qRT-PCR reactions were conducted using the PerfecCTa SYBR Green Supermix low Rox real-time PCR kit (Quanta Biosciences) in a Stratagene MX3005P™ thermocycler. Reactions (15 μ L) were performed in duplicate and contained 3 μ L of cDNA and 100 nM of gene-specific primer sets (forward and reverse). The amplification program consisted of an initial denaturing step at 94 °C for 2 min, followed by 40 cycles of 20 sec at 94 °C, 20 sec at 55 °C, and 20 sec at 68 °C. Fluorescence was read after the 55 °C annealing step in each cycle. To obtain melting curves for analysis of gene product specificity, fluorescence was read after the amplification step at 68 °C in the final cycle. The comparative CT ($\Delta\Delta$ CT) method (Livak and Schmittgen, 2001) was used to quantify the relative levels of each RNA transcript. The Δ CT values were calculated using β -actin mRNA or GAPDH (CT value) as the internal control. The $\Delta\Delta$ CT values were determined using the appropriate control samples as the reference values. Relative levels of mRNAs of the gene of interest were calculated using the formulas $2^{(-\Delta\Delta$ CT)}.

2.2.8.4 Protein-RNA interaction by RNA-IP

A549 cells (2×10^6) were infected with ZIKV (MOI=5) for 48 hrs. Cells were washed with ice-cold PBS once, removed from plates using a cell scraper and then pelleted at 800xg for 5 min at 4 °C. Cells were re-suspended in RNA-IP buffer (Table 2.5) containing 1x protease inhibitor cocktail and the RNase inhibitor RNaseOUT. To avoid non-specific binding of proteins to beads, protein G-sepharose beads were first incubated with 5% BSA in RNA-IP buffer, followed by incubation overnight at 4 °C with rabbit anti-G3BP1, goat anti-TIAR or mouse anti-myc. Subsequently, cell lysates were incubated with the antibody-bead complexes for 2 hrs at 4 °C followed by five washes with RNA-IP buffer containing RNaseOUT. Aliquots of the protein-antibody-bead complexes were boiled and processed for SDS-PAGE and immunoblotting while the rest of the complexes were added to RNA extraction buffer and processed for RNA extraction.

2.2.9 Luciferase reporter assays

The day before transfection, A549 cells (1×10^5) and HEK293T cells (2.5×10^5) were seeded into 12-well plates as described in Section 2.2.2.2. To detect IFN induction, the IRF3 promoter-driven firefly luciferase reporter plasmid p55-CIB-Luc (provided by T. Taniguchi, University of Tokyo, Japan), the NF- κ B promoter-driven reporter plasmid pNF- κ B-Luc (Stratagene) or the IFN- β promoter-driven reporter plasmid p125-luc (ref) was co-transfected with the renilla luciferase reporter plasmid pRL-TK (Promega) as a transfection control. Where indicated, poly(I:C) was co-transfected or transfected into cells following expression of luciferase reporters. For detection of IFN-mediated signaling, cells were transfected with the ISG56 promoter-driven reporter plasmid pGL3B/561 (a gift from Dr. Ganes C. Sen, Lerner Research Institute of the Cleveland Clinic, USA), the ISRE promoter-driven reporter plasmid pGL4 ISRE (Promega) or the GAS promoter-

driven reporter plasmid pGAS-Luc (Stratagene) together with a renilla luciferase reporter plasmid (as transfection control). IFN signaling was induced by treatment with Type- I, II or III IFNs for the indicated time periods.

Cell lysates were harvested at indicated time periods in 200 μ l Luciferase Lysis buffer (Table 2.5). To enhance lysis, samples were frozen at -80°C for at least 30 min and then thawed at room temperature. For luciferase assays, the samples were aliquoted in duplicates for reading of firefly as well as renilla luciferase activities. The firefly luciferase substrate D-luciferin was prepared at a final concentration of 70 μM in Luciferase Assay Buffer (Table 2.5). For renilla luciferase measurements, the substrate coelenterazine was prepared at a final concentration of 1.4 μM in Luciferase Assay Buffer without DTT and ATP. The specific substrates were added to samples and incubated in the absence of light for 5 min. Luciferase activities were measured using an Illuminator plate reader BioTek. The relative reporter activity of specific promoters was calculated by normalization to the renilla luciferase reporter activity in the corresponding samples.

2.2.10 Cell viability assay

To control for cytotoxic effects of siRNAs or drugs used in this thesis work, viability assays were performed using the CellTiter-Glo® Luminescent Cell Viability Assay system (Promega) which measures ATP levels. Cells transfected with siRNAs or treated with drugs, were harvested at the indicated times after once wash with PBS. Cells were lysed by suspending in 200 μL of PBS and then freezing at -80°C (minimum of 20 min) followed by thawing. The lysates were then aliquoted in duplicate in wells of 96-well plates. Luciferase substrates (D-luciferin or Coelenterazine; Gold Biotechnology) were then added to each sample (1:1 of v/v ratio) followed

by incubation for 5 min at room temperature. Luminescence values were then read using an Illuminator plate reader.

Chapter 3 Flavivirus infection impairs peroxisome biogenesis and antiviral signaling

A version of this chapter has been published in:

“*You, J., ***Hou, S.**, Malik-Soni, N., Xu, Z., Kumar, A., Rachubinski, R.A., Frappier, L., Hobman, T.C. (2015) Flavivirus Infection Impairs Peroxisome Biogenesis and Early Antiviral Signaling. *J Virol.* 2015 Dec;89(24):12349-61. doi: 10.1128/JVI.01365-15.”

*Authors contributed equally

3.1 Rationale

Flaviviruses replicate relatively slowly and like most viruses, their genomes encode a very limited number of proteins (10 in this case). To ensure efficient viral replication, it is essential that they encode multifunctional proteins to evade host immune defenses. The capsid protein is the first viral protein to be synthesized in infected cells, and it is produced in vast excess for what is needed for genome packaging (reviewed in (Urbanowski et al., 2008)). Intriguingly, although viral replication occurs entirely in the cytoplasm, a large pool of capsid is targeted to the nucleus and nucleolus (Bulich and Aaskov, 1992; Mori et al., 2005). Although the functional significance of this phenomenon is still unclear, it is possible that these nuclear capsid proteins perform non-structural functions apart from genome packaging (Urbanowski et al., 2008).

The non-structural role of capsid proteins is supported by the observations that capsid proteins interact with diverse cellular factors involved in different signaling pathways (Table 3.1). For instance, WNV capsids have been shown to modulate apoptosis (Urbanowski and Hobman, 2013), neuro-inflammation (Marle et al., 2007), tight junction protein turnover (Medigeschi et al., 2009), as well as transcriptional and translation control (Bhuvanakantham et al., 2010), suggesting an important role of this viral structural component in the regulation of host immune responses and viral pathogenesis. Similarly, DENV capsid has been shown to interact with components of several cellular processes including apoptosis (Netsawang et al., 2010, 2014), lipid droplet biogenesis (Samsa et al., 2009; Carvalho et al., 2011) and nucleosome formation (Balinsky et al., 2013), further demonstrating the non-structural functions of flavivirus capsid proteins in modulating cellular processes during viral infection.

Table 3.1 Non-structural functions of flavivirus capsids in modulating cellular pathways

Flavivirus	Capsid-binding host factor	Effect on cellular pathway	Reference
DENV	DAXX	Disrupts interaction between CD137 and NFκB, thus inducing CD137-mediated apoptosis	(Limjindaporn et al., 2007; Netsawang et al., 2010; Nagila et al., 2011; Netsawang et al., 2014)
	Core histones (H2A, H2B, H3 and H4)	Inhibits nucleosome formation	(Colpitts et al., 2011)
	Lipid droplet	Binds lipid droplets and may facilitate viral replication	(Samsa et al., 2009; Carvalho et al., 2012; Iglesias et al., 2015; Martins et al., 2012)
	Nucleolin	Hijacks nucleolin for viral morphogenesis	(Balinsky et al., 2013)
JEV	B23	Exploits B23 for capsid nucleolar localization and viral replication	(Tsuda et al., 2006)
	Caprin-1	Hijacks Caprin-1 for viral RNA replication and inhibits stress granule formation	(Kato et al., 2013)
	Unknown	Mediates virus-induced autophagy	(Wang et al., 2015)
WNV	DDX56	Binds DDX56 which is required for virion assembly	(Xu et al., 2011; Xu and Hobman, 2012; Reid and Hobman, 2017)
	I ^{2PP2A}	Interacts and augments I ^{2PP2A} activity	(Hunt et al., 2007)
	Jab1	Induces cytotoxicity which is negated by binding of Jab1	(Oh et al., 2006)
	MKRN1	Induces cytotoxicity which is reduced by binding of MKRN1	(Ko et al., 2010)

Table 3.1 (continued)

	Unknown	Blocks apoptosis in a PI3K-dependent manner	(Urbanowski and Hobman, 2013)
WNV	Unknown	Induces lysosomal degradation of tight junction proteins	(Medigeshi et al., 2009)
	Unknown	Activates glia cells and induces neuroinflammation	(Marle et al., 2007)
	Hsp70 and cofactors	Hijacks these host proteins for viral replication and virion assembly in human and insect cells	(Oh and Song, 2006; Taguwa et al., 2015)
DENV, WNV	Importin α/β	Importin-mediated nuclear localization of capsid benefits WNV production	(Bhuvanankantham et al., 2009, 2010)
	PEX19	Binds to PEX19 and impedes peroxisome biogenesis	(You et al., 2015)
	Sec3p	Targets Sec3p for proteasomal degradation and inhibits its antiviral activity	(Bhuvanankantham et al., 2010)
YFV (and other flaviviruses)	*N.A.	Sequesters viral dsRNA and thus inhibits Dicer-mediated RNAi activity in mosquito cells	(Samuel et al., 2016)
ZIKV	G3BP1 and Caprin-1	Capsid-mediated sequestration of these host factors potentially contributes to inhibition of stress granule formation	(Hou et al., 2017)

*N.A., not applicable

In collaboration with Dr. Lori Frappier (University of Toronto), our laboratory identified >20 putative human DENV and WNV capsid-binding partners by proteomic analyses. Among these candidates is PEX19, which binds the capsids of both viruses. PEX19 is required for the biogenesis of peroxisomes, which are membranous organelles that regulate lipid metabolism, oxidative homeostasis and innate immune signaling (reviewed in (Smith and Aitchison, 2013)). PEX19 serves as a chaperone that facilitates PMP-membrane assembly and *de novo* peroxisome formation (reviewed in Sections *1.2.2.2* and *1.2.2.3*). Genetic ablation of *PEX19* results in loss of peroxisomes and associated functions. Accordingly, binding of flavivirus capsids to PEX19 could potentially interfere with its activity, leading to dysregulation of peroxisome biogenesis and peroxisomal functions. Since my thesis focuses on understanding how flaviviruses evade cellular defenses, I decided to investigate the interplay between flaviviruses and the peroxisome-mediated antiviral response.

As the first attempt to explore the functional significance of capsid-PEX19 interaction, my colleague Dr. Jae Hwan You and I set out to examine whether DENV and WNV infection alters the number of peroxisomes and the protein level of PEX19. In parallel, we confirmed the interaction between capsid proteins and PEX19 during viral infection. Subsequently, we determined whether capsid expression alone alters peroxisome abundance. To determine if flaviviruses inhibit peroxisome-mediated antiviral response, we examined the induction of Type-III IFN (IFN- λ) expression during viral infection. Finally, to establish a signaling link between PEX19 and the peroxisome-mediated antiviral program, we measured the induction of IFN- λ expression in *PEX19*-silenced cells.

3.2 Results

3.2.1 DENV and WNV capsid proteins interact with PEX19

In order to confirm the interaction between PEX19 and capsid proteins in the context of viral infection, A549 cells were infected with DENV or WNV (MOI = 5) for 48 hrs and then subjected to co-immunoprecipitation (co-IP) using antibodies to PEX19 or capsid proteins. We selected 48 h.p.i as the sample collection time point because the maximum viral replication (as determined by plaque assays) and by extension, viral protein expression, was usually achieved at this time. Data from reciprocal co-IP in Figure 3.1 show that PEX19 forms stable complexes with the capsid proteins in DENV- and WNV-infected cells.

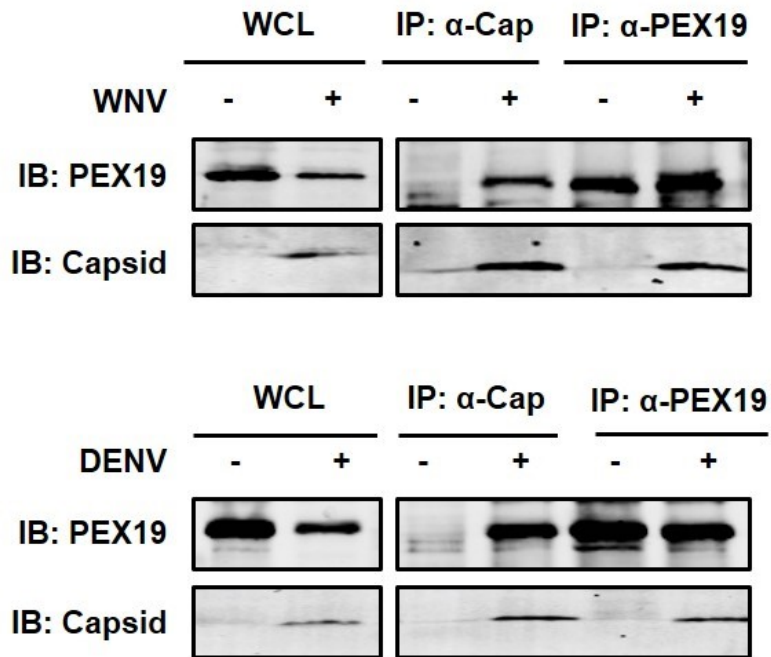


Figure 3.1 Flavivirus capsid proteins interact with PEX19. A549 cells were infected with WNV or DENV-2 (MOI = 5). Forty-eight hours later lysates were subjected to co-immunoprecipitation with rabbit anti-WNV capsid (upper panel), guinea pig anti-DENV capsid (lower panel) or rabbit anti-PEX19 antibody followed by SDS-PAGE and immunoblotting. IB, immunoblotting, IP, immunoprecipitation, WCL, whole-cell lysate. N = 3

To visualize the effect of virus infection on PEX19 localization, we performed confocal microscopy analyses. A549 cells were infected with DENV or WNV virus (MOI = 2) for 24 hrs after which endogenous PEX19 and viral capsid proteins were detected using the indicated antibodies. As shown in Figure 3.2A, PEX19 exhibited a typical cytoplasmic localization and disperse distribution in mock cells, a pattern which is consistent with its role as the cytosolic chaperone for newly synthesized PMPs (Jones et al., 2004). In contrast, in cells infected with DENV or WNV, the PEX19 signal was concentrated in areas that were enriched for capsid proteins, possibly sites of viral replication and/or assembly (Figure 3.2A). Co-localization analysis using Pearson correlation coefficient (PCC) indicated partial co-localization between PEX19 and capsid proteins (Figure 3.2B). This method measures the linear correlation between two variables (Royal Society, 1895) and in this case, pixel intensities from the PEX19 and capsid channels. The PCC value falls between -1 and +1; and the closer it is to +1, the higher the degree of colocalization between the two channels. The average PCC values in DENV- and WNV-infected cells were 0.6 and 0.5 respectively, suggesting a partial colocalization between capsids and PEX19. In conclusion, our microscopy analysis is consistent with co-immunoprecipitation data showing an interaction between PEX19 and flavivirus capsid proteins.

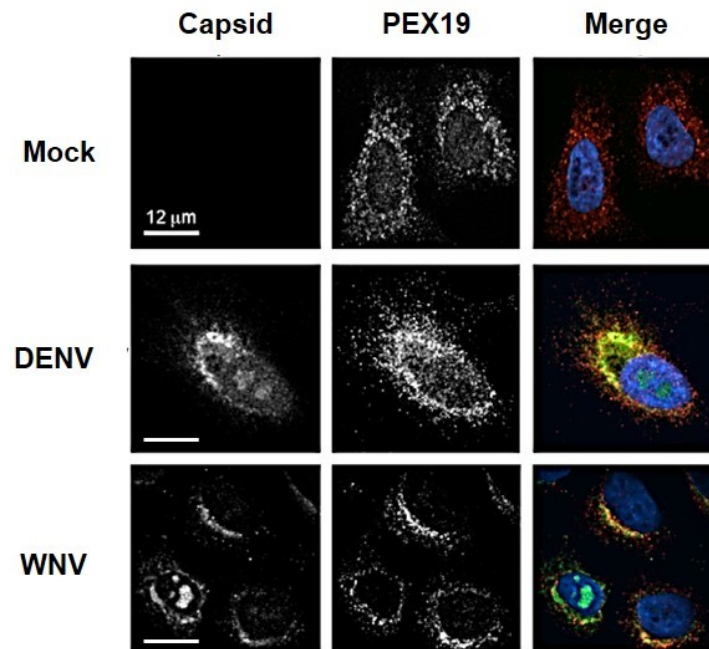
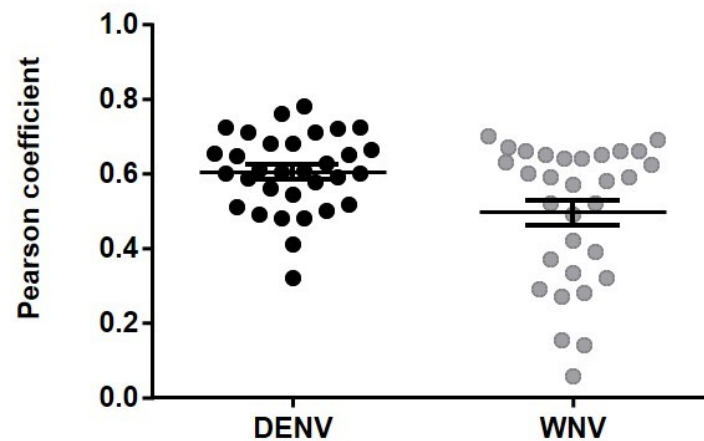
A**B**

Figure 3.2 PEX19 partially co-localizes with capsid proteins during flavivirus infection. A. A549 cells were infected with DENV-2 or WNV (MOI = 2) for 24 hrs and then processed for indirect immunofluorescence microscopy using a guinea pig anti-WNV or -DENV capsid and rabbit anti-PEX19. Primary antibodies were detected using donkey anti-guinea pig Alexa 488 and donkey anti-rabbit Alexa 546. Images were acquired on a spinning disk confocal microscope equipped with a 60X oil lens. Scale bar = 12 μm. Nuclei were stained with DAPI. **B.** Co-localization analysis of PEX19 and capsid proteins (represented by Pearson correlation coefficient; PCC) was performed using Volocity software. A minimum of 10 cells were used per sample and all PCC values from 3 independent experiments were plotted.

3.2.2 Flavivirus infection leads to PEX19 degradation

To investigate the functional consequence of capsid-PEX19 interaction, we first examined the effect of flavivirus infection on steady state PEX19 protein levels using immunoblot analysis. Figure 3.3A revealed that levels of PEX19 protein were reduced 30 to 40% in DENV- and WNV-infected cells respectively. Since capsid proteins bind PEX19, we next determined whether expression of capsids alone could induce degradation of this host factor. To increase the percentage of capsid-expressing cells, in instead of using plasmid-based transfection, we transduced A549 cells with lentiviruses encoding DENV or WNV capsids at a high multiplicity of transduction (MOT = 10). Quantification of immunoblots indicated that expression of either capsid protein alone did not trigger significant degradation of PEX19 (Figure 3.3B). However, because viral proteins do not usually function in isolation (Klema et al., 2015), it is possible that virus-induced degradation of PEX19 requires interaction or coordination between the capsid proteins and other viral components.

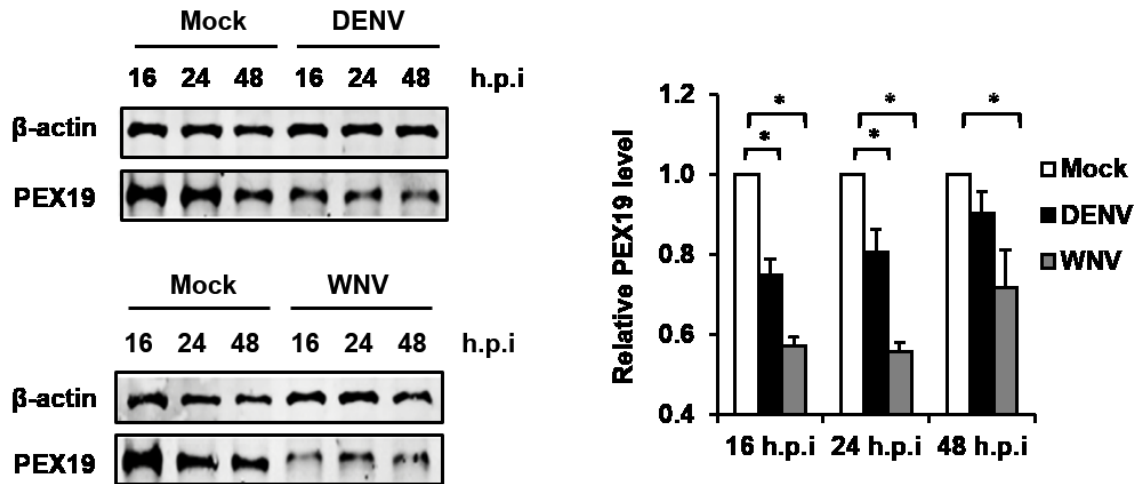
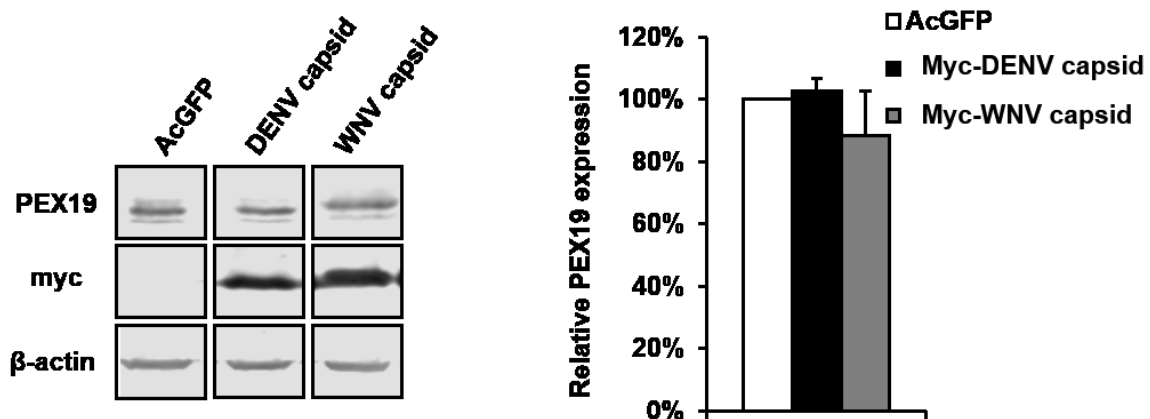
A**B**

Figure 3.3 Flavivirus infection reduces levels of PEX19 protein. **A.** A549 cells were infected with WNV or DENV-2 (MOI = 2) for the indicated time periods after which lysates were prepared for immunoblotting with rabbit anti-PEX19, guinea pig anti-DENV capsid and anti-WNV capsid antibodies. **B.** A549 cells were transduced (MOT = 10) with lentiviruses encoding an AcGFP (control), myc-DENV or myc-WNV capsids for 48 hrs. Lysates were collected and processed for immunoblotting using a mouse anti-myc antibody and rabbit anti-PEX19 antibody. Levels of β -actin are shown as a loading control. Quantification of PEX19 expression (relative to PEX19 levels in mock samples) was performed using Image Studio Lite 5.0 software. The relative levels of PEX19 were represented on the bar graphs (right panels). * $P < 0.05$; N = 3

To gain mechanistic insight into how flaviviruses induce loss of PEX19, infected cells were treated with inhibitors that block proteasome- (MG132) or lysosome- (BAF-A1) dependent degradation and relative levels of PEX19 were determined. As shown in Figure 3.4A, addition of MG132 resulted in an increase in the total level of ubiquitinated proteins, as indicated by a darker smear of ubiquitin staining, indicating that this inhibitor was having the desired effect on the proteasomal degradation pathway. Similarly, BAF-A1 treatment induced an upregulation in LC3B-II levels (Tumbarello et al., 2012), indicating that the lysosomal degradation machinery was negatively impacted (Figure 3.4A). While treatment of BAF-A1 did not prevent loss of PEX19 in WNV- or DENV-infected cells, in cells treated with MG132, loss of PEX19 due to infection was moderately abrogated (Figure 3.4B). However, as indicated by the altered levels of capsids in Figure 3.4A, interference of the proteasomal and lysosomal pathways seems to have an impact on viral replication (Heaton and Randall, 2010; Fernandez-Garcia et al., 2011; Byk et al., 2016) thus confounding our analyses. Further experiments are required to identify the cellular pathway(s) in which PEX19 is degraded during flavivirus infection.

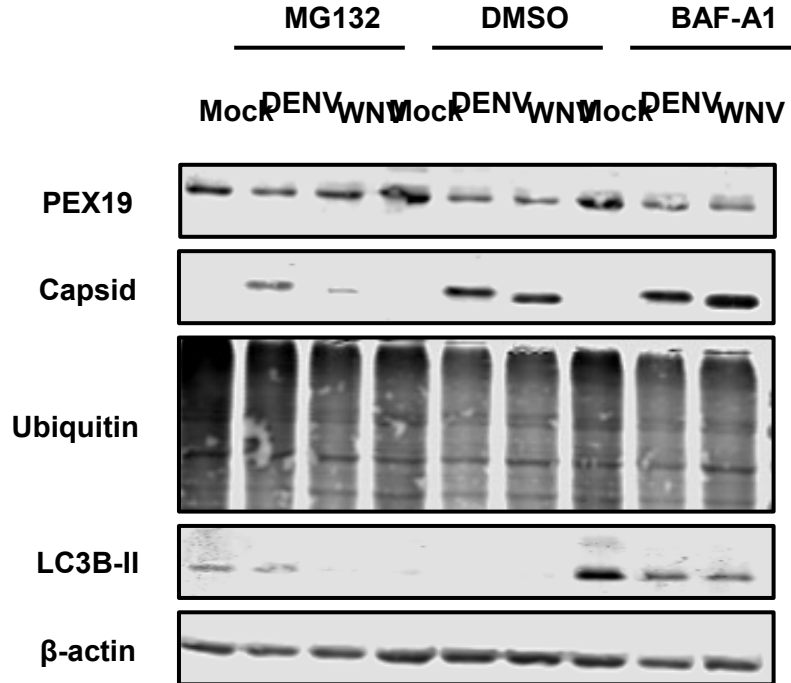
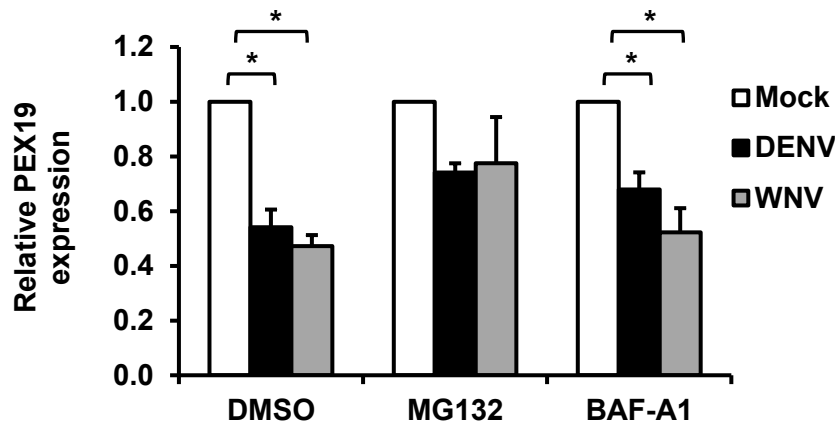
A**B**

Figure 3.4 The effect of proteasome and lysosome inhibitors on virus-induced degradation of PEX19. **A.** A549 cells were infected with WNV or DENV-2 (MOI = 2) for 24 hrs and then treated with DMSO, MG132 (20 μ M) or baflomycin-A1 (BAF-A1; 400 nM) for 12 hrs. Cell lysates analyzed by immunoblotting with rabbit anti-PEX19 and guinea pig anti-capsid antibodies. As positive controls for drug treatments, the levels of ubiquitinated proteins and the autophagy maker LC3B-II were measured by immunoblotting. Levels of β -actin serve as a loading control. **B.** Relative PEX19 expression was quantified using Image Studio Lite software. * P < 0.05; N = 3

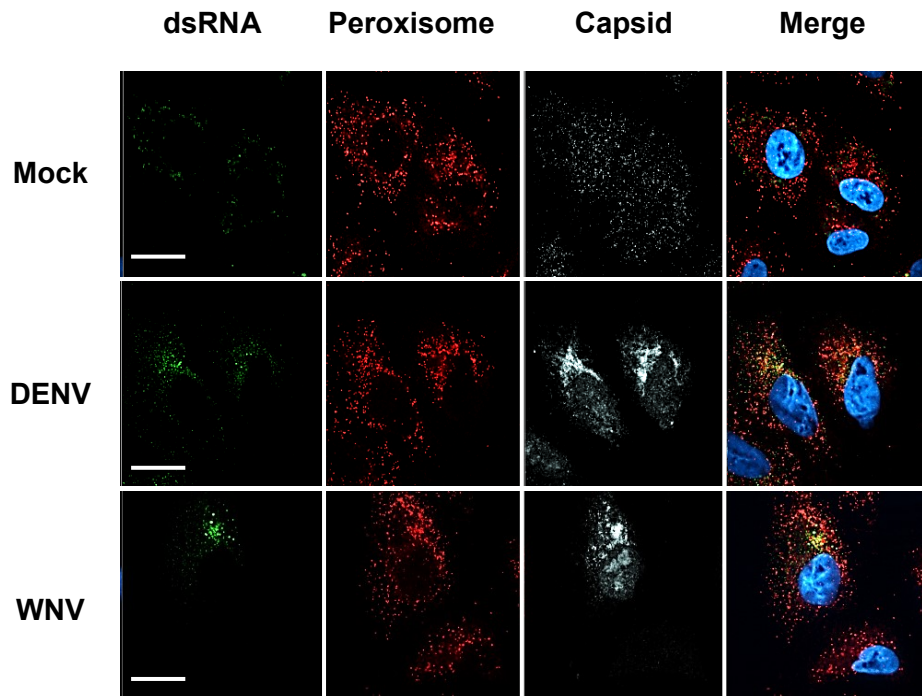
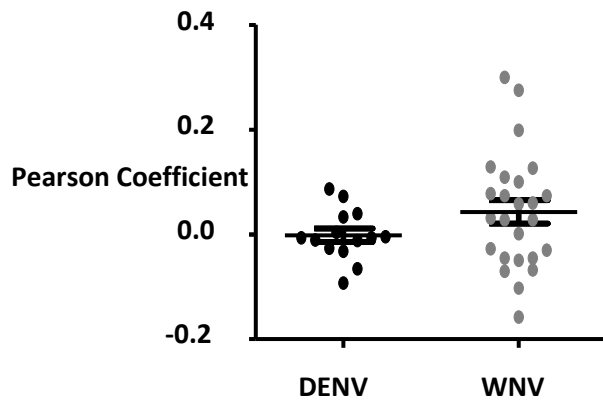
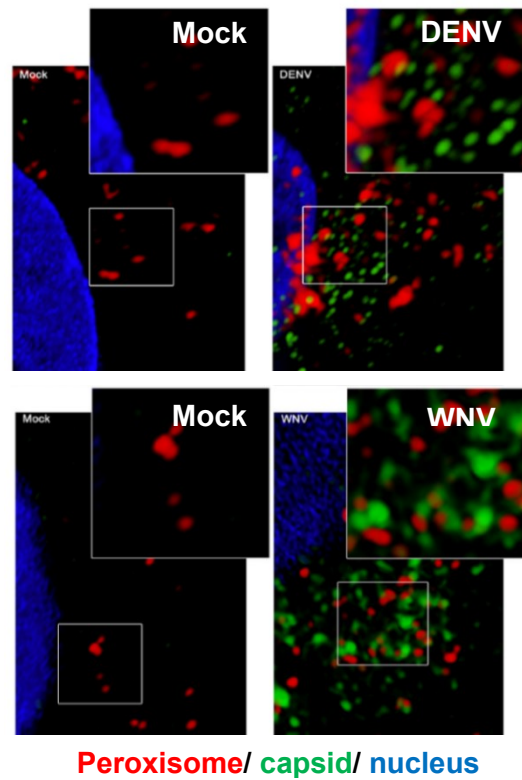
3.2.3 Flavivirus infection alters peroxisome distribution

As mentioned earlier, PEX19 is required for peroxisome biogenesis by facilitating the membrane insertion of PMPs as well as budding of peroxisomal precursors from the ER (Schmidt et al., 2012). Accordingly, capsid protein-mediated sequestration and infection-induced degradation of PEX19 could lead to defects in peroxisome formation and therefore alterations in peroxisome biology. To test this possible scenario, we first examined the distribution of peroxisomes in mock- and DENV- or WNV-infected cells. Peroxisomes were identified using an antibody to the tripeptide SKL (Szilard et al., 1995), a targeting motif found at the carboxyl termini of many peroxisomal matrix proteins (Gould et al., 1989). We selected SKL as the peroxisome marker to ensure that all organelles identified in our study were functional, since peroxisomal “ghosts” which lack matrix enzymes have been reported in cells defective in peroxisomal matrix import (Santos et al., 1992).

In mock-infected cells, SKL-positive puncta were dispersed throughout the cytoplasm (Figure 3.5A). In contrast, infection with DENV or WNV resulted in clustering of peroxisomes to areas enriched in capsid-positive structures (Figure 3.5A). Since components of some plant viruses (e.g., Tombusviruses) have been shown to traffic to peroxisomes to facilitate genome synthesis (Panavas et al., 2005; Rochon et al., 2014), we next investigated whether flavivirus replication takes place at this organelle in addition to the endoplasmic reticulum, the main site of replication and assembly. To identify replication complexes, an antibody specific for dsRNA, an intermediate of RNA virus replication, was utilized. Although distribution of peroxisomes was altered by viral infection, no significant overlap between dsRNA and peroxisomes was evident (Figure 3.5A and B), suggesting that flavivirus replication does not occur in association with this organelle. In addition, structured illumination microscopy (SIM), a form of super-resolution microscopy,

revealed no evidence of co-localization between capsid proteins (green channel) and peroxisomes (red channel) as signals from the corresponding channels did not significantly overlap (i.e., lack of yellow signal on the merge images) (Figure 3.5C).

Figure 3.5 Flavivirus infection alters peroxisome distribution. **A.** A549 cells were infected with WNV or DENV-2 (MOI = 2) for 24 hrs. Cells were processed for indirect immunofluorescence using guinea pig anti-WNV or -DENV capsid antibodies. Viral replication complexes and peroxisomes were detected using mouse anti-dsRNA and rabbit anti-SKL antibodies respectively. Primary antibodies were detected using donkey anti-mouse Alexa 488, donkey anti-rabbit Alexa 546 and goat anti-guinea pig Alexa 647. Nuclei were stained with DAPI. Images were acquired using a spinning disk confocal microscope equipped with a 60X oil lens. Scale bar = 12 μ m. **B.** Co-localization analysis of dsRNA- and SKL-positive structures using Pearson correlation coefficient was performed using Volocity software. **C.** Viral infection and indirect immunofluorescence microscopy was performed as described in (A). Images were acquired using SIM on a DeltaVision OMX microscopy. N = 3.

A**B****C**

3.2.4 Flavivirus infection leads to reduction in peroxisome numbers

To determine whether flavivirus infection alters peroxisome abundance, we utilized SIM to compare the numbers of peroxisomes in mock-infected and virus-infected cells. We chose SIM because it offers a higher resolution (~8-fold in 3 dimensions) compared to confocal microscopy, thus rendering a better separation of clustering objects. According to data in Figure 3.3A, the maximum reduction in PEX19 levels was achieved at or before 16 h.p.i.; and because the turnover of peroxisomes takes approximately 2 days in cultured mammalian cells (Huybrechts et al., 2009), we originally selected 64-72 h.p.i as the fixation time point. Due to noticeable cytopathic effect, we later adjusted the protocol to process samples at 48 h.p.i when infected cells were still relatively healthy (according to the shape of nuclei stained by DAPI) for imaging. Quantitation of peroxisome numbers revealed that DENV- and WNV-infected cells contained 30-35% fewer peroxisomes than mock-infected cells (Figure 3.6).

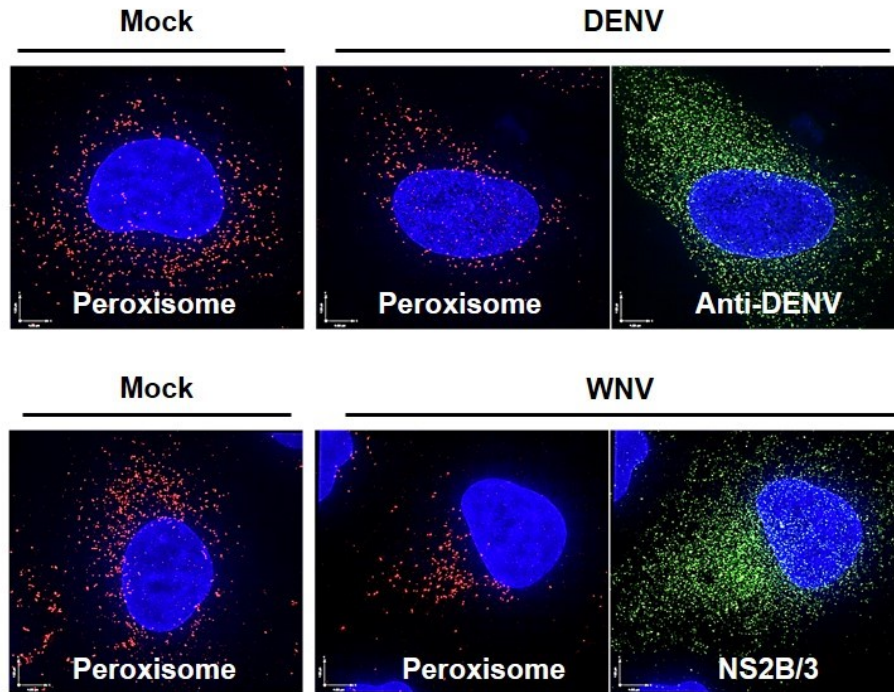
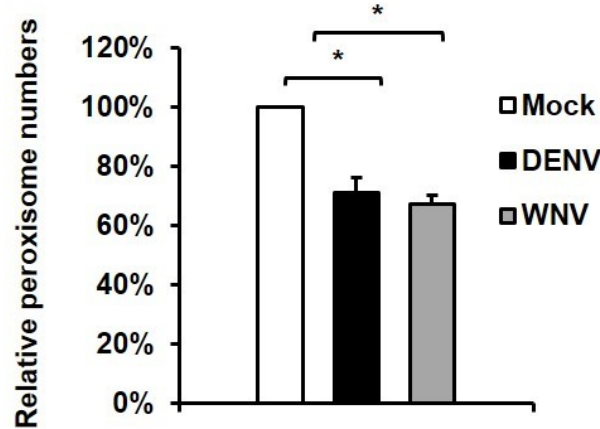
A**B**

Figure 3.6 Flavivirus infection reduces peroxisome numbers. A. A549 cells were infected with WNV or DENV-2 (MOI = 2) for 48 hrs. Cells were then processed for indirect immunofluorescence using anti-WNV NS2B/3 or anti-DENV antibodies. Peroxisomes were detected using a rabbit anti-SKL antibody. Primary antibodies were detected using donkey anti-mouse Alexa 488 and donkey anti-rabbit Alexa 568. Nuclei were stained with DAPI. Images were acquired and reconstructed using SIM. Scale bar = 4 μ m **B.** Quantification of peroxisome numbers was performed using Volocity software. A minimum of 15 cells were used for each sample. * $P < 0.05$; N = 3

Next, to determine whether the virus-induced reduction in peroxisome abundance was due to defects in the peroxisome division pathway, we measured the size of peroxisomes in individual cells and generated size distribution curves accordingly. The logic was that, if viral infection impairs peroxisome division, we would expect to see fewer small peroxisomes and more large peroxisomes. Figure 3.7 shows that the sizes of peroxisomes in mock- and flavivirus-infected cells were similar, indicating that DENV and WNV infection does not impact the peroxisomal division pathway significantly.

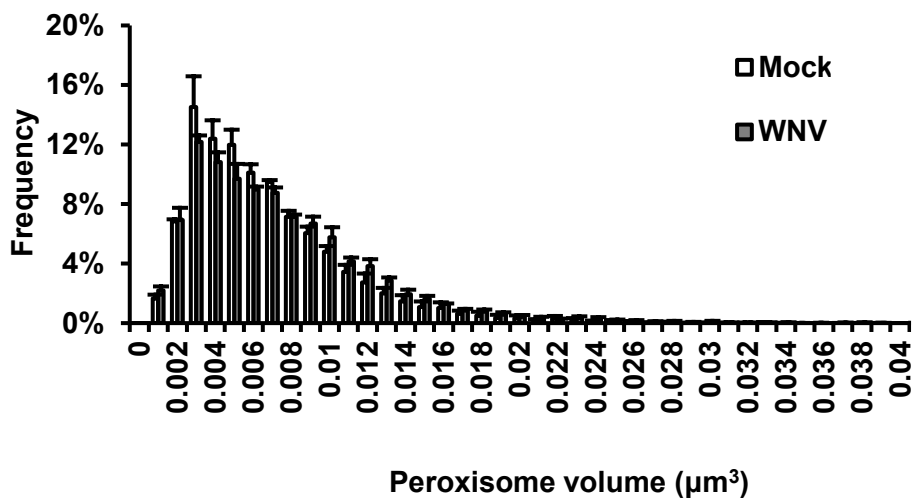
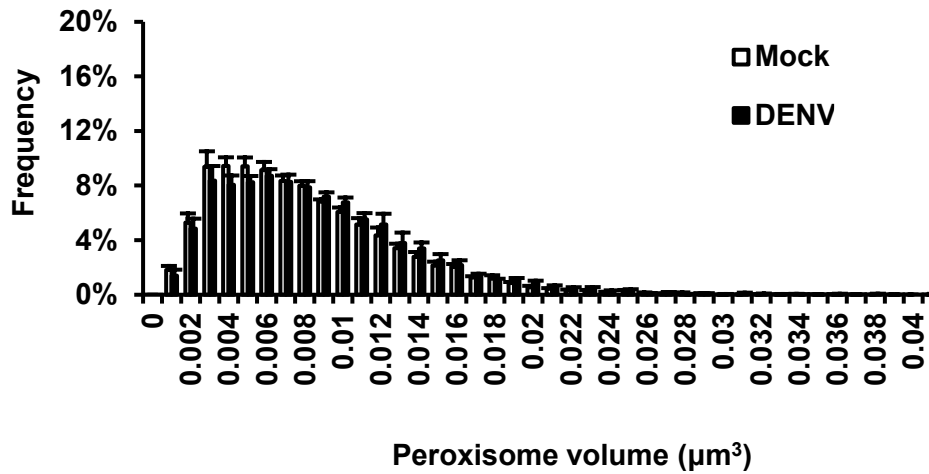


Figure 3.7 Flavivirus infection does not alter peroxisome size. A549 cells were infected with DENV-2 (top panel) or WNV (bottom panel) (MOI = 2) for 48 hrs. Cells were processed for indirect immunofluorescence using anti-WNV NS2B/3 or anti-DENV antibodies. Peroxisomes were visualized by staining with rabbit anti-SKL antibody. Primary antibodies were detected using donkey anti-mouse Alexa 488 and donkey anti-rabbit Alexa 568. Images were acquired and reconstructed using SIM. Quantification of peroxisome sizes was performed using Volocity software. A minimum of 15 cells were used for quantification in each sample. N = 3

3.2.5 Capsid protein expression leads to reduction in peroxisome numbers

To determine if the virus-induced effects on peroxisomes could be recapitulated by expression of capsid protein alone, we examined the localization and abundance of peroxisomes in A549 cells transfected with plasmids encoding DENV or WNV capsid proteins. Ectopic expression of enhanced green fluorescent protein (eGFP) was used as the negative control. As shown in Figure 3.8A, capsid protein expression caused clustering of peroxisomes in the perinuclear region similar to what was observed in infected cells. Moreover, the average number of peroxisomes in capsid-expressing cells was ~20% lower than those expressing eGFP (Figure 3.8B). Therefore, our findings suggest that capsid proteins are at least partially responsible for the altered peroxisome abundance during viral infection and that other viral determinants may also contribute to this process.

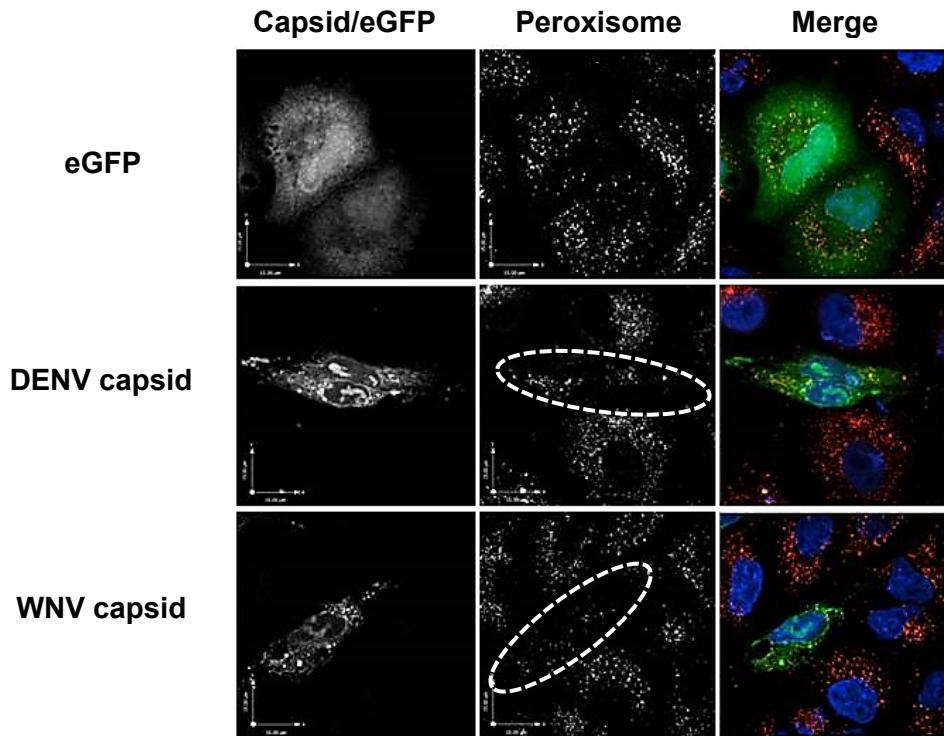
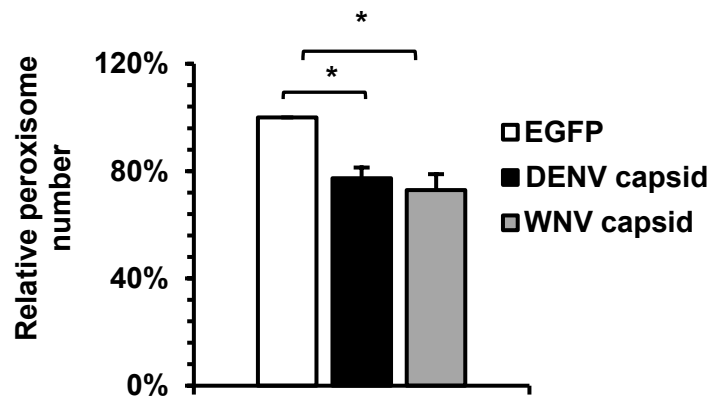
A**B**

Figure 3.8 Expression of capsid proteins lead to reduction in peroxisome numbers. A. A549 cells were transfected with plasmids encoding eGFP, DENV capsid or WNV capsids for 24 hrs. Cells were then processed for indirect immunofluorescence using guinea pig anti-DENV-2 capsid or anti-WNV capsid antibodies. Peroxisomes were detected using rabbit anti-SKL antibody. Primary antibodies were detected using donkey anti-guinea pig Alexa 488 and donkey anti-rabbit Alexa 546. Nuclei were stained with DAPI. Images were acquired using a spinning disk confocal microscope equipped with a 60X oil objective lens. Scale bar = 15 μ m. **B.** A minimum of 15 cells were analyzed for the average peroxisome numbers using Volocity software. * P <0.05; N = 3

3.2.6 *Flaviviruses suppress Type-III IFN induction*

A number of fairly recent studies have shown that the antiviral adaptor molecule MAVS localizes to peroxisomal membranes and mediates induction of Type- I and Type- III IFN response through peroxisomes (Dixit et al., 2010; Ferreira et al., 2016; Odendall et al., 2014). Accordingly, we predicted that reduction in peroxisome numbers would negatively affect the antiviral response initiated at this organelle. To test this hypothesis, we examined the ability of cells to stimulate IFN- λ expression during DENV and WNV infection. Figure 3.9A shows that, following transfection of cells with the viral dsRNA analogue poly(:C), levels of *ifn- λ* transcripts were dramatically increased in mock-infected cells. However, in cells infected with DENV or WNV, induction of *ifn- λ* transcripts was reduced by >80%.

Because expression of capsid proteins in the absence of other viral proteins can downregulate peroxisome numbers (Figure 3.8B), we next examined whether expression of these viral proteins dampened antiviral signaling. To increase the proportion of cells expressing capsid within an experimental population, a lentivirus delivery system was utilized to introduce DENV and WNV capsid into A549 cells. Unexpectedly, capsid expression did not significantly affect the relative induction of *ifn- λ* following poly(I:C) stimulation compared to cells expressing AcGFP (Figure 3.9B). These results indicate that capsid proteins alone are not sufficient to block IFN induction.

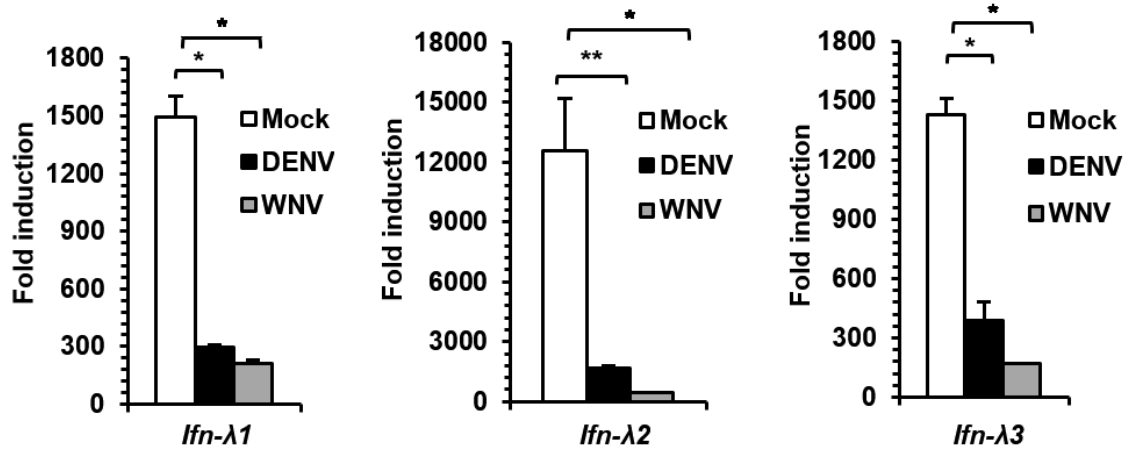
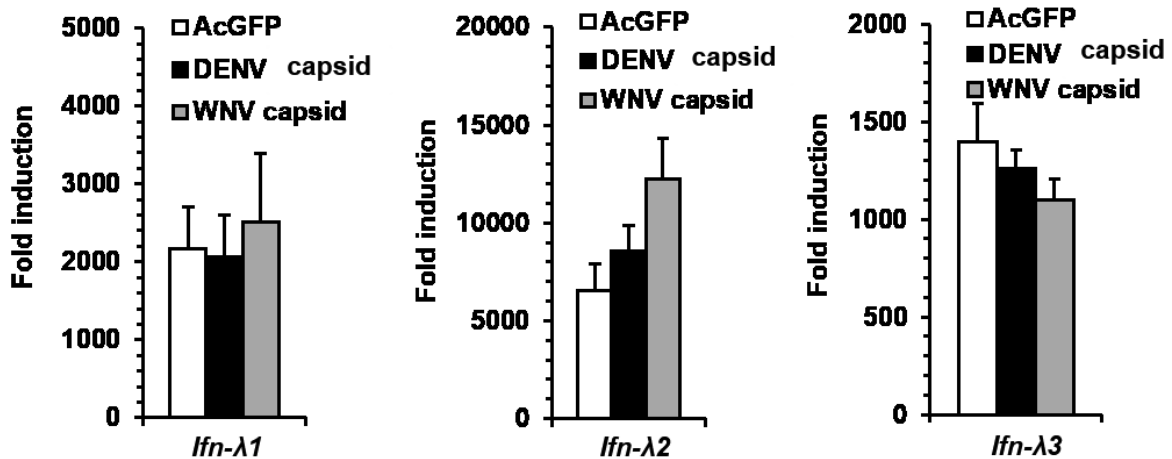
A**B**

Figure 3.9 Flavivirus infection inhibits type-III IFN (IFN- λ) production. **A.** A549 cells were infected with WNV or DENV-2 (MOI=2) for 10-12 hrs. Cells were then transfected with 4 μ g of poly(I:C) or pCMV-5 plasmid for 12 hrs to induce expression of *ifn- λ* genes. **B.** A549 cells were transduced with lentiviruses encoding AcGFP, myc-DENV capsid or myc-WNV capsids. Forty-eight hours later, cells were transfected with 4 μ g of poly(I:C) or pCMV-5 plasmid for 12 hrs to induce *ifn- λ* genes. Cell lysates were collected and processed for RNA extraction. The relative fold induction of *IFN- λ* genes was determined by qRT-PCR. * P <0.05, ** P <0.01; N = 4

3.2.7 The peroxisome biogenesis factor PEX19 plays a role in the IFN response

Since viral infection induced PEX19 degradation (Figure 3.3A), we reasoned that the virus-induced reduction of PEX19 could be a novel mechanism by which flaviviruses antagonize the host IFN system. To address this, we needed to determine whether PEX19 plays a role in the expression of IFN- λ . A549 cells were transiently transfected with siRNAs to knockdown expression of and then *ifn- λ* expression was measured following poly(I:C) treatment. The siRNAs reduced PEX19 protein by approximately 80% and this was associated with ~2-fold reduction in *ifn- λ* transcript levels compared to cells transfected with non-silencing siRNAs (Figure 3.10). These data suggest that PEX19 is somewhat important for IFN induction and that it could be a restriction factor for flavivirus replication. To test the latter, we measured viral titers from *PEX19*-silenced A549 cells infected with WNV and DENV. To our surprise, we observed a small but significant reduction in both DENV and WNV virion production in cells deficient in PEX19 particularly at 24 h.p.i (Figure 3.11). Taken together, these data suggest that while PEX19 regulates the host Type-III IFN response, it also plays a role in the viral life cycle.

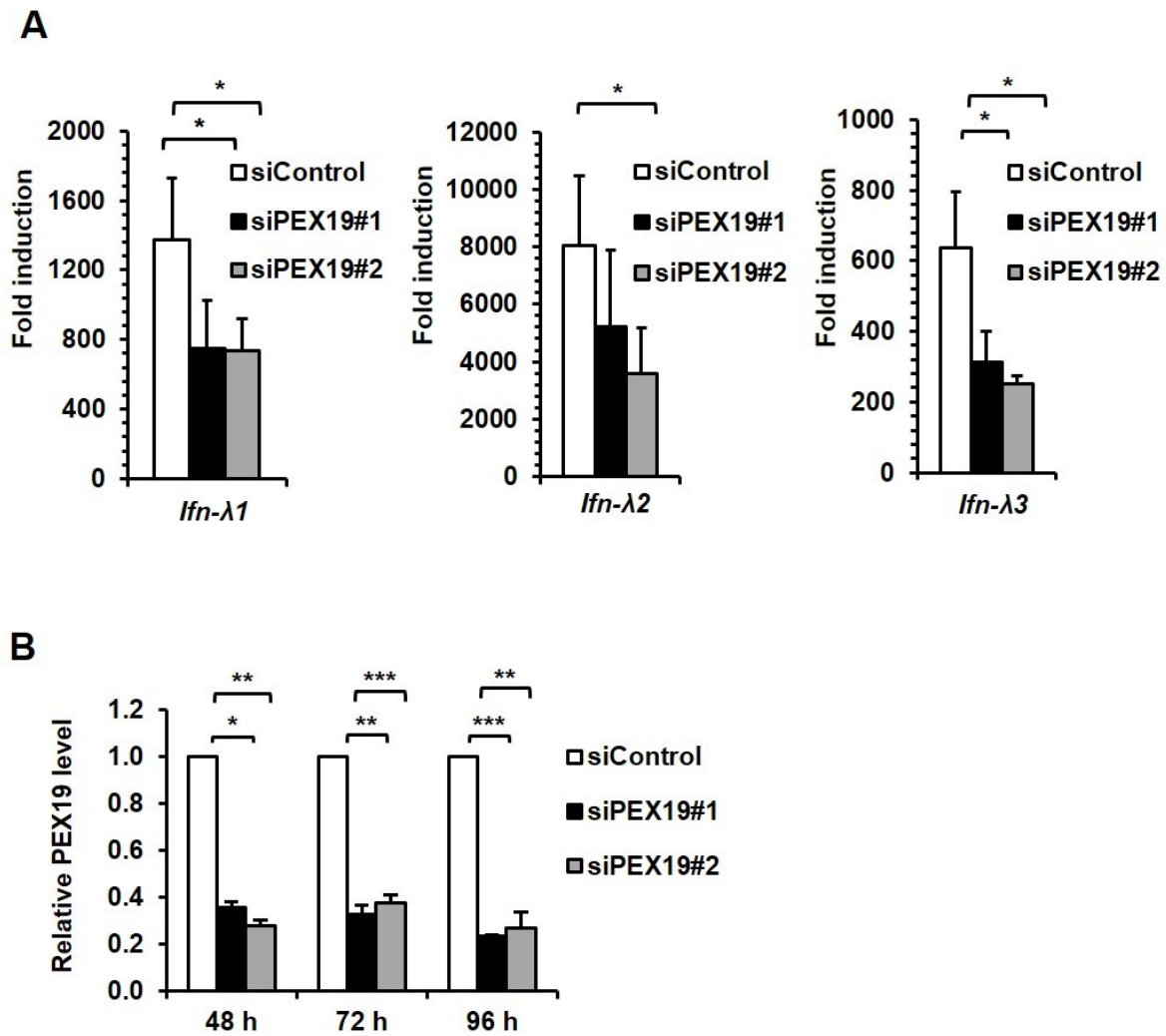


Figure 3.10 *PEX19*-silencing reduces *ifn-λ* expression. **A.** A549 cells were infected with WNV or DENV-2 (MOI = 2) for 10-12 hrs. Cells were then transfected with 4 μ g of poly(I:C) or pCMV-5 plasmid for 12 hrs to induce expression of *ifn-λ* genes. Cell lysates were processed for RNA extraction and immunoblotting. The relative fold induction of *ifn-λ* transcripts was determined by qRT-PCR. **B.** Following immunoblotting, the silencing efficiency of *PEX19* was determined using Image Studio Lite 5.0 software. * $P < 0.05$, ** $P < 0.01$, *** $P < 0.001$; N = 4

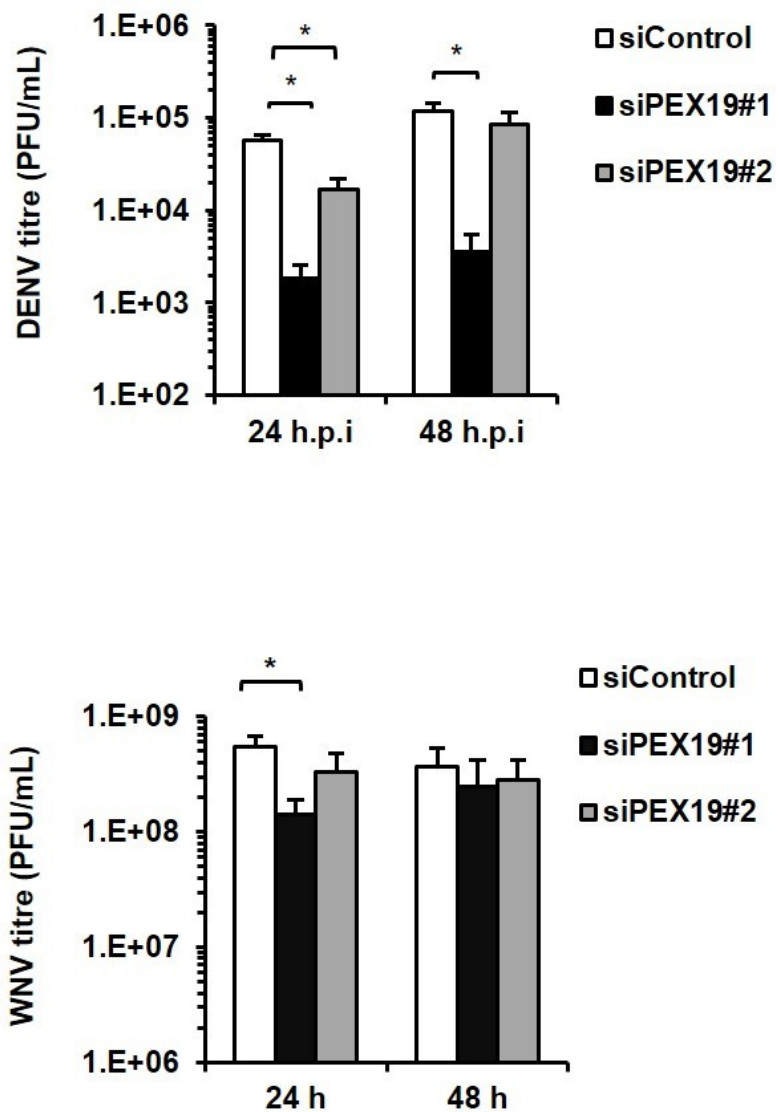


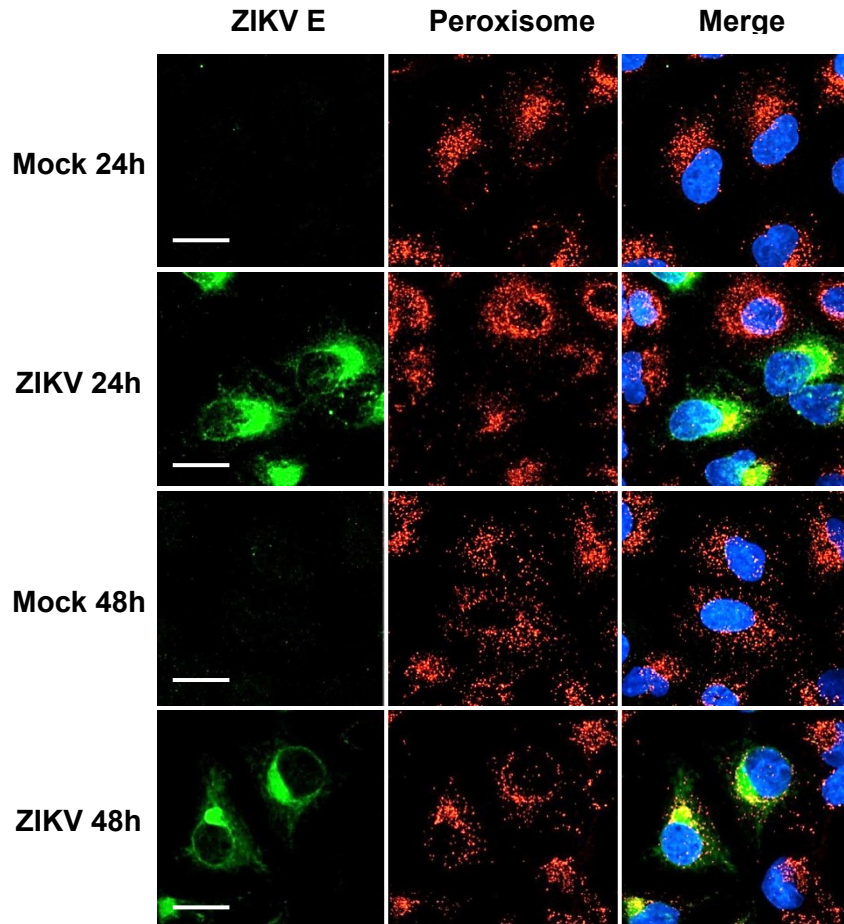
Figure 3.11 *PEX19*-silencing reduces DENV and WNV production. A549 cells were transfected with siControl or siRNAs specific for *PEX19* for 48 hrs. Cells were then infected with DENV-2 (top panel) or WNV (bottom panel) (MOI = 0.5). Cell supernatants were collected 48 h.p.i and viral titers were determined by plaque assay. * $p < 0.05$; N = 4

3.2.8 ZIKV infection leads to reduction in peroxisome abundance

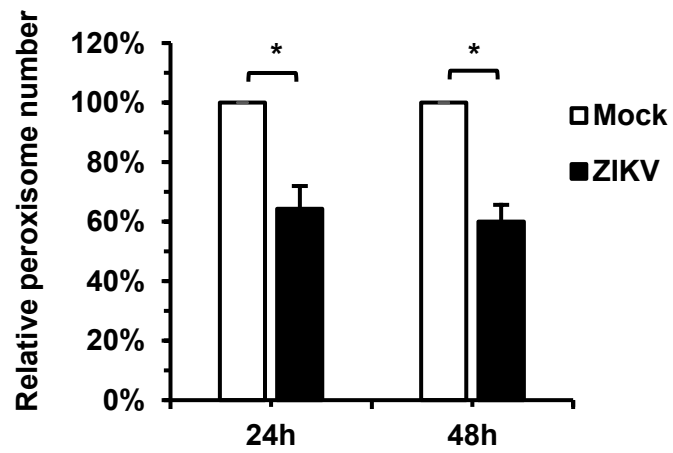
To determine whether other flaviviruses also alter peroxisome biogenesis, we investigated the effect of ZIKV infection on peroxisome abundance using confocal microscopy. As shown in Figure 3.12A, similar to what was observed for DENV and WNV, ZIKV infection induced clustering of peroxisomes into areas enriched for the viral E protein. Quantification of peroxisomes also revealed that ZIKV infection was associated with significant loss of peroxisomes at 24 and 48 h.p.i. (Figure 3.12B), suggesting that modulation of peroxisome biology may be a common phenomenon during flavivirus infection.

Figure 3.12 ZIKV infection reduces peroxisome numbers. **A.** A549 cells were infected with ZIKV (MOI = 2) for 24 hrs and 48 hrs. Fixed cells were processed for indirect immunofluorescence using a mouse anti-flavivirus E protein antibody. Peroxisomes were visualized by staining with a rabbit anti-PEX14 antibody. Primary antibodies were detected using donkey anti-mouse Alexa 488 and donkey anti-rabbit Alexa 546. Nuclei were stained with DAPI. Images were acquired using a spinning disk confocal microscope equipped with a 60X oil lens. Scale bar = 12 μ m. **B.** Quantification of peroxisome numbers was performed using Volocity software. A minimum of 15 cells were used per sample. * $P < 0.05$; N = 3

A



B



3.2.9 Different peroxisome biogenesis factors play different roles in IFN induction

Since we showed that PEX19 plays a role in the Type-III IFN system, we asked the question whether other peroxisomal biogenesis factors influence this antiviral pathway. To address this, we transiently silenced several peroxisomal proteins involved in regulation of membrane assembly (PEX3 and PEX16), matrix protein import (PEX5, PEX7 and PEX13) and organelle division (PEX11 β). Transfection of poly(I:C) was then used to stimulate IFN expression. Similar to what was observed with *PEX19*-silenced cells, expression of both IFN- β and IFN- λ 2 was significantly reduced in cells deficient in *PEX3* (Figure 3.13, top panel). While knockdown of *PEX7*, *PEX13* or *PEX11 β* did not alter IFN expression significantly, silencing of *PEX5* resulted in upregulation of IFNs (Figure 3.13, bottom panel). Although further experiments are needed to confirm these findings (e.g., by transfection of a different gene-specific siRNA), our data suggest that different peroxisomal biogenesis factors may play differential roles in the IFN system.

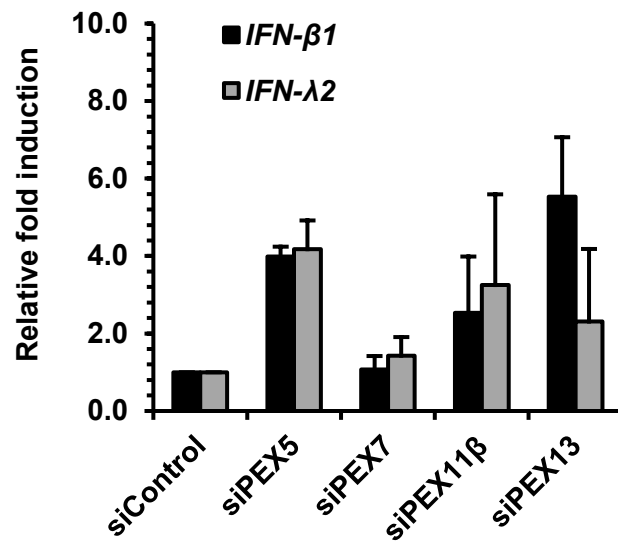
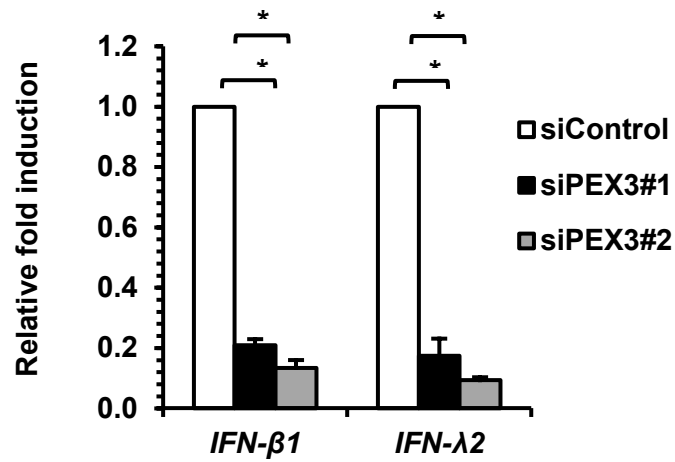


Figure 3.13 Transient silencing of *PEX* genes differentially affects induction of type-I and type-III IFNs. A549 cells were transfected with the indicated siRNAs. Forty-eight hours later, 2 μg of poly(I:C) was transfected into cells to stimulate IFN expression. Twelve-hours later, total RNAs were isolated and processed for qRT-PCR to determine the relative induction of *ifn-β1* and *ifn-λ2*. * $P < 0.05$. N = 3

3.3 Summary

In this chapter, we have shown that flaviviruses modulate peroxisome biogenesis to interfere with innate immune signaling. This is likely due in part to the interaction between capsid proteins and the peroxisome biogenesis factor PEX19. Initially, this novel host-virus interaction was confirmed in the context of DENV and WNV infections, during which a significant loss of PEX19 was also observed. Given the important function of PEX19 in peroxisome biogenesis, we postulated that binding of capsid proteins as well as reduction in PEX19 impairs peroxisome biogenesis. Indeed, altered peroxisome distribution as well as reduced peroxisome numbers were observed in DENV-, WNV-, and ZIKV-infected cells. These effects could largely be recapitulated by expression of the capsid proteins in transiently transfected cells, suggesting a role of this viral determinant in modulating peroxisome biology. Moreover, we revealed that potent suppression of *ifn-λ* transcript expression correlated with a decrease in peroxisome abundance and PEX19 during viral infection, an observation consistent with previous findings that peroxisomes are important antiviral signaling platforms (Dixit et al., 2010). We also identified a novel function for PEX19 in regulating the induction of Type-III IFNs. Preliminary findings suggest that other peroxisomal biogenesis factors may be important for the IFN pathway as well. Together, for the first time, our study demonstrates that manipulation of peroxisomes may be a common mechanism by which flaviviruses and potentially other viruses evade cellular antiviral defenses. Future studies will be focused on dissecting the molecular signaling events that occur at the peroxisomal membrane to regulate host antiviral signaling. In addition, investigating the effect of viral infection on other peroxisomal functions including redox homeostasis and lipid metabolism will also be useful.

Chapter 4 Zika virus inhibits the induction and downstream signaling of Type-I interferon response

A version of this chapter has been published in:

“*Kumar, A., ***Hou, S.**, Airo, A.M., Limonta, D., Mancinelli, V., Branton, W., Power, C., Hobman, T.C. 2016. Zika virus inhibits Type- I interferon production and downstream signaling. *EMBO Rep* 17:1766–1775.”

*Authors contributed equally

4.1 Rationale

Since its resurgence in late 2015, ZIKV has spread across the Americas, creating huge economic and health burdens in endemic areas. Depending upon the context, ZIKV infection can lead to serious complications including congenital defects and Guillain-Barré syndrome. Based on evidence from clinical and animal studies, this flavivirus possesses a unique ability to cross different anatomical barriers (e.g., the placenta and the fetal BBB) and replicate in diverse tissues and cell types (e.g., placenta, eyes, testes and fetal brain cells) (Adams Waldorf et al., 2016; Bhatnagar, 2016; Calvet et al., 2016; Govero et al., 2016; Mansuy et al., 2016; Miner et al., 2016). Together, these studies suggest that ZIKV is able to overcome host antiviral defenses and establish productive infections. Recently, several animal studies have demonstrated that mice with a defective IFN response suffer higher viral burdens and increased pathologies (Govero et al., 2016; Lazear et al., 2016; Miner et al., 2016; Tripathi et al., 2017), indicating that the host IFN system plays a paramount role in controlling ZIKV replication and pathogenesis.

As discussed in Section *1.2.1.2*, the IFN system consists of an induction phase, which leads to production and release of IFNs; and an IFN-dependent signaling phase, where binding of IFNs to receptors initiates a signaling cascade that induces transcription of a large panel of antiviral genes, ISGs. Previous studies have shown that productive replication of flaviviruses is linked to their ability to interfere with IFN response pathways. For example, DENV utilizes the viral protein NS5 to target STAT2, a critical transcriptional activator of ISGs, for proteasomal degradation; and the inability of DENV NS5 to reduce murine STAT2 renders these species refractory to viral infections (Ashour et al., 2009; Morrison et al., 2013; Tripathi et al., 2017). Among flaviviruses, ZIKV is more similar to DENV than most other members of this family and therefore, we sought to determine if and how ZIKV antagonizes the host IFN system to favor viral replication.

To investigate the molecular strategies used by ZIKV to suppress this cellular antiviral defense, we first examined the kinetics of dsRNA-stimulated antiviral signaling in response to ZIKV infection. In addition, we characterized viral replication and susceptibility to dsRNA and IFN treatments. Finally, we identified key signaling steps that were targeted by ZIKV as well as the viral determinants involved in the subversion of host IFN system.

4.2 Results

4.2.1 ZIKV inhibits the host cell IFN response

The IFN system provides one of the first lines of cellular defense against pathogens and therefore, many viruses have developed mechanisms to delay and/or suppress this antiviral program (Table 1.1). As a first step towards understanding how ZIKV may affect the IFN system, we monitored the kinetics of IFN induction and downstream signaling over the course of infection in A549 cells. As shown in Figure 4.1A, A549 cells activated expression of *ifn- β* and the ISG *ifit1* (interferon-induced protein with tetratricopeptide repeats 1) in response to ZIKV infection. IFIT1 is one of the antiviral effectors that is induced during flavivirus infection (Pichlmair et al., 2011; Szretter et al., 2012; Kimura et al., 2013). At 18 h.p.i., levels of *ifn- β* and *ifit1* induction were only increased <6-fold. In contrast, expression of these two genes was increased well over 100-fold at 24 and 48 h.p.i.. This may indicate that the virus delays the IFN response during early stages of infection.

To further investigate the interplay between ZIKV and the IFN system, we next assessed how ZIKV replication was affected by activation of an antiviral response before infection and at early time points post-infection. Cells were transfected with the viral dsRNA analogue poly(I:C) prior to or after viral infection and then relative levels of viral RNAs were assessed using qRT-PCR. As shown in Figure 4.1B (left panel), pre-treatment of A549 cells with poly(I:C) reduced

ZIKV replication by >80%, indicating that the virus was highly susceptible to a pre-existing antiviral state. In contrast, viral RNA level was largely unaffected when poly(I:C) was added after infection was established (Figure 4.1B, right panel), suggesting that the virus subverts the host antiviral response. To further test this scenario, we measured the levels of *ifn-β* and *ifit1* transcripts following poly(I:C) stimulation in cells infected with ZIKV. As expected, during ZIKV infection, induction of both *ifn-β* and *ifit1* was dramatically reduced (>80%) compared to mock-infected cells (Figure 4.1C), indicating that ZIKV actively blocks the dsRNA-stimulated antiviral signaling.

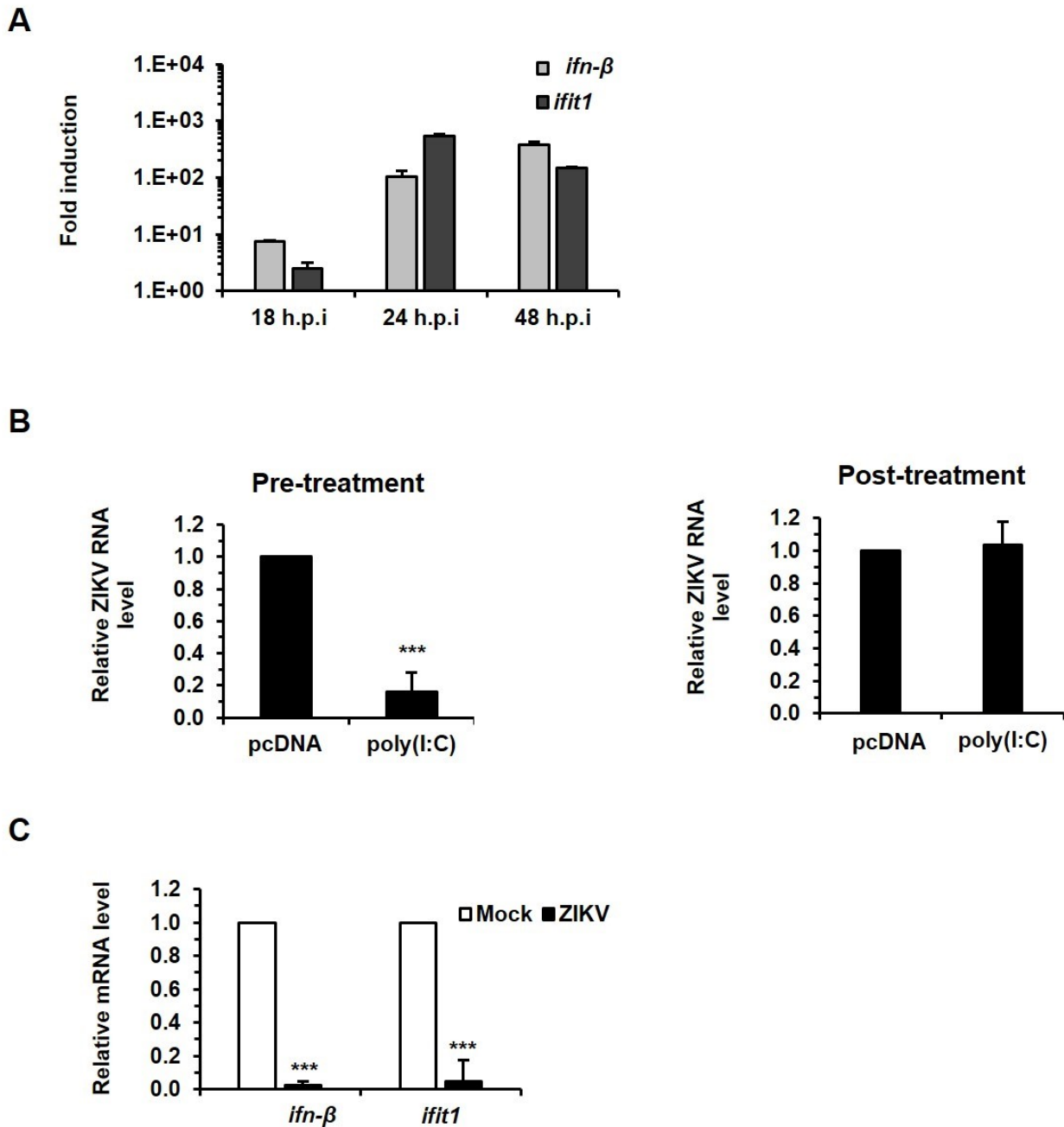


Figure 4.1 ZIKV inhibits the host IFN response. **A.** A549 cells were infected with ZIKV (MOI = 2) for the indicated time periods after which cell lysates were processed for qRT-PCR to determine the relative levels of *ifn-β* and *ifit1*. **B** and **C.** A549 cells were transfected with or without poly(I:C) for 6 hrs and then infected with ZIKV (MOI = 3) for 18 hrs (Pre-treatment). Alternatively, cells were infected with ZIKV first for 6 hrs and then transfected with poly(I:C) for 12 hrs (Post-treatment). Relative levels of **(B)** viral RNA as well as **(C)** *ifn-β* and *ifit1* transcripts were determined by qRT-PCR. *** $P < 0.001$; N = 3.

Next, luciferase reporter assays were performed to determine whether ZIKV inhibits the promoter activity of IFIT1, an ISG which can be induced by IRF3 and IFNs independently as it contains both an IRF3-binding site and an interferon-stimulated response element (*ISRE*) (Grandvaux et al., 2002). Consistent to what was observed with the effect of ZIKV infection on *ifn-β* and *ifit1* transcript levels, relative luciferase activity was repressed by 50% in ZIKV-infected cells compared to control cells (Figure 4.2A). Depending upon the flavivirus, different viral proteins have been implicated in subversion of the host IFN system (Table 1.1). To identify which ZIKV proteins antagonize the IFN response, we expressed individual viral proteins in HEK293T cells and measured poly(I:C)-induced IFIT1 promoter activity. Figure 4.2B shows that IFIT1 promoter activity was affected by multiple ZIKV proteins albeit to varying degrees. The strongest suppression (~70%) was observed in cells expressing NS5 while moderate inhibition (~40%) was observed in E- or NS4A-expressing cells. Together, these data indicate that ZIKV deploys effective countermeasures to the host IFN system, primarily through the actions of viral proteins E, NS4A and NS5.

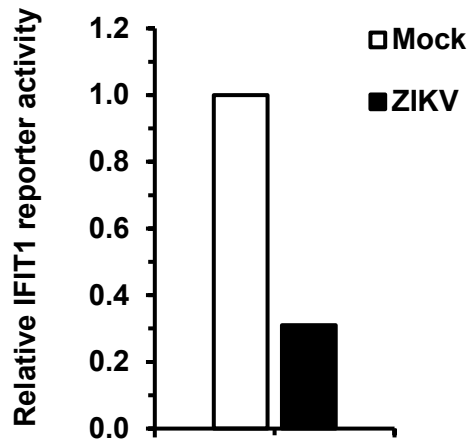
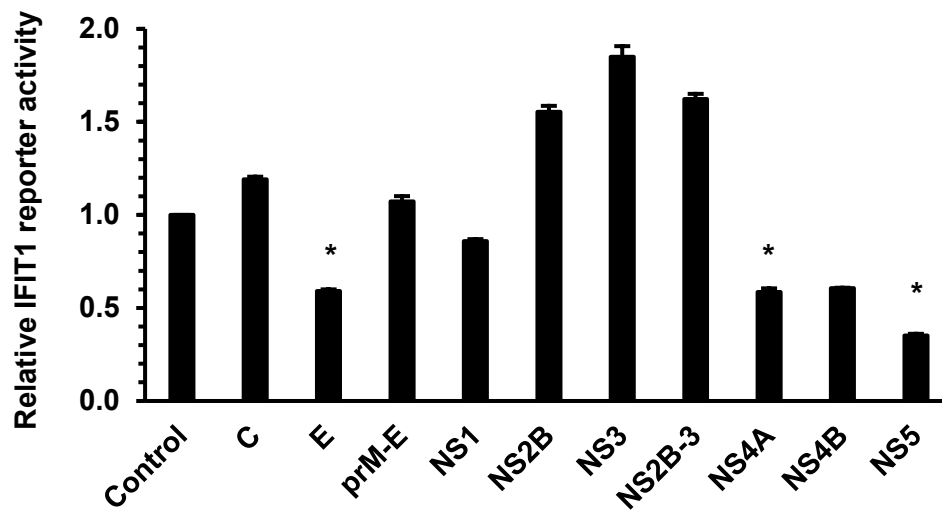
A**B**

Figure 4.2 Multiple ZIKV proteins inhibit IFIT1 promoter activity. **A.** A549 cells were infected with ZIKV (MOI = 5) for 16 hrs and then co-transfected with plasmids encoding IFIT1 promoter-driven firefly luciferase, constitutively active renilla luciferase construct as well as poly(I:C). Cell lysates were harvested and processed for luciferase activity. N = 2. **B.** HEK293T cells were transfected with plasmids encoding individual ZIKV proteins, an IFIT1 promoter-driven firefly luciferase, renilla luciferase and poly(I:C). Cell lysates were then harvested and subjected to luciferase assays. * $P < 0.05$; N = 3

4.2.2 ZIKV inhibits the induction of Type- I IFN expression

As indicated by the repressed promoter activity of IFIT1 (Figure 4.2A), an ISG whose expression can be triggered by IRF3 and IFNs independently (Grandvaux et al., 2002), ZIKV may interfere with the induction and/or downstream signaling of the IFN response. To identify the signaling step(s) targeted by ZIKV, we next asked the question whether and how IFN induction may be affected. To address this, poly(I:C)-induced IFN- β -driven promoter activity was measured during ZIKV infection. Consistent with what was observed with *ifn- β* transcripts, the activity of the IFN- β -dependent promoter was reduced almost-10 fold in ZIKV-infected cells (Figure 4.3A) indicating that the virus inhibits the induction of Type- I IFN response. Since efficient expression of IFN- β requires the transcription factors IRF3 and NF κ B, we next examined the effect of infection on IRF3-driven and NF κ B-driven promoters. Similar to the IFN- β -dependent promoter, poly(I:C)-induced activation of IRF3- and NF κ B-dependent transcription was suppressed (>90% and 75% respectively) by ZIKV infection (Figure 4.3A).

To identify the specific viral component(s) that interfere with Type- I IFN production, we measured the promoter activities driven by IFN- β , IRF3 and NF κ B in HEK293T cells expressing individual ZIKV proteins. The only viral protein which significantly reduced NF κ B-dependent transcriptional activity was NS5 and the effect was moderate (Figure 4.3B). In contrast, three viral proteins, NS1, NS4A and NS5, suppressed the activities of IFN- β - and IRF3-dependent promoters; NS5 had the greatest effect (Figure 4.3B). Interestingly, NS2A expression augmented NF κ B-mediated promoter function by >2-fold (Figure 4.3B), possibly implicating this viral protein in pro-inflammatory pathways (Hamel et al., 2017). Taken together, these data suggest that the viral proteins NS1, NS4A and NS5 act to suppress IFN production during ZIKV infection.

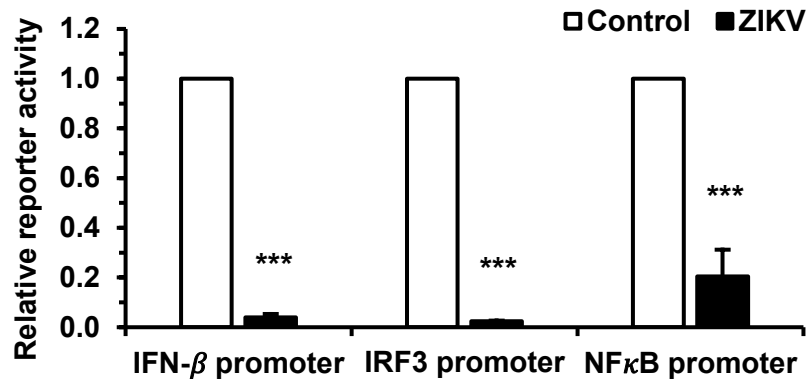
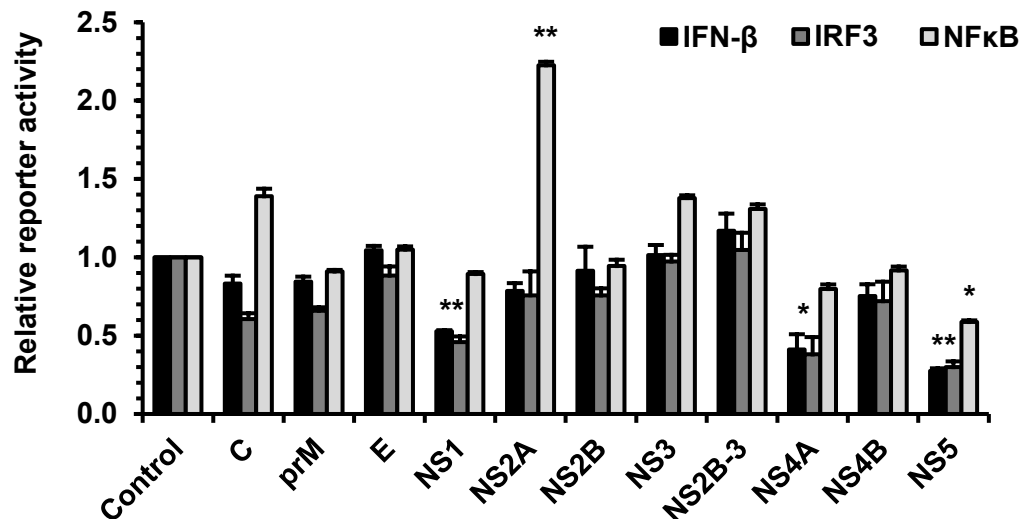
A**B**

Figure 4.3 ZIKV blocks the induction of type-I IFN response. **A.** A549 cells were infected with ZIKV (MOI = 5) for 16 hrs and then transfected with the indicated promoter-driven firefly luciferase plasmids and a constitutively active renilla luciferase construct, as well as 1 μ g of poly(I:C). After 8 hrs, cell lysates were harvested and processed for luciferase assay. **B.** HEK293T cells were transfected with plasmids encoding individual ZIKV proteins, an IFN- β , IRF3 or NF κ B promoter-driven firefly luciferase plasmid and a constitutively active renilla luciferase construct, as well as 0.4 μ g of poly(I:C). Twenty-four hours later, cell lysates were harvested and subjected to luciferase assay. *C* = capsid; *E* = envelope, * P <0.05, ** P <0.01, *** P <0.001; $N = 3$

To gain further insights into how ZIKV proteins interfere with Type- I IFN expression, we measured the effect of NS1, NS4A and NS5 on IFN- β - and IRF3-driven promoter activities following induction by over-expression of TBK1 or a constitutively active IRF3 (IRF3(5D)). TBK1 is a critical mediator of IFN induction by phosphorylating IRF3; it is shown to be targeted by DENV as well as WNV (Dalrymple et al., 2015). Data from luciferase reporter assay indicate that all three ZIKV proteins suppressed TBK1-stimulated IFN- β - and IRF3-mediated promoter activities (Figure 4.4). In cells expressing NS1, both reporter activities were rescued upon induction by IRF3(5D) expression. In contrast, NS4A and NS5 retained their abilities to inhibit both reporter activities in IRF3(5D)-expressing cells (Figure 4.4). These data suggest that repression of IFN induction by ZIKV NS1, NS4A and NS5 occurs at the TBK1 level and that NS4A and NS5 may also deploy mechanisms to subvert signaling downstream of IRF3 activation.

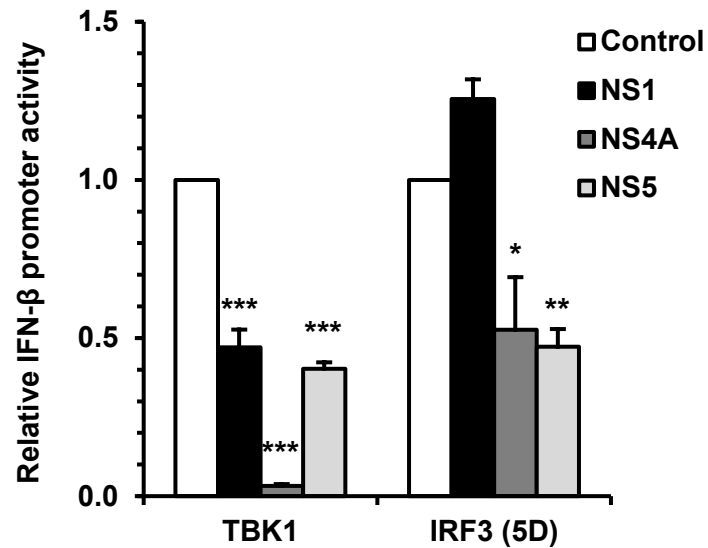
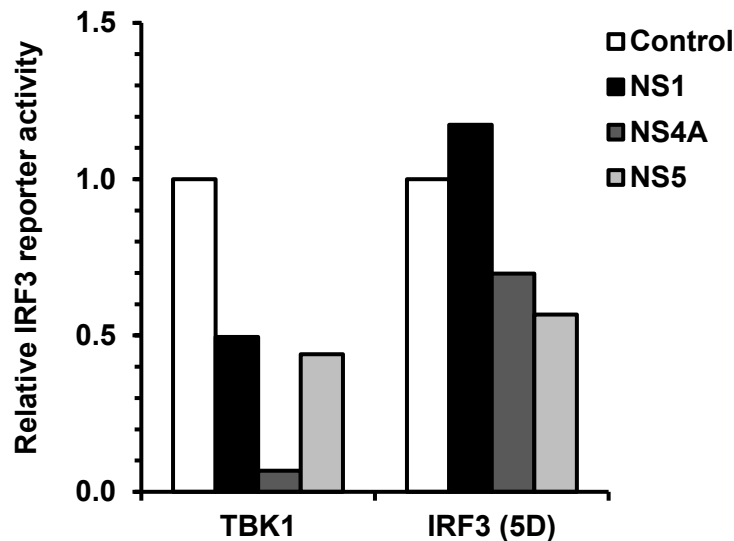
A**B**

Figure 4.4 ZIKV NS1, NS4A and NS5 block TBK1-mediated IFN induction. A. HEK293T cells were co-transfected with plasmids encoding ZIKV NS1, NS4A or NS5, an IFN- β promoter-driven firefly luciferase plasmid and a constitutively active renilla luciferase construct, as well as 0.5 μ g of plasmids encoding TBK1 or a constitutively active form of IRF3(5D). Twenty-four hours later, cell lysates were harvested and subjected to luciferase assay. * P <0.05, ** P <0.01, *** P <0.001; N = 3. **B.** The same experimental procedure was performed as described in (A) with the exception that the IFN- β luciferase reporter construct was replaced by an IRF3 promoter-driven firefly luciferase plasmid. N = 2

4.2.3 ZIKV blocks Type-I and -III IFN signaling

Initiation of the IFN effector phase is dependent on the interaction between IFNs and their cognate receptors, which then leads to transcriptional activation of ISGs with diverse antiviral functions (Figure 1.4). Due to the potent antiviral effect of IFNs, flaviviruses have evolved ways to interfere with the IFN-dependent signaling cascade (Table 1.1).

To understand how ZIKV modulates IFN signaling, we first determined whether virus replication is sensitive to IFN treatment administered before or after viral infection has started. The qRT-PCR data in Figure 4.5A (left panel) indicate that ZIKV replication was inhibited by pre-treatment of cells with Type- I (IFN- α), Type- II (IFN- γ), and Type- III (IFN- λ) IFNs. While Type- I and -III IFNs reduced replication by ~10-fold, Type-II IFN only inhibited replication by 50%. In contrast, addition of IFNs after virus infection was established did not significantly affect replication (Figure 4.5A, right panel). These data suggest that although ZIKV is sensitive to the IFN-stimulated antiviral response, the virus can efficiently block IFN signaling after infection is established.

To determine which IFN signaling pathway is affected by virus infection, we measured the levels of *ifit1* transcripts in ZIKV-infected cells following IFN stimulation. qRT-PCR analyses revealed that *ifit1* induction by IFN- α and IFN- λ , but not IFN- γ , were suppressed >80% in ZIKV-infected cells (Figure 4.5B). This suggests that the virus targets specific IFN signaling pathways (i.e. Type-I and -III but not Type- II).

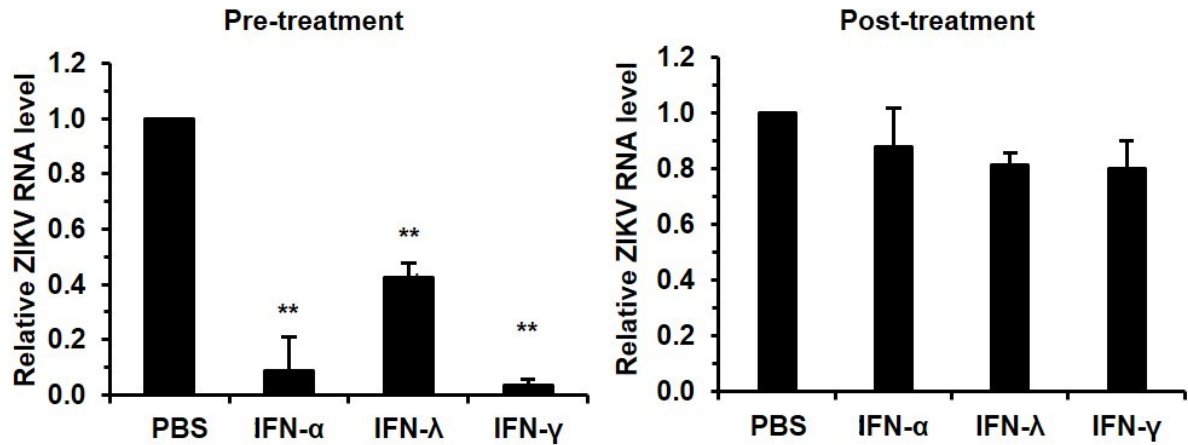
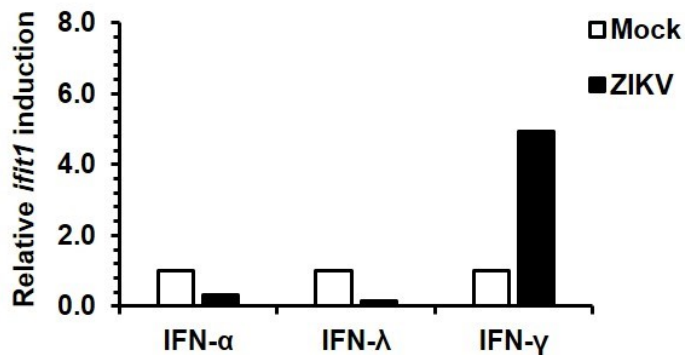
A**B**

Figure 4.5 ZIKV suppresses Type-I and -III IFN signaling. **A.** A549 cells were treated with PBS (as negative control), IFN- α (100 U/mL), IFN- λ (200 ng/mL) or IFN- γ (10 U/mL) for 6 hrs, after which they were infected with ZIKV (MOI = 3) for 18 hrs (Pre-treatment). Alternatively, cells were first infected with ZIKV for 6 hrs followed by treatment with IFNs for 12 hrs (Post-treatment). Total RNA was isolated and relative ZIKV RNA levels were determined by qRT-PCR. * P <0.05, ** P <0.01; N = 3. **B.** A549 cells were infected with ZIKV (MOI=3) for 6 hrs and then treated with PBS or IFNs for 12 hrs using the same concentrations as described in (A). Total RNAs were isolated and relative *ifit1* levels were determined by qRT-PCR. N = 2.

To confirm this finding, we utilized luciferase reporter assays to measure Type-I/-III as well as Type- II IFN signaling through the *ISRE* and *GAS* promoters respectively. Consistent with the data in Figure 4.5B, activity of the *ISRE* promoter was reduced by 50% in ZIKV-infected cells whereas *GAS*-dependent transcription was not significantly affected (Figure 4.6A). Taken together, these data indicate that ZIKV selectively impedes Type-I and -III IFN signaling; moreover, they suggest that a host factor(s) common to Type- I and -III but absent from the Type-II IFN pathway could be a target of ZIKV.

To determine which viral components subvert(s) IFN signaling, we expressed individual ZIKV proteins in HEK293T cells and examined their effects on *ISRE* promoter in response to IFN- α stimulation. While expression of prM-E had a significant but modest effect, NS5 strongly reduced (>90%) *ISRE*-dependent IFN signaling (Figure 4.6B). In summary, these data indicate that ZIKV interferes with the effector phase of Type-I and -III IFN response, a process mediated primarily by the viral protein NS5.

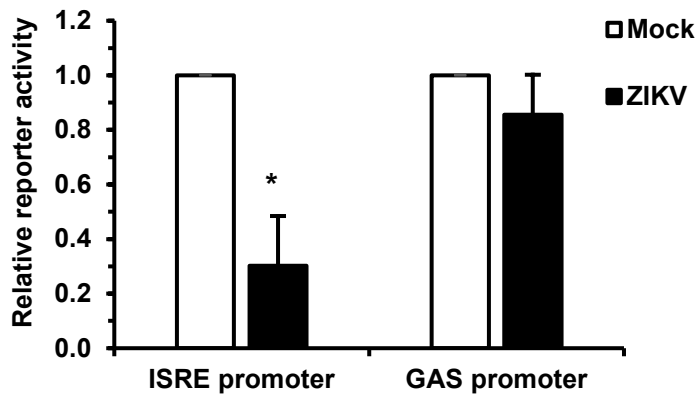
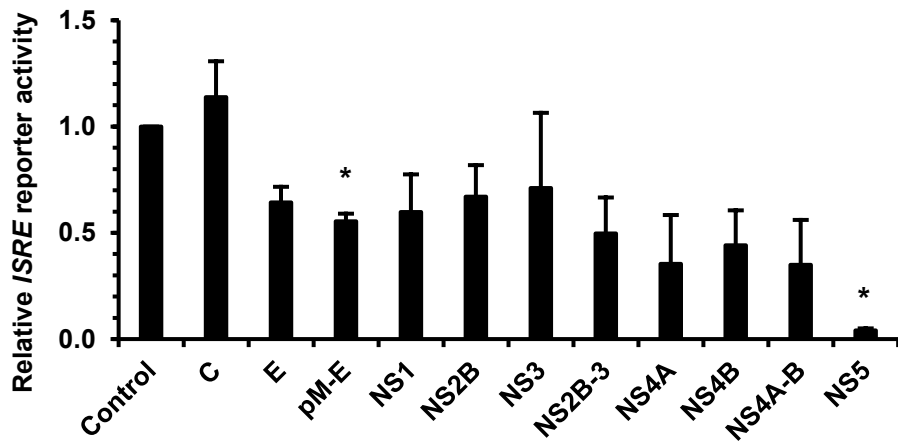
A**B**

Figure 4.6 ZIKV NS5 blocks Type-I and -III IFN signaling. **A.** A549 cells were infected with ZIKV (MOI = 5) for 6 hrs and then transfected with an *ISRE*- or *GAS*-promoter-driven firefly luciferase construct together with a constitutively active renilla luciferase construct. Sixteen-hours later, cells were treated with IFN- α (100 U/ml) or IFN- γ (10 U/ml) for 2 hrs to stimulate IFN signaling. Cell lysates were harvested and processed for luciferase assay. **B.** HEK293T cells were transfected with ZIKV protein expression constructs together with an *ISRE* promoter-driven firefly luciferase plasmid as well as a constitutively active renilla luciferase construct. After 24 hrs, they were treated with IFN- α (100 U/mL) to stimulate IFN signaling. Ten-hours later, cell lysates were harvested and subjected to luciferase assay. *C* = capsid; *E* = envelope. * $P < 0.05$; N = 3

4.2.4 ZIKV infection induces proteasomal degradation of human STAT2

STAT2 is an essential transcriptional activator of ISGs induced by Type-I and Type-III IFNs; however, it is not involved in the Type-II IFN signaling cascade (Figure 1.4). Accordingly, we speculated that interfering with STAT2 could be a critical mechanism by which ZIKV inhibits Type-I and Type-III IFN pathways. To test this possibility, we first examined whether levels of STAT2 protein were affected by ZIKV infection. Immunoblotting revealed that STAT2 was almost completely abolished in ZIKV-infected cells by 24 h.p.i. while STAT1 levels remained unchanged (Figure 4.7A). To further verify this finding, we performed confocal microscopy and monitored STAT2 nuclear translocation in A549 cells as well as primary human fetal astrocytes (HFAs), a cell type shown to have physiological relevance in ZIKV pathogenesis (Hamel et al., 2017). As shown in Figure 4.7B, almost all of the mock-infected cells contained nuclear STAT2 following IFN- α treatment. However, in ZIKV-infected A549 and primary HFAs, very little STAT2 signal was detected, confirming that ZIKV indeed induces loss of STAT2.

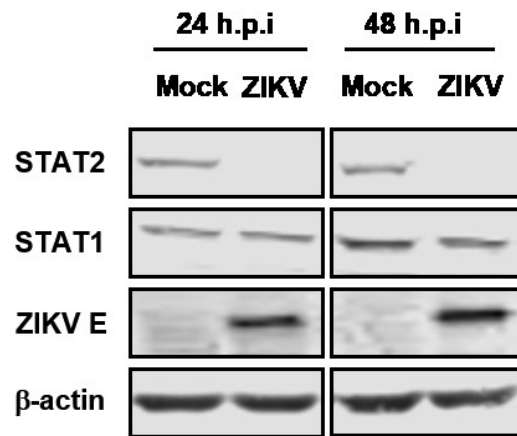
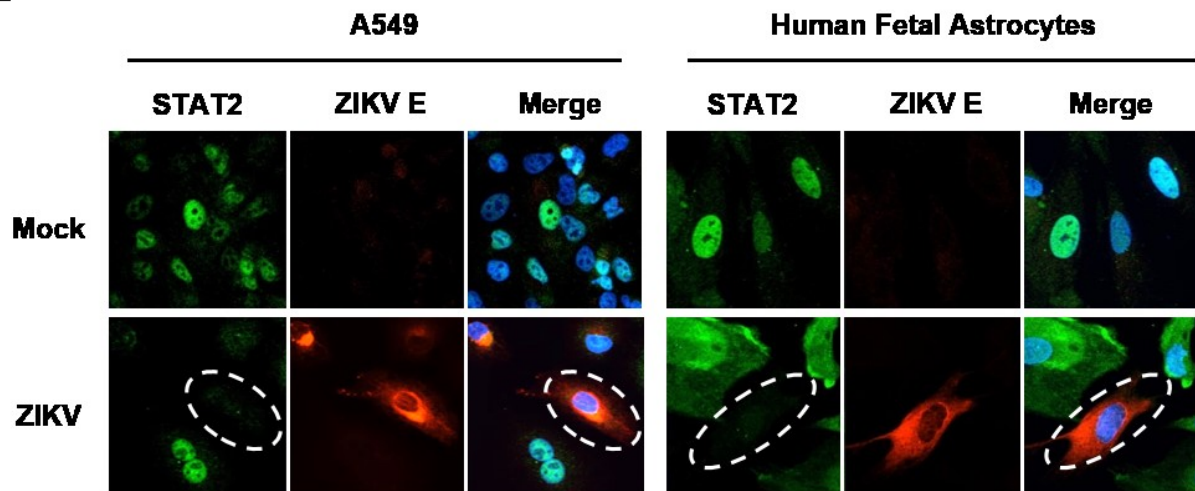
A**B**

Figure 4.7 ZIKV NS5 induces STAT2 degradation in human cells. **A.** A549 cells were infected with ZIKV (MOI = 5) for 24 and 48 hrs, after which cell lysates were processed for SDS-PAGE and immunoblotting using antibodies to endogenous STAT1 and STAT2. Levels of the viral envelope (E) protein and cellular β -actin were used as the infection and loading controls respectively. **B.** A549 cells (MOI = 2) or human primary fetal astrocytes (MOI = 5) were infected with ZIKV for 24 and 48 hrs respectively, after which IFN- α (100 U/mL) was added for 2 hrs to stimulate STAT nuclear translocation. Cells were then processed for indirect immunofluorescence. STAT2 was detected using a rabbit anti-human STAT2 antibody while infected cells were identified by staining with a mouse anti-E protein antibody. Primary antibodies were detected using donkey anti-rabbit Alexa 488 and donkey anti-mouse Alexa 546. Nuclei were stained with DAPI. Images were acquired on a spinning disk confocal microscope equipped with a 40X oil objective lens. Dashed line white circles indicate ZIKV-infected cells. N = 3

To gain insight into the nature of virus-induced STAT2 degradation, we treated cells with inhibitors of the proteasome (MG132 and epoxomicin) and lysosome (bafilomycin-A1; BAF-A1) and monitored STAT2 levels during ZIKV infection. Immunoblotting analyses in Figure 4.8 show that ZIKV-induced degradation of STAT2 was largely abrogated by proteasome inhibitors, whereas BAF-A1 treatment did not prevent loss of STAT2. Taken together, these data indicate that inhibition of IFN signaling is mediated in part by ZIKV-induced degradation of STAT2 through the proteasome.

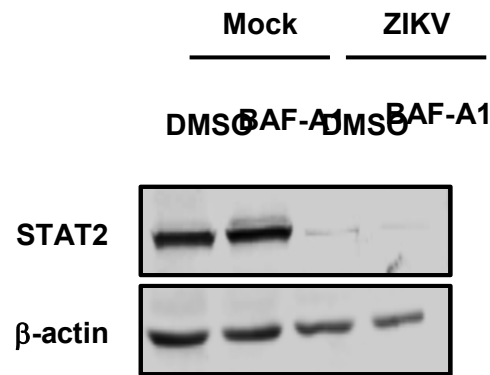
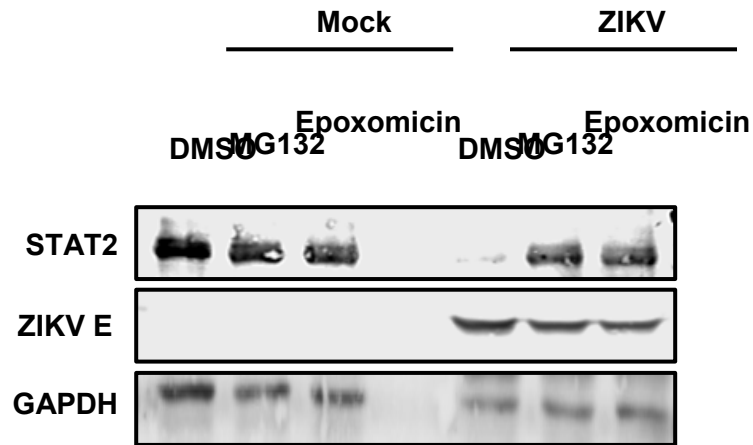


Figure 4.8 ZIKV-induced degradation of STAT2 requires the proteasome. A549 cells were infected with ZIKV (MOI = 5) for 24 hrs and then treated with DMSO (as the negative control), MG132 (20 μ M) or epoxomicin (400 nM) for 12 hrs (top panel). In parallel, A549 cells infected with ZIKV for 24 hrs were treated with baflomycin-A1 (BAF-A1; 400 nM) for 12 hrs (bottom panel). Cell lysates were harvested and processed for SDS-PAGE and immunoblotting. Endogenous STAT2 was detected with a rabbit anti-human STAT2 antibody. Cellular GAPDH or β -actin and ZIKV envelope (E) protein were detected by the appropriate antibodies and used as the loading and infection controls respectively; N = 3

4.2.5 ZIKV infection does not induce degradation of mouse STAT2

Previous studies have shown that DENV-induced degradation of STAT2 is species-specific; that is, while the virus causes degradation of human STAT2, the murine counterpart is resistant to DENV (Ashour et al., 2010). To determine whether ZIKV can induce STAT2 degradation in the murine system, we examined IFN- α -stimulated STAT2 nuclear translocation in mouse embryonic fibroblasts (MEFs) using confocal microscopy. Microscopy analysis rather than immunoblotting was utilized because ZIKV poorly infects MEFs and therefore single-cell based detection was the preferable assay.

Following treatment with IFN- α , STAT2 was observed in the nuclei of mock and ZIKV-infected MEFs (Figure 4.9A). This suggests that ZIKV does not induce degradation of STAT2 nor affects its translocation to the nucleus in mouse cells. As such, STAT2 could be a major restriction factor of ZIKV replication in mice. Consistent with this theory, transient silencing of STAT2 in MEFs by siRNA resulted in increased replication of ZIKV (Figure 4.9B). Together, these data reaffirm the importance of IFN signaling in limiting ZIKV infection. Moreover, they support the possibility that STAT2-deficient mice could serve as an alternative animal model for flavivirus pathogenesis studies. Indeed, soon after the publication of our study, another research group established a STAT2^{-/-} mouse model for ZIKV infection, which has revealed novel insights into viral virulence and pathogenesis (Tripathi et al., 2017).

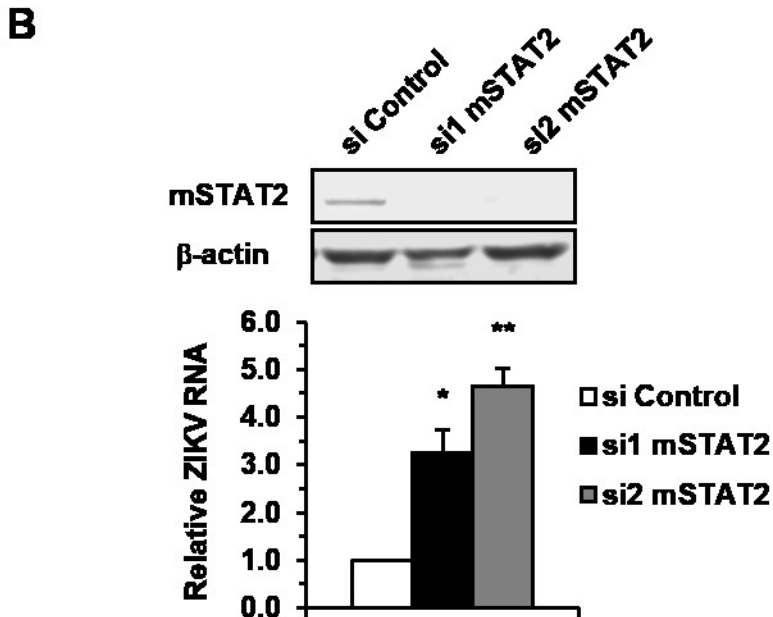
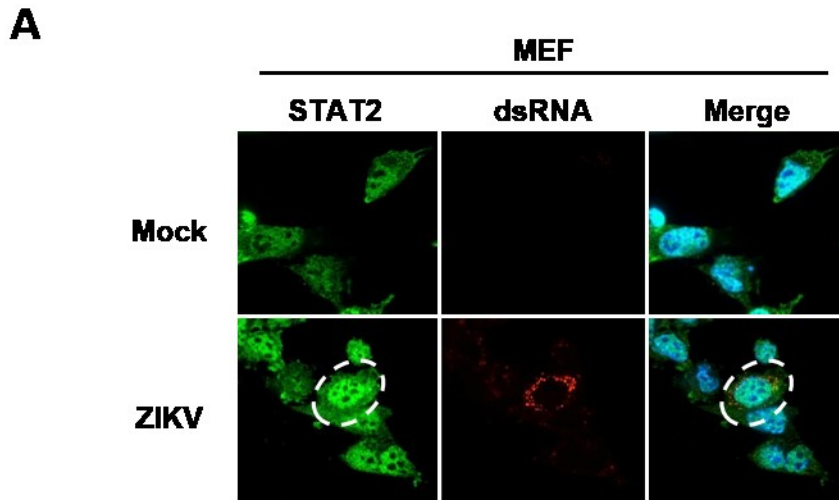


Figure 4.9 ZIKV does not induce degradation of murine STAT2. **A.** Mouse embryonic fibroblasts (MEF) were infected with ZIKV (MOI = 5) for 48 hrs after which IFN- α (200 U/mL) was added for 2 hrs. Samples were then processed for indirect immunofluorescence. Rabbit anti-mouse STAT2 and mouse anti-dsRNA antibodies were used to detect STAT2 and infected cells respectively. Primary antibodies were detected using donkey anti-rabbit Alexa 488 and donkey anti-mouse Alexa 546. Nuclei were stained with DAPI. Images were acquired on a spinning disk confocal microscope with a 40X oil objective lens. Dashed-line white circles indicate ZIKV-positive cells. **B.** Mouse STAT2 (mSTAT2) in MEFs was transiently depleted by transfection of specific siRNAs for 48 hrs, after which cells were infected with ZIKV (MOI = 5) for another 48 hrs. Silencing efficiency was determined by immunoblotting with mouse anti-STAT2. Levels of β -actin serve as the loading control. Relative ZIKV RNA was measured by qRT-PCR. * $P < 0.05$, ** $P < 0.01$; N = 3

4.2.6 ZIKV NS5 protein induces degradation of human STAT2

To identify the viral component(s) required for STAT2 degradation, we examined nuclear translocation of STAT2 in A549 cells expressing individual ZIKV proteins. Confocal microscopy was utilized to facilitate single cell-based analysis. This method was preferable because some of the viral proteins were found to be expressed at relatively low levels when immunoblotting was used for analyses. Figure 4.10 shows that with the exception of NS5, none of the viral proteins affected nuclear accumulation of STAT2 in IFN- α -treated cells. In NS5-expressing cells, the STAT2 signal was almost completely absent similar to what was observed in ZIKV-infected cells. This suggests that NS5 is the key determinant for inducing degradation of STAT2 during ZIKV infection.

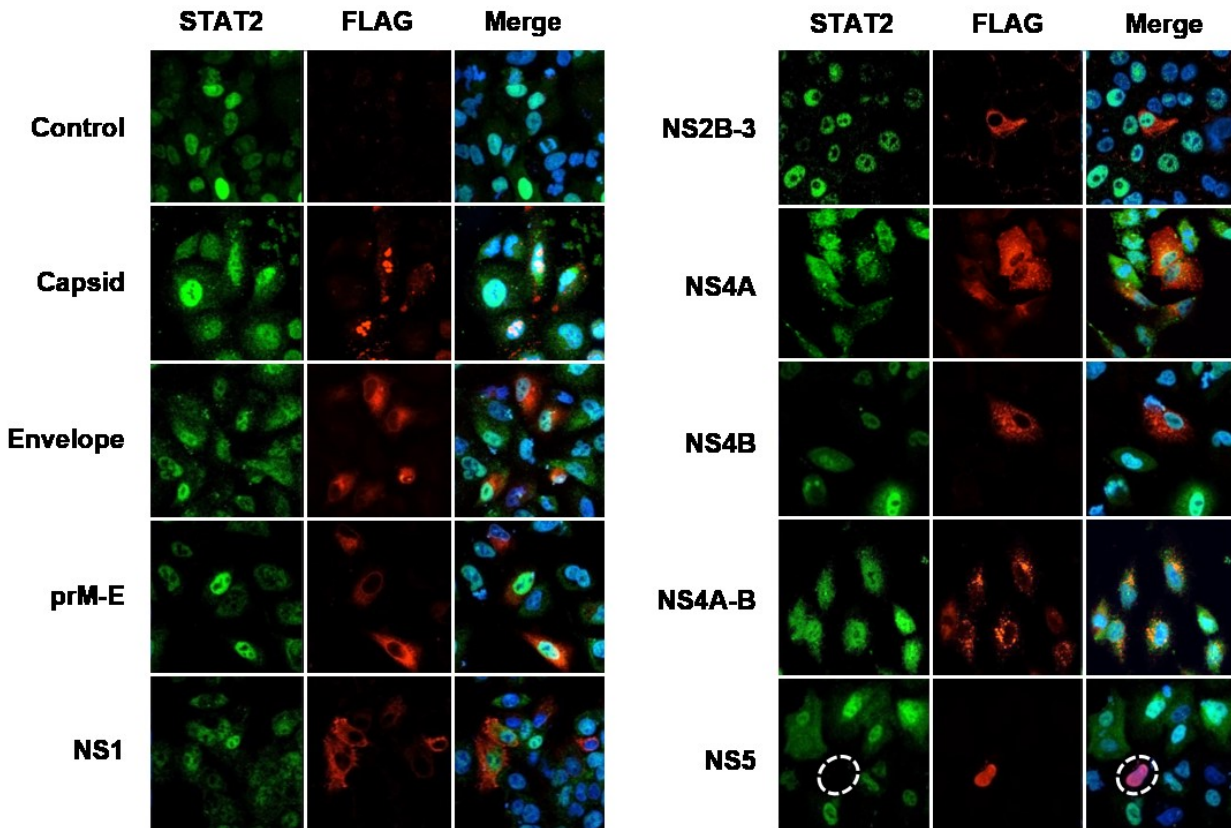
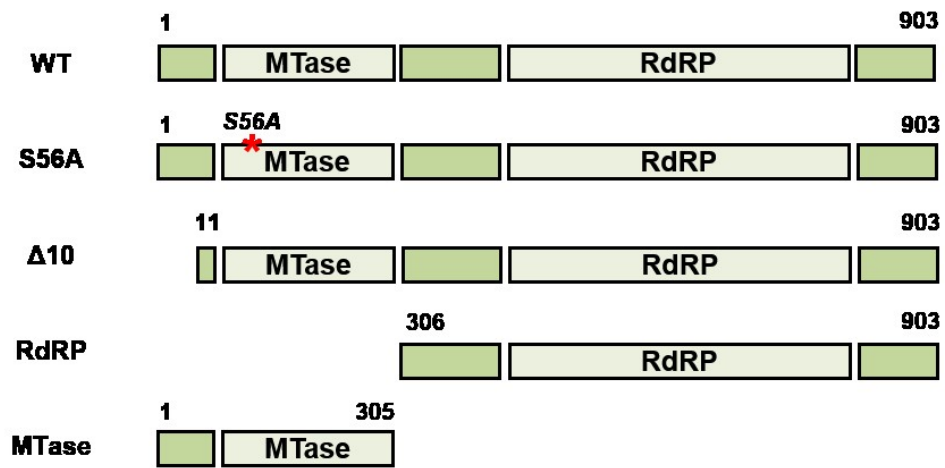
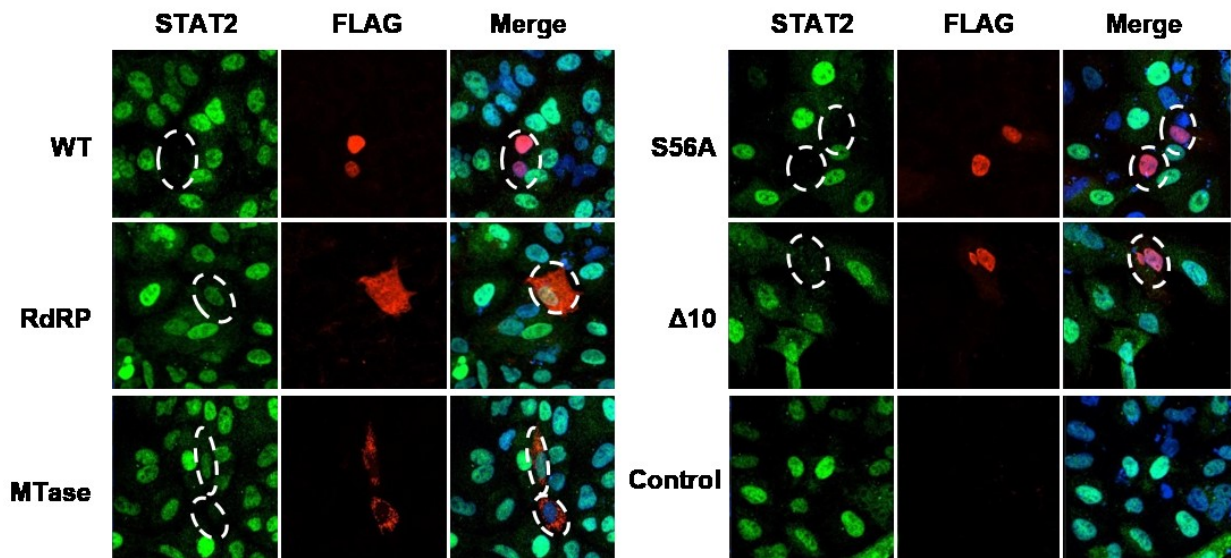
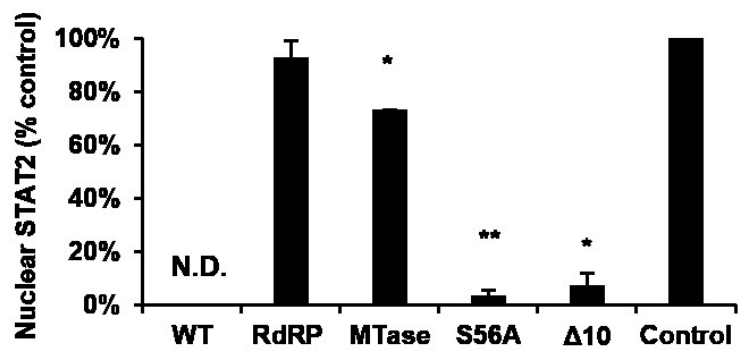


Figure 4.10 Expression of ZIKV NS5 induces STAT2 degradation in human cells. A549 cells were transfected with a control plasmid pcDNA-3.1 or plasmids encoding individual FLAG-tagged ZIKV proteins. At 48 hrs post-transfection, cells were treated with IFN- α (100 U/mL) for 2 hrs and then processed for indirect immunofluorescence. Rabbit anti-human STAT2 and mouse anti-FLAG antibodies were used to detect endogenous STAT2 and transfected cells respectively. Primary antibodies were detected using donkey anti-rabbit Alexa 488 and donkey anti-mouse Alexa 546. Nuclei were stained with DAPI. Images were acquired on a spinning disk confocal microscope with a 40X oil objective lens. NS5-positive cells are indicated by dashed line white circles; N = 3

To further investigate the nature of NS5-mediated STAT2 degradation, we transfected plasmids encoding a number of different NS5 constructs in A549 cells and examined their effect on STAT2 nuclear translocation. These NS5 constructs included a mutant lacking the amino-terminal 10 amino acid residues ($\Delta 10$), the methyltransferase (MTase) domain of NS5, the RNA-dependent RNA polymerase (RdRP) domain and a mutant lacking MTase activity (S56A) (Figure 4.11A). Of these constructs, only the $\Delta 10$ mutant induced loss of STAT2 to a degree that was similar to wild type NS5 (Figure 4.11B and C). This observation illustrates an important distinction between NS5 proteins of DENV and ZIKV. Specifically, unlike ZIKV NS5, the first 10 amino acid residues of DENV NS5 are required for degradation of STAT2 (Ashour et al., 2009).

With respect to the domain of ZIKV NS5 that mediates STAT2 degradation, the data are inconclusive. Specifically, while expression of the NS5 RdRP domain did not trigger STAT2 reduction, in many of the cells expressing the MTase domain, STAT2 signals were noticeably lower (Figure 4.11B). However, the effect of MTase domain on STAT2 was much less dramatic than the full length NS5 (Figure 4.11B), which indicate that other regions of this viral protein contribute to STAT2 degradation. Moreover, MTase activity was not required for STAT2 degradation as evidenced by the fact that expression of the S56A mutant retained the ability to efficiently degrade STAT2 (Figure 4.11C).

Figure 4.11 Neither the MTase nor the RdRP domain of ZIKV NS5 is sufficient to induce efficient degradation of STAT2. **A.** Schematic representation of the ZIKV NS5 expression constructs. **B.** A549 cells were transfected with a control plasmid pcDNA-3.1 or the NS5 expression constructs as shown in (A). At 48 hrs post-transfection, cells were treated with IFN- α (100 U/mL) for 2 hrs and then processed for indirect immunofluorescence. STAT2 and FLAG epitope-tagged proteins were detected using rabbit anti-human STAT2 and mouse anti-FLAG antibodies. Primary antibodies were detected using donkey anti-rabbit Alexa 488 and donkey anti-mouse Alexa 546. Nuclei were stained with DAPI. Images were acquired on a spinning disk confocal microscope with a 40X oil objective lens. NS5-positive cells are indicated by dashed line white circles. **C.** The percentage of cells containing nuclear STAT2 was determined using the Volocity image analysis software. A minimum of 20 cells were counted for each sample. *N.D.*= not detected. * P <0.05; $N = 3$

A**B****C**

4.2.7 ZIKV NS5 interacts with human STAT2 through its MTase domain

Since DENV NS5 was shown to interact with STAT2 (Ashour et al., 2009), we next explored potential interaction between ZIKV NS5 and this antiviral protein by co-immunoprecipitation assay. FLAG-tagged wild-type NS5 was expressed in HEK293T cells which were then treated with the proteasome inhibitor epoxomicin to ensure that sufficient amount of STAT2 was available for binding. Co-immunoprecipitation and immunoblotting revealed that STAT2 forms a stable complex with FLAG-NS5 (Figure 4.12A). As a first attempt to map the domain(s) of NS5 required for binding STAT2, we used the NS5 constructs described in Figure 4.10A for co-immunoprecipitation and immunoblotting. These analyses revealed that STAT2 interacts with the MTase domain of NS5 (Figure 4.12B). Moreover, neither the first 10 amino acids of NS5 nor the MTase activity was required for NS5-STAT2 interaction. Together, our data demonstrate that ZIKV NS5 interacts with STAT2 through the MTase domain, a process that is likely a key step in the eventual degradation of this antiviral protein during viral infection.

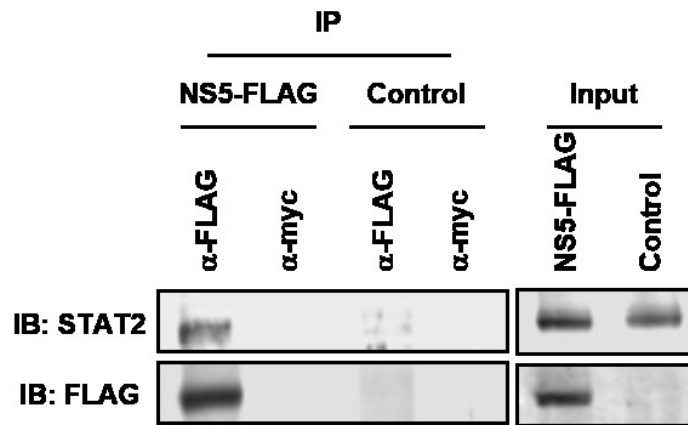
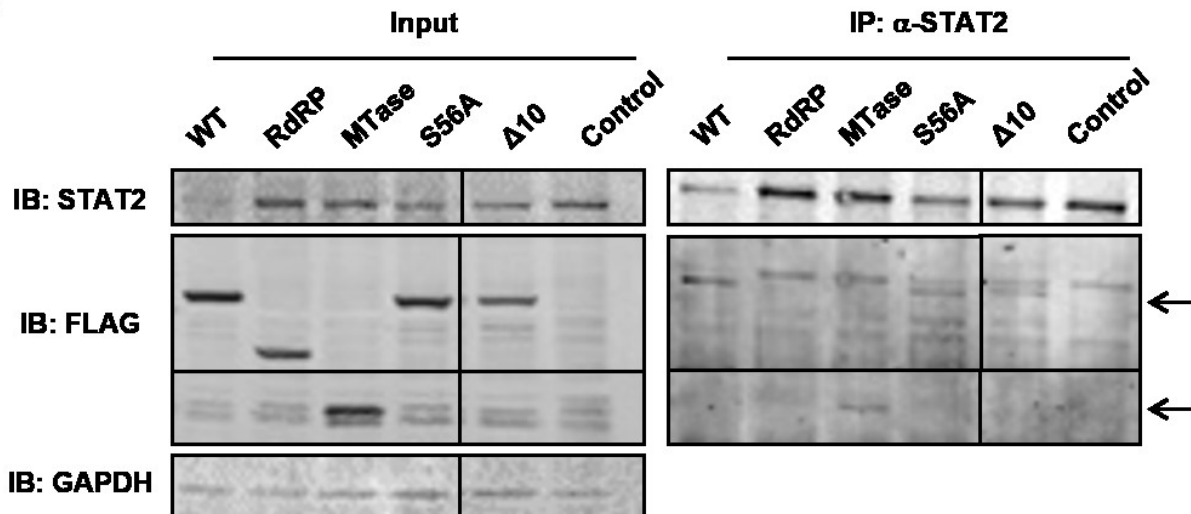
A**B**

Figure 4.12 ZIKV NS5 interacts with human STAT2. **A.** A549 cells were transfected with plasmids encoding FLAG-tagged ZIKV NS5 or a control plasmid pcDNA-3.1 for 24 hrs and then treated with epoxomicin (400 nM) for 24 hrs. Cells were harvested and processed for co-immunoprecipitation using mouse anti-FLAG or anti-myc antibodies followed by SDS-PAGE and immunoblotting. **B.** A549 cells were transfected with expression plasmids encoding FLAG-tagged wild type (WT) NS5, NS5 mutants or domains or a control plasmid (pcDNA-3.1) for 48 hrs. Cells were harvested and processed for co-immunoprecipitation using rabbit anti-human STAT2 antibody followed by SDS-PAGE and immunoblotting with anti-STAT2 and anti-FLAG. Levels of GAPDH serve as the loading control. Arrows indicate NS5 or NS5 mutants/domain co-immunoprecipitated with STAT2. *IP* = immunoprecipitation; *IB* = immunoblotting. Arrows indicate the co-IP WT NS5 and NS5 mutants; N = 2

4.3 Summary

In this chapter, we investigated the molecular mechanisms by which ZIKV interferes with the host IFN response. Initially, we observed a delayed IFN response during the early stages of viral infection, which suggests an active viral countermeasure to the host defense system. Supporting this scenario, we showed that ZIKV replication was resistant to poly(I:C) and IFN treatments after infection was established. This indicates that the virus effectively inhibits antiviral signaling. ZIKV suppresses IFN expression likely by interfering with the transcriptional activity driven by IRF3 and NF κ B. The viral proteins NS1, NS4A and NS5 may play a role in this process. Similar to DENV, ZIKV was found to induce proteasomal degradation of STAT2. This results in blocking Type-I and –III IFN signalling, a phenomenon that is species-specific. This process is mediated by NS5, which was found to interact with STAT2 through its MTase domain. Together, our experiments have revealed multiple strategies employed by ZIKV to counteract the host IFN system. Further understanding of this viral antagonism could in turn reveal important aspects of the host-virus interface that may be used as novel therapeutic targets.

Chapter 5 Zika virus hijacks stress granule proteins and modulates the host stress response

A version of this chapter has been published in:

“***Hou, S.**, *Kumar, A., Xu, Z., Airo, A.M., Stryapunina, I., Wong, C. P., Branton, W., Tcheshnokov, E., Götte, M., Power, C., Hobman, T.C. 2017. Zika virus hijacks stress granule proteins and modulates the host stress response. *J Virol.* doi:10.1128/JVI.00474-17.”

*Authors contributed equally

5.1 Rationale

Stress response pathways are integral to cellular antiviral systems. Activation of these pathways can lead to cap-dependent translation arrest and stress granule (SG) formation, which aid in restricting viral replication as well as regulating cell survival (White and Lloyd, 2012). SGs are dynamic cytoplasmic RNA granules that serve as temporary sites to store stalled translation initiation complexes (Kedersha et al., 2000, 2002). As such, they are essential for maintaining RNA homeostasis during cellular stress. SG aggregation can be induced through phosphorylation of the eukaryote translation initiation factor eIF2 α by the kinases HRI, PERK, GCN2 and PKR in response to heat-shock and oxidative stress, ER stress, nutrient starvation and viral dsRNA respectively (Chong et al., 1992; Dever et al., 1993; Harding et al., 1999). Subsequently, phosphorylated eIF2 α interferes with the GTP exchange activity of eIF2B, leading to reduced availability of ternary complexes and therefore suppressed translation initiation (Sudhakar et al., 2000). Upon binding of key nucleating factors such as G3BP1/2, TIA-1 and TIAR, the stalled pre-initiation complexes (containing mRNA) become further condensed, resulting in formation of SGs (Kedersha et al., 1999; Gilks et al., 2004; Matsuki et al., 2013).

Because SGs can limit the access of viruses to the cellular protein translation machinery, several flaviviruses have evolved ways to inhibit SG assembly (Table 1.2). For instance, DENV and WNV have been shown to re-direct the SG factors TIA-1 and TIAR to promote viral genome synthesis, a process that also blocks formation of SGs (Emara and Brinton, 2007). Similarly, JEV prevents SG formation by hijacking the SG-associated protein Caprin-1 for viral replication (Kato et al., 2013). Although suppression of SGs was also reported during ZIKV infection (Roth et al., 2017; Basu et al., 2017), the viral determinants and molecular mechanism(s) involved remain largely unknown.

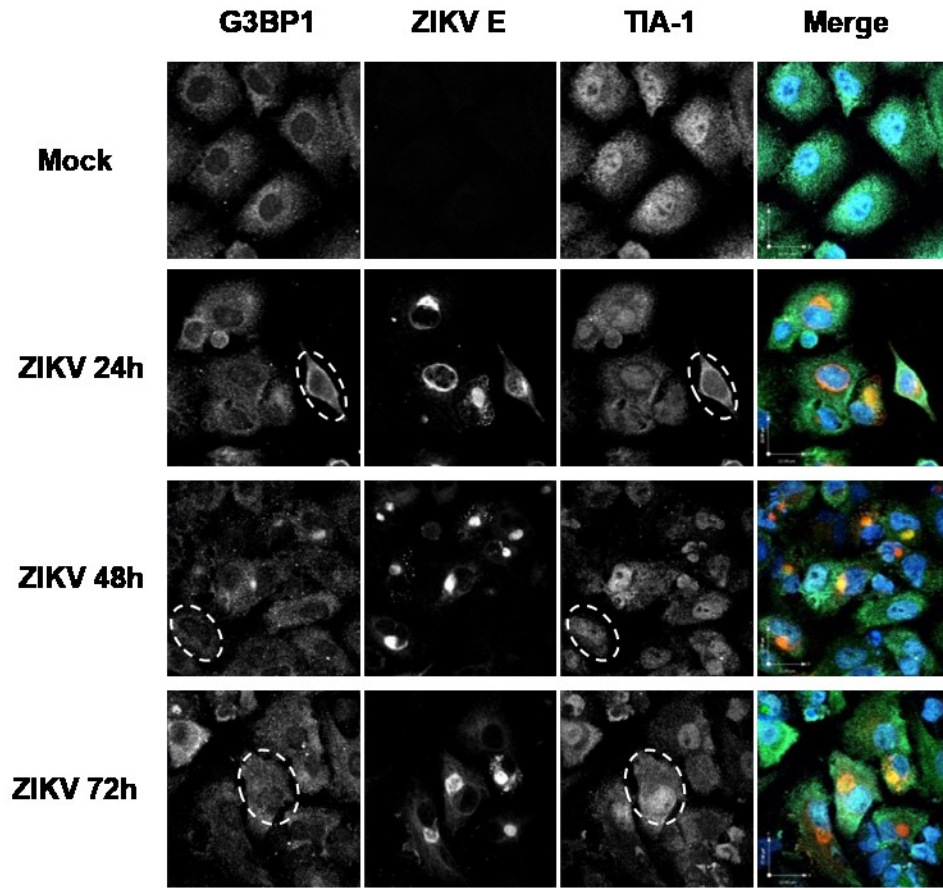
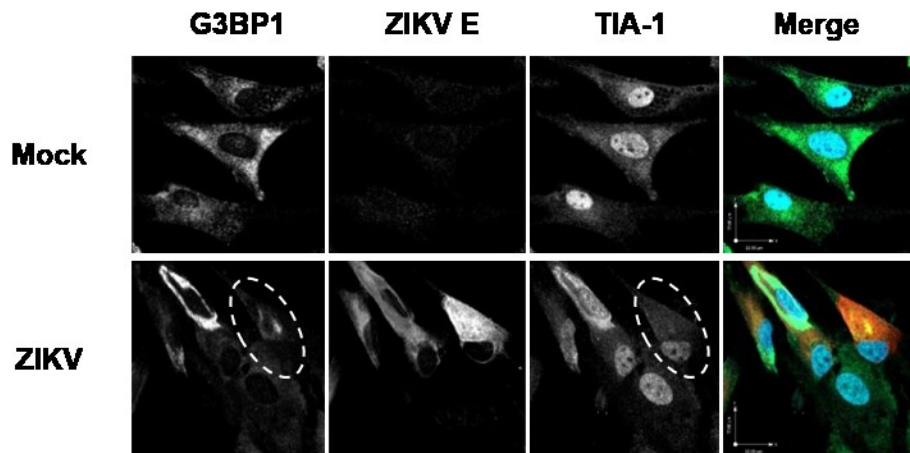
In this chapter, the mechanism(s) by which ZIKV manipulates the cellular stress response pathways were investigated. These analyses included examining the effects of viral infection and protein expression on induction of stress responses and SG formation. Experiments were also designed to understand the functional relevance of SG components in the viral life cycle.

5.2 Results

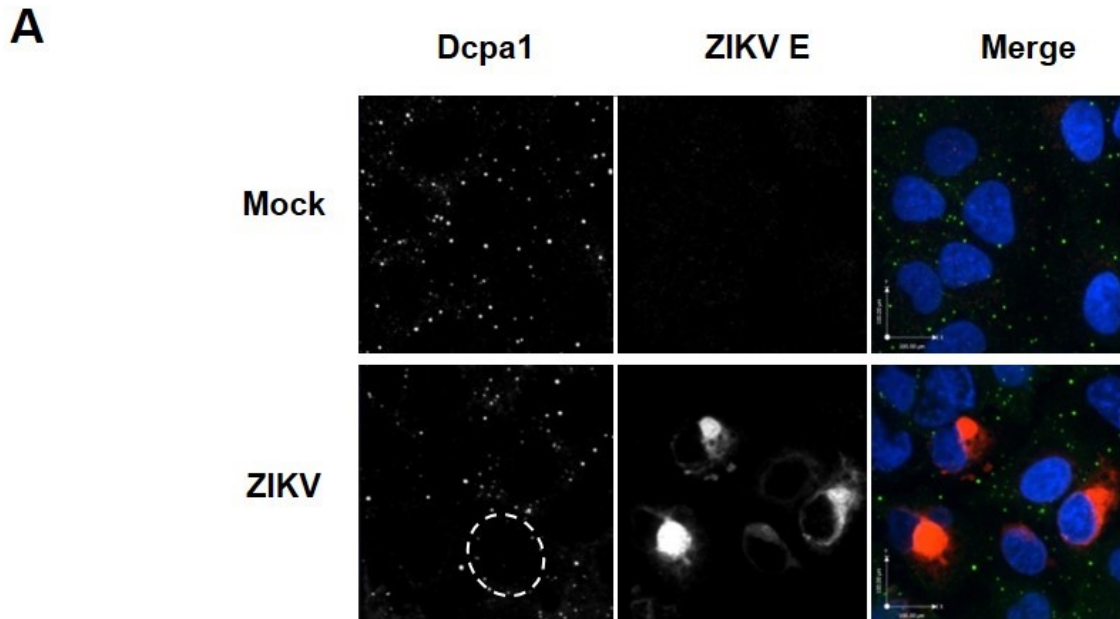
5.2.1 ZIKV infection does not induce robust SG formation

During infection of mammalian cells by certain RNA viruses (e.g. HCV), formation of SGs is induced in a timely manner (Garaigorta et al., 2012; Ruggieri et al., 2012). As a first step toward understanding how ZIKV infection affects stress response pathways, we monitored the kinetics of SG assembly over the course of infection by confocal microscopy. To visualize SGs, double-positive staining of G3BP1 and TIA-1 was employed whereas ZIKV-positive cells were identified using an antibody to the flavivirus E protein. As shown in Figure 5.1A, A549 cells infected with ZIKV at 24, 48 and 72 h.p.i contained very few G3BP1/TIA-1-positive foci in the cytoplasm, indicating that viral replication does not robustly induce SG aggregation at these time points. To confirm this finding in a more physiologically relevant system, we determined whether SGs were formed in ZIKV-infected primary human fetal astrocytes (HFAs), a brain cell type recently reported to support ZIKV replication (Hamel et al., 2017; Retallack et al., 2016). Figure 5.1B shows that, similar to what was observed in A549 cells, ZIKV infection did not induce SG assembly in HFAs at 48 h.p.i.

Figure 5.1 ZIKV infection does not induce robust SG formation. A549 cells (**A**) and primary human fetal astrocytes (**B**) were infected with ZIKV (MOI = 3 and 5 respectively) for the indicated time periods before processing for indirect immunofluorescence. SGs were identified by double-staining with rabbit anti-G3BP1 and goat anti-TIA-1. Virus-infected cells were identified by staining with a mouse antibody to E protein. Primary antibodies were detected using donkey anti-rabbit Alexa 488, donkey anti-mouse Alexa 546 and chicken anti-goat Alexa 647. Nuclei were stained with DAPI. Images were acquired on a spinning disk confocal microscope equipped with a 40X oil objective lens. Scale bar = 22 μ m. Dashed line white circles indicate ZIKV-positive cells. N = 3

A**B**

Processing bodies (P-bodies), another type of RNA granules, are major sites of cellular RNA degradation and known to exchange contents with SGs during cellular stress (reviewed in (Anderson and Kedersha, 2009)). Unlike SGs, P-bodies are normally always present in the cytoplasm of mammalian cells and their abundance can be upregulated in response to stress. Next, we quantified the numbers of P-bodies in cells infected with ZIKV. An antibody to the P-body resident de-capping protein (Dcp1a) was utilized to identify these RNA granules in fixed cells. In mock-infected cells, Dcp1a-positive puncta (15-20/cell) were dispersed throughout the cytoplasm (Figure 5.2A and B). No significant change in the number or distribution of P-bodies was observed in ZIKV-infected cells as identified by positive E-protein staining (Figure 5.2 A and B). Taken together, these data indicate that ZIKV infection does not induce robust SG formation nor does it alter the abundance of P-bodies in A549 cells.



B



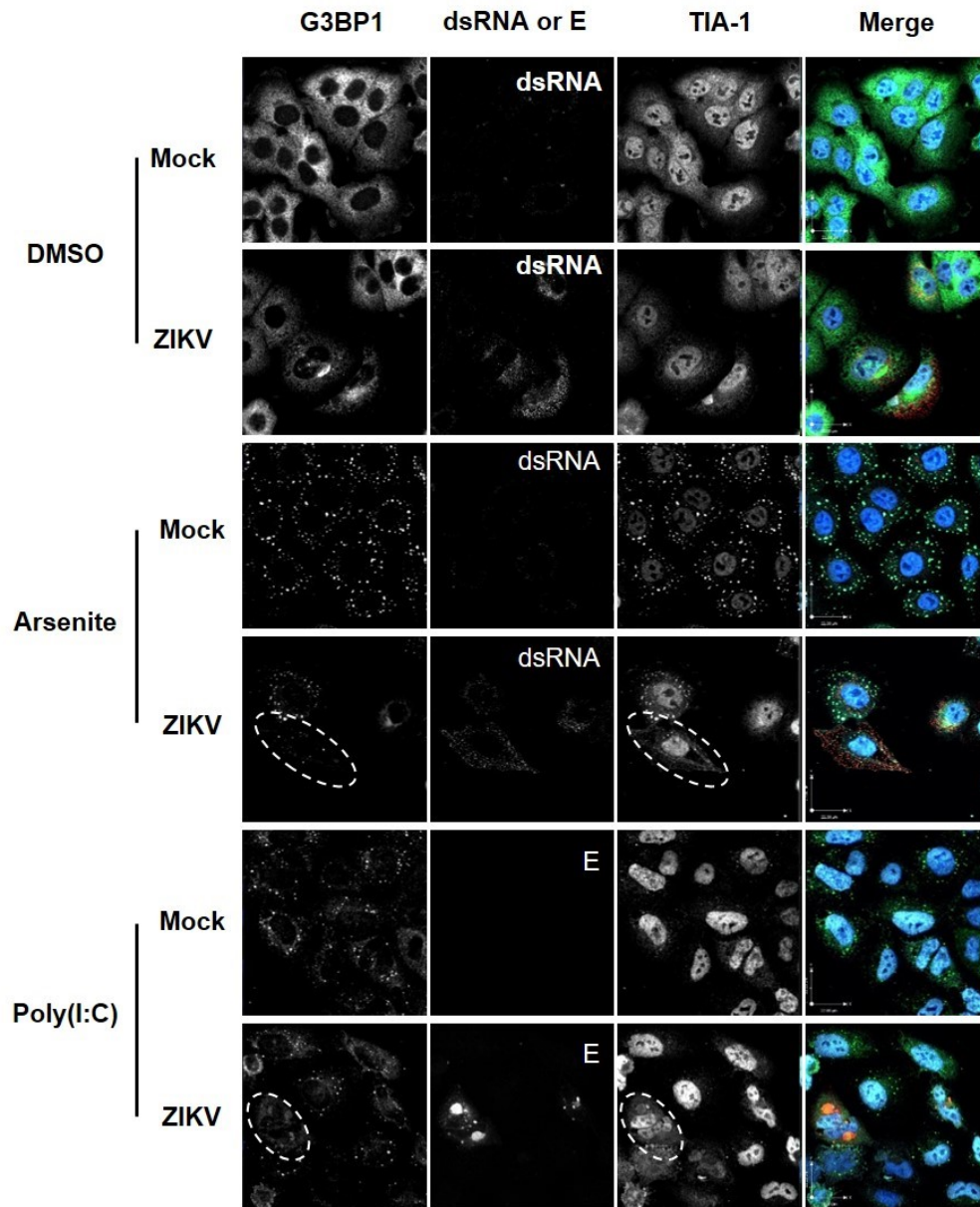
Figure 5.2 ZIKV infection does not alter P-body abundance. **A.** A549 cells were infected with ZIKV (MOI = 3) for 48 hrs and then processed for indirect immunofluorescence. P-bodies and virus infected cells were identified using rabbit anti-Dcpa1 mouse anti-E protein respectively. Primary antibodies were detected with donkey anti-rabbit Alexa 488 and donkey anti-mouse Alexa 546. Nuclei were stained with DAPI. Images were acquired on a spinning disk confocal microscope equipped with a 40X oil objective lens. Scale bar = 22 μ m **B.** Average numbers of P-bodies were determined using Volocity software. A minimum of 30 cells were used for each sample. Dashed line white circles indicate ZIKV-positive cells. N = 3

5.2.2 ZIKV inhibits SG formation induced by various stress stimuli

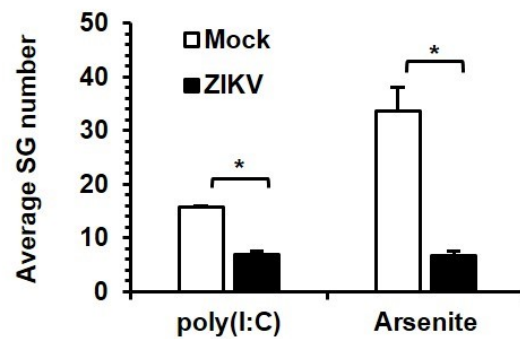
Inhibition of SG biogenesis is not uncommon in flavivirus-infected cells. For instance, DENV and WNV have been shown to block SG formation induced by oxidative stress (Emara and Brinton, 2007a; Roth et al., 2017). The lack of SG formation observed in infected cells could be due to active countermeasures employed by ZIKV. To explore this further, we measured the numbers of SGs at 24 h.p.i following treatment with two different stress stimuli, sodium arsenite and poly(I:C), which induce phosphorylation of eIF2 α through the kinases HRI and PKR respectively. By quantifying G3BP1/TIA-1 double-positive foci, we observed a significant reduction in SG numbers in ZIKV-infected A549 cells, despite differences in SG abundance induced by arsenite and poly(I:C) (Figure 5.3A and B). Specifically, in mock-infected cells, ~20 and 40 SGs were formed following stimulation with poly(I:C) and arsenite respectively whereas ZIKV-infected cells treated with these agents contained ~50% and 75% less SGs (Figure 5.3B). This indicates that the virus actively blocks SG assembly triggered through the HRI and PKR-mediated stress response pathways. To determine whether this phenomenon could be recapitulated in primary HFAs, we quantified the number of SGs in mock and infected HFAs following treatment with arsenite. Similar to the effect observed in A549 cells, ZIKV infection strongly reduced the abundance of arsenite-induced SGs in HFAs (Figure 5.4A and B), confirming that the virus suppresses SG formation triggered by oxidative stress.

Figure 5.3 ZIKV inhibits SG formation induced by arsenite and poly(I:C). **A.** A549 cells were infected with ZIKV (MOI = 3) for 24 hrs and then treated with or without sodium arsenite (0.5 mM) for 30 min or transfected with 0.4 μ g of poly(I:C) for 12 hrs. Cells were fixed and processed for indirect immunofluorescence. SGs were identified using rabbit anti-G3BP1 and goat anti-TIA-1. Virus-infected cells were identified using mouse antibodies to viral E protein or dsRNA. Primary antibodies were detected using donkey anti-rabbit Alexa 488, donkey anti-mouse Alexa 546 and chicken anti-goat Alexa 647. Nuclei were stained with DAPI. Images were acquired on a spinning disk confocal microscope equipped with a 40X oil lens. Scale bar = 22 μ m **B.** Quantification of SG numbers was performed using Volocity software. A minimum of 30 cells were used per sample. Dashed line white circles indicate ZIKV-positive cells. *** $P < 0.001$; N = 3.

A



B



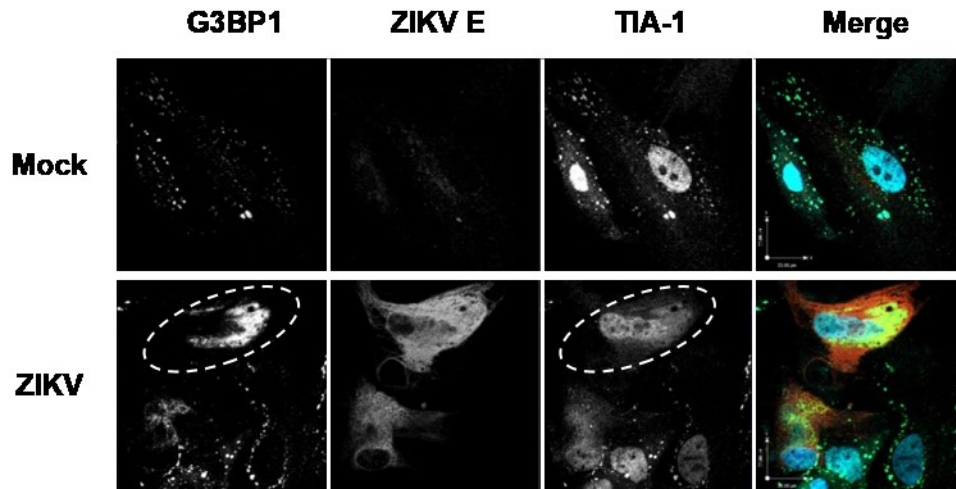
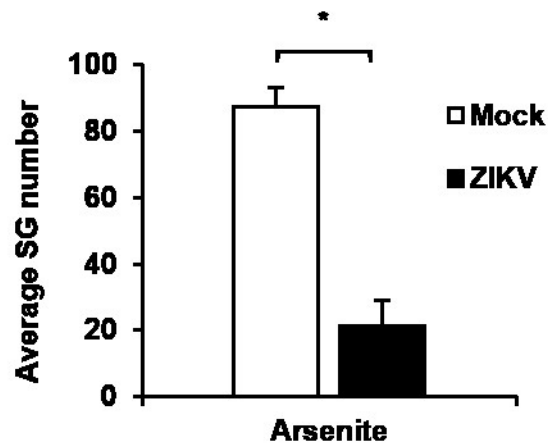
A**B**

Figure 5.4 ZIKV inhibits SG formation in primary human fetal astrocytes (HFAs). **A.** HFAs were infected with ZIKV (MOI = 5) for 48 hrs. Prior to processing for indirect immunofluorescence, cells were treated with sodium arsenite (0.5 mM) for 30 min. SGs were identified using rabbit anti-G3BP1 and goat anti-TIA-1. Virus-infected cells were identified using mouse anti-E protein. Primary antibodies were detected using donkey anti-rabbit Alexa 488, donkey anti-mouse Alexa 546 and chicken anti-goat Alexa 647. Nuclei were stained with DAPI. Images were acquired on a spinning disk confocal microscope equipped with a 40X oil objective lens. Scale bar = 22 μ m **B.** Quantification of SG numbers was performed using Volocity software. A minimum of 15 cells were used per sample. Dashed line white circles indicate ZIKV-positive cells. *** $P < 0.001$; N = 3.

5.2.3 ZIKV inhibits SG formation induced by hippuristanol

Apart from sodium arsenite and poly(I:C), stressors that target translation initiation factors besides eIF2 α can also trigger SG formation (Cencic and Pelletier, 2016). To investigate whether inhibition of SG assembly by ZIKV occurs in an eIF2 α -independent manner, we measured the number of SGs in mock and infected A549 cells following treatment with hippuristanol, an inhibitor of the translation initiation factor eIF4A (Bordeleau et al., 2005; Cencic and Pelletier, 2016). ZIKV infection reduced the number of hippuristanol-induced SGs by an average of 60% (Figure 5.5A and B), indicating that the virus also prevents SG assembly through a pathway that does not require eIF2 α phosphorylation. Together, these data illustrate that ZIKV inhibits SG biogenesis induced by multiple stress stimuli.

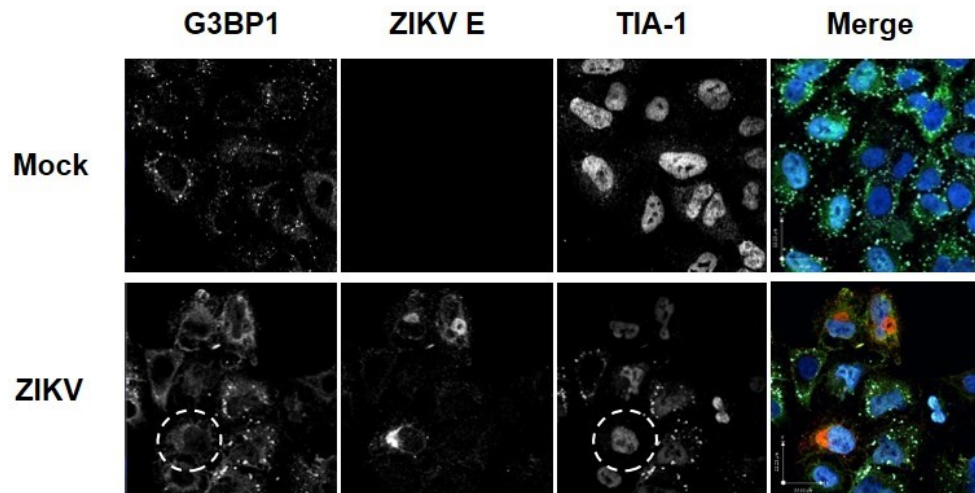
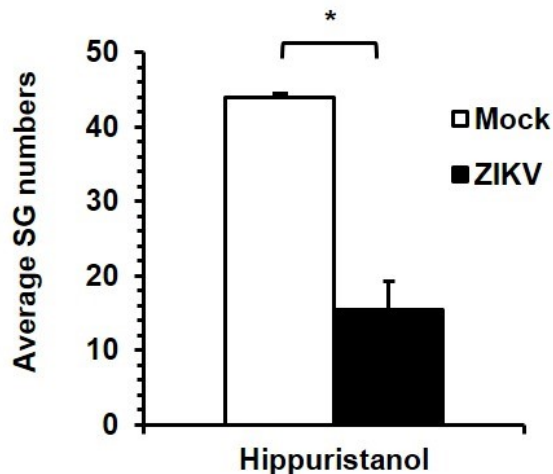
A**B**

Figure 5.5 ZIKV inhibits SG formation induced by hippuristanol. **A.** A549 cells were infected with ZIKV (MOI = 3) for 24 hrs and then treated with hippuristanol (1 μ M) for 25 min before processing for indirect immunofluorescence. SGs were identified using rabbit anti-G3BP1 and goat anti-TIA-1. Virus-infected cells were identified using mouse anti-E protein. Primary antibodies were detected using donkey anti-rabbit Alexa 488, donkey anti-mouse Alexa 546 and chicken anti-goat Alexa 647. Nuclei were stained with DAPI. Images were acquired on a spinning disk confocal microscope equipped with a 40X oil lens. Scale bar = 22 μ m **B.** The numbers of SGs were quantified using Volocity software. A minimum of 30 cells were counted per sample. Dashed line white circles indicate ZIKV-positive cells. * P <0.05; N = 3.

5.2.4 ZIKV infection activates the host stress response through PKR and the unfolded protein response (UPR)

To identify the signaling step(s) targeted by ZIKV to subvert SG formation, we next examined whether activation of the stress response pathways *per se* was affected by infection. Since both the PKR- and UPR-mediated signaling cascades are induced during infection by several flaviviruses (Ambrose and Mackenzie, 2011; Garaigorta et al., 2012; Peña and Harris, 2011; Yu et al., 2006), we monitored the kinetics of PKR and UPR activation as well as phosphorylation of the downstream target eIF2 α over the course of ZIKV infection in A549 cells and primary HFAs. Using immunoblot analyses, we detected significant upregulation of phospho-PKR at 24, 48 and 60 h.p.i and increased levels of phospho-eIF2 α at 24 and 48 h.p.i in A549 cells (Figure 5.6, left panel). Similar results were observed in infected HFAs, in which upregulation of phospho-PKR and phospho-eIF2 α was induced at 24 and 48 h.p.i. (Figure 5.6, right panel). These data suggest that ZIKV triggers phosphorylation of PKR and eIF2 α during later stages of infection. As shown in Figure 5.6 (bottom panel), spliced *XBPI* transcripts (detected by PCR followed by electrophoresis and ethidium bromide staining) were upregulated as early as 12 h.p.i. and this process was sustained for at least 60 h.p.i. Splicing of *XBPI* is mediated by the ER stress sensor IRE1 α (Figure 1.8) and therefore it serves as an indicator of UPR activation. As such, our data demonstrate that ZIKV infection in A549 cells triggers the stress response pathways mediated through PKR and the UPR, albeit with slightly different kinetics.

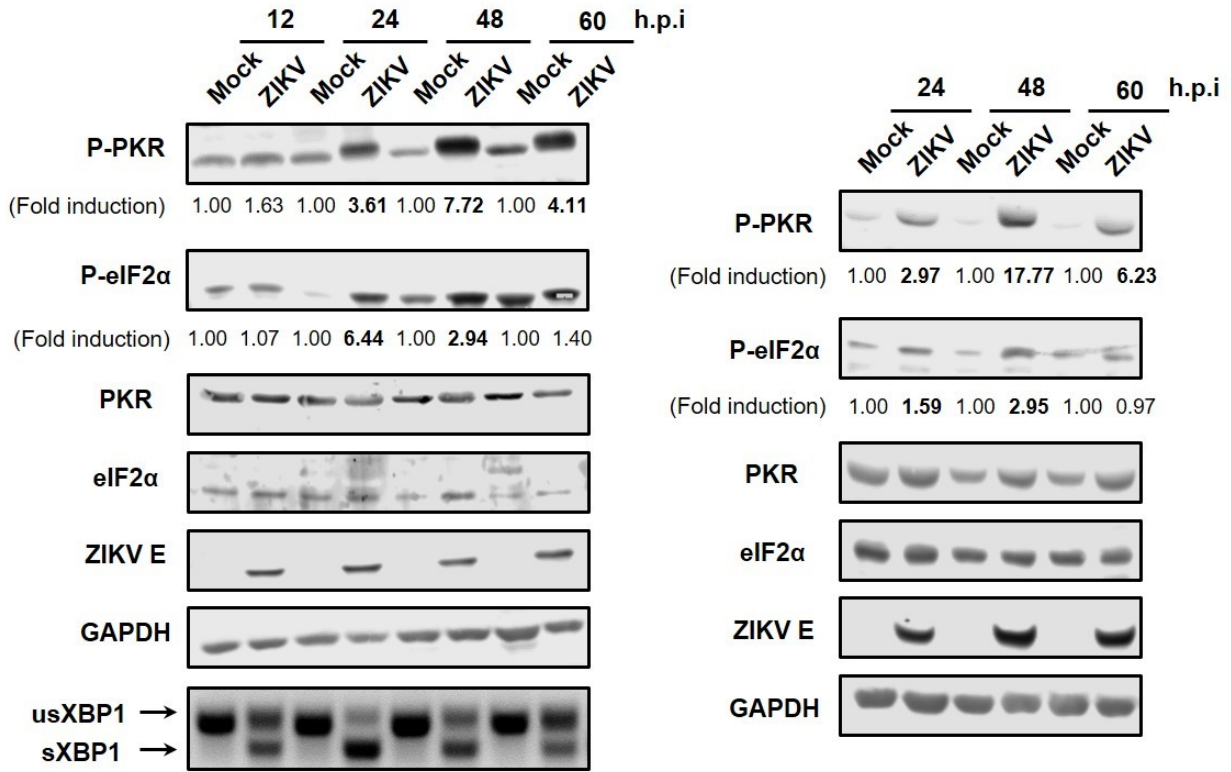
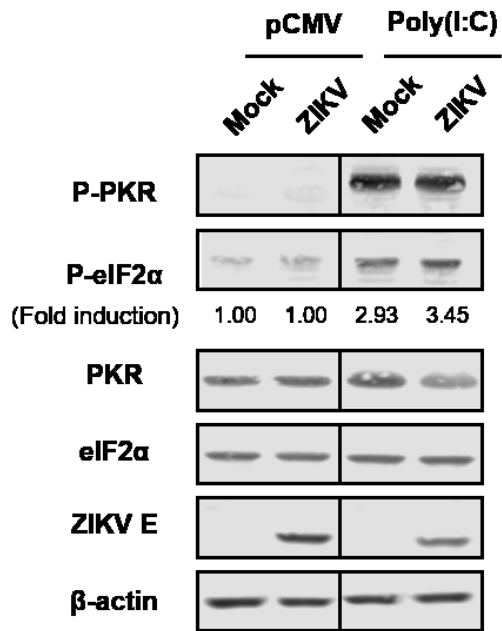
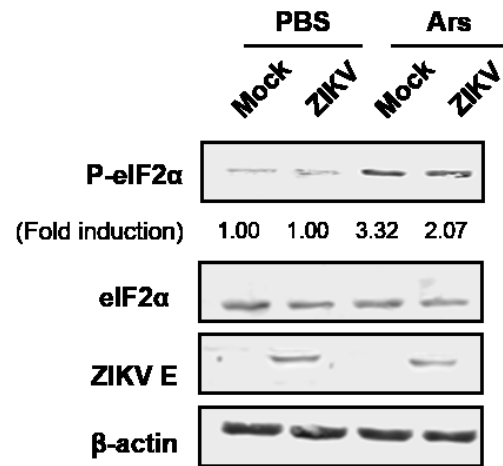
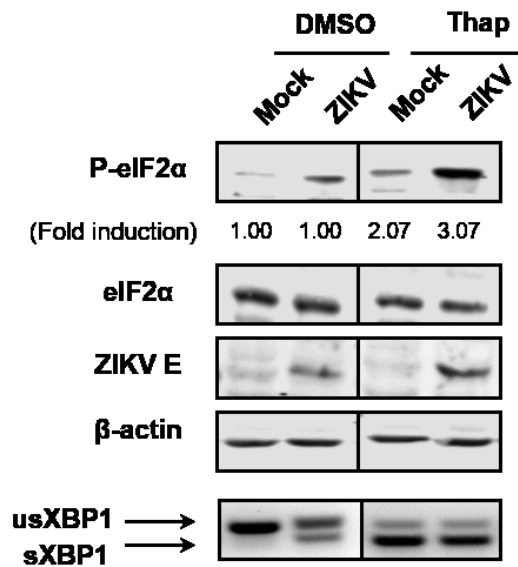


Figure 5.6 ZIKV infection activates the stress response pathways. A549 cells (left panel) and primary human fetal astrocytes (right panel) were infected with ZIKV (MOI = 5) for the indicated time periods after which total cell lysates were processed for immunoblotting. For A549 cells, samples were also processed for RT-PCR followed by agarose gel electrophoresis (bottom panel). Total PKR, phospho-PKR (P-PKR), total eIF2 α and phospho-eIF2 α (P-eIF2 α) were detected using the appropriate antibodies. Levels of GAPDH and ZIKV envelope protein (ZIKV E) are shown as loading and infection controls respectively. Quantification of P-PKR and P-eIF2 α induction (relative to mock-infected samples) was performed using the software Image Studio Lite and the average fold induction was shown below the corresponding immunoblots. Bolded numbers indicate statistical significance in P-PKR and P-eIF2 α induction determined by Student's *t*-test ($P < 0.05$). N = 4. Agarose gel electrophoresis following PCR was performed to detect spliced *XBPI* (sXBP1) and unspliced *XBPI* (usXBP1) transcripts from A49 cells. N = 3

To determine if the lack of eIF2 α phosphorylation at 12 h.p.i. was due to active suppression by the virus, we examined the effect of ZIKV infection on eIF2 α phosphorylation following stimulation by different stress pathway activators. A549 cells were treated with poly(I:C), arsenite or the ER stress inducer thapsigargin (thap) at 12 and 16 h.p.i. respectively and then relative levels of phospho-eIF2 α were determined by immunoblotting. As shown in Figure 5.7A-C, treatment of mock-infected cells with stress pathway activators lead to marked increases in phospho-eIF2 α and splicing of *XBPI* mRNA (in thapsigargin-treated samples). Similar results were observed in ZIKV-infected cells indicating that infection does not suppress stress-mediated activation of PKR, UPR or phosphorylation of eIF2 α . These data suggest that the virus-induced block in SG assembly occurs at a downstream signaling step(s).

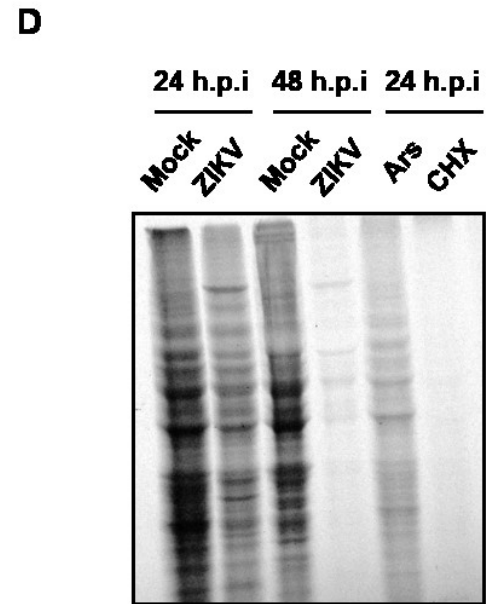
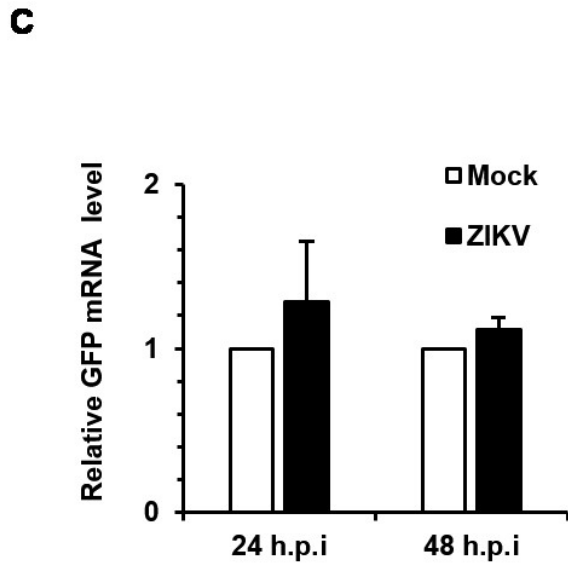
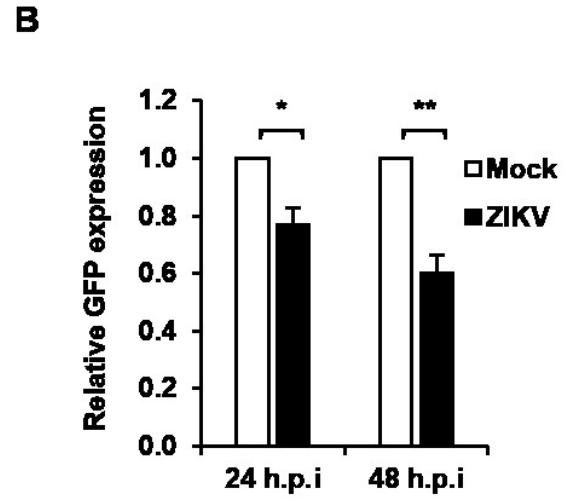
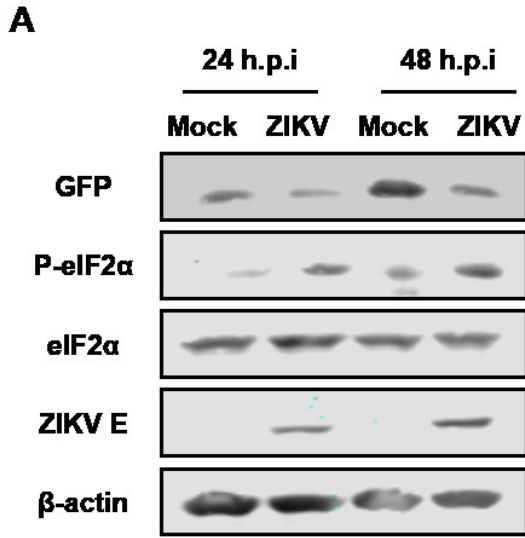
Figure 5.7 ZIKV infection does not block the induction of host stress response. A and B. A549 cells were infected with ZIKV (MOI = 3) for 12 hrs and then (A) transfected with 0.5 μ g of pCMV-3.1 or poly(I:C) for 2 hrs or (B) treated with PBS or sodium arsenite (Ars; 0.5 mM) for 1 hr. Cell lysates were harvested and processed for immunoblotting. C. A549 cells were infected with ZIKV (MOI = 5) for 16 hrs and then treated with DMSO or thapsigargin (Thap; 1 μ M) for 1 hr. Total cell lysates and RNAs were processed for immunoblotting (top panel) and RT-PCR followed by agarose gel electrophoresis (bottom panel) respectively. Total PKR, phospho-PKR (P-PKR), total eIF2 α and phospho-eIF2 α (P-eIF2 α) were detected using appropriate antibodies. Levels of β -actin and ZIKV envelope protein (ZIKV E) are shown as loading and infection controls respectively. Quantification of P-eIF2 α was performed using Image Studio Lite software and the average fold induction (relative to non-stimulated samples) from three independent experiments was shown below the corresponding immunoblot. Student's *t*-test was performed and no statistical significance was identified in P-eIF2 α induction. Spliced *XBPI* (sXBPI) and unspliced *XBPI* (usXBPI) transcripts were detected by agarose gel electrophoresis. N = 3

A**B****C**

5.2.5 ZIKV infection leads to protein translation arrest

Although induction of the stress response has been demonstrated in studies of other flaviviruses (Blázquez et al., 2014; Yu et al., 2006), whether these infections lead to translation arrest has not been documented in most cases. Since we showed that ZIKV infection activates phosphorylation of eIF2 α , we next investigated whether translation repression ensues. We first determined how viral infection affects expression of an ectopic reporter cassette encoding AcGFP delivered into A549 cells via lentivirus-based transduction. Consistent with earlier observations, phospho-eIF2 α was upregulated at 24 and 48 h.p.i. (Figure 5.8A). While levels of the viral E protein increased during this period, levels of AcGFP protein expression were significantly reduced (>40%) in ZIKV-infected cells (Figure 5.8B). This reduction was not due to altered transcription as *AcGFP* mRNA levels were similar between mock and infected samples (Figure 5.8C). Next, an [³⁵S] protein-labeling assay was performed to determine the effect of viral infection on the rate of cellular protein synthesis. Nascent protein synthesis was significantly reduced in ZIKV-infected cells (Figure 5.8D), suggesting that ZIKV infection leads to translation arrest in A549 cells, despite continuous production of viral proteins. Our finding is in agreement with a recent study demonstrating that flavivirus infections generally induce protein translation shut-off in Huh-7 cells (Roth et al., 2017).

Figure 5.8 ZIKV infection inhibits host cell protein synthesis. **A.** A549 cells transduced with pTRIP-AcGFP lentivirus (MOT = 2) were infected 12 hrs later with ZIKV (MOI = 5). Cell lysates were harvested at 24 and 48 h.p.i. for **(B)** immunoblotting and **(C)** qRT-PCR analyses. AcGFP was detected with a goat anti-GFP. Levels of total eIF2 α and phospho-eIF2 α (P-eIF2 α) are detected using specific antibodies produced from rabbit. Levels of β -actin and ZIKV envelope protein (ZIKV E) are shown as loading and infection controls respectively. **B.** The relative levels of GFP protein in mock and ZIKV-infected cells were determined using Image Studio Lite software. * $P < 0.05$; ** $P < 0.01$. **C.** Total RNA was extracted from mock and ZIKV-infected cells and processed for qRT-PCR to determine the relative mRNA levels of *ACTB* and *GFP*. **D.** A549 cells were infected with ZIKV (MOI = 5) for 24 and 48 hrs. Following depletion of amino acids for 1 hr, cells were incubated with 110 μ Ci/mL of [³⁵S] cysteine and methionine for 2 hrs. Cell lysates were harvested and processed for SDS-PAGE and autoradiography. Sodium arsenite (Ars; 0.5 mM) and cycloheximide (CHX; 50 μ M) were added 30 min prior to [³⁵S] labeling as controls. N = 3

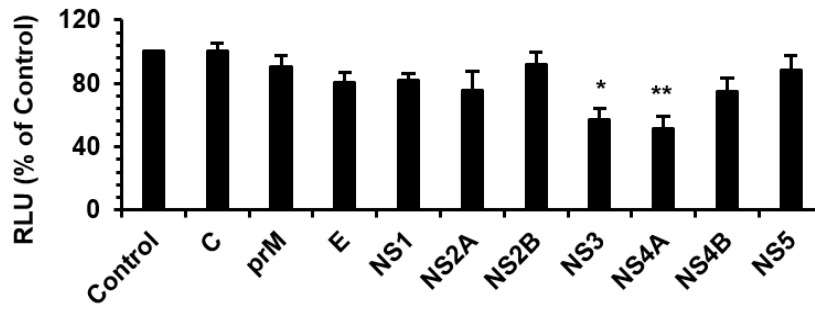
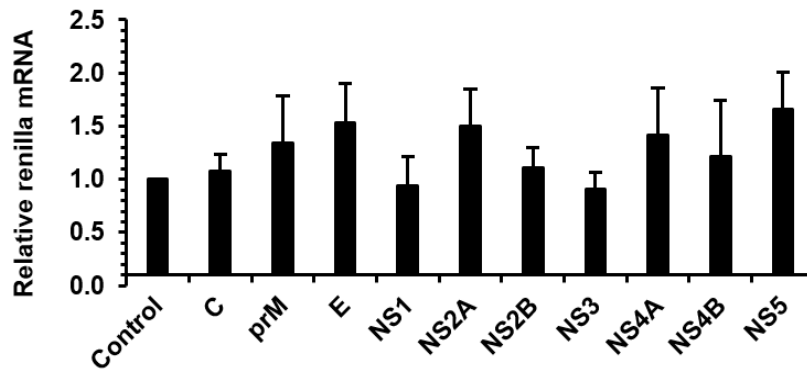
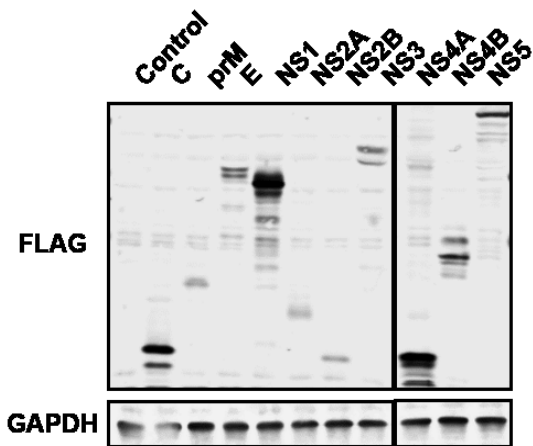
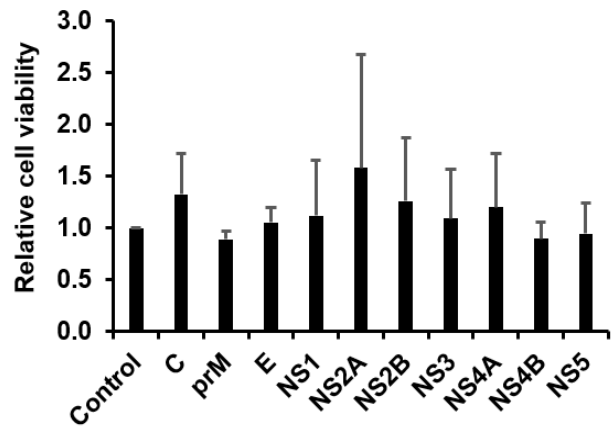
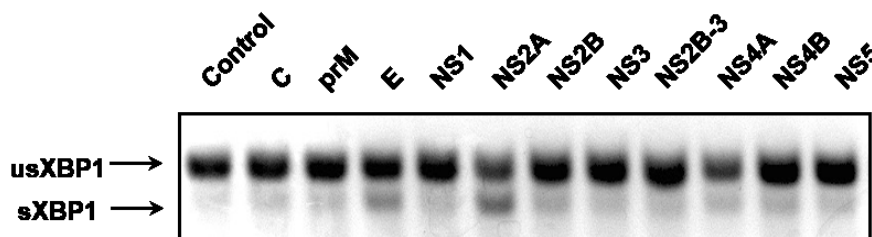


5.2.6 ZIKV proteins NS3 and NS4A promote protein translation arrest

To identify the viral component(s) that facilitate translation arrest, we expressed individual ZIKV proteins together with a renilla luciferase reporter in HEK293T cells and measured their effect on luciferase activity. Immunoblot analyses confirmed the expression of individual ZIKV proteins (Figure 5.9C) and ATP assay revealed no significant impact of viral protein expression on cell viability (Figure 5.9D). As shown in Figure 5.9A, with the exception of NS3 and NS4A, expression of ZIKV proteins did not alter luciferase activity. However, reporter activity was reduced ~40% in cells expressing NS3 or NS4A. The reduced luciferase activity in NS3 or NS4A expressing cells was not due to altered cellular transcription as mRNA levels of the renilla reporter were similar to that in control cells (Figure 5.9B). These data suggest that NS3 and/or NS4A play a role in promoting protein translation repression during ZIKV infection.

Previous studies have implicated a number of flavivirus proteins in inducing UPR signaling (Ambrose and Mackenzie, 2011; Umareddy et al., 2007). Since ZIKV infection leads to activation of the UPR (Figure 5.6, bottom panel), next sought to determine which viral proteins were involved in this process. HEK293T cells were transfected with individual ZIKV protein expression constructs and the levels of spliced *XBPI* transcripts were determined by RT-PCR and agarose gel electrophoresis. As shown in Figure 5.9E, expression of the E protein and NS2A triggered splicing of *XBPI* mRNA. While we have show that ZIKV employs different viral factors to modulate stress response pathways, the precise molecular mechanisms mediating these processes remain to be elucidated.

Figure 5.9 Expression of NS3 or NS4A inhibits protein translation. A-D. HEK293T cells were co-transfected with plasmids encoding ZIKV proteins and a renilla luciferase reporter. Forty-eight hours post-transfection, cell lysates were subjected to **(A)** luciferase assays to quantify relative reporter activity, **(B)** qRT-PCR analyses to quantify relative levels of reporter mRNA, **(C)** immunoblotting to confirm protein expression and **(D)** ATP assay to analyze cell viability. * $P < 0.05$; ** $P < 0.01$. **E.** HEK293T cells were transfected with plasmids encoding ZIKV proteins for 24 hrs. Total RNA was isolated and processed for RT-PCR followed by agarose gel electrophoresis to detect spliced *XBPI* (sXBPI) and unspliced *XBPI* (usXBPI) transcripts. *C* = capsid, *E* = envelope; N = 3.

A**B****C****D****E**

5.2.7 ZIKV infection does not alter expression of SG proteins

One of the known viral mechanisms to antagonize SG formation is through direct cleavage of key nucleating factors. For example, the poliovirus protease 3Cpro cleaves the SG proteins G3BP and eIF4GI (White et al., 2007; White and Lloyd, 2011). To determine whether ZIKV inhibits SG aggregation by cleaving or altering the expression of SG-associated proteins, immunoblot analysis was performed to determine the levels of G3BP1, TIA-1 and TIAR in A549 cells infected with ZIKV. The data from these experiments reveal that levels of these SG components were unchanged in response to ZIKV infection nor was there any evidence of virus-induced cleavage of G3BP1, TIA-1 or TIAR (Figure 5.10A).

Post-translational modification of SG assembly factors can also affect biogenesis of these RNA granules (Tourrière et al., 2003; Dolzhanskaya et al., 2006; Kwon et al., 2007). For example, arsenite-induced SG formation is dependent on dephosphorylation of G3BP1 at serine 149 (Tourrière et al., 2003). Accordingly, we investigated whether phosphorylation of G3BP1 was affected by ZIKV infection. Immunoblot analyses showed that comparable levels of phospho-G3BP1 were detected in both mock- and ZIKV-infected cells at 18 h.p.i, regardless of whether cells were treated with arsenite (Ars) or thapsigargin (Thap) (Figure 5.10B). Because neither of the stress treatments induced noticeable dephosphorylation of G3BP1, our results were inconclusive and further experiments are needed to address the question whether post-translational modifications of SG proteins are affected by ZIKV upon stress stimulation.

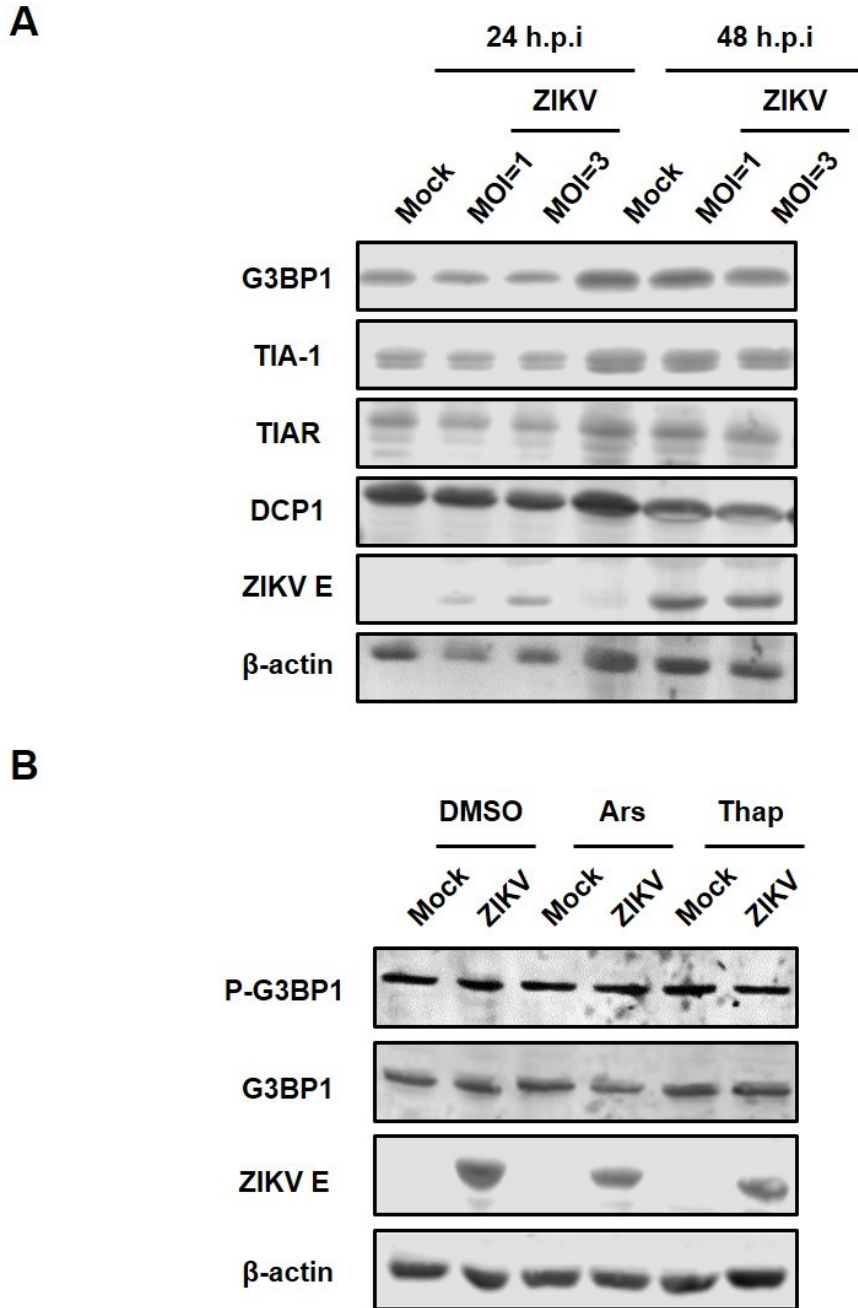


Figure 5.10 ZIKV infection does not affect steady state levels of SG-associated proteins.

A. A549 cells infected with ZIKV (MOI = 1 or 3) were harvested at 24 and 48 h.p.i. after which levels of G3BP1, TIA-1, TIAR and Dcp1 were determined by immunoblotting using the appropriate antibodies. Levels of β -actin and ZIKV envelope protein (ZIKV E) are shown as loading and infection controls respectively. **B.** A549 cells infected with ZIKV (MOI = 5) for 16 hrs were then treated with or without sodium arsenite (Ars; 0.5 mM) or thapsigargin (Thap; 1 μ M) for 1 hr. Levels of total G3BP1 and phospho-G3BP1 (P-G3BP1) were determined by immunoblotting using a rabbit anti-G3BP1 or anti-phospho-G3BP1 antibody. Levels of β -actin and ZIKV envelope protein (ZIKV E) are shown as loading and infection controls respectively.

N = 2

5.2.8 ZIKV infection does not disrupt the microtubule network

Since microtubule-mediated transport of translationally stalled mRNPs is important for SG assembly (Ivanov et al., 2003), we next examined the effect of ZIKV infection on microtubule network integrity. As a positive control, A549 cells were treated with nocodazole, an inhibitor of microtubule polymerization (Vasquez et al., 1997). As shown in Figure 5.11, microtubules as represented by β -tubulin-positive structures maintained a normal filamentous architecture in ZIKV-infected cells at 48 h.p.i. suggesting that the microtubule network was not significantly disrupted by this flavivirus.

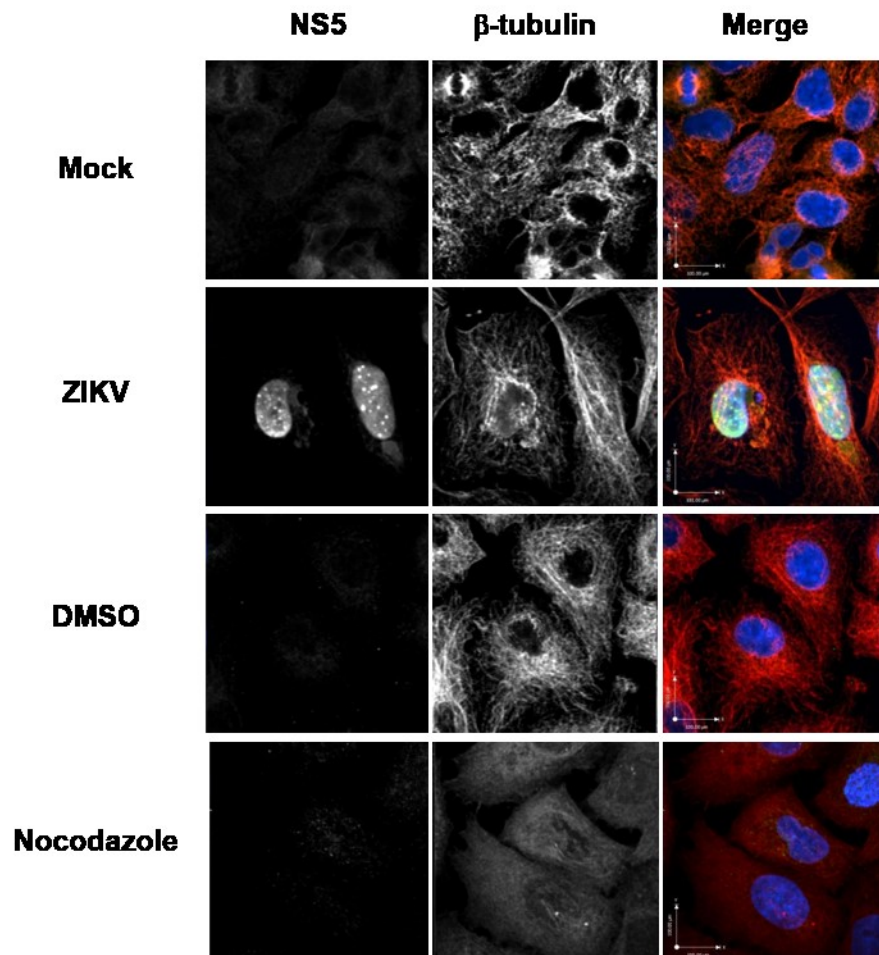


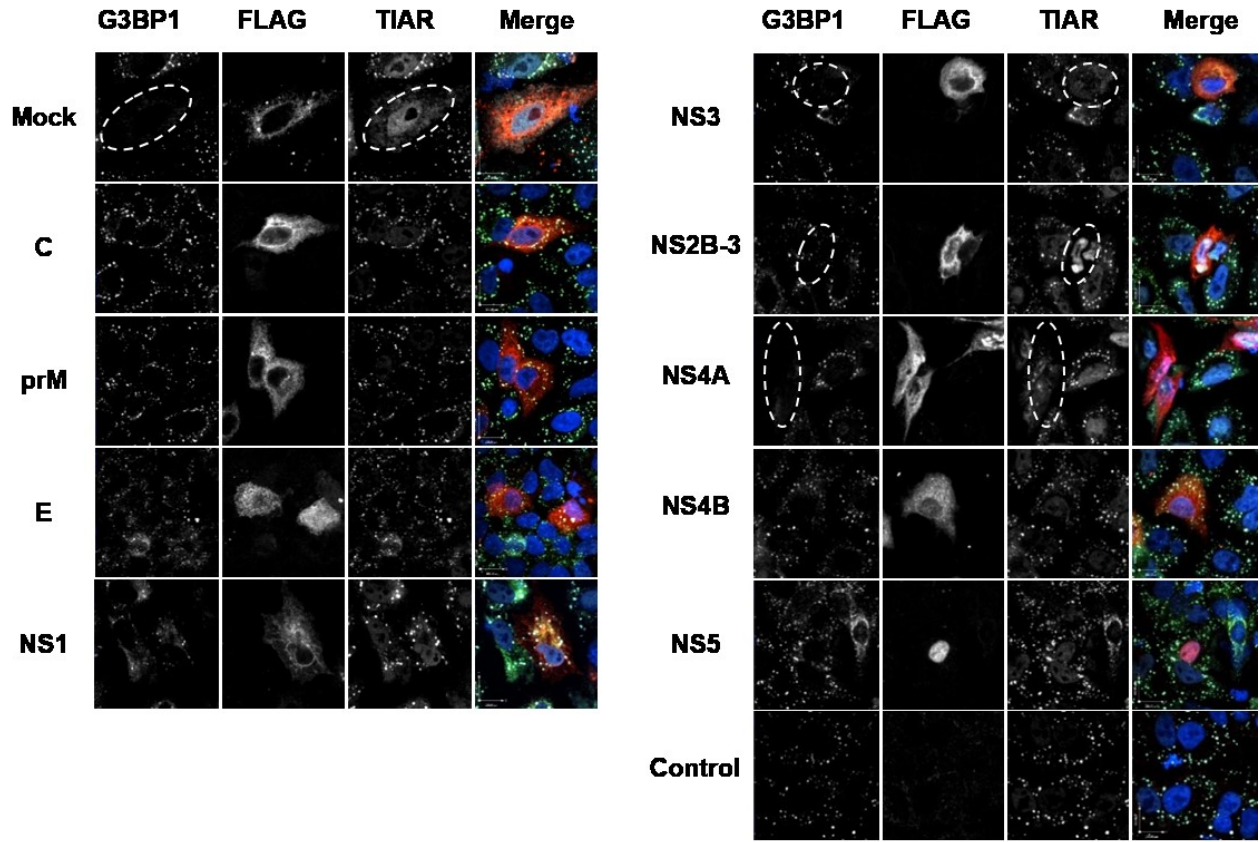
Figure 5.11 ZIKV infection does not disrupt the microtubule network. A549 cells were infected with ZIKV (MOI = 3) for 48 hrs and processed for indirect immunofluorescence. As controls, cells were treated with DMSO or nocodazole (10 μ M) for 8 hrs. Infected cells were detected using goat anti-NS5. Microtubules were stained with a mouse anti- β -tubulin. Primary antibodies were detected using donkey anti-goat Alexa 488 and donkey anti-mouse Alexa 546. Nuclei were stained with DAPI. Images were acquired on a spinning-disk confocal microscope equipped with a 60X oil objective lens. Scale bar = 100 μ m. N = 2

5.2.9 Inhibition of SG formation is mediated by the viral capsid protein, NS3, NS2B-3 and NS4A

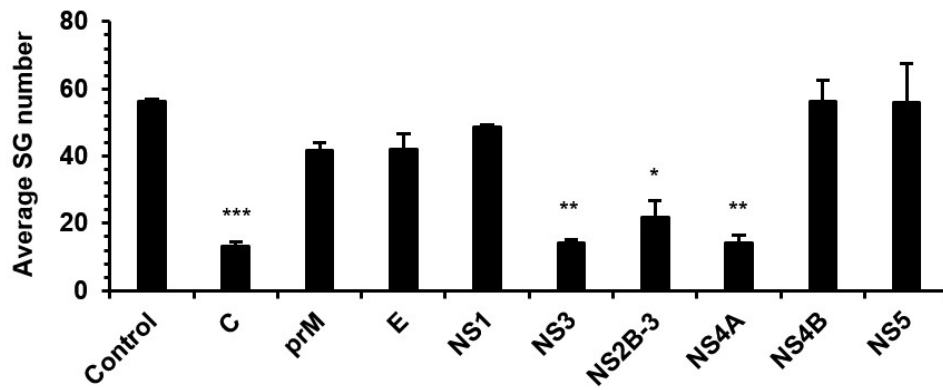
Based on the data described above, the signaling step(s) targeted by ZIKV to disrupt SG assembly is likely downstream of where formation of translationally silenced mRNP occurs. To identify the viral component(s) responsible for interfering with SG biogenesis, we expressed individual FLAG-tagged ZIKV proteins in A549 cells and then treated cells with hippuristanol to induce SG formation. SGs were identified by double-positive staining for G3BP1 and TIAR as described above. As shown in Figure 5.12, most of the ZIKV proteins did not block hippuristanol-induced SG formation. However, in cells expressing capsid, NS3/NS2B-3 or NS4A, the average numbers of SGs in each cell were reduced by ~70-80% (Figure 5.12B). In some cells expressing these viral proteins, G3BP1/TIAR-positive structures (as indicated by the dash-line white circles) were virtually absent (Figure 5.12A).

Figure 5.12 Expression of ZIKV capsid, NS3, NS2B-3 or NS4A blocks SG formation. A. A549 cells were transfected with the indicated ZIKV expression plasmids for 48 hrs and then treated with hippuristanol (1 μ M) for 25 min before processing for indirect immunofluorescence. Samples were incubated with mouse anti-FLAG epitope, rabbit anti-G3BP1 and goat anti-TIAR antibodies. Primary antibodies were detected using donkey anti-rabbit Alexa 488, donkey anti-mouse Alexa 546 and chicken anti-goat Alexa 647. Nuclei were stained with DAPI. Images were acquired using a spinning-disk confocal microscope equipped with a 60X oil objective lens. Scale bar = 100 μ m. **B.** Numbers of SGs in transfected cells were quantified using Volocity software. A minimum of 15 cells were used for each sample. Dash line white circles indicate capsid-, NS3-, NS2B-3- or NS4A-positive cells. *C* = capsid, *E* = envelope; * P <0.05, ** P <0.01, *** P <0.001; $N = 3$.

A



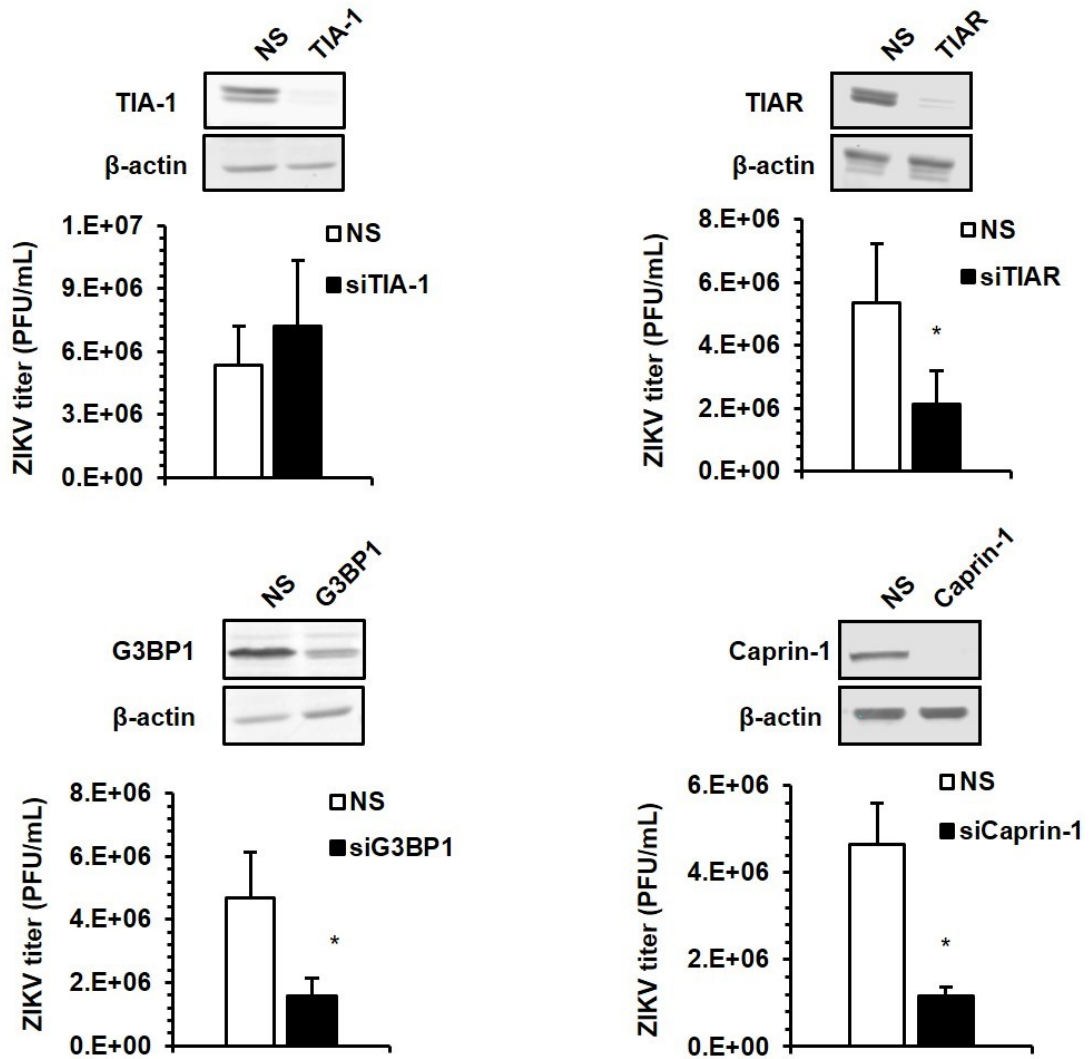
B



5.2.10 The SG proteins G3BP1, TIAR and Caprin-1 are important for ZIKV replication

Since other flaviviruses including DENV, WNV and JEV are known to exploit SG components to promote viral replication (Emara and Brinton, 2007; Katoh et al., 2013), we examined whether some of the key SG assembly factors play a role in the ZIKV life cycle. Levels of G3BP1, TIA-1, TIAR and Caprin-1 were transiently reduced by transfection of siRNAs in A549 cells followed by ZIKV infection and plaque assays to determine how loss of these SG components affected viral titers. Compared to cells transfected with non-silencing (NS) siRNAs, knockdown of G3BP1, TIAR and Caprin-1, but not TIA-1, resulted in ~70% reduction in ZIKV titers (Figure 5.13A), suggesting that these host proteins positively regulate the viral life cycle. The decreased viral titres were not due to altered cell viability by siRNA treatment as indicated by the cell viability assay (Figure 5.13B).

A



B

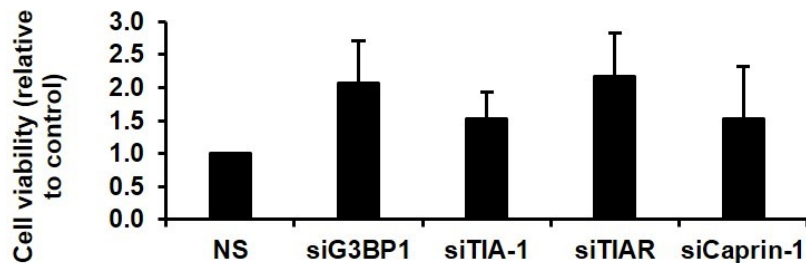


Figure 5.13 The SG components G3BP1, TIAR and Caprin-1 are important for ZIKV replication. A549 cells were transfected with non-silencing siRNA (NS) or siRNAs specific for G3BP1, TIAR, TIA-1 or Caprin-1 for 48 hrs. **A.** Cells were then infected with ZIKV (MOI = 0.5) for additional 48 hrs after which they were processed for immunoblotting (to assess knockdown efficiency) and plaque assays to determine viral titers. **B.** siRNA-treated (uninfected) cells were processed for cell viability assay. * $P < 0.05$, ** $P < 0.01$; N = 3

5.2.11 ZIKV capsid protein interacts with G3BP1 and Caprin-1

Since expression of ZIKV capsid, NS3 and NS4A inhibit SG assembly (Figure 5.12), we next determined whether these viral proteins interact with the SG factors that were shown to be involved in viral replication (Figure 5.13A). We expressed the corresponding FLAG-tagged viral proteins in HEK293T cells and then performed co-immunoprecipitation assays to identify associated host proteins. NS1 was included as a negative control as it had little effect on SG formation (Figure 5.12). Because capsid, NS3, G3BP1 and TIAR are RNA-binding proteins, cell lysates were treated with the nuclease benzonase (which degrades both DNAs and RNAs) to reduce non-specific RNA-mediated interactions. Immunoblotting revealed that capsid protein forms a stable complex with G3BP1 and Caprin-1 but not TIAR (Figure 5.14). This may indicate that capsid-mediated sequestration of G3BP1 and Caprin-1 is one mechanism by which ZIKV blocks SG formation. Although none of these SG components were found to interact with NS3 or NS4A in the co-immunoprecipitation assay, we cannot exclude the possibility that these viral proteins interact with other SG factors.

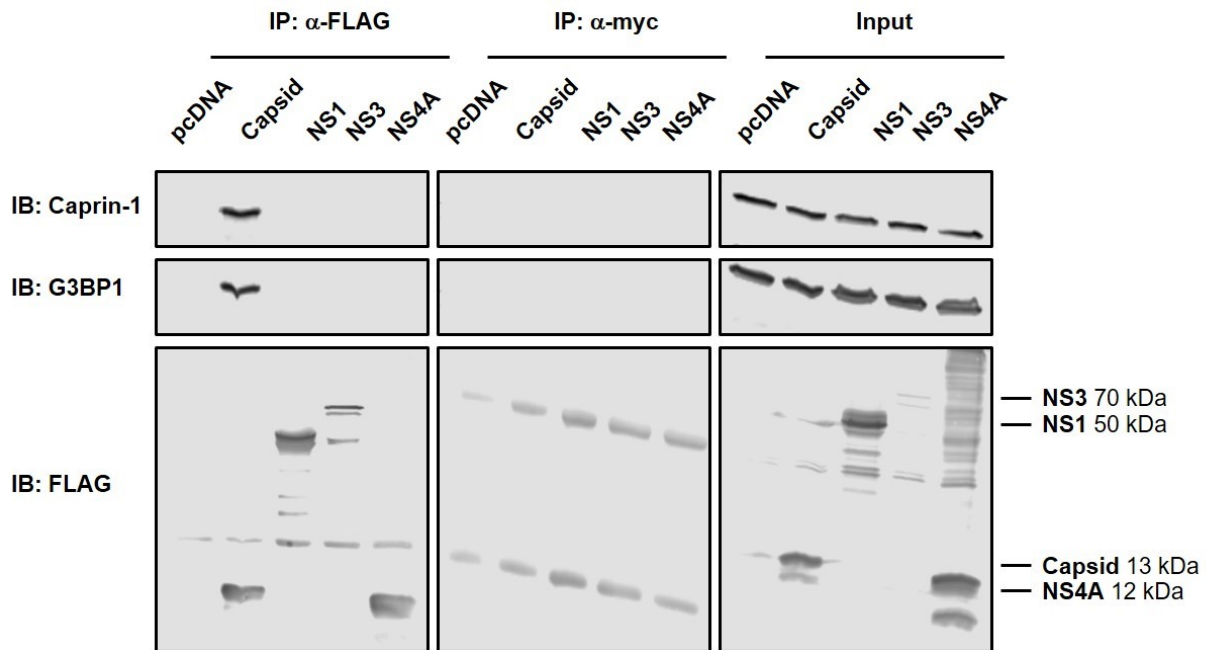


Figure 5.14 ZIKV capsid protein interacts with G3BP1 and Caprin-1. HEK293T cells were transfected with the indicated ZIKV protein expression constructs or a control plasmid pcDNA-3.1(-) for 48 hrs. Cell lysates were harvested and processed for immunoprecipitation using mouse anti-FLAG or anti-myc (negative control) antibodies followed by immunoblotting. Mouse anti-FLAG or anti-myc, rabbit anti-G3BP1 and rabbit anti-Caprin-1 antibodies were used to detect the FLAG-tagged viral proteins and endogenous G3BP1 as well as Caprin-1. The viral proteins and their corresponding protein molecular sizes are indicated. IP, immunoprecipitation; IB, immunoblotting; N = 3

Apart from viral proteins, viral RNA can also modulate SG assembly. For instance, WNV and DENV RNAs were shown to recruit TIA-1 and TIAR for genome replication, a process that was also thought to inhibit SG formation (Emara and Brinton, 2007). To determine if ZIKV RNA binds G3BP1 and/or TIAR, RNA-immunoprecipitation using antibodies to G3BP1 or TIAR was performed. An anti-myc antibody was used as a negative control. As shown in Figure 5.15A, a significant amount of ZIKV RNA associated with anti-G3BP1 but not anti-TIAR or anti-myc co-immunoprecipitations. Figure 5.15B confirms that levels of viral RNA in the starting material (infected cell lysate) were high indicating a robust infection of the cells. Moreover, the immunoblot data in Figure 5.15C confirm that both TIAR and G3BP1 were immunoprecipitated. Of note, even though much more TIAR appeared to be recovered, no ZIKV RNA was detected in the co-immunoprecipitation with anti-TIAR antibody. These data suggest that viral RNA-mediated sequestration of G3BP1 may constitute an additional means by which SG assembly is prevented during ZIKV infection.

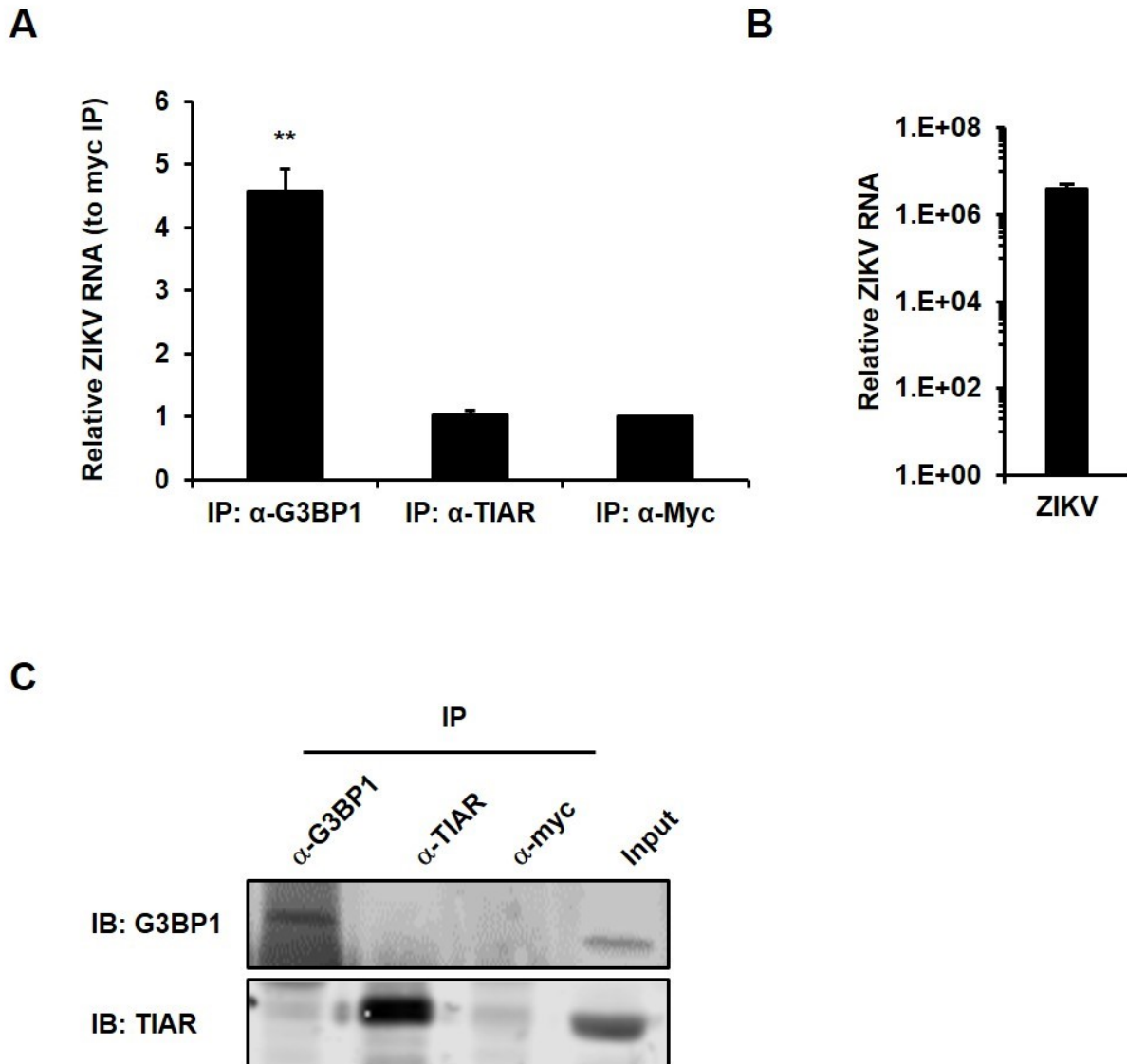
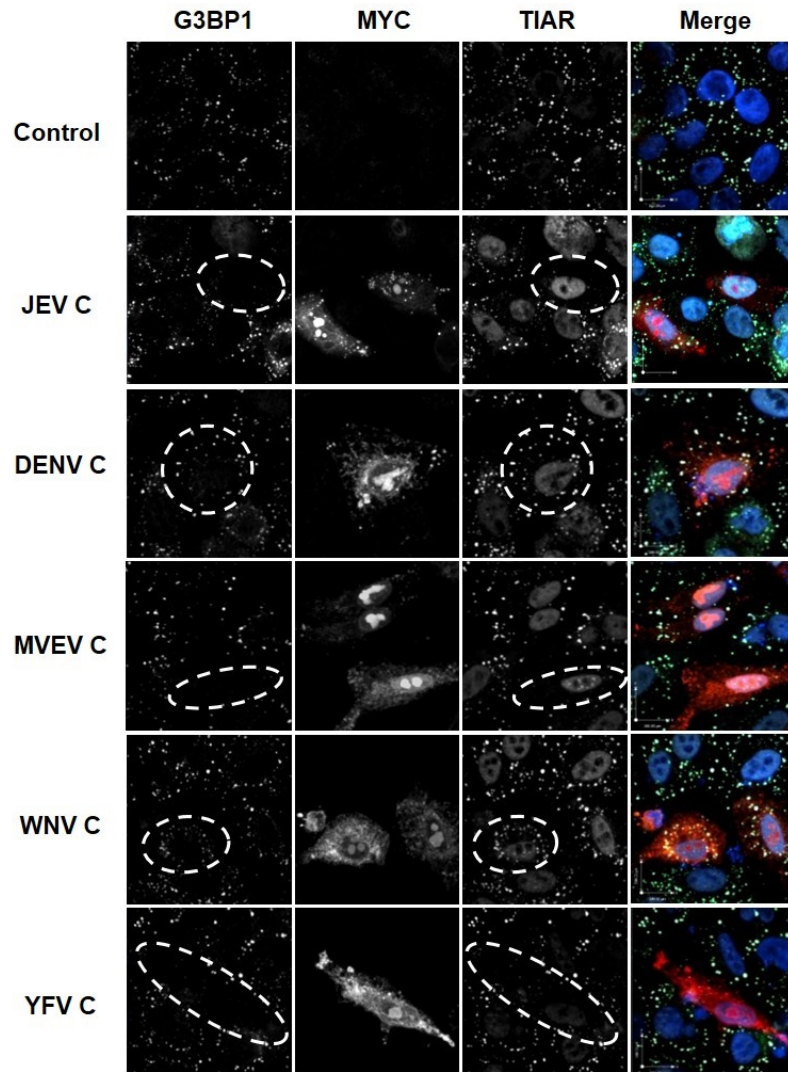
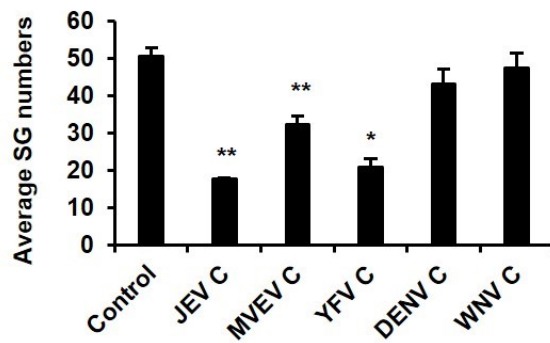
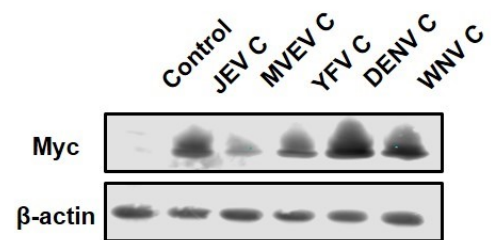


Figure 5.15 ZIKV RNA binds G3BP1. A549 cells were infected with ZIKV (MOI=5) for 48 hrs after which cell lysates were prepared. Rabbit anti-G3BP1, goat anti-TIAR or mouse anti-myc antibodies were used for immunoprecipitation. **A.** RNAs isolated from the immunoprecipitates were extracted and processed for qRT-PCR. The relative levels of ZIKV RNA were determined by normalization to the CT value obtained from myc-immunoprecipitation samples. $*P<0.05$ **B.** Relative ZIKV RNA in the infected sample was determined by normalization to the CT value obtained from mock-infected cells. **C.** Immunoprecipitation efficiency was determined by immunoblot analysis using anti-G3BP1 and anti-TIAR antibodies. IP, immunoprecipitation; IB, immunoblotting; N = 3.

5.2.12 Capsid proteins of MVEV and YFV inhibit SG formation

Since capsid proteins of ZIKV (Figure 5.12) and JEV interfere with SG assembly ((Kato et al., 2013), we next examined whether capsids of other flaviviruses also suppress SG biogenesis. Myc-tagged capsids from JEV, DENV, MVEV, WNV and YFV were expressed in A549 cells and the average numbers of hippuristanol-induced SGs were determined by quantitative confocal microscopy. Immunoblot analyses confirmed similar expression levels of all capsid proteins (Figure 5.16C). Depending upon the particular capsid protein, different effects on SG formation were observed. Whereas expression of DENV and WNV capsids had little effect on SG assembly, the numbers of SGs in cells expressing JEV, MVEV and YFV capsids were reduced by ~ 65%, 35% and 60% respectively (Figure 5.16A and B). Taken together, these data suggest that capsid-mediated interference of SG assembly is a common strategy employed by multiple flaviviruses to subvert the antiviral function of SGs.

Figure 5.16 Expression of flavivirus capsid proteins have differential effects on SG formation. **A.** A549 cells were transfected with plasmids encoding capsid proteins from Japanese encephalitis (JEV), Dengue (DENV), West Nile (WNV), yellow fever (YFV) and Murray Valley encephalitis (MVEV) viruses or empty vector (Control) for 48 hrs. Cells were treated with hippuristanol (1 μ M) for 25 min before processing for indirect immunofluorescence. SGs were identified using rabbit anti-G3BP1 and goat anti-TIAR. Transfected cells expression capsid proteins were identified using mouse anti-myc. Primary antibodies were detected using donkey anti-rabbit Alexa 488, donkey anti-mouse Alexa 546 and chicken anti-goat Alexa 647. Nuclei were stained with DAPI. Images were acquired using a spinning-disk confocal microscope equipped with a 60X oil objective lens. Scale bar = 100 μ m. **B.** SG numbers in transfected cells were quantified using Volocity software. A minimum of 15 cells were used for each sample. Dashed line white circles indicate capsid-positive cells. * P <0.05. **C.** HEK293T cells were transfected with the indicated expression plasmids and 48 hrs later cell lysates were harvested and processed for immunoblotting analysis. The myc-tagged capsids were visualized by an anti-myc antibody. β -actin was utilized as the loading control. N = 3.

A**B****C**

5.3 Summary

In this chapter, we undertook a mechanistic approach to understand how ZIKV infection modulates the host stress response. In contrast to what was observed in an very recent study (Roth et al., 2017), ZIKV infection leads to robust induction of cellular stress response signaling, resulting in phosphorylation of eIF2 α as well as translation shut-off. The latter process is likely mediated by the viral proteins NS3 and/or NS4A. Despite activating this antiviral program, ZIKV strongly inhibits the formation of SGs triggered by various stress stimuli. Further analyses indicated that ZIKV targets a signaling step downstream of stalled translation initiation in order to block SG assembly. The capsid, NS3, NS2B-3 and NS4A were identified as viral suppressors of SG formation. For capsid at least, its inhibitory effect on SG biogenesis may result from sequestering SG components G3BP1 and Caprin-1, both of which are implicated in the viral life cycle. Analyses revealed that other (but not all) flavivirus capsid proteins impair SG assembly. Based on these data, we speculate that recruitment of SG-associated proteins by specific viral factors including capsid protein facilitates replication of ZIKV and potentially other flaviviruses, while at the same time preventing formation of SGs. Future studies should focus on determining precisely how SG assembly factors function in flavivirus replication.

Chapter 6 Discussion and Perspectives

6.1 Synopsis

Compared to large DNA viruses such as herpesviruses and poxviruses, the genome coding capacities of flaviviruses are relatively small. Therefore, it is necessary that they encode multi-functional proteins in order to interfere with host antiviral systems and establish productive infections. My thesis work focused on how flavivirus components (proteins and RNA) antagonize various cellular defense pathways. First, we showed that flaviviruses such as DENV and WNV interfere with peroxisome biogenesis in part (or whole) by capsid protein-mediated sequestering of the peroxisome biogenesis factor PEX19. Virus infection also induced PEX19 degradation and the resulting decrease in peroxisome numbers is thought to diminish the IFN response. The mechanisms by which a newly emerging pathogen, ZIKV impedes the host IFN system was also explored. As well as identifying multiple ZIKV proteins that impair IFN induction and downstream signaling, we showed that the virus modulates the cellular stress response and hijacks the stress granule components G3BP1, TIAR and Caprin-1 likely to benefit replication.

6.2 Interaction between flaviviruses and peroxisomes

Peroxisomes are highly dynamic organelles as they perform diverse metabolic functions and are able to alter their contents, abundance and sizes in response to environmental cues (reviewed (Mast et al., 2015)). Studies have shown that peroxisomes regulate the metabolism of signaling molecules such as reactive oxidative species (ROS) and that they “crosstalk” with other organelles through signaling cascades to coordinate their own activities and proliferation (reviewed in (Nordgren et al., 2013; Mast et al., 2015)). In this regard, it is not surprising that peroxisomes are viewed as signaling platforms that regulate cellular processes.

6.2.1 Peroxisomes as signaling platforms

Over the past few decades, scientists have gained substantial insights into peroxisome biology and metabolic functions, but the roles of these organelles in regulating signaling pathways is only beginning to be understood. Recent evidence showing that these organelles function as signaling platforms is based on the observations that they regulate ROS metabolism, which are important mediators of multiple cellular pathways (Tal et al., 2009; Le Belle et al., 2011; Anastasiou et al., 2011; Lee et al., 2013).

Peroxisomes participate in both generation and degradation of ROS. Peroxisome-based β -oxidation of fatty acids produces H_2O_2 , which can cause oxidative stress in cell. To counteract this, levels of H_2O_2 can be reduced by the actions of catalases. Decreased catalase levels and/or activity is linked to oxidative stress-induced cytotoxicity as well as organismal aging (Wood et al., 2006). In addition, ROS can induce an inflammatory response by triggering NF κ B activation, which leads to production of pro-inflammatory cytokines (Schreck et al., 1991; Asehnoune et al., 2004). Accordingly, peroxisomes may influence the ROS-mediated stress response and the pro-inflammatory pathway during viral infections (Raung et al., 2001; Olagnier et al., 2014; Basu et al., 2017). Consistent with this idea, studies using *in vitro* and mouse models have shown that treatment with anti-oxidants or peroxisome proliferative agents can alleviate JEV-induced inflammation as well as neuropathogenesis (Dutta et al., 2009; Sehgal et al., 2012).

Peroxisomes have also been linked to turnover of intracellular structures through mTORC1 (mammalian target of rapamycin complex 1), a negative regulator of autophagy. The activity of mTORC1 is repressed by the kinase ataxia-telangiectasia mutated (ATM) as well as the tuberous sclerosis complex (TSC) which is composed of TSC1, TSC2 and Rheb (Zhang et al., 2015). A number of studies revealed that ATM, TSC1 and TSC2 interact with the peroxisome biogenesis

factors PEX19 and PEX5, which facilitate localization of these mTORC1 suppressors to the peroxisomal membrane where they regulate ROS-induced mTORC1 signaling (Watters et al., 1999; Zhang et al., 2013, 2015). While the precise mechanism of membrane integration and the signaling molecules involved remain elusive, this finding supports a scenario in which peroxisomes provide a platform for molecular interactions and coordination of multiple signaling processes.

6.2.2 Peroxisome-mediated antiviral signaling

Another breakthrough that implicated peroxisomes as signaling organelles was the observation that the adaptor molecule MAVS localizes to peroxisomal membrane (Dixit et al., 2010). MAVS was originally discovered as an outer mitochondrial membrane protein (Seth et al., 2005). Structural and functional analyses revealed the importance of MAVS oligomerization (Tang and Wang, 2009; Hou et al., 2011) and mitochondrial dynamics (Koshiba et al., 2011) in RLR-mediated antiviral signaling. Based on the current knowledge of mitochondrial MAVS, several predictions can be made regarding how this antiviral mediator is regulated at peroxisomes.

In the initial study by Dixit and colleagues, a small pool of MAVS was found to localize to peroxisomes in mouse and human cell lines (Dixit et al., 2010). MAVS may be inserted into the membrane of peroxisomes in a way similar to other tail-anchored PMPs such as Mff and Fis1, a process that is likely dependent on PEX19 and PEX3 (Halbach et al., 2006; Yagita et al., 2013). However, this remains to be demonstrated experimentally.

Following detection of viral RNA, RLR interacts with MAVS through their caspase activation and recruitment domain (CARDs), leading to oligomerization of MAVS on the mitochondrial membrane (Hou et al., 2011). The intermolecular interactions between CARD

domains mediate formation of MAVS aggregates in a prion-like manner (Hou et al., 2011). Subsequent recruitment of signaling molecules including TBK1 and IKK ϵ that are required for the activation of downstream transcription factors IRF3 and NF κ B is dependent on both the CARD and transmembrane domain of MAVS (Seth et al., 2005; Hou et al., 2011). This suggests that mitochondrial membrane association is a prerequisite for efficient signal transduction. Accordingly, it is likely that peroxisomal MAVS oligomerizes upon activation by RLR and association with peroxisomal membrane is required for downstream signaling. In addition, peroxisomal MAVS may form signaling synapses with its counterparts on mitochondria and MAM (mitochondria-associated membrane) through CARD-mediated interactions. Consistent with this idea, spatial contacts between MAVS among these subcellular structures have been described in a human hepatocyte cell line during HCV infection (Horner et al., 2011); however, to what extent each of these structures contribute to IFN induction is not clear.

Several modulators of mitochondrial dynamics have been implicated in regulating MAVS function. For instance, components of the mitochondria fusion machinery, mitofusion 1 (Mfn1) and OPA1, promote RLR-signaling, whereas the mitochondria fission proteins Fis1 and DRP1 suppress RLR-MAVS signal transduction (Castanier et al., 2010). Our microscopic analyses revealed no significant morphological changes in peroxisomes during flavivirus infection although the distribution of the organelles was altered and the numbers were reduced. However, because peroxisome elongation is a transient process (reviewed in (Smith and Aitchison, 2013b)), we cannot rule out the possibility that peroxisome morphogenesis has occurred but we failed to detect such changes by imaging of fixed cells. If peroxisomal dynamics indeed influence the activation of MAVS, peroxisome biogenesis factors such as those involved in the division pathway (i.e., PEX11, DRP, Mff and Fis1) may play key roles in this process. Based on our preliminary data,

transient silencing of *PEX* genes exerts differential effect on IFN expression following stimulation by poly(I:C). These observations posit a scenario in which different peroxins perform distinct functions to regulate peroxisome dynamics and thus modulate the antiviral response from this location.

Regulation of RLR-mediated signaling is also dependent on post-translational modification of MAVS (reviewed in (Belgnaoui et al., 2011)). For example, both ubiquitination and phosphorylation of MAVS have been shown to influence MAVS-mediated IFN induction (Arimoto et al., 2007; Pan et al., 2014; Liu et al., 2015, 2017). Little is known about the modulators of peroxisomal MAVS or the composition of the associated signaling complex. Peroxisomal MAVS may recruit the same mediators for functional activation and/or signal transduction; or it may utilize a different subset of regulatory molecules. If the latter is true, it is tempting to speculate that subcellular localization of MAVS dictates signaling outcomes through the recruitment of unique signaling mediators. Mass spectrometry of peroxisomal MAVS-binding partners as well as gene silencing analyses can help identify regulators and components of the MAVS-associated signaling complex at peroxisomes.

Finally, it has been shown that mitochondrial membrane potential ($\Delta\Psi_m$) and oxidative stress can influence MAVS oligomerization (Tal et al., 2009; Koshiba et al., 2011; Zhao et al., 2012). Although peroxisomes do not generate a membrane potential like mitochondria, they are important players in ROS metabolism. As such, peroxisome-regulated ROS metabolism may affect MAVS activation and/or downstream signaling.

6.2.3 Modulation of peroxisome biogenesis and antiviral signaling by flaviviruses

Given that peroxisomes contain MAVS and can mediate innate immune signaling, it is conceivable that viruses deploy strategies to antagonize this antiviral system. Our study (detailed in chapter 3) is the first report demonstrating a direct interaction between flaviviruses and peroxisomes. While the precise mechanism remains elusive, our data posit the following scenarios to explain how flaviviruses may interfere with peroxisome biogenesis and the antiviral signaling conducted through this organelle (Figure 6.1).

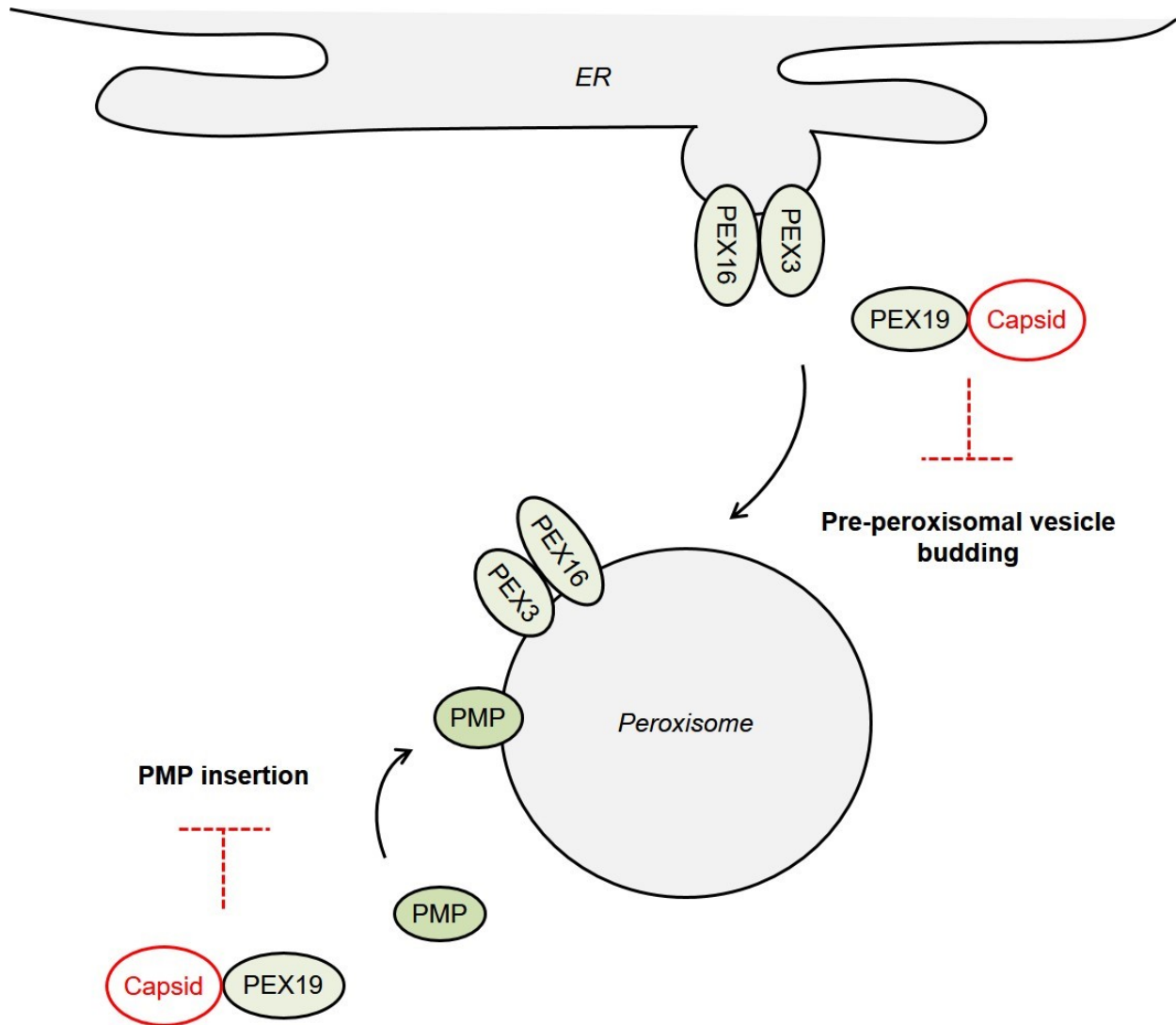


Figure 6.1 Model to account for how flaviviruses interfere with peroxisome biogenesis. PEX19 is a cytosolic chaperone required for insertion of peroxisomal membrane proteins (PMPs) through interaction with the membrane docking complex composed of PEX3 and PEX16. In addition, PEX19 interacts with PEX3 and facilitates budding of pre-peroxisomal vesicles from the ER during *de novo* peroxisome formation. I propose that binding of flavivirus capsid proteins to PEX19 interferes with the ability of this peroxin to interact with PEX3 and/or PMPs, thereby disrupting the membrane assembly process as well as pre-peroxisomal vesicle budding. Dashed red lines indicate speculative processes that require further experimental validation.

First, capsid protein-dependent sequestration and virus-induced degradation of PEX19 may impair the chaperone activity of this peroxin and thus membrane integration of PMPs. While we did not detect dramatic alterations in PMP localization in infected cells or in cells expressing capsid proteins, it is still possible that the function of PEX19 was affected through interaction with capsids. Instead of analyzing cells that were fixed at selected time-points, photo/pulse-chase-labelling assays could be utilized to monitor the localizations of PEX19-dependent PMPs tagged with a photo-activated fluorescent protein (Kim et al., 2006). In parallel, co-immunoprecipitation analyses could be used to determine whether binding of PEX19 to cargos or to the docking complex PEX3/PEX16 is impaired by viral infection or capsid expression.

Second, loss of PEX19 function leads to defects in *de novo* peroxisome formation. It has been reported that interaction between PEX19 and PEX3 is essential for budding of pre-peroxisomal vesicles from the ER in mammalian cells (Schmidt et al., 2012). Our study showed that viral infection leads to reduced peroxisome numbers, a process that is unlikely due to changes in the peroxisome division pathway because sizes of the organelles are not significantly affected by infection. However, it is unclear whether this phenomenon is the direct result of defects in the formation and/or budding of pre-peroxisomal vesicles. To address this question, *de novo* peroxisome biogenesis could be examined in the presence of viral infection or capsid protein expression using cells devoid of peroxisomes (such as *PEX19*-, *PEX3*- or *PEX16*-null human fibroblasts). Nascent organelle formation could be induced by ectopic expression of the missing peroxin (South and Gould, 1999; Honsho et al., 2002; Tam et al., 2005; Kim et al., 2006). If *de novo* peroxisome biogenesis were affected, we would expect to see less peroxisomes formed from the ER in infected and/or capsid-expressing cells.

Third, reduction in PEX19 levels and peroxisome numbers dampen peroxisomal MAVS-mediated antiviral signaling. Since targeting of MAVS (a membrane protein) to peroxisomes likely relies on PEX19, reduction of this peroxin may decrease the pool of MAVS available for signal transduction from this organelle. Our data showing that DENV/WNV infection suppresses IFN- λ induction correlate with the reduction seen in PEX19 and peroxisome numbers. To address this further, analyses of MAVS localization as well as PEX19-MAVS interaction in infected cells could be performed. My data also indicate that PEX19 has a role in Type-III IFN production (as demonstrated by *in vitro* RNAi assay) and therefore, degradation of this peroxin in infected cells would be expected to negatively impact antiviral signaling. Similarly, reduction of peroxisomes may lead to redistribution of MAVS to other subcellular structures, thereby changing the outcome of antiviral response. Consistent with this speculation, a previous study demonstrated that increased peroxisomal localization of MAVS due to disruption in MAM-mitochondria contacts is associated with elevated IFN- β expression (Horner et al., 2011). As suggested by Horner *et al.*, this phenomenon occurs possibly because when MAVS is localized to peroxisomes, it is not constrained by negative regulators such as NLRX1 at mitochondria (Moore et al., 2008), thus resulting in increased signal transduction.

Lastly, maintenance of peroxisomes is governed by biogenesis and degradation; the latter process is mediated through selective autophagy also known as pexophagy (Iwata et al., 2006). Previous studies have shown that flaviviruses such as DENV and WNV activate the autophagic pathway (Beatman et al., 2012; Heaton and Randall, 2010). Thus, it is possible that accelerated degradation of peroxisomes due to upregulated pexophagy contributes in part to reduced peroxisome abundance in infected cells. To test this idea, we could examine how peroxisome

numbers in infected cells are affected by treatment with autophagy inhibitors and/or loss of proteins required for autophagy.

6.2.4 Perspective: the role of peroxisomes in flavivirus replication and pathogenesis

The identification of peroxisomes as targets for flaviviruses opens up new opportunities for research as well as antiviral developments. Apart from counteracting the IFN system, capsid protein dependent-sequestration of PEX19 or other peroxins may facilitate virus replication. Consistent with this idea, we observed that knockdown of *PEX19* led to decreased virus production. Because PEX19 is responsible for PMP peroxisomal targeting as well as peroxisome biogenesis, it is also possible that reduced PMP and/or peroxisomal functions due to *PEX19* silencing has deleterious effects on virus replication (Tanner et al., 2014). To investigate this further, it would be of interest to determine the effects of silencing other peroxins on viral replication as well as innate immune signaling.

From a clinical perspective, it would be intriguing to explore the use of peroxisome proliferative drugs to improve innate immune response and treat viral infections. A recent *in vivo* study showed that administration of fenofibrate, a reagent that induces peroxisome proliferation through the peroxisome proliferative activated-receptor α (PPAR α) pathway, has an anti-inflammatory effects on JEV-infected mice and alleviates virus-induced neurotoxicity (Sehgal et al., 2012). Fenofibrate belongs to a class of plasma-lipid lowering drugs called fibrates (Issemann and Green, 1990), which are used to treat certain metabolic symptoms such as high blood triglyceride levels. In rodent models, both the hypolipidemic and neuroprotective functions of fibrates are thought to be mediated through PPAR α -dependent peroxisome proliferation (Reddy and Krishnakantha, 1975; Deplanque et al., 2003; Gray et al., 2011); however, whether these compounds induce peroxisome proliferation in human cells is unknown. Recent high throughput

screening has identified novel peroxisome proliferative agents independent of PPAR in human hepatocyte cell lines (Chiu et al., 2014). It is tempting to speculate that candidates with anti-inflammatory, anti-oxidant, and/or antiviral capacity may be used to treat WNV and JEV-induced encephalitis.

6.3 The immune evasion strategies of ZIKV

ZIKV re-emerged less than three years ago but the pace of research discovery in this area has been impressive as evidenced by the explosion of knowledge regarding viral biology and pathogenesis. This rapid success is due in part to related studies on other flaviviruses. For instance, animal models of DENV have recently been shown to support ZIKV replication and revealed the essential antiviral roles of IFNs during ZIKV infection (Govero et al., 2016; Lazear et al., 2016; Tang et al., 2016; Tripathi et al., 2017).

6.3.1 Interference with IFN induction

IFN induction is the first step through which a host cell mounts a rapid antiviral response and “signals” to neighboring cells that a pathogen has been detected. Genetic ablation of the transcription factors IRF3 and IRF7 impairs IFN production, leading to increased viral burden and mortality in mice infected with flaviviruses (Chen et al., 2013; Lazear et al., 2013, 2016). Not surprisingly, inhibiting IFN expression is of advantage to many viruses, particularly during the early stages of infection. Based on studies from our laboratory and others, ZIKV deploys both common and unique strategies to antagonize the production of IFNs.

In chapter 4, data was presented showing that ZIKV inhibits IFN induction at the level of TBK1 and IRF3 by the viral proteins NS1, NS4A and NS5. This observation was later confirmed by another group who also reported that ZIKV NS1 and NS4B prevent TBK1 phosphorylation

through direct binding (Wu et al., 2017). A similar strategy was reported earlier for DENV and WNV, which utilize NS4B/NS4A to block TBK1 activation (Dalrymple et al., 2015b); however, whether these viral proteins actually bind to the host kinase is unknown. Although our data do not exclude the possibility of NS1-TBK1 interaction, the findings by Wu *et al* are intriguing as mature NS1 resides in the ER lumen or is secreted whereas TBK1 is a cytosolic kinase. An important question then is how can these two proteins physically interact. A plausible answer is that binding of NS1 to TBK1 is mediated by a host factor, which is anchored to the ER membrane and interacts with TBK1. The adaptor molecule STING is a potential candidate since it resides at the ER membrane and activates TBK1 downstream of cGAS-signaling (Tanaka and Chen, 2012). During flavivirus infection, STING mediates IFN induction and virus-mediated cleavage of this host protein impairs IFN expression (Aguirre et al., 2012). Binding of ZIKV NS1 to STING within the ER lumen may interfere with its ability to activate TBK1, a situation that would prevent downstream signaling. Understanding how the luminal domain of STING affects its activity may shed more light on this issue. Finally, it is possible that the reported interaction between NS1 and TBK1 is in fact an artifact resulting from *in vitro* immunoprecipitation, in which lysis of cellular membranes may allow for release of NS1 into the cytosol to bind TBK1. In this case, NS1-mediated inhibition of TBK1 may involve targeting of signaling component(s) that regulate TBK1 function.

Our data indicate that ZIKV NS4A also interferes with TBK1-directed antiviral signaling. In contrast, Wu and colleagues reported that NS4B is a viral suppressor of TBK1 activation (Wu et al., 2017a). Sequence alignment reveals that NS4A utilized in the two studies share the same amino acid sequence while a conserved mutation (valine to methionine) was found in the NS4B protein (Figure 6.2), suggesting that strain specificity does not play a major role in the observed

discrepancy. It is possible that different experimental conditions (e.g., utilizing different antiviral stimuli) and analytic approaches (i.e., qRT-PCR vs. luciferase assay) contribute to the different experimental outcomes. Apart from inhibiting TBK1, we suspect that NS4A also interferes with a signaling step downstream of IRF3 activation (Figure 6.3) since this viral protein was able to inhibit IRF3-driven promoter activity upon stimulation by a constitutively active IRF3. Potential mechanisms include blocking the dimerization of IRF3 and/or its nuclear translocation. Of note, we showed that ZIKV NS4A also induces translation arrest and therefore, it is possible that the observed reduced IFN induction was due in part to decreased production of cellular proteins needed for this process.

Z1106033	2123	FGVMEALGTLPGHMTERFQEIDNLAVL	2150
PF13/251013-18	2123	FGVMEALGTLPGHMTERFQEIDNLAVL	2150
Z1106033	2151	MRAETGSRPYKAAAQLPETLETIMLLGLLGTVSLGIFFVLMRNKGIGKM	2200
PF13/251013-18	2151	MRAETGSRPYKAAAQLPETLETIMLLGLLGTVSLGIFFVLMRNKGIGKM	2200
Z1106033	2201	GFGMVTLGASAWLMWLSEIEPARIACVLIVVFLLLVLIPEPEKQRSPQD	2250
PF13/251013-18	2201	GFGMVTLGASAWLMWLSEIEPARIACVLIVVFLLLVLIPEPEKQRSPQD	2250
Z1106033	2251	NQMAIIMVAVGLLGLITANELGWLERTKSDSLHLMGRREEGATIGFSMD	2300
PF13/251013-18	2251	NQMAIIMVAVGLLGLITANELGWLERTKSDSLHLMGRREEGATIGFSMD	2300
Z1106033	2301	IDLRPASAWAIYAALTFITPAVQHAVTTSYNNYSLMAMATQAGVLFMG	2350
PF13/251013-18	2301	IDLRPASAWAIYAALTFITPAVQHAVTTSYNNYSLMAMATQAGVLFMG	2350
Z1106033	2351	KGMPFYAWDFGVPLLMIGCYSQLTPLTLIVAIILLVAHYMYLIPGLQAAA	2400
PF13/251013-18	2351	KGMPFYAWDFGVPLLMIGCYSQLTPLTLIVAIILLVAHYMYLIPGLQAAA	2400
Z1106033	2401	ARAAQKRTAAGIMKNPVVDGIVVTDIDTMTIDPQVEKMGQVLLIAVAVS	2450
PF13/251013-18	2401	ARAAQKRTAAGIMKNPVVDGIVVTDIDTMTIDPQVEKMGQVLLIAVAVS	2450
Z1106033	2451	SAILSRTAWGWGEAGALITAATSTLWEGSPNKYWNSSTATSLCNIFRGSY	2500
PF13/251013-18	2451	SAILSRTAWGWGEAGALITAATSTLWEGSPNKYWNSSTATSLCNIFRGSY	2500
Z1106033	2501	LAGASLIYTVTRNAGLVKRRGGGTGETLGEKWKARLNQMSALEFYSYKKS	2550
PF13/251013-18	2501	LAGASLIYTVTRNAGLVKRRGGGTGETLGEKWKARLNQMSALEFYSYKKS	2550
Z1106033	2551	GITEVCREEARRALKDGVATGGHAVSRGSAKLRWLVERGYLPYQKVIDL	2600
PF13/251013-18	2551	GITEVCREEARRALKDGVATGGHAVSRGSAKLRWLVERGYLPYQKVIDL	2600
Z1106033	2601	GCGRGGWSYYAATIRKQVEVKGYTKGGPGHEEFLVQSYGWNIVRLKSGV	2650
PF13/251013-18	2601	GCGRGGWSYYAATIRKQVEVKGYTKGGPGHEEFLVQSYGWNIVRLKSGV	2650
Z1106033	2651	DVFHMAAEPDCLLLCDIGESSSSPEVEEARTLRVLSMVGDWLEKRPGAF	2700
PF13/251013-18	2651	DVFHMAAEPDCLLLCDIGESSSSPEVEEARTLRVLSMVGDWLEKRPGAF	2700
Z1106033	2701	IKVLCPYTSTMMETLERLQRRYGGGLVRVPLSRNSTHEMYWVSGAKSNTI	2750
PF13/251013-18	2701	IKVLCPYTSTMMETLERLQRRYGGGLVRVPLSRNSTHEMYWVSGAKSNTI	2750
Z1106033	2751	KSVSTTSQLLLGRMDGPRRPV	2771
PF13/251013-18	2751	KSVSTTSQLLLGRMDGPRRPV	2771

Figure 6.2 Sequence alignment of the NS4A-B region within the polyprotein of ZIKV strains Z1106033 and PF13/251013-18. The full length polypeptide sequences of ZIKV isolates Z1106033 (utilized in the study by Wu *et al.*) and strain PF13/251013-18 (utilized in our study) were obtained from NCBI (accession number KX369547.1 and KU312312.1 respectively). Sequence alignment was performed using the protein sequence pairwise alignment program EMBOSS needle (EMBL-EBI). Red box indicates the one amino acid residue difference between NS4A-B proteins of the two strains.

ZIKV NS5 also inhibits TBK1- and IRF3-directed signaling but it is not clear if this involves direct binding or through interference with components of the TBK1/IRF3-associated signaling complex. A recent study demonstrated that JEV NS5 inhibits IRF3 and NF κ B nuclear translocation by disrupting their interaction with the nuclear-import cargo receptor, importin α/β (Ye et al., 2017). By analogy, it is possible that ZIKV NS5 impedes nuclear transport of these transcription factors using a similar strategy. Since a significant proportion of NS5 localizes to the nucleus, it would be of interest to determine whether this viral protein hinders the transcriptional activity of IRF3 and/or NF κ B (Figure 6.3).

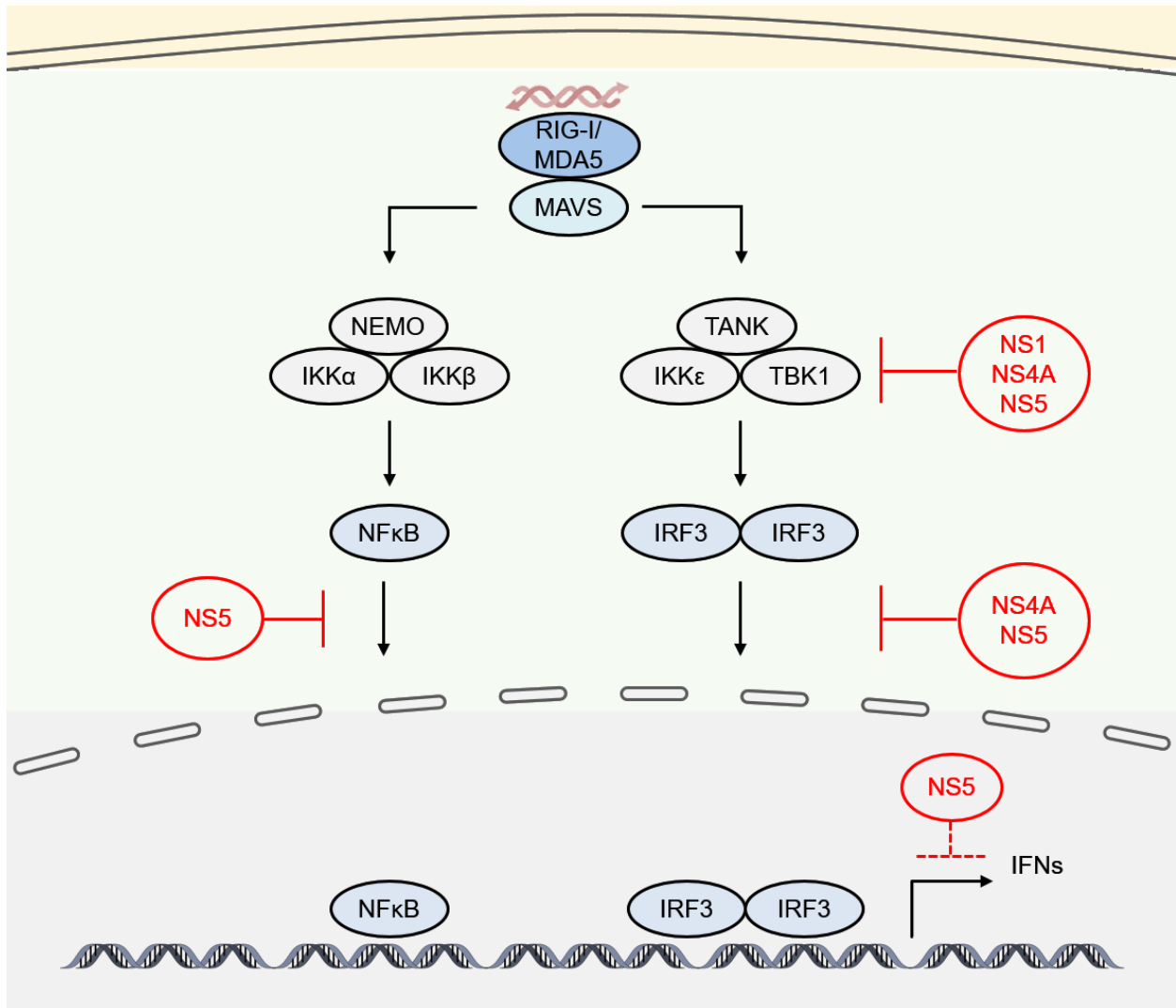


Figure 6.3 How ZIKV non-structural proteins inhibit interferon (IFN) induction and signaling. During ZIKV infection, the IFN response can be induced by the cytosolic helicases RIG-I/MDA5, which recognize unique structures within viral dsRNA, leading to activation of the adaptor protein MAVS and the downstream kinase complexes NEMO/IKK α /IKK β and TBK1/IKK ϵ /TANK. These kinases phosphorylate the transcription factors IRF3 and the inhibitor of NF- κ B, leading to the activation of IRF3 and NF- κ B. The activated transcription factors translocate into the nucleus and promote the expression of *ifn* genes. The viral proteins NS1, NS4A and NS5 were shown to inhibit IFN induction by blocking the function of TBK1. NS4A and NS5 also interfere with signal transduction downstream of IRF3 activation. Finally, NS5 reduces signaling downstream of NF κ B stimulation and may directly interfere with IRF3-mediated IFN transcription. Dashed red lines indicate speculative processes that require experimental validation.

6.3.2 Interference with IFN signaling

Inhibition of IFN-signaling is well documented for flaviviruses. Studies by our group and others showed that ZIKV NS5 targets human STAT2 for proteasomal degradation, thereby preventing ISG expression (Grant et al., 2016; Kumar et al., 2016). Degradation of STAT2 has also been reported in cells infected with respiratory syncytial virus (Elliott et al., 2007; Whelan et al., 2016), Nipah virus (Rodriguez et al., 2004) and the DENV (Ashour et al., 2009; Morrison et al., 2013), all of which exploit the cellular ubiquitin-proteasome system to induce loss of STAT2.

Although the NS5 of ZIKV and DENV is an important weapon to antagonize the host IFN pathway, a number of mechanistic differences between the two viruses are worth noting. First, proteolytic processing of the DENV NS5 precursor (at a site upstream of its N-terminus) is required for reducing STAT2 levels (Ashour et al., 2009). In contrast, we showed that this is not required for ZIKV NS5 to bind to and trigger STAT2 degradation. Second, the methyltransferase (MTase) domain of DENV NS5 (between amino acid residues 11 and residue 306) is required for STAT2 binding (Morrison et al., 2013) and the preceding 10 amino acid residues are needed to induce degradation of this host factor (Ashour et al., 2009). While ZIKV NS5 also utilizes the MTase domain to interact with STAT2, the 10 amino acid residues at its N-terminus are not required for STAT2 degradation. Alignment of the N-terminal regions of DENV and ZIKV NS5 reveals three differences in the first 10 amino acid residues (Figure 6.4). It is known that the threonine (T) and glycine (G) residues at positions 2 and 3 of DENV NS5 are important for recruiting the putative E3 ubiquitin ligase UBR4 to promote STAT2 reduction (Morrison et al., 2013). Assuming that it also acts as a scaffold like DENV NS5, sequences within the RdRP domain of ZIKV NS5 (between residue 306 and residue 903) may facilitate its binding to an E3 ligase, the identity of which remains to be determined (Figure 6.5).

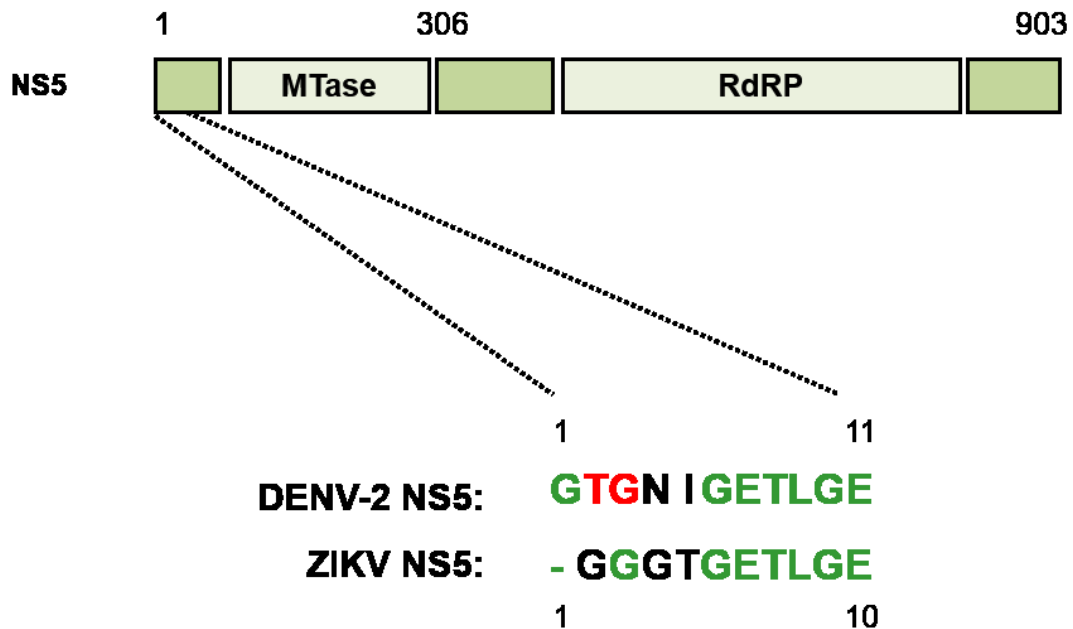


Figure 6.4 Sequence alignment of the amino terminal ends of DENV-2 and ZIKV NS5 proteins. A schematic representation of flavivirus NS5 protein showing methyltransferase (MTase) and RNA-dependent RNA polymerase (RdRP) domains (top panel). The full length sequences of ZIKV NS5 and DENV-2 NS5 were obtained from NCBI (accession number KX369547.1 and NC_001474.2 respectively). Sequence alignment was performed using the Vector NTI software (Thermo Fisher Scientific) (bottom panel). Green letters indicate identical residues; black letters indicate unique residues; and red letters indicate residues known to be required for inducing STAT2 degradation during DENV infection (Morrison et al., 2013).

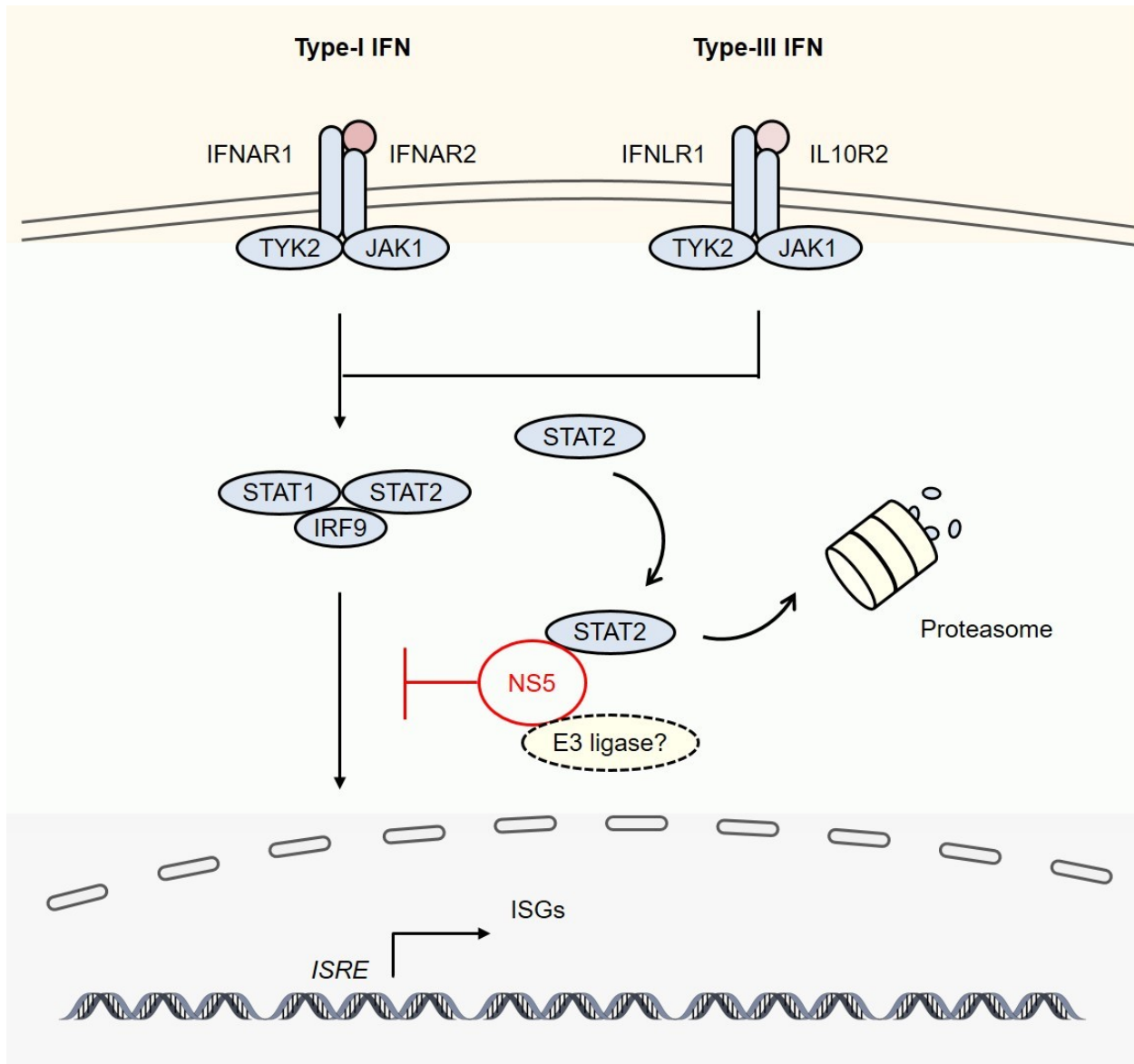


Figure 6.5 Model to account for how ZIKV NS5 protein affects type-I/III interferon (IFN) signaling. IFN signaling is induced following binding of type-I IFNs to the cell surface receptors IFNAR1 and IFNAR2, or type-III IFNs to IFNLR1 and IL10R2. This leads to activating phosphorylation of the downstream kinases JAK1 and TYK2 which then phosphorylate the transcription factors STAT1 and STAT2. The transcription factors heterodimerize and then form a complex with IRF9 to facilitate *ISRE* promoter-mediated expression of IFN-stimulated genes (ISGs). ZIKV NS5 acts as a scaffold to link STAT2 and an as yet unidentified E3 ubiquitin ligase. Ubiquitination of STAT2 leads to its degradation through the proteasome. Dashed line indicates speculative processes and require further experimental validation.

STAT2 degradation during DENV and ZIKV infection is a species-specific process. Loss of STAT2 occurs during ZIKV infection of human and monkey cell lines, but STAT2 of murine origin is resistant to this process (Kumar et al., 2016; Grant et al., 2016). From virus-host perspective this makes sense because humans and non-human primates are the primary mammalian hosts for DENV and ZIKV. The inability of DENV NS5 to bind murine STAT2 could explain (at least partly) why murine STAT2 is resistant to degradation (Ashour et al., 2010), but whether this is also true for ZIKV NS5 remains to be determined. These findings may provide the basis for development of new animal models for DENV and ZIKV. For most DENV and ZIKV pathogenesis studies, mice strains that lack a fully functioning IFN system are employed. Consequently, virus-induced symptoms or pathologies developed in these animals are likely exaggerated. Developing mice that express human STAT2 instead of the murine orthologue may be a more relevant model for studying flavivirus pathogenesis and testing new antiviral therapeutics such as those described below.

6.3.3 Perspective: targeting NS5-STAT2 interaction as a novel antiviral strategy

The viral polymerase is a key target for antiviral development due to its essential role in viral replication. Several pharmaceutical inhibitors have demonstrated *in vitro* pan-serotype activity by targeting specific sites of DENV NS5 engaged in viral RNA-binding and polymerization (Lim et al., 2016). Recently, the crystal structure of a full-length ZIKV NS5 has been resolved (Godoy et al., 2017; Zhao et al., 2017). A few compounds which were shown to suppress replication of other flaviviruses were also demonstrated to reduce ZIKV replication (Retallack et al., 2016; Zmurko et al., 2016). While it is important to improve the specificity and potency of antivirals targeting the enzymatic functions of NS5, identifying inhibitors that can disrupt the NS5-STAT2 interface may be a new avenue for therapeutic development. Depending

on the target site(s), successful candidates may or may not inhibit NS5 enzymatic activities but instead prevent degradation of STAT2 and thus promote a robust IFN response. Characterizing key residue(s) in NS5 required for interaction with STAT2 may help shed more light onto this potential antiviral strategy.

6.4 How ZIKV modulates the host cell stress response

The ability to maintain homeostasis during cellular stress is vital for the health and survival of a cell. In mammals, this task is mostly accomplished by the stress response system, which induces expression of stress-coping molecules, activation of pro-survival pathways, protein translation arrest as well as SG formation. As the stress response can exert both proviral and antiviral effects, flaviviruses including ZIKV have evolved ways to tailor this cellular system to their advantage.

6.4.1 Activation of PKR and UPR signaling

During genome replication, flaviviruses produce dsRNA that can be detected by the cytosolic helicases such as RLR family members and the protein kinase PKR. Although it is still unclear how these viral RNA sensors gain access to viral replication complexes, RLRs are crucial for initiating antiviral responses during flavivirus infection. However, the role of PKR is more controversial. While one report showed that PKR-deficient mice suffer aggravated pathology and increased lethality following WNV infection (Samuel et al., 2006), *in vitro* studies suggest that this kinase is dispensable for controlling DENV replication (Diamond and Harris, 2001; Roth et al., 2017). We showed that ZIKV infection induces activation of PKR but whether or how this kinase affects replication of the virus is not yet clear.

Consistent with the observation that it activates PKR, ZIKV infection also leads to phosphorylation of eIF2 α , a well-known downstream target of PKR. However, whether this is mediated by PKR remains unclear as eIF2 α can also be phosphorylated by the ER transmembrane kinase PERK following UPR activation. Our data revealed that the UPR or at least the IRE1 α -arm of UPR signaling is stimulated upon ZIKV infection. Although we could not detect PERK activation (i.e., phosphorylation of PERK) using immunoblotting, there are reasons to believe that PERK-mediated UPR signaling is also induced. First, all three ER stress sensors, IRE1 α , PERK and ATF6, are regulated by BiP, which releases them to become fully active when it is bound by accumulating misfolded and unfolded proteins during ER stress (Bertolotti et al., 2000; Shen et al., 2002). Therefore, in theory, the three arms of UPR signaling are triggered in parallel by ER stress stimuli and in this case, by ZIKV infection. Second, ZIKV infection does not inhibit eIF2 α phosphorylation induced by the ER stressor thapsigargin, indicating that the virus does not interfere with the function of PERK. Taken together, these data suggest that ZIKV-induced phosphorylation of eIF2 α is mediated by PKR and/or PERK.

While we showed that ZIKV induces (rather than inhibits) eIF2 α phosphorylation, a number of earlier studies reported different findings. In these studies, infection of mammalian cells with DENV, WNV, JEV and ZIKV did not significantly upregulate phospho-eIF2 α levels (Ambrose and Mackenzie, 2011; Elbahesh et al., 2011; Tu et al., 2012b; Roth et al., 2017). In the report by Roth *et al.*, DENV and ZIKV were shown to impair eIF2 α phosphorylation induced by exogenous stress through an undefined mechanism (Roth et al., 2017). The discrepancy between these studies may be due to use of different cell lines (i.e., Huh-7 vs. A549 cells) and/or virus strains (i.e., ZIKV MR766 strain and PL-Cal strain). Further analyses are needed to understand how strain and cell type specificity may affect stress response induction.

6.4.2 Induction of protein translation arrest

While a number of studies reported that WNV and DENV evade host translation shut-off (Ambrose and Mackenzie, 2011; Peña and Harris, 2011), Roth and colleagues observed a general repression of protein translation during flavivirus infection. Consistent with this observation, our data showed that ZIKV infection triggers global inhibition of cellular protein synthesis, a process likely associated with phosphorylation of eIF2 α and mediated by the viral proteins NS3 and NS4A. However, we do not know how these viral factors promote translation arrest since no significant activation of UPR signaling, and by extension, PERK, was observed in cells expressing either viral protein. Further analysis is needed to determine whether expression of NS3 or NS4A alone induces PERK activation, eIF2 α phosphorylation and/or interferes with component(s) of the translation initiation complexes.

Regarding UPR signaling, we observed an increase of *XBPI* transcript splicing in cells expressing E protein or NS2A of ZIKV; but how these viral factors activate IRE1 α and potentially other arms of UPR signaling is unknown. Studies have shown that the E protein of DENV and JEV interacts with the protein chaperone BiP to facilitate viral replication (Limjindaporn et al., 2009; Nain et al., 2017). Therefore, it is possible that ZIKV E protein and NS2A hijack BiP, leading to activation of the ER stress sensors. These viral proteins may also directly bind and activate IRE1 α , whose function is induced through binding of unfolded proteins (Gardner and Walter, 2011). As suggested for DENV and JEV (Yu et al., 2006), activation of the XBP1 pathway can promote cell survival by alleviating ER burden thus benefiting ZIKV replication. Future studies are needed to characterize the role IRE1 α -XBP1 signaling in the host stress response to ZIKV infection.

An expected consequence of virus-induced translation shut-off is restriction of viral protein synthesis. However, it seems that ZIKV and other flaviviruses have evolved ways to evade this antiviral response (Roth et al., 2017). In the course of our studies, we observed continuous production of viral proteins over the course of ZIKV infection (particularly between 12 and 48 h.p.i.). Several scenarios that are not mutually exclusive could explain this phenomenon. First, ZIKV may utilize a cap-independent pathway for genome translation. *In vitro* studies suggest that translation of DENV genome still occurs when the cap-dependent pathway is inhibited (Edgil et al., 2006). This is further supported by the observation that expression of a dysfunctional eIF4E (i.e., phospho-mutants), which fails to bind the cap structure and initiate cap-dependent mRNA translation, has little impact on DENV replication (Roth et al., 2017). Second, inhibition of protein synthesis may occur in an oscillating fashion, which creates windows of opportunity for viral polyprotein synthesis. Consistent with this idea, the degree of protein translation arrest is coordinated with expression of the phosphatase 1c cofactor GADD34 (growth arrest and DNA damage-inducible protein) upon dsRNA stimulation (Dalet et al., 2017). GADD34 facilitates dephosphorylation of eIF2 α and is essential for translation recovery to permit “pulse” production of IFN- β . Since increased expression of GADD34 was observed in DENV-infected cells (Peña and Harris, 2011; Roth et al., 2017), it is tempting to speculate that other flaviviruses including ZIKV upregulate this host factor to overcome translation repression, thereby allowing viral protein synthesis to occur. Third, flavivirus genomic RNA may contain elements that allow it to out-compete cellular mRNAs for the pool of active translational factors during cellular translation arrest. Lastly, as suggested by Roth *et al.*, specific viral protein(s) may facilitate the recruitment of the translation machinery to the viral genome under stress conditions.

6.4.3 Inhibition of SG formation

While a number of RNA viruses including respiratory syncytial virus and HCV stimulate formation of SGs (Lindquist et al., 2010; Garaigorta et al., 2012b), flaviviruses including DENV, WNV and JEV have been reported to block SG biogenesis (Emara and Brinton, 2007; Katoh et al., 2013; Roth et al., 2017). Our data indicate that ZIKV also inhibits SG assembly in a human lung epithelial cell line as well as in primary human fetal astrocytes, suggesting that modulation of SG biogenesis may be of clinical significance in fetal neuropathogenesis.

Several picornaviruses such as poliovirus and encephalomyocarditis virus (White et al., 2007b; Ng et al., 2013) block SG formation by cleaving cellular proteins necessary for SG biogenesis. However, based on our data, this does not appear to occur in ZIKV-infected cells nor does the virus seem to alter phosphorylation of G3BP1 (which can also affect SG formation). Deacetylation, methylation and poly-ADP ribosylation as well of SG components are also known to drive SG condensation (Kwon et al., 2007; Tsai et al., 2016). At the present time, we do not know if ZIKV or other flaviviruses affect these post-translational modifications of SG factors.

Co-opting SG-associated proteins to benefit virus replication or other aspects of the virus life cycle has been documented for Chikungunya virus (Fros et al., 2012), Sindbis virus (Cristea et al., 2010), HCV (Ariumi et al., 2011; Garaigorta et al., 2012) as well as WNV and DENV (Emara and Brinton, 2007). Our research suggests that the SG components G3BP1, Caprin-1 and TIAR are important for the ZIKV life cycle; however the mechanisms are not yet known. One possibility is that they facilitate viral genome synthesis similar to what was proposed for TIA-1/TIAR during DENV and WNV infection (Emara and Brinton, 2007), a scenario supported by the observation that G3BP1 binds to ZIKV genomic RNA. Based on transfection studies, only the capsid protein was shown to stably associate with G3BP1 and Caprin-1. However, we cannot rule out the

possibility that a pool of these host proteins also interact with component(s) of the viral replication complex during infection. Another possibility is that SG proteins promote the transition from genome translation to genome replication or vice versa as G3BP1 has been implicated in the translational regulation of certain cellular mRNAs (Ortega et al., 2010) as well as Sindbis virus genomic RNA (Cristea et al., 2010). SG assembly factors may also facilitate virion assembly and/or production as has been reported for HCV infection (Garaigorta et al., 2012); but so far, there is no hard evidence for this during flavivirus infection.

A consequence of co-opting SG proteins for other purposes would be inhibition of SG formation. We identified the viral capsid, NS3, NS2B-3 and NS4A as suppressors of SG assembly, providing the first evidence that ZIKV proteins modulate SG biogenesis. In the case of capsid proteins, it is likely that they inhibit SG assembly by sequestering G3BP1 as well as Caprin-1. We also observed reduced SG formation in cells expressing capsid proteins of MVEV or YFV. Because we only tested for interaction between ZIKV proteins and a small number of SG components, we cannot exclude the possibility that other viral proteins inhibit SG formation by sequestering other SG factors. Taken together, our data posit the following scenarios during ZIKV infection: 1) phosphorylation of eIF2 α and translation arrest occurs in response to viral infection; and 2) multiple viral proteins and genomic RNA sequester SG-associated proteins (e.g., G3BP1 and Caprin-1) to benefit viral replication and/or assembly, a process that also serves to block the antiviral function of SGs (Figure 6.6).

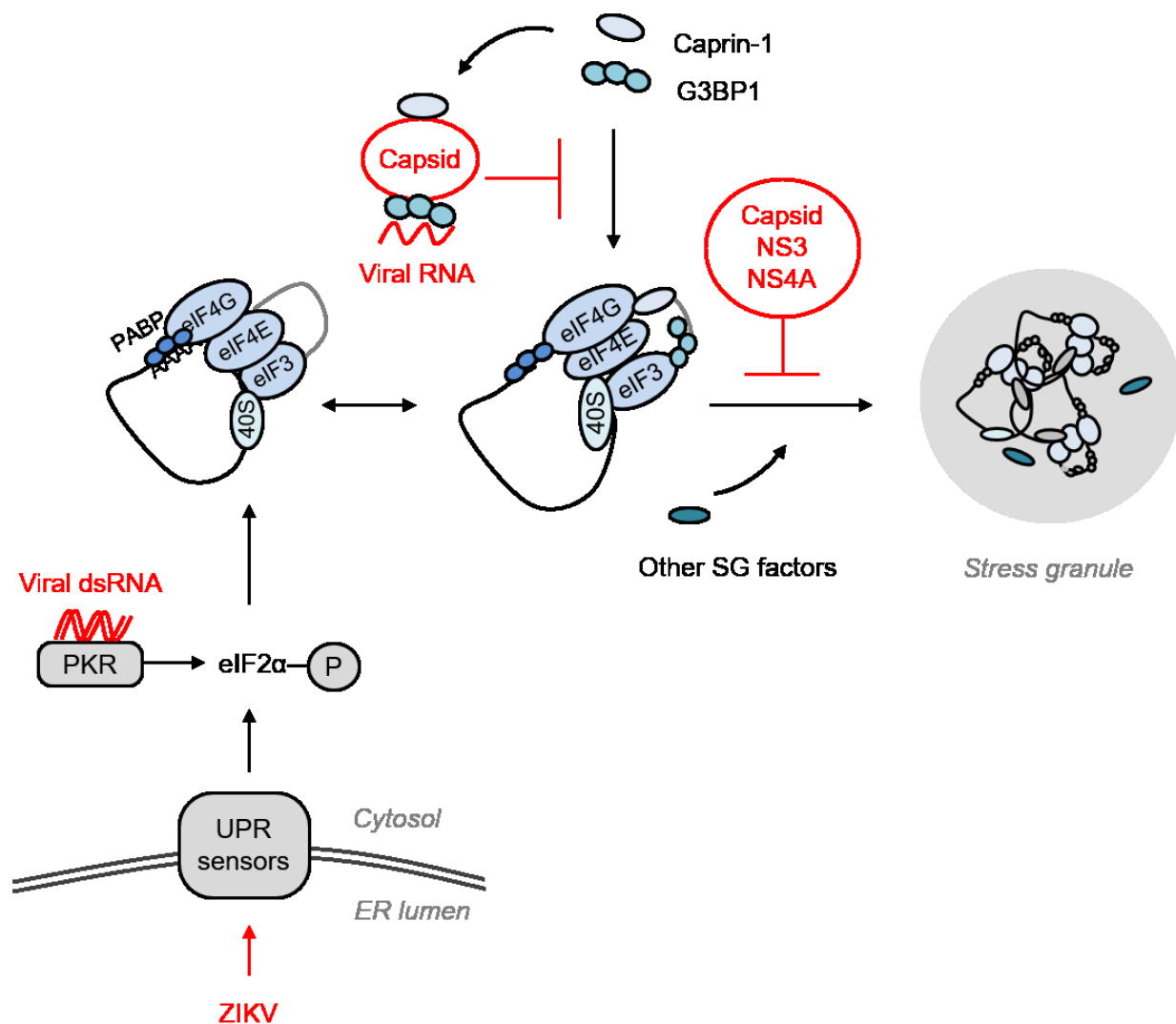


Figure 6.6 Modulation of the stress response by ZIKV. ZIKV infection leads to activation of the dsRNA-activated protein kinase PKR and the unfolded protein response (UPR) in the ER. This results in phosphorylation of the translation initiation factor eIF2 α , leading to decreased ternary complexes and thus reduced translation initiation. Normally, binding of host factors such as G3BP1 and Caprin-1 promotes condensation of stalled initiation complexes and formation of stress granules (SGs). During ZIKV infection though, capsid protein and viral genomic RNA sequester G3BP1 as well as Caprin-1 to promote viral replication through an unknown mechanism. The capsid protein as well as NS3 and NS4A further block SG assembly downstream of translationally silenced mRNP formation.

Cells infected with flaviviruses also contain noncoding subgenomic flaviviral RNAs (sfRNAs), which are pathogenic determinants generated from incomplete degradation of genomic RNAs by the host ribonuclease Xrn1 (Pijlman et al., 2008). Interestingly, sfRNAs of DENV were shown to bind G3BP1, G3BP2 and Caprin-1 during infection (Bidet et al., 2014). Since ZIKV was recently shown to produce sfRNA (Akiyama et al., 2016), it is possible that sequestration of SG-associated factors by sfRNAs also contributes to infection-induced inhibition of SG assembly.

While we focused on determining how ZIKV interferes with the SG assembly process, it is also possible that the virus alter the disassembly pathway of these RNA granules. Disassembly of SGs has been shown to correlate with recovery in cellular protein synthesis (Mazroui et al., 2007) and may involve dissociation of SG contents and/or release of mRNA from granules to resume translation (Buchan and Parker, 2009). A number of RNA-binding proteins have been implicated in promoting SG disassembly including Staufen and Grb7. Over-expression of Staufen can inhibit SG assembly possibly by stabilizing mRNA-polysome interaction (Thomas et al., 2005) while phosphorylation of Grb7 is required to weaken its interaction with HuR, TIA-1 and certain mRNAs (Tsai et al., 2008) from SGs. Accordingly, determining the levels, post-translational modifications of and potential viral interaction with SG disassembly factors such as Staufen and Grb7 could provide further insights into the mechanism by which ZIKV modulate the SG pathway.

6.4.4 Perspective: physiological consequences of stress response modulation

In this study, we focused on understanding the mechanisms by which ZIKV modulates the stress response, but how the altered stress response pathways may impact the host cell remains largely unknown. Formation of SGs can prevent apoptosis through reduction of ROS (Takahashi et al., 2013) as well as through sequestration of the receptor for activated C-kinase (RACK1) into the RNA granules (Arimoto et al., 2008). RACK1 facilitates activation of the apoptotic pathway

mediated through p38 and JNK MAPK in response to certain stress stimuli (Arimoto et al., 2008). Accordingly, suppression of SG assembly may augment levels of intracellular ROS and RACK1-mediated apoptosis in ZIKV-infected cells, potentially contributing to tissue damage in the placenta as well as neurotoxicity in the developing fetus (Retallack et al., 2016). Monitoring the stress response during viral persistence in physiologically relevant cell types may provide novel insights into ZIKV-induced congenital disorders.

6.5 Concluding remarks

As obligate intracellular parasites, viruses have evolved diverse strategies to exploit host cell machineries to create favorable environments for replication. To achieve this goal, virtually all RNA viruses including flaviviruses encode multi-functional proteins. From the small capsid protein to the comparatively large polymerase, flavivirus proteins have been shown to interact with a growing list of host factors likely as means to facilitate viral replication and evade antiviral systems. Characterizing these host-virus interactions not only provides insights into virus biology but also advances our knowledge of the cellular processes involved. As demonstrated in this thesis work, interactions between flavivirus components and antiviral pathways have revealed novel functions of peroxisomal proteins and SG factors in the viral life cycle. In turn, these findings underscore the importance of peroxisomes as signaling organelles, the IFN system and the cellular stress response in controlling viral infections. Further elucidating the interactions between flaviviruses and the host cell signaling pathways warrants promise for development of new animal models and therapeutic strategies.

Reference

- Adams Waldorf, K.M., Stencel-Baerenwald, J.E., Kapur, R.P., Studholme, C., Boldenow, E., Vornhagen, J., Baldessari, A., Dighe, M.K., Thiel, J., Merillat, S., Armistead, B., Tisoncik-Go, J., Green, R.R., Davis, M.A., Dewey, E.C., Fairgrieve, M.R., Gatenby, J.C., Richards, T., Garden, G.A., Diamond, M.S., Juul, S.E., Grant, R.F., Kuller, L., Shaw, D.W.W., Ogle, J., Gough, G.M., Lee, W., English, C., Hevner, R.F., Dobyns, W.B., Gale Jr, M., Rajagopal, L., 2016. Fetal brain lesions after subcutaneous inoculation of Zika virus in a pregnant nonhuman primate. *Nat Med* advance online publication. doi:10.1038/nm.4193
- Agrawal, G., Fassas, S.N., Xia, Z.-J., Subramani, S., 2016. Distinct requirements for intra-ER sorting and budding of peroxisomal membrane proteins from the ER. *J. Cell Biol.* 212, 335–348. doi:10.1083/jcb.201506141
- Agrawal, G., Joshi, S., Subramani, S., 2011. Cell-free sorting of peroxisomal membrane proteins from the endoplasmic reticulum. *Proc. Natl. Acad. Sci. U.S.A.* 108, 9113–9118. doi:10.1073/pnas.1018749108
- Aguirre, S., Maestre, A.M., Pagni, S., Patel, J.R., Savage, T., Gutman, D., Maringer, K., Bernal-Rubio, D., Shabman, R.S., Simon, V., Rodriguez-Madoz, J.R., Mulder, L.C.F., Barber, G.N., Fernandez-Sesma, A., 2012. DENV Inhibits Type I IFN Production in Infected Cells by Cleaving Human STING. *PLoS Pathog* 8, e1002934. doi:10.1371/journal.ppat.1002934
- Akiyama, B.M., Laurence, H.M., Massey, A.R., Costantino, D.A., Xie, X., Yang, Y., Shi, P.-Y., Nix, J.C., Beckham, J.D., Kieft, J.S., 2016. Zika virus produces noncoding RNAs using a multi-pseudoknot structure that confounds a cellular exonuclease. *Science* 354, 1148–1152. doi:10.1126/science.aah3963
- Albertini, M., Rehling, P., Erdmann, R., Girzalsky, W., Kiel, J.A.K.W., Veenhuis, M., Kunau, W.-H., 1997. Pex14p, a Peroxisomal Membrane Protein Binding Both Receptors of the Two PTS-Dependent Import Pathways. *Cell* 89, 83–92. doi:10.1016/S0092-8674(00)80185-3
- Albornoz, A., Carletti, T., Corazza, G., Marcello, A., 2014. The Stress Granule Component TIA-1 Binds Tick-Borne Encephalitis Virus RNA and Is Recruited to Perinuclear Sites of Viral Replication To Inhibit Viral Translation. *J. Virol.* 88, 6611–6622. doi:10.1128/JVI.03736-13
- Alcon-LePoder, S., Drouet, M.-T., Roux, P., Frenkiel, M.-P., Arborio, M., Durand-Schneider, A.-M., Maurice, M., Blanc, I.L., Gruenberg, J., Flamand, M., 2005. The Secreted Form of Dengue Virus Nonstructural Protein NS1 Is Endocytosed by Hepatocytes and Accumulates in Late Endosomes: Implications for Viral Infectivity. *J. Virol.* 79, 11403–11411. doi:10.1128/JVI.79.17.11403-11411.2005
- Allison, S.L., Schlich, J., Stiasny, K., Mandl, C.W., Heinz, F.X., 2001. Mutational evidence for an internal fusion peptide in flavivirus envelope protein E. *J. Virol.* 75, 4268–4275. doi:10.1128/JVI.75.9.4268-4275.2001
- Alvarez, D.E., Lodeiro, M.F., Ludueña, S.J., Pietrasanta, L.I., Gamarnik, A.V., 2005. Long-range RNA-RNA interactions circularize the dengue virus genome. *J. Virol.* 79, 6631–6643. doi:10.1128/JVI.79.11.6631-6643.2005

- Ambrose, R.L., Mackenzie, J.M., 2011. West Nile virus differentially modulates the unfolded protein response to facilitate replication and immune evasion. *J. Virol.* 85, 2723–2732. doi:10.1128/JVI.02050-10
- Anastasiou, D., Pouligiannis, G., Asara, J.M., Boxer, M.B., Jiang, J., Shen, M., Bellinger, G., Sasaki, A.T., Locasale, J.W., Auld, D.S., Thomas, C.J., Heiden, M.G.V., Cantley, L.C., 2011. Inhibition of Pyruvate Kinase M2 by Reactive Oxygen Species Contributes to Cellular Antioxidant Responses. *Science* 334, 1278–1283. doi:10.1126/science.1211485
- Anchisi, S., Guerra, J., Garcin, D., 2015. RIG-I ATPase Activity and Discrimination of Self-RNA versus Non-Self-RNA. *mBio* 6. doi:10.1128/mBio.02349-14
- Anderson, P., Kedersha, N., 2009. RNA granules: post-transcriptional and epigenetic modulators of gene expression. *Nat Rev Mol Cell Biol* 10, 430–436. doi:10.1038/nrm2694
- Apte-Sengupta, S., Sirohi, D., Kuhn, R.J., 2014. Coupling of replication and assembly in flaviviruses. *Current Opinion in Virology* 9, 134–142. doi:10.1016/j.coviro.2014.09.020
- Aranovich, A., Hua, R., Rutenberg, A.D., Kim, P.K., 2014. PEX16 contributes to peroxisome maintenance by constantly trafficking PEX3 via the ER. *J Cell Sci* 127, 3675–3686. doi:10.1242/jcs.146282
- Araujo, L.M., Ferreira, M.L.B., Nascimento, O.J., Araujo, L.M., Ferreira, M.L.B., Nascimento, O.J., 2016. Guillain-Barré syndrome associated with the Zika virus outbreak in Brazil. *Arquivos de Neuro-Psiquiatria* 74, 253–255. doi:10.1590/0004-282X20160035
- Arimoto, K., Fukuda, H., Imajoh-Ohmi, S., Saito, H., Takekawa, M., 2008. Formation of stress granules inhibits apoptosis by suppressing stress-responsive MAPK pathways. *Nat Cell Biol* 10, 1324–1332. doi:10.1038/ncb1791
- Arimoto, K., Takahashi, H., Hishiki, T., Konishi, H., Fujita, T., Shimotohno, K., 2007. Negative regulation of the RIG-I signaling by the ubiquitin ligase RNF125. *PNAS* 104, 7500–7505. doi:10.1073/pnas.0611551104
- Ariumi, Y., Kuroki, M., Kushima, Y., Osugi, K., Hijikata, M., Maki, M., Ikeda, M., Kato, N., 2011. Hepatitis C Virus Hijacks P-Body and Stress Granule Components around Lipid Droplets. *J. Virol.* 85, 6882–6892. doi:10.1128/JVI.02418-10
- Arjona, A., Ledizet, M., Anthony, K., Bonafé, N., Modis, Y., Town, T., Fikrig, E., 2007. West Nile virus envelope protein inhibits dsRNA-induced innate immune responses. *J. Immunol.* 179, 8403–8409.
- Asehounne, K., Strassheim, D., Mitra, S., Kim, J.Y., Abraham, E., 2004. Involvement of Reactive Oxygen Species in Toll-Like Receptor 4-Dependent Activation of NF- κ B. *The Journal of Immunology* 172, 2522–2529. doi:10.4049/jimmunol.172.4.2522
- Ashour, J., Laurent-Rolle, M., Shi, P.-Y., García-Sastre, A., 2009. NS5 of dengue virus mediates STAT2 binding and degradation. *J. Virol.* 83, 5408–5418. doi:10.1128/JVI.02188-08
- Ashour, J., Morrison, J., Laurent-Rolle, M., Belicha-Villanueva, A., Plumlee, C.R., Bernal-Rubio, D., Williams, K.L., Harris, E., Fernandez-Sesma, A., Schindler, C., García-Sastre, A., 2010. Mouse STAT2 Restricts Early Dengue Virus Replication. *Cell Host & Microbe* 8, 410–421. doi:10.1016/j.chom.2010.10.007
- Avirutnan, P., Fuchs, A., Hauhart, R.E., Somnuk, P., Youn, S., Diamond, M.S., Atkinson, J.P., 2010. Antagonism of the complement component C4 by flavivirus nonstructural protein NS1. *J. Exp. Med.* 207, 793–806. doi:10.1084/jem.20092545
- Avirutnan, P., Hauhart, R.E., Somnuk, P., Blom, A.M., Diamond, M.S., Atkinson, J.P., 2011. Binding of flavivirus nonstructural protein NS1 to C4b binding protein modulates complement activation. *J. Immunol.* 187, 424–433. doi:10.4049/jimmunol.1100750

- Avirutnan, P., Zhang, L., Punyadee, N., Manuyakorn, A., Puttikhunt, C., Kasinrerak, W., Malasit, P., Atkinson, J.P., Diamond, M.S., 2007. Secreted NS1 of dengue virus attaches to the surface of cells via interactions with heparan sulfate and chondroitin sulfate E. *PLoS Pathog.* 3, e183. doi:10.1371/journal.ppat.0030183
- Bai, F., Kong, K.-F., Dai, J., Qian, F., Zhang, L., Brown, C.R., Fikrig, E., Montgomery, R.R., 2010. A Paradoxical Role for Neutrophils in the Pathogenesis of West Nile Virus. *J Infect Dis* 202, 1804–1812. doi:10.1086/657416
- Balinsky, C.A., Schmeisser, H., Ganesan, S., Singh, K., Pierson, T.C., Zoon, K.C., 2013. Nucleolin Interacts with the Dengue Virus Capsid Protein and Plays a Role in Formation of Infectious Virus Particles. *J. Virol.* 87, 13094–13106. doi:10.1128/JVI.00704-13
- Barouch, D.H., Thomas, S.J., Michael, N.L., 2017. Prospects for a Zika Virus Vaccine. *Immunity* 46, 176–182. doi:10.1016/j.immuni.2017.02.005
- Basu, M., Courtney, S.C., Brinton, M.A., 2017. Arsenite-induced stress granule formation is inhibited by elevated levels of reduced glutathione in West Nile virus-infected cells. *PLOS Pathogens* 13, e1006240. doi:10.1371/journal.ppat.1006240
- Bayer, A., Lennemann, N.J., Ouyang, Y., Bramley, J.C., Morosky, S., Marques, E.T.D.A., Cherry, S., Sadovsky, Y., Coyne, C.B., 2016. Type III Interferons Produced by Human Placental Trophoblasts Confer Protection against Zika Virus Infection. *Cell Host & Microbe* 19, 705–712. doi:10.1016/j.chom.2016.03.008
- Bayless, N.L., Greenberg, R.S., Swigut, T., Wysocka, J., Blish, C.A., 2016. Zika Virus Infection Induces Cranial Neural Crest Cells to Produce Cytokines at Levels Detrimental for Neurogenesis. *Cell Host & Microbe* 0. doi:10.1016/j.chom.2016.09.006
- Beasley, D.W.C., Whiteman, M.C., Zhang, S., Huang, C.Y.-H., Schneider, B.S., Smith, D.R., Gromowski, G.D., Higgs, S., Kinney, R.M., Barrett, A.D.T., 2005. Envelope Protein Glycosylation Status Influences Mouse Neuroinvasion Phenotype of Genetic Lineage 1 West Nile Virus Strains. *J. Virol.* 79, 8339–8347. doi:10.1128/JVI.79.13.8339-8347.2005
- Beatman, E., Oyer, R., Shives, K.D., Hedman, K., Brault, A.C., Tyler, K.L., David Beckham, J., 2012. West Nile virus growth is independent of autophagy activation. *Virology* 433, 262–272. doi:10.1016/j.virol.2012.08.016
- Beatty, P.R., Puerta-Guardo, H., Killingbeck, S.S., Glasner, D.R., Hopkins, K., Harris, E., 2015. Dengue virus NS1 triggers endothelial permeability and vascular leak that is prevented by NS1 vaccination. *Science Translational Medicine* 7, 304ra141-304ra141. doi:10.1126/scitranslmed.aaa3787
- Belgnaoui, S.M., Paz, S., Hiscott, J., 2011. Orchestrating the interferon antiviral response through the mitochondrial antiviral signaling (MAVS) adapter. *Current Opinion in Immunology* 23, 564–572. doi:10.1016/j.coi.2011.08.001
- Bender, S., Reuter, A., Eberle, F., Einhorn, E., Binder, M., Bartenschlager, R., 2015. Activation of Type I and III Interferon Response by Mitochondrial and Peroxisomal MAVS and Inhibition by Hepatitis C Virus. *PLoS Pathog.* 11, e1005264. doi:10.1371/journal.ppat.1005264
- Bertolotti, A., Zhang, Y., Hendershot, L.M., Harding, H.P., Ron, D., 2000. Dynamic interaction of BiP and ER stress transducers in the unfolded-protein response. *Nat Cell Biol* 2, 326–332. doi:10.1038/35014014
- Besnard, M., Lastère, S., Teissier, A., Musso, D., 2014. Evidence of perinatal transmission of Zika virus, French Polynesia, December 2013 and February 2014 [WWW Document].

- URL <http://www.eurosurveillance.org/ViewArticle.aspx?ArticleId=20751> (accessed 3.7.17).
- Best, S.M., Morris, K.L., Shannon, J.G., Robertson, S.J., Mitzel, D.N., Park, G.S., Boer, E., Wolfinger, J.B., Bloom, M.E., 2005. Inhibition of interferon-stimulated JAK-STAT signaling by a tick-borne flavivirus and identification of NS5 as an interferon antagonist. *J. Virol.* 79, 12828–12839. doi:10.1128/JVI.79.20.12828-12839.2005
- Betsem, E., Kaidarova, Z., Stramer, S.L., Shaz, B., Sayers, M., LeParc, G., Custer, B., Busch, M.P., Murphy, E.L., 2017. Correlation of West Nile Virus Incidence in Donated Blood with West Nile Neuroinvasive Disease Rates, United States, 2010–2012. *Emerging Infect. Dis.* 23, 212–219. doi:10.3201/eid2302.161058
- Bhatnagar, J., 2016. Zika Virus RNA Replication and Persistence in Brain and Placental Tissue - Volume 23, Number 3—March 2017 - *Emerging Infectious Disease journal - CDC*. doi:10.3201/eid2303.161499
- Bhatnagar, J., Rabeneck, D.B., Martines, R.B., Reagan-Steiner, S., Ermias, Y., Estetter, L.B.C., Suzuki, T., Ritter, J., Keating, M.K., Hale, G., Gary, J., Muehlenbachs, A., Lambert, A., Lanciotti, R., Oduyebo, T., Meaney-Delman, D., Bolaños, F., Saad, E.A.P., Shieh, W.-J., Zaki, S.R., 2017. Zika Virus RNA Replication and Persistence in Brain and Placental Tissue. *Emerging Infect. Dis.* 23, 405–414. doi:10.3201/eid2303.161499
- Bhatt, S., Gething, P.W., Brady, O.J., Messina, J.P., Farlow, A.W., Moyes, C.L., Drake, J.M., Brownstein, J.S., Hoen, A.G., Sankoh, O., Myers, M.F., George, D.B., Jaenisch, T., Wint, G.R.W., Simmons, C.P., Scott, T.W., Farrar, J.J., Hay, S.I., 2013. The global distribution and burden of dengue. *Nature* 496, 504–507. doi:10.1038/nature12060
- Bhuvanankantham, R., Cheong, Y.K., Ng, M.-L., 2010. West Nile virus capsid protein interaction with importin and HDM2 protein is regulated by protein kinase C-mediated phosphorylation. *Microbes Infect.* 12, 615–625. doi:10.1016/j.micinf.2010.04.005
- Bhuvanankantham, R., Chong, M.-K., Ng, M.-L., 2009. Specific interaction of capsid protein and importin- α / β influences West Nile virus production. *Biochem. Biophys. Res. Commun.* 389, 63–69. doi:10.1016/j.bbrc.2009.08.108
- Bhuvanankantham, R., Li, J., Tan, T.T.T., Ng, M.-L., 2010. Human Sec3 protein is a novel transcriptional and translational repressor of flavivirus. *Cell. Microbiol.* 12, 453–472. doi:10.1111/j.1462-5822.2009.01407.x
- Bidet, K., Dadlani, D., Garcia-Blanco, M.A., 2014. G3BP1, G3BP2 and CAPRIN1 Are Required for Translation of Interferon Stimulated mRNAs and Are Targeted by a Dengue Virus Non-coding RNA. *PLoS Pathog* 10, e1004242. doi:10.1371/journal.ppat.1004242
- Biedenbender, R., Bevilacqua, J., Gregg, A.M., Watson, M., Dayan, G., 2011. Phase II, Randomized, Double-Blind, Placebo-Controlled, Multicenter Study to Investigate the Immunogenicity and Safety of a West Nile Virus Vaccine in Healthy Adults. *J Infect Dis* 203, 75–84. doi:10.1093/infdis/jiq003
- Blazevic, J., Rouha, H., Bradt, V., Heinz, F.X., Stiasny, K., 2016. Membrane Anchors of the Structural Flavivirus Proteins and Their Role in Virus Assembly. *J. Virol.* 90, 6365–6378. doi:10.1128/JVI.00447-16
- Blázquez, A.-B., Escribano-Romero, E., Merino-Ramos, T., Saiz, J.-C., Martín-Acebes, M.A., 2014. Stress responses in flavivirus-infected cells: activation of unfolded protein response and autophagy. *Front Microbiol* 5, 266. doi:10.3389/fmicb.2014.00266

- Boon, J.A. den, Ahlquist, P., 2010. Organelle-Like Membrane Compartmentalization of Positive-Strand RNA Virus Replication Factories. *Annual Review of Microbiology* 64, 241–256. doi:10.1146/annurev.micro.112408.134012
- Bordeleau, M.-E., Matthews, J., Wojnar, J.M., Lindqvist, L., Novac, O., Jankowsky, E., Sonenberg, N., Northcote, P., Teesdale-Spittle, P., Pelletier, J., 2005. Stimulation of mammalian translation initiation factor eIF4A activity by a small molecule inhibitor of eukaryotic translation. *Proc. Natl. Acad. Sci. U.S.A.* 102, 10460–10465. doi:10.1073/pnas.0504249102
- Borden, E.C., Sen, G.C., Uze, G., Silverman, R.H., Ransohoff, R.M., Foster, G.R., Stark, G.R., 2007. Interferons at age 50: past, current and future impact on biomedicine. *Nat Rev Drug Discov* 6, 975–990. doi:10.1038/nrd2422
- Brasil, P., Pereira, J.P.J., Moreira, M.E., Ribeiro Nogueira, R.M., Damasceno, L., Wakimoto, M., Rabello, R.S., Valderramos, S.G., Halai, U.-A., Salles, T.S., Zin, A.A., Horovitz, D., Daltro, P., Boechat, M., Raja Gabaglia, C., Carvalho de Sequeira, P., Pilotto, J.H., Medialdea-Carrera, R., Cotrim da Cunha, D., Abreu de Carvalho, L.M., Pone, M., Machado Siqueira, A., Calvet, G.A., Rodrigues Baião, A.E., Neves, E.S., Nassar de Carvalho, P.R., Hasue, R.H., Marschik, P.B., Einspieler, C., Janzen, C., Cherry, J.D., Bispo de Filippis, A.M., Nielsen-Saines, K., 2016. Zika Virus Infection in Pregnant Women in Rio de Janeiro. *New England Journal of Medicine* 375, 2321–2334. doi:10.1056/NEJMoal602412
- Brinton, M.A., 2002. THE MOLECULAR BIOLOGY OF WEST NILE VIRUS: A New Invader of the Western Hemisphere. *Annual Review of Microbiology* 56, 371–402. doi:10.1146/annurev.micro.56.012302.160654
- Buchan, J.R., Parker, R., 2009. Eukaryotic Stress Granules: The Ins and Out of Translation. *Mol Cell* 36, 932. doi:10.1016/j.molcel.2009.11.020
- Bulich, R., Aaskov, J.G., 1992. Nuclear localization of dengue 2 virus core protein detected with monoclonal antibodies. *Journal of General Virology* 73, 2999–3003. doi:10.1099/0022-1317-73-11-2999
- Byk, L.A., Iglesias, N.G., Maio, F.A.D., Gebhard, L.G., Rossi, M., Gamarnik, A.V., 2016. Dengue Virus Genome Uncoating Requires Ubiquitination. *mBio* 7, e00804-16. doi:10.1128/mBio.00804-16
- Cai, X., Chiu, Y.-H., Chen, Z.J., 2014. The cGAS-cGAMP-STING Pathway of Cytosolic DNA Sensing and Signaling. *Molecular Cell* 54, 289–296. doi:10.1016/j.molcel.2014.03.040
- Calvet, G., Aguiar, R.S., Melo, A.S.O., Sampaio, S.A., de Filippis, I., Fabri, A., Araujo, E.S.M., de Sequeira, P.C., de Mendonça, M.C.L., de Oliveira, L., Tschoeke, D.A., Schrago, C.G., Thompson, F.L., Brasil, P., Dos Santos, F.B., Nogueira, R.M.R., Tanuri, A., de Filippis, A.M.B., 2016. Detection and sequencing of Zika virus from amniotic fluid of fetuses with microcephaly in Brazil: a case study. *Lancet Infect Dis* 16, 653–660. doi:10.1016/S1473-3099(16)00095-5
- Campbell, G.L., Hills, S.L., Fischer, M., Jacobson, J.A., Hoke, C.H., Hombach, J.M., Marfin, A.A., Solomon, T., Tsai, T.F., Tsu, V.D., Ginsburg, A.S., 2011. WHO | Estimated global incidence of Japanese encephalitis: a systematic review [WWW Document]. WHO. URL <http://www.who.int/bulletin/volumes/89/10/10-085233/en/> (accessed 3.7.17).
- Cao-Lormeau, V.-M., Blake, A., Mons, S., Lastère, S., Roche, C., Vanhomwegen, J., Dub, T., Baudouin, L., Teissier, A., Larre, P., Vial, A.-L., Decam, C., Choumet, V., Halstead, S.K., Willison, H.J., Musset, L., Manuguerra, J.-C., Despres, P., Fournier, E., Mallet, H.-

- P., Musso, D., Fontanet, A., Neil, J., Ghawché, F., 2016. Guillain-Barré Syndrome outbreak associated with Zika virus infection in French Polynesia: a case-control study. *The Lancet* 387, 1531–1539. doi:10.1016/S0140-6736(16)00562-6
- Capeding, M.R., Tran, N.H., Hadinegoro, S.R.S., Ismail, H.I.H.M., Chotpitayasunondh, T., Chua, M.N., Luong, C.Q., Rusmil, K., Wirawan, D.N., Nallusamy, R., Pitisuttithum, P., Thisyakorn, U., Yoon, I.-K., van der Vliet, D., Langevin, E., Laot, T., Hutagalung, Y., Frago, C., Boaz, M., Wartel, T.A., Tornieporth, N.G., Saville, M., Bouckenoghe, A., 2014. Clinical efficacy and safety of a novel tetravalent dengue vaccine in healthy children in Asia: a phase 3, randomised, observer-masked, placebo-controlled trial. *The Lancet* 384, 1358–1365. doi:10.1016/S0140-6736(14)61060-6
- Carvalho, F.A., Carneiro, F.A., Martins, I.C., Assunção-Miranda, I., Faustino, A.F., Pereira, R.M., Bozza, P.T., Castanho, M., Mohana-Borges, R., Da Poian, A.T., Santos, N.C., 2011. Dengue virus capsid protein binding to hepatic lipid droplets is K⁺-dependent and mediated by droplets surface proteins. *J. Virol.* doi:10.1128/JVI.06796-11
- Carvalho, F.A., Carneiro, F.A., Martins, I.C., Assunção-Miranda, I., Faustino, A.F., Pereira, R.M., Bozza, P.T., Castanho, M.A.R.B., Mohana-Borges, R., Da Poian, A.T., Santos, N.C., 2012. Dengue virus capsid protein binding to hepatic lipid droplets (LD) is potassium ion dependent and is mediated by LD surface proteins. *J. Virol.* 86, 2096–2108. doi:10.1128/JVI.06796-11
- Castanier, C., Garcin, D., Vazquez, A., Arnoult, D., 2010. Mitochondrial dynamics regulate the RIG-I-like receptor antiviral pathway. *EMBO reports* 11, 133–138. doi:10.1038/embor.2009.258
- Cauchemez, S., Besnard, M., Bompard, P., Dub, T., Guillemette-Artur, P., Eyrolle-Guignot, D., Salje, H., Kerkhove, M.D.V., Abadie, P.V., Garel, C., Fontanet, P.A., Mallet, H.-P., 2016. Association between Zika virus and microcephaly in French Polynesia, 2013–2015: a retrospective study. *Lancet (London, England)* 387, 2125. doi:10.1016/S0140-6736(16)00651-6
- CDC, 2016a. West Nile virus disease cases and deaths reported to CDC by year and clinical presentation, 1999–2015 [WWW Document]. Final Cumulative Maps & Data for 1999–2015. URL https://www.cdc.gov/westnile/resources/pdfs/data/1-wnv-disease-cases-by-year_1999-2015_07072016.pdf (accessed 3.7.17).
- CDC, 2016b. Florida investigation links four recent Zika cases to local mosquito-borne virus transmission [WWW Document]. CDC Press Releases. URL <http://www.cdc.gov.login.ezproxy.library.ualberta.ca/media/releases/2016/p0729-florida-zika-cases.html> (accessed 2.4.17).
- CDC, 2013. Omsk Hemorrhagic Fever Distribution Map | Omsk Hemorrhagic Fever | CDC [WWW Document]. URL <https://www.cdc.gov/vhf/omsk/outbreaks/distribution-map.html> (accessed 3.9.17).
- Ceccaldi, P.-F., Longuet, P., Mandelbrot, L., 2007. [Emerging viral infectious diseases and pregnancy]. *Gynecol Obstet Fertil* 35, 339–342. doi:10.1016/j.gyobfe.2007.02.020
- Cencic, R., Pelletier, J., 2016. Hippuristanol - A potent steroid inhibitor of eukaryotic initiation factor 4A. *Translation* 4, e1137381. doi:10.1080/21690731.2015.1137381
- Chambers, T.J., Halevy, M., Nestorowicz, A., Rice, C.M., Lustig, S., 1998. West Nile virus envelope proteins: nucleotide sequence analysis of strains differing in mouse neuroinvasiveness. *Journal of General Virology* 79, 2375–2380. doi:10.1099/0022-1317-79-10-2375

- Chambers, T.J., Weir, R.C., Grakoui, A., McCourt, D.W., Bazan, J.F., Fletterick, R.J., Rice, C.M., 1990. Evidence that the N-terminal domain of nonstructural protein NS3 from yellow fever virus is a serine protease responsible for site-specific cleavages in the viral polyprotein. *Proc. Natl. Acad. Sci. U.S.A.* 87, 8898–8902.
- Chan, Y.K., Gack, M.U., 2016. A phosphomimetic-based mechanism of dengue virus to antagonize innate immunity. *Nat Immunol* 17, 523–530. doi:10.1038/ni.3393
- Chan, Y.K., Gack, M.U., 2015. RIG-I-like receptor regulation in virus infection and immunity. *Current Opinion in Virology, Antiviral strategies • Virus structure and expression* 12, 7–14. doi:10.1016/j.coviro.2015.01.004
- Chatel-Chaix, L., Cortese, M., Romero-Brey, I., Bender, S., Neufeldt, C.J., Fischl, W., Scaturro, P., Schieber, N., Schwab, Y., Fischer, B., Ruggieri, A., Bartenschlager, R., 2016. Dengue Virus Perturbs Mitochondrial Morphodynamics to Dampen Innate Immune Responses. *Cell Host & Microbe* 20, 342–356. doi:10.1016/j.chom.2016.07.008
- Chen, H.-W., King, K., Tu, J., Sanchez, M., Luster, A.D., Shresta, S., 2013. The Roles of IRF-3 and IRF-7 in Innate Antiviral Immunity against Dengue Virus. *The Journal of Immunology* 191, 4194–4201. doi:10.4049/jimmunol.1300799
- Chen, J., Ng, M.M.-L., Chu, J.J.H., 2015. Activation of TLR2 and TLR6 by Dengue NS1 Protein and Its Implications in the Immunopathogenesis of Dengue Virus Infection. *PLOS Pathogens* 11, e1005053. doi:10.1371/journal.ppat.1005053
- Chiu, H.-C., Hannemann, H., Heesom, K.J., Matthews, D.A., Davidson, A.D., 2014. High-Throughput Quantitative Proteomic Analysis of Dengue Virus Type 2 Infected A549 Cells. *PLoS ONE* 9, e93305. doi:10.1371/journal.pone.0093305
- Chong, K.L., Feng, L., Schappert, K., Meurs, E., Donahue, T.F., Friesen, J.D., Hovanessian, A.G., Williams, B.R., 1992. Human p68 kinase exhibits growth suppression in yeast and homology to the translational regulator GCN2. *EMBO J.* 11, 1553–1562.
- Chu, J.J.H., Ng, M.L., 2004. Infectious entry of West Nile virus occurs through a clathrin-mediated endocytic pathway. *J. Virol.* 78, 10543–10555. doi:10.1128/JVI.78.19.10543-10555.2004
- Clum, S., Ebner, K.E., Padmanabhan, R., 1997. Cotranslational membrane insertion of the serine proteinase precursor NS2B-NS3(Pro) of dengue virus type 2 is required for efficient in vitro processing and is mediated through the hydrophobic regions of NS2B. *J. Biol. Chem.* 272, 30715–30723.
- Cohen, G.B., Rangan, V.S., Chen, B.K., Smith, S., Baltimore, D., 2000. The Human Thioesterase II Protein Binds to a Site on HIV-1 Nef Critical for CD4 Down-regulation. *J. Biol. Chem.* 275, 23097–23105. doi:10.1074/jbc.M000536200
- Colpitts, T.M., Barthel, S., Wang, P., Fikrig, E., 2011. Dengue virus capsid protein binds core histones and inhibits nucleosome formation in human liver cells. *PLoS ONE* 6, e24365. doi:10.1371/journal.pone.0024365
- Costa, H.E., Gouilly, J., Mansuy, J.-M., Chen, Q., Levy, C., Cartron, G., Veas, F., Al-Daccak, R., Izopet, J., Jabrane-Ferrat, N., 2016. ZIKA virus reveals broad tissue and cell tropism during the first trimester of pregnancy. *Scientific Reports* 6, 35296. doi:10.1038/srep35296
- Courtney, S.C., Scherbik, S.V., Stockman, B.M., Brinton, M.A., 2012. West Nile Virus Infections Suppress Early Viral RNA Synthesis and Avoid Inducing the Cell Stress Granule Response. *J. Virol.* 86, 3647–3657. doi:10.1128/JVI.06549-11

- Cristea, I.M., Rozjabek, H., Molloy, K.R., Karki, S., White, L.L., Rice, C.M., Rout, M.P., Chait, B.T., MacDonald, M.R., 2010. Host factors associated with the Sindbis virus RNA-dependent RNA polymerase: role for G3BP1 and G3BP2 in virus replication. *J. Virol.* 84, 6720–6732. doi:10.1128/JVI.01983-09
- Dalet, A., Argüello, R.J., Combes, A., Spinelli, L., Jaeger, S., Fallet, M., Manh, T.-P.V., Mendes, A., Perego, J., Reverendo, M., Camosseto, V., Dalod, M., Weil, T., Santos, M.A., Gatti, E., Pierre, P., 2017. Protein synthesis inhibition and GADD34 control IFN- β heterogeneous expression in response to dsRNA. *The EMBO Journal* 36, 761–782. doi:10.15252/embj.201695000
- Dalrymple, N.A., Cimica, V., Mackow, E.R., 2015. Dengue Virus NS Proteins Inhibit RIG-I/MAVS Signaling by Blocking TBK1/IRF3 Phosphorylation: Dengue Virus Serotype 1 NS4A Is a Unique Interferon-Regulating Virulence Determinant. *mBio* 6. doi:10.1128/mBio.00553-15
- Dammai, V., Subramani, S., 2001. The Human Peroxisomal Targeting Signal Receptor, Pex5p, Is Translocated into the Peroxisomal Matrix and Recycled to the Cytosol. *Cell* 105, 187–196. doi:10.1016/S0092-8674(01)00310-5
- de Araújo, T.V.B., Rodrigues, L.C., de Alencar Ximenes, R.A., de Barros Miranda-Filho, D., Montarroyos, U.R., de Melo, A.P.L., Valongueiro, S., de Albuquerque, M. de F.P.M., Souza, W.V., Braga, C., Filho, S.P.B., Cordeiro, M.T., Vazquez, E., Di Cavalcanti Souza Cruz, D., Henriques, C.M.P., Bezerra, L.C.A., da Silva Castanha, P.M., Dhalia, R., Marques-Júnior, E.T.A., Martelli, C.M.T., 2016. Association between Zika virus infection and microcephaly in Brazil, January to May, 2016: preliminary report of a case-control study. *The Lancet Infectious Diseases* 16, 1356–1363. doi:10.1016/S1473-3099(16)30318-8
- de Oliveira Dias, J.R., Ventura, C.V., Borba, P.D., de Paula Freitas, B., Pierroti, L.C., do Nascimento, A.P., de Moraes, N.S.B., Maia, M., Belfort, R., 2017. INFANTS WITH CONGENITAL ZIKA SYNDROME AND OCULAR FINDINGS FROM SÃO PAULO, BRAZIL: SPREAD OF INFECTION. *Retin Cases Brief Rep.* doi:10.1097/ICB.0000000000000518
- Delille, H.K., Agricola, B., Guimaraes, S.C., Borta, H., Luers, G.H., Fransen, M., Schrader, M., 2010. Pex11p{beta}-mediated growth and division of mammalian peroxisomes follows a maturation pathway. *Journal of Cell Science* 123, 2750. doi:10.1242/jcs.062109
- Deplanque, D., Gelé, P., Pétrault, O., Six, I., Furman, C., Bouly, M., Nion, S., Dupuis, B., Leys, D., Fruchart, J.-C., Cecchelli, R., Staels, B., Duriez, P., Bordet, R., 2003. Peroxisome Proliferator-Activated Receptor- α Activation as a Mechanism of Preventive Neuroprotection Induced by Chronic Fenofibrate Treatment. *J. Neurosci.* 23, 6264–6271.
- Dever, T.E., Chen, J.J., Barber, G.N., Cigan, A.M., Feng, L., Donahue, T.F., London, I.M., Katze, M.G., Hinnebusch, A.G., 1993. Mammalian eukaryotic initiation factor 2 alpha kinases functionally substitute for GCN2 protein kinase in the GCN4 translational control mechanism of yeast. *Proc. Natl. Acad. Sci. U.S.A.* 90, 4616–4620.
- Dey, M., Cao, C., Dar, A.C., Tamura, T., Ozato, K., Sicheri, F., Dever, T.E., 2005. Mechanistic link between PKR dimerization, autophosphorylation, and eIF2alpha substrate recognition. *Cell* 122, 901–913. doi:10.1016/j.cell.2005.06.041
- Diamond, M.S., Gale Jr., M., 2012. Cell-intrinsic innate immune control of West Nile virus infection. *Trends in Immunology* 33, 522–530. doi:10.1016/j.it.2012.05.008

- Diamond, M.S., Harris, E., 2001. Interferon Inhibits Dengue Virus Infection by Preventing Translation of Viral RNA through a PKR-Independent Mechanism. *Virology* 289, 297–311. doi:10.1006/viro.2001.1114
- Diamond, M.S., Pierson, T.C., 2015. Molecular Insight into Dengue Virus Pathogenesis and Its Implications for Disease Control. *Cell* 162, 488–492. doi:10.1016/j.cell.2015.07.005
- Dick, G.W.A., Kitchen, S.F., Haddow, A.J., 1952. Zika virus. I. Isolations and serological specificity. *Trans. R. Soc. Trop. Med. Hyg.* 46, 509–520.
- Dixit, E., Boulant, S., Zhang, Y., Lee, A.S.Y., Odendall, C., Shum, B., Hacohen, N., Chen, Z.J., Whelan, S.P., Fransen, M., Nibert, M.L., Superti-Furga, G., Kagan, J.C., 2010. Peroxisomes are signaling platforms for antiviral innate immunity. *Cell* 141, 668–681. doi:10.1016/j.cell.2010.04.018
- Dobler, G., Gniel, D., Petermann, R., Pfeffer, M., 2012. Epidemiology and distribution of tick-borne encephalitis. *Wien Med Wochenschr* 162, 230–238. doi:10.1007/s10354-012-0100-5
- Dolzhanskaya, N., Merz, G., Aletta, J.M., Denman, R.B., 2006. Methylation regulates the intracellular protein-protein and protein-RNA interactions of FMRP. *Journal of Cell Science* 119, 1933–1946. doi:10.1242/jcs.02882
- Dong, H., Chang, D.C., Hua, M.H.C., Lim, S.P., Chionh, Y.H., Hia, F., Lee, Y.H., Kukkaro, P., Lok, S.-M., Dedon, P.C., Shi, P.-Y., 2012. 2'-O Methylation of Internal Adenosine by Flavivirus NS5 Methyltransferase. *PLoS Pathog* 8, e1002642. doi:10.1371/journal.ppat.1002642
- Driggers, R.W., Ho, C.-Y., Korhonen, E.M., Kuivanen, S., Jääskeläinen, A.J., Smura, T., Rosenberg, A., Hill, D.A., DeBiasi, R.L., Vezina, G., Timofeev, J., Rodriguez, F.J., Levanov, L., Razak, J., Iyengar, P., Hennenfent, A., Kennedy, R., Lanciotti, R., du Plessis, A., Vapalahti, O., 2016. Zika Virus Infection with Prolonged Maternal Viremia and Fetal Brain Abnormalities. *New England Journal of Medicine* 0, null. doi:10.1056/NEJMoa1601824
- Duffy, M.R., Chen, T.-H., Hancock, W.T., Powers, A.M., Kool, J.L., Lanciotti, R.S., Pretrick, M., Marfel, M., Holzbauer, S., Dubray, C., Guillaumot, L., Griggs, A., Bel, M., Lambert, A.J., Laven, J., Kosoy, O., Panella, A., Biggerstaff, B.J., Fischer, M., Hayes, E.B., 2009. Zika Virus Outbreak on Yap Island, Federated States of Micronesia. *New England Journal of Medicine* 360, 2536–2543. doi:10.1056/NEJMoa0805715
- Dutta, K., Ghosh, D., Basu, A., 2009. Curcumin Protects Neuronal Cells from Japanese Encephalitis Virus-Mediated Cell Death and also Inhibits Infective Viral Particle Formation by Dysregulation of Ubiquitin-Proteasome System. *J Neuroimmune Pharmacol* 4, 328–337. doi:10.1007/s11481-009-9158-2
- Duve, C.D., Baudhuin, P., 1966. Peroxisomes (microbodies and related particles). *Physiological Reviews* 46, 323–357.
- Edgil, D., Polacek, C., Harris, E., 2006. Dengue virus utilizes a novel strategy for translation initiation when cap-dependent translation is inhibited. *J. Virol.* 80, 2976–2986. doi:10.1128/JVI.80.6.2976-2986.2006
- El Magraoui, F., Bäumer, B.E., Platta, H.W., Baumann, J.S., Girzalsky, W., Erdmann, R., 2012. The RING-type ubiquitin ligases Pex2p, Pex10p and Pex12p form a heteromeric complex that displays enhanced activity in an ubiquitin conjugating enzyme-selective manner. *FEBS J.* 279, 2060–2070. doi:10.1111/j.1742-4658.2012.08591.x

- Elbahesh, H., Scherbik, S.V., Brinton, M.A., 2011. West Nile virus infection does not induce PKR activation in rodent cells. *Virology* 421, 51–60. doi:10.1016/j.virol.2011.08.008
- Elgersma, Y., Kwast, L., Klein, A., Voorn-Brouwer, T., van den Berg, M., Metzger, B., America, T., Tabak, H.F., Distel, B., 1996. The SH3 domain of the *Saccharomyces cerevisiae* peroxisomal membrane protein Pex13p functions as a docking site for Pex5p, a mobile receptor for the import PTS1-containing proteins. *J. Cell Biol.* 135, 97–109.
- Elliott, J., Lynch, O.T., Suessmuth, Y., Qian, P., Boyd, C.R., Burrows, J.F., Buick, R., Stevenson, N.J., Touzelet, O., Gadina, M., Power, U.F., Johnston, J.A., 2007. Respiratory Syncytial Virus NS1 Protein Degrades STAT2 by Using the Elongin-Cullin E3 Ligase. *Journal of Virology* 81, 3428. doi:10.1128/JVI.02303-06
- Elshuber, S., Allison, S.L., Heinz, F.X., Mandl, C.W., 2003. Cleavage of protein prM is necessary for infection of BHK-21 cells by tick-borne encephalitis virus. *J. Gen. Virol.* 84, 183–191. doi:10.1099/vir.0.18723-0
- Emara, M.M., Brinton, M.A., 2007a. Interaction of TIA-1/TIAR with West Nile and dengue virus products in infected cells interferes with stress granule formation and processing body assembly. *PNAS* 104, 9041–9046. doi:10.1073/pnas.0703348104
- Emara, M.M., Brinton, M.A., 2007b. Interaction of TIA-1/TIAR with West Nile and dengue virus products in infected cells interferes with stress granule formation and processing body assembly. *PNAS* 104, 9041–9046. doi:10.1073/pnas.0703348104
- Erdmann, R., Schliebs, W., 2005. Peroxisomal matrix protein import: the transient pore model. *Nat Rev Mol Cell Biol* 6, 738–742. doi:10.1038/nrm1710
- Evans, J.D., Crown, R.A., Sohn, J.A., Seeger, C., 2011. West Nile virus infection induces depletion of IFNAR1 protein levels. *Viral Immunol.* 24, 253–263. doi:10.1089/vim.2010.0126
- Evans, J.D., Seeger, C., 2007. Differential effects of mutations in NS4B on West Nile virus replication and inhibition of interferon signaling. *J. Virol.* 81, 11809–11816. doi:10.1128/JVI.00791-07
- Fernandez-Garcia, M.-D., Meertens, L., Bonazzi, M., Cossart, P., Arenzana-Seisdedos, F., Amara, A., 2011. Appraising the roles of CBL1 and the ubiquitin/proteasome system for flavivirus entry and replication. *J. Virol.* 85, 2980–2989. doi:10.1128/JVI.02483-10
- Ferreira, A.R., Magalhães, A.C., Camões, F., Gouveia, A., Vieira, M., Kagan, J.C., Ribeiro, D., 2016. Hepatitis C virus NS3-4A inhibits the peroxisomal MAVS-dependent antiviral signalling response. *Journal of Cellular and Molecular Medicine* 20, 750. doi:10.1111/jcmm.12801
- Filomatori, C.V., Lodeiro, M.F., Alvarez, D.E., Samsa, M.M., Pietrasanta, L., Gamarnik, A.V., 2006. A 5' RNA element promotes dengue virus RNA synthesis on a circular genome. *Genes Dev.* 20, 2238–2249. doi:10.1101/gad.1444206
- Flamand, M., Megret, F., Mathieu, M., Lepault, J., Rey, F.A., Deubel, V., 1999. Dengue virus type 1 nonstructural glycoprotein NS1 is secreted from mammalian cells as a soluble hexamer in a glycosylation-dependent fashion. *J. Virol.* 73, 6104–6110.
- Fros, J.J., Domeradzka, N.E., Baggen, J., Geertsema, C., Flipse, J., Vlak, J.M., Pijlman, G.P., 2012. Chikungunya virus nsP3 blocks stress granule assembly by recruitment of G3BP into cytoplasmic foci. *J. Virol.* 86, 10873–10879. doi:10.1128/JVI.01506-12
- Fujiki, Y., Matsuzono, Y., Matsuzaki, T., Fransen, M., 2006. Import of peroxisomal membrane proteins: the interplay of Pex3p- and Pex19p-mediated interactions. *Biochim. Biophys. Acta* 1763, 1639–1646. doi:10.1016/j.bbamcr.2006.09.030

- Fujiki, Y., Yagita, Y., Matsuzaki, T., 2012. Peroxisome biogenesis disorders: Molecular basis for impaired peroxisomal membrane assembly: In metabolic functions and biogenesis of peroxisomes in health and disease. *Biochimica et Biophysica Acta (BBA) - Molecular Basis of Disease* 1822, 1337–1342. doi:10.1016/j.bbadis.2012.06.004
- Gandre-Babbe, S., Blik, A.M. van der, 2008. The Novel Tail-anchored Membrane Protein Mff Controls Mitochondrial and Peroxisomal Fission in Mammalian Cells. *Mol. Biol. Cell* 19, 2402–2412. doi:10.1091/mbc.E07-12-1287
- Garaigorta, U., Heim, M.H., Boyd, B., Wieland, S., Chisari, F.V., 2012. Hepatitis C Virus (HCV) Induces Formation of Stress Granules Whose Proteins Regulate HCV RNA Replication and Virus Assembly and Egress. *J. Virol.* 86, 11043–11056. doi:10.1128/JVI.07101-11
- Garcia-Blanco, M.A., Vasudevan, S.G., Bradrick, S.S., Nichitta, C., 2016. Flavivirus RNA transactions from viral entry to genome replication. *Antiviral Research* 134, 244–249. doi:10.1016/j.antiviral.2016.09.010
- Gardner, B.M., Walter, P., 2011. Unfolded Proteins Are Ire1-Activating Ligands That Directly Induce the Unfolded Protein Response. *Science* 333, 1891–1894. doi:10.1126/science.1209126
- Getts, D.R., Terry, R.L., Getts, M.T., Müller, M., Rana, S., Shrestha, B., Radford, J., Rooijen, N.V., Campbell, I.L., King, N.J.C., 2008. Ly6c+ “inflammatory monocytes” are microglial precursors recruited in a pathogenic manner in West Nile virus encephalitis. *Journal of Experimental Medicine* 205, 2319–2337. doi:10.1084/jem.20080421
- Ghoshal, A., Das, S., Ghosh, S., Mishra, M.K., Sharma, V., Koli, P., Sen, E., Basu, A., 2007. Proinflammatory mediators released by activated microglia induces neuronal death in Japanese encephalitis. *Glia* 55, 483–496. doi:10.1002/glia.20474
- Gilfoy, F.D., Mason, P.W., 2007. West Nile Virus-Induced Interferon Production Is Mediated by the Double-Stranded RNA-Dependent Protein Kinase PKR. *J. Virol.* 81, 11148–11158. doi:10.1128/JVI.00446-07
- Gilks, N., Kedersha, N., Ayodele, M., Shen, L., Stoecklin, G., Dember, L.M., Anderson, P., 2004. Stress Granule Assembly Is Mediated by Prion-like Aggregation of TIA-1. *Mol. Biol. Cell* 15, 5383–5398. doi:10.1091/mbc.E04-08-0715
- Gillespie, L.K., Hoenen, A., Morgan, G., Mackenzie, J.M., 2010. The endoplasmic reticulum provides the membrane platform for biogenesis of the flavivirus replication complex. *J. Virol.* 84, 10438–10447. doi:10.1128/JVI.00986-10
- Goasdoué, K., Miller, S.M., Colditz, P.B., Björkman, S.T., 2016. Review: The blood-brain barrier; protecting the developing fetal brain. *Placenta*. doi:10.1016/j.placenta.2016.12.005
- Godoy, A.S., Lima, G.M.A., Oliveira, K.I.Z., Torres, N.U., Maluf, F.V., Guido, R.V.C., Oliva, G., 2017. Crystal structure of Zika virus NS5 RNA-dependent RNA polymerase. *Nature Communications* 8, 14764. doi:10.1038/ncomms14764
- Gollins, S.W., Porterfield, J.S., 1986. The uncoating and infectivity of the flavivirus West Nile on interaction with cells: effects of pH and ammonium chloride. *J. Gen. Virol.* 67 (Pt 9), 1941–1950. doi:10.1099/0022-1317-67-9-1941
- Gollins, S.W., Porterfield, J.S., 1985. Flavivirus infection enhancement in macrophages: an electron microscopic study of viral cellular entry. *J. Gen. Virol.* 66 (Pt 9), 1969–1982. doi:10.1099/0022-1317-66-9-1969

- Goncalvez, A.P., Engle, R.E., Claire, M.S., Purcell, R.H., Lai, C.-J., 2007. Monoclonal antibody-mediated enhancement of dengue virus infection in vitro and in vivo and strategies for prevention. *PNAS* 104, 9422–9427. doi:10.1073/pnas.0703498104
- Goodfellow, J.A., Willison, H.J., 2016. Guillain-Barre syndrome: a century of progress. *Nat Rev Neurol* 12, 723–731. doi:10.1038/nrneurol.2016.172
- Gotuzzo, E., Yactayo, S., Córdova, E., 2013. Efficacy and Duration of Immunity after Yellow Fever Vaccination: Systematic Review on the Need for a Booster Every 10 Years. *Am J Trop Med Hyg* 89, 434–444. doi:10.4269/ajtmh.13-0264
- Gould, E., Solomon, T., 2008. Pathogenic flaviviruses. *The Lancet* 371, 500–509. doi:10.1016/S0140-6736(08)60238-X
- Gould, S.J., Keller, G.A., Hosken, N., Wilkinson, J., Subramani, S., 1989. A conserved tripeptide sorts proteins to peroxisomes. *J. Cell Biol.* 108, 1657–1664.
- Govero, J., Esakky, P., Scheaffer, S.M., Fernandez, E., Drury, A., Platt, D.J., Gorman, M.J., Richner, J.M., Caine, E.A., Salazar, V., Moley, K.H., Diamond, M.S., 2016. Zika virus infection damages the testes in mice. *Nature* 540, 438–442. doi:10.1038/nature20556
- Grandvaux, N., Servant, M.J., tenOever, B., Sen, G.C., Balachandran, S., Barber, G.N., Lin, R., Hiscott, J., 2002. Transcriptional Profiling of Interferon Regulatory Factor 3 Target Genes: Direct Involvement in the Regulation of Interferon-Stimulated Genes. *J. Virol.* 76, 5532–5539. doi:10.1128/JVI.76.11.5532-5539.2002
- Grant, A., Ponia, S.S., Tripathi, S., Balasubramaniam, V., Miorin, L., Sourisseau, M., Schwarz, M.C., Sánchez-Seco, M.P., Evans, M.J., Best, S.M., García-Sastre, A., 2016. Zika Virus Targets Human STAT2 to Inhibit Type I Interferon Signaling. *Cell Host & Microbe* 0. doi:10.1016/j.chom.2016.05.009
- Gray, E., Ginty, M., Kemp, K., Scolding, N., Wilkins, A., 2011. Peroxisome proliferator-activated receptor- α agonists protect cortical neurons from inflammatory mediators and improve peroxisomal function. *European Journal of Neuroscience* 33, 1421–1432. doi:10.1111/j.1460-9568.2011.07637.x
- Guirakhoo, F., Heinz, F.X., Mandl, C.W., Holzmann, H., Kunz, C., 1991. Fusion activity of flaviviruses: comparison of mature and immature (prM-containing) tick-borne encephalitis virions. *J. Gen. Virol.* 72 (Pt 6), 1323–1329. doi:10.1099/0022-1317-72-6-1323
- Guo, J.-T., Hayashi, J., Seeger, C., 2005. West Nile virus inhibits the signal transduction pathway of alpha interferon. *J. Virol.* 79, 1343–1350. doi:10.1128/JVI.79.3.1343-1350.2005
- Guzman, M.G., Halstead, S.B., Artsob, H., Buchy, P., Farrar, J., Gubler, D.J., Hunsperger, E., Kroeger, A., Margolis, H.S., Martínez, E., Nathan, M.B., Pelegrino, J.L., Simmons, C., Yoksan, S., Peeling, R.W., 2010. Dengue: a continuing global threat. *Nat. Rev. Microbiol.* 8, S7-16. doi:10.1038/nrmicro2460
- Guzman, M.G., Harris, E., 2015. Dengue. *The Lancet* 385, 453–465. doi:10.1016/S0140-6736(14)60572-9
- Gyure, K.A., 2009. West Nile Virus Infections. *Journal of Neuropathology and Experimental Neurology* 68, 1053–1060. doi:10.1097/NEN.0b013e3181b88114
- Hadinegoro, S.R., Arredondo-García, J.L., Capeding, M.R., Deseda, C., Chotpitayasunondh, T., Dietze, R., Hj Muhammad Ismail, H.I., Reynales, H., Limkittikul, K., Rivera-Medina, D.M., Tran, H.N., Bouckennooghe, A., Chansinghakul, D., Cortés, M., Fanouillere, K., Forrat, R., Frago, C., Gailhardou, S., Jackson, N., Noriega, F., Plennevaux, E., Wartel,

- T.A., Zambrano, B., Saville, M., 2015. Efficacy and Long-Term Safety of a Dengue Vaccine in Regions of Endemic Disease. *New England Journal of Medicine* 373, 1195–1206. doi:10.1056/NEJMoa1506223
- Halbach, A., Landgraf, C., Lorenzen, S., Rosenkranz, K., Volkmer-Engert, R., Erdmann, R., Rottensteiner, H., 2006. Targeting of the tail-anchored peroxisomal membrane proteins PEX26 and PEX15 occurs through C-terminal PEX19-binding sites. *J Cell Sci* 119, 2508–2517. doi:10.1242/jcs.02979
- Halstead, S.B., 2007. Dengue. *The Lancet* 370, 1644–1652. doi:10.1016/S0140-6736(07)61687-0
- Hamel, R., Ferraris, P., Wichit, S., Diop, F., Talignani, L., Pompon, J., Garcia, D., Liégeois, F., Sall, A.A., Yssel, H., Missé, D., 2017a. African and Asian Zika virus strains differentially induce early antiviral responses in primary human astrocytes. *Infect. Genet. Evol.* 49, 134–137. doi:10.1016/j.meegid.2017.01.015
- Hamel, R., Ferraris, P., Wichit, S., Diop, F., Talignani, L., Pompon, J., Garcia, D., Liégeois, F., Sall, A.A., Yssel, H., Missé, D., 2017b. African and Asian Zika virus strains differentially induce early antiviral responses in primary human astrocytes. *Infect. Genet. Evol.* 49, 134–137. doi:10.1016/j.meegid.2017.01.015
- Harding, H.P., Zhang, Y., Ron, D., 1999. Protein translation and folding are coupled by an endoplasmic-reticulum-resident kinase. *Nature* 397, 271–274. doi:10.1038/16729
- Hayes, E.B., Sejvar, J.J., Zaki, S.R., Lanciotti, R.S., Bode, A.V., Campbell, G.L., 2005. Virology, Pathology, and Clinical Manifestations of West Nile Virus Disease. *Emerging Infectious Diseases* 11, 1174. doi:10.3201/eid1108.050289b
- He, Z., Zhu, X., Wen, W., Yuan, J., Hu, Y., Chen, J., An, S., Dong, X., Lin, C., Yu, J., Wu, J., Yang, Y., Cai, J., Li, J., Li, M., 2016. Dengue Virus Subverts Host Innate Immunity by Targeting Adaptor Protein MAVS. *Journal of Virology* 90, 7219. doi:10.1128/JVI.00221-16
- Heaton, N.S., Randall, G., 2010. Dengue Virus-Induced Autophagy Regulates Lipid Metabolism. *Cell Host & Microbe* 8, 422–432. doi:10.1016/j.chom.2010.10.006
- Hirsch, A.J., Smith, J.L., Haese, N.N., Broeckel, R.M., Parkins, C.J., Kreklywich, C., DeFilippis, V.R., Denton, M., Smith, P.P., Messer, W.B., Colgin, L.M.A., Ducore, R.M., Grigsby, P.L., Hennebold, J.D., Swanson, T., Legasse, A.W., Axthelm, M.K., MacAllister, R., Wiley, C.A., Nelson, J.A., Streblow, D.N., 2017. Zika Virus infection of rhesus macaques leads to viral persistence in multiple tissues. *PLOS Pathogens* 13, e1006219. doi:10.1371/journal.ppat.1006219
- Hoepfner, D., Schildknecht, D., Braakman, I., Philippsen, P., Tabak, H.F., 2005. Contribution of the Endoplasmic Reticulum to Peroxisome Formation. *Cell* 122, 85–95. doi:10.1016/j.cell.2005.04.025
- Holden, K.L., Harris, E., 2004. Enhancement of dengue virus translation: role of the 3' untranslated region and the terminal 3' stem-loop domain. *Virology* 329, 119–133. doi:10.1016/j.virol.2004.08.004
- Honsho, M., Hiroshige, T., Fujiki, Y., 2002. The Membrane Biogenesis Peroxin Pex16p TOPOGENESIS AND FUNCTIONAL ROLES IN PEROXISOMAL MEMBRANE ASSEMBLY. *J. Biol. Chem.* 277, 44513–44524. doi:10.1074/jbc.M206139200
- Horner, S.M., Liu, H.M., Park, H.S., Briley, J., Gale, M., 2011. Mitochondrial-associated endoplasmic reticulum membranes (MAM) form innate immune synapses and are

- targeted by hepatitis C virus. *Proc Natl Acad Sci U S A* 108, 14590–14595.
doi:10.1073/pnas.1110133108
- Hou, F., Sun, L., Zheng, H., Skaug, B., Jiang, Q.-X., Chen, Z.J., 2011. MAVS Forms Functional Prion-like Aggregates to Activate and Propagate Antiviral Innate Immune Response. *Cell* 146, 448–461. doi:10.1016/j.cell.2011.06.041
- Hou, S., Kumar, A., Xu, Z., Airo, A.M., Stryapunina, I., Wong, C. P., Branton, W., Tchesnokov, E., Götte, M., Power, C., Hobman, T.C. 2017. Zika virus hijacks stress granule proteins and modulates the host stress response. *J Virol*. doi:10.1128/JVI.00474-17
- Hsieh, S.-C., Tsai, W.-Y., Wang, W.-K., 2010. The length of and nonhydrophobic residues in the transmembrane domain of dengue virus envelope protein are critical for its retention and assembly in the endoplasmic reticulum. *J. Virol.* 84, 4782–4797. doi:10.1128/JVI.01963-09
- Hua, R., Gidda, S.K., Aranovich, A., Mullen, R.T., Kim, P.K., 2015. Multiple Domains in PEX16 Mediate Its Trafficking and Recruitment of Peroxisomal Proteins to the ER. *Traffic* 16, 832–852. doi:10.1111/tra.12292
- Hua, R., Kim, P.K., 2016. Multiple paths to peroxisomes: Mechanism of peroxisome maintenance in mammals. *Biochimica et Biophysica Acta (BBA) - Molecular Cell Research, Assembly, Maintenance and Dynamics of Peroxisomes* 1863, 881–891. doi:10.1016/j.bbamcr.2015.09.026
- Hubálek, Z., Rudolf, I., 2012. Tick-borne viruses in Europe. *Parasitol Res* 111, 9–36. doi:10.1007/s00436-012-2910-1
- Hung, S.L., Lee, P.L., Chen, H.W., Chen, L.K., Kao, C.L., King, C.C., 1999. Analysis of the steps involved in Dengue virus entry into host cells. *Virology* 257, 156–167. doi:10.1006/viro.1999.9633
- Hunt, T.A., Urbanowski, M.D., Kakani, K., Law, L.-M.J., Brinton, M.A., Hobman, T.C., 2007. Interactions between the West Nile virus capsid protein and the host cell-encoded phosphatase inhibitor, I2PP2A. *Cell. Microbiol.* 9, 2756–2766. doi:10.1111/j.1462-5822.2007.01046.x
- Iglesias, N.G., Mondotte, J.A., Byk, L.A., De Maio, F.A., Samsa, M.M., Alvarez, C., Gamarnik, A.V., 2015. Dengue Virus Uses a Non-Canonical Function of the Host GBF1-Arf-COPI System for Capsid Protein Accumulation on Lipid Droplets. *Traffic* 16, 962–977. doi:10.1111/tra.12305
- Ishak, R., Tovey, D.G., Howard, C.R., 1988. Morphogenesis of Yellow Fever Virus 17D in Infected Cell Cultures. *Journal of General Virology* 69, 325–335. doi:10.1099/0022-1317-69-2-325
- Ishikawa, T., Yamanaka, A., Konishi, E., 2014. A review of successful flavivirus vaccines and the problems with those flaviviruses for which vaccines are not yet available. *Vaccine* 32, 1326–1337. doi:10.1016/j.vaccine.2014.01.040
- Issemann, I., Green, S., 1990. Activation of a member of the steroid hormone receptor superfamily by peroxisome proliferators. *Nature* 347, 645–650. doi:10.1038/347645a0
- Ivanov, P.A., Chudinova, E.M., Nadezhdina, E.S., 2003. Disruption of microtubules inhibits cytoplasmic ribonucleoprotein stress granule formation. *Experimental Cell Research* 290, 227–233. doi:10.1016/S0014-4827(03)00290-8
- Ivashkiv, L.B., Donlin, L.T., 2014. Regulation of type I interferon responses. *Nat Rev Immunol* 14, 36–49. doi:10.1038/nri3581

- Iwamoto, M., Jernigan, D.B., Guasch, A., Trepka, M.J., Blackmore, C.G., Hellinger, W.C., Pham, S.M., Zaki, S., Lanciotti, R.S., Lance-Parker, S.E., DiazGranados, C.A., Winquist, A.G., Perlino, C.A., Wiersma, S., Hillyer, K.L., Goodman, J.L., Marfin, A.A., Chamberland, M.E., Petersen, L.R., West Nile Virus in Transplant Recipients Investigation Team, 2003. Transmission of West Nile virus from an organ donor to four transplant recipients. *N. Engl. J. Med.* 348, 2196–2203. doi:10.1056/NEJMoa022987
- Iwata, J., Ezaki, J., Komatsu, M., Yokota, S., Ueno, T., Tanida, I., Chiba, T., Tanaka, K., Kominami, E., 2006. Excess peroxisomes are degraded by autophagic machinery in mammals. *J. Biol. Chem.* 281, 4035–4041. doi:10.1074/jbc.M512283200
- Jacobson, E.R., Ginn, P.E., Troutman, J.M., Farina, L., Stark, L., Klenk, K., Burkhalter, K.L., Komar, N., 2005. West Nile virus infection in farmed American alligators (*Alligator mississippiensis*) in Florida. *J. Wildl. Dis.* 41, 96–106. doi:10.7589/0090-3558-41.1.96
- Jan, L.R., Yang, C.S., Trent, D.W., Falgout, B., Lai, C.J., 1995. Processing of Japanese encephalitis virus non-structural proteins: NS2B-NS3 complex and heterologous proteases. *J. Gen. Virol.* 76 (Pt 3), 573–580. doi:10.1099/0022-1317-76-3-573
- Janjindamai, W., Pruekprasert, P., 2003. Perinatal dengue infection: a case report and review of literature. *Southeast Asian J. Trop. Med. Public Health* 34, 793–796.
- Jentes, E.S., Pomeroy, G., Gershman, M.D., Hill, D.R., Lemarchand, J., Lewis, R.F., Staples, J.E., Tomori, O., Wilder-Smith, A., Monath, T.P., 2011. The revised global yellow fever risk map and recommendations for vaccination, 2010: consensus of the Informal WHO Working Group on Geographic Risk for Yellow Fever. *The Lancet Infectious Diseases* 11, 622–632. doi:10.1016/S1473-3099(11)70147-5
- Jones, J.M., Morrell, J.C., Gould, S.J., 2004. PEX19 is a predominantly cytosolic chaperone and import receptor for class 1 peroxisomal membrane proteins. *J Cell Biol* 164, 57–67. doi:10.1083/jcb.200304111
- Joshi, S., Agrawal, G., Subramani, S., 2012. Phosphorylation-dependent Pex11p and Fis1p interaction regulates peroxisome division. *Mol. Biol. Cell* 23, 1307–1315. doi:10.1091/mbc.E11-09-0782
- Kato, H., Takahashi, K., Fujita, T., 2011. RIG-I-like receptors: cytoplasmic sensors for non-self RNA. *Immunological Reviews* 243, 91–98. doi:10.1111/j.1600-065X.2011.01052.x
- Katoh, H., Okamoto, T., Fukuhara, T., Kambara, H., Morita, E., Mori, Y., Kamitani, W., Matsuura, Y., 2013. Japanese Encephalitis Virus Core Protein Inhibits Stress Granule Formation through an Interaction with Caprin-1 and Facilitates Viral Propagation. *J. Virol.* 87, 489–502. doi:10.1128/JVI.02186-12
- Kawai, T., Takahashi, K., Sato, S., Coban, C., Kumar, H., Kato, H., Ishii, K.J., Takeuchi, O., Akira, S., 2005. IPS-1, an adaptor triggering RIG-I- and Mda5-mediated type I interferon induction. *Nat Immunol* 6, 981–988. doi:10.1038/ni1243
- Kedersha, N., Chen, S., Gilks, N., Li, W., Miller, I.J., Stahl, J., Anderson, P., 2002. Evidence That Ternary Complex (eIF2-GTP-tRNAⁱ Met)-Deficient Preinitiation Complexes Are Core Constituents of Mammalian Stress Granules. *Mol. Biol. Cell* 13, 195–210. doi:10.1091/mbc.01-05-0221
- Kedersha, N., Cho, M.R., Li, W., Yacono, P.W., Chen, S., Gilks, N., Golan, D.E., Anderson, P., 2000. Dynamic Shuttling of Tia-1 Accompanies the Recruitment of mRNA to Mammalian Stress Granules. *The Journal of Cell Biology* 151, 1257–1268. doi:10.1083/jcb.151.6.1257

- Kedersha, N., Stoecklin, G., Ayodele, M., Yacono, P., Lykke-Andersen, J., Fritzler, M.J., Scheuner, D., Kaufman, R.J., Golan, D.E., Anderson, P., 2005. Stress granules and processing bodies are dynamically linked sites of mRNP remodeling. *J Cell Biol* 169, 871–884. doi:10.1083/jcb.200502088
- Kedersha, Nancy L., Gupta, M., Li, W., Miller, I., Anderson, P., 1999. RNA-Binding Proteins Tia-1 and Tiar Link the Phosphorylation of Eif-2 α to the Assembly of Mammalian Stress Granules. *The Journal of Cell Biology* 147, 1431–1442. doi:10.1083/jcb.147.7.1431
- Khromykh, Alexander A., Meka, H., Guyatt, K.J., Westaway, E.G., 2001. Essential Role of Cyclization Sequences in Flavivirus RNA Replication. *J. Virol.* 75, 6719–6728. doi:10.1128/JVI.75.14.6719-6728.2001
- Khromykh, A. A., Varnavski, A.N., Sedlak, P.L., Westaway, E.G., 2001. Coupling between replication and packaging of flavivirus RNA: evidence derived from the use of DNA-based full-length cDNA clones of Kunjin virus. *J. Virol.* 75, 4633–4640. doi:10.1128/JVI.75.10.4633-4640.2001
- Khromykh, A.A., Westaway, E.G., 1996. RNA binding properties of core protein of the flavivirus Kunjin. *Archives of Virology* 141, 685–699. doi:10.1007/BF01718326
- Kim, K., Shresta, S., 2016. Neuroteratogenic Viruses and Lessons for Zika Virus Models. *Trends in Microbiology* 24, 622–636. doi:10.1016/j.tim.2016.06.002
- Kim, P.K., Mullen, R.T., Schumann, U., Lippincott-Schwartz, J., 2006. The origin and maintenance of mammalian peroxisomes involves a de novo PEX16-dependent pathway from the ER. *J. Cell Biol.* 173, 521–532. doi:10.1083/jcb.200601036
- Kimura, T., Katoh, H., Kayama, H., Saiga, H., Okuyama, M., Okamoto, T., Umemoto, E., Matsuura, Y., Yamamoto, M., Takeda, K., 2013. Ifit1 Inhibits Japanese Encephalitis Virus Replication through Binding to 5' Capped 2'-O Unmethylated RNA. *J. Virol.* 87, 9997–10003. doi:10.1128/JVI.00883-13
- Klema, V.J., Padmanabhan, R., Choi, K.H., 2015. Flaviviral Replication Complex: Coordination between RNA Synthesis and 5'-RNA Capping. *Viruses* 7, 4640–4656. doi:10.3390/v7082837
- Klenk, K., Snow, J., Morgan, K., Bowen, R., Stephens, M., Foster, F., Gordy, P., Beckett, S., Komar, N., Gubler, D., Bunning, M., 2004. Alligators as West Nile virus amplifiers. *Emerging Infect. Dis.* 10, 2150–2155. doi:10.3201/eid1012.040264
- Knoblach, B., Rachubinski, R.A., 2010. Phosphorylation-dependent activation of peroxisome proliferator protein PEX11 controls peroxisome abundance. *J. Biol. Chem.* 285, 6670–6680. doi:10.1074/jbc.M109.094805
- Ko, A., Lee, E.-W., Yeh, J.-Y., Yang, M.-R., Oh, W., Moon, J.-S., Song, J., 2010. MKRN1 induces degradation of West Nile virus capsid protein by functioning as an E3 ligase. *J. Virol.* 84, 426–436. doi:10.1128/JVI.00725-09
- Kobayashi, S., Tanaka, A., Fujiki, Y., 2007. Fis1, DLP1, and Pex11p coordinately regulate peroxisome morphogenesis. *Exp. Cell Res.* 313, 1675–1686. doi:10.1016/j.yexcr.2007.02.028
- Koch, A., Thiemann, M., Grabenbauer, M., Yoon, Y., McNiven, M.A., Schrader, M., 2003. Dynamin-like Protein 1 Is Involved in Peroxisomal Fission. *J. Biol. Chem.* 278, 8597–8605. doi:10.1074/jbc.M211761200
- Kong, K.-F., Delroux, K., Wang, X., Qian, F., Arjona, A., Malawista, S.E., Fikrig, E., Montgomery, R.R., 2008. Dysregulation of TLR3 impairs the innate immune response to West Nile virus in the elderly. *J. Virol.* 82, 7613–7623. doi:10.1128/JVI.00618-08

- Koshiba, T., Yasukawa, K., Yanagi, Y., Kawabata, S., 2011. Mitochondrial Membrane Potential Is Required for MAVS-Mediated Antiviral Signaling. *Sci. Signal.* 4, ra7-ra7. doi:10.1126/scisignal.2001147
- Kraemer, M.U., Sinka, M.E., Duda, K.A., Mylne, A.Q., Shearer, F.M., Barker, C.M., Moore, C.G., Carvalho, R.G., Coelho, G.E., Bortel, W.V., Hendrickx, G., Schaffner, F., Elyazar, I.R., Teng, H.-J., Brady, O.J., Messina, J.P., Pigott, D.M., Scott, T.W., Smith, D.L., Wint, G.W., Golding, N., Hay, S.I., 2015. The global distribution of the arbovirus vectors *Aedes aegypti* and *Ae. albopictus*. *eLife* 4, e08347. doi:10.7554/eLife.08347
- Kumar, A., Hou, S., Airo, A.M., Limonta, D., Mancinelli, V., Branton, W., Power, C., Hobman, T.C., 2016. Zika virus inhibits type-I interferon production and downstream signaling. *EMBO Rep.* 17, 1766–1775. doi:10.15252/embr.201642627
- Kümmerer, B.M., Rice, C.M., 2002. Mutations in the yellow fever virus nonstructural protein NS2A selectively block production of infectious particles. *J. Virol.* 76, 4773–4784.
- Kwon, S., Zhang, Y., Matthias, P., 2007. The deacetylase HDAC6 is a novel critical component of stress granules involved in the stress response. *Genes Dev.* 21, 3381–3394. doi:10.1101/gad.461107
- Laurent-Rolle, M., Boer, E.F., Lubick, K.J., Wolfenbarger, J.B., Carmody, A.B., Rockx, B., Liu, W., Ashour, J., Shupert, W.L., Holbrook, M.R., Barrett, A.D., Mason, P.W., Bloom, M.E., García-Sastre, A., Khromykh, A.A., Best, S.M., 2010. The NS5 protein of the virulent West Nile virus NY99 strain is a potent antagonist of type I interferon-mediated JAK-STAT signaling. *J. Virol.* 84, 3503–3515. doi:10.1128/JVI.01161-09
- Lazarow, P.B., 2011. Viruses exploiting peroxisomes. *Curr. Opin. Microbiol.* 14, 458–469. doi:10.1016/j.mib.2011.07.009
- Lazear, H.M., Govero, J., Smith, A.M., Platt, D.J., Fernandez, E., Miner, J.J., Diamond, M.S., 2016. A Mouse Model of Zika Virus Pathogenesis. *Cell Host & Microbe* 19, 720–730. doi:10.1016/j.chom.2016.03.010
- Lazear, H.M., Lancaster, A., Wilkins, C., Suthar, M.S., Huang, A., Vick, S.C., Clepper, L., Thackray, L., Brassil, M.M., Virgin, H.W., Nikolich-Zugich, J., Moses, A.V., Gale, M., Jr., Früh, K., Diamond, M.S., 2013. IRF-3, IRF-5, and IRF-7 Coordinately Regulate the Type I IFN Response in Myeloid Dendritic Cells Downstream of MAVS Signaling. *PLoS Pathog* 9, e1003118. doi:10.1371/journal.ppat.1003118
- Le Belle, J.E., Orozco, N.M., Paucar, A.A., Saxe, J.P., Mottahedeh, J., Pyle, A.D., Wu, H., Kornblum, H.I., 2011. Proliferative Neural Stem Cells Have High Endogenous ROS Levels that Regulate Self-Renewal and Neurogenesis in a PI3K/Akt-Dependant Manner. *Cell Stem Cell* 8, 59–71. doi:10.1016/j.stem.2010.11.028
- Lee, E., Stocks, C.E., Amberg, S.M., Rice, C.M., Lobigs, M., 2000. Mutagenesis of the Signal Sequence of Yellow Fever Virus prM Protein: Enhancement of Signalase Cleavage In Vitro Is Lethal for Virus Production. *J. Virol.* 74, 24–32. doi:10.1128/JVI.74.1.24-32.2000
- Lee, J.-G., Baek, K., Soetandyo, N., Ye, Y., 2013. Reversible inactivation of deubiquitinases by reactive oxygen species in vitro and in cells. *Nature Communications* 4, 1568. doi:10.1038/ncomms2532
- Li, C., Xu, D., Ye, Q., Hong, S., Jiang, Y., Liu, X., Zhang, N., Shi, L., Qin, C.-F., Xu, Z., 2016. Zika Virus Disrupts Neural Progenitor Development and Leads to Microcephaly in Mice. *Cell Stem Cell* 19, 120–126. doi:10.1016/j.stem.2016.04.017

- Li, Deng, C.-L., Ye, H.-Q., Zhang, H.-L., Zhang, Q.-Y., Chen, D.-D., Zhang, P.-T., Shi, P.-Y., Yuan, Z.-M., Zhang, B., 2016. Transmembrane Domains of NS2B Contribute to both Viral RNA Replication and Particle Formation in Japanese Encephalitis Virus. *J. Virol.* 90, 5735–5749. doi:10.1128/JVI.00340-16
- Li, X., Gould, S.J., 2002. PEX11 promotes peroxisome division independently of peroxisome metabolism. *The Journal of Cell Biology* 156, 643–651. doi:10.1083/jcb.200112028
- Lim, S.M., Koraka, P., Osterhaus, A.D.M.E., Martina, B.E.E., 2011. West Nile Virus: Immunity and Pathogenesis. *Viruses* 3, 811–828. doi:10.3390/v3060811
- Lim, S.P., Noble, C.G., Seh, C.C., Soh, T.S., Sahili, A.E., Chan, G.K.Y., Lescar, J., Arora, R., Benson, T., Nilar, S., Manjunatha, U., Wan, K.F., Dong, H., Xie, X., Shi, P.-Y., Yokokawa, F., 2016. Potent Allosteric Dengue Virus NS5 Polymerase Inhibitors: Mechanism of Action and Resistance Profiling. *PLOS Pathogens* 12, e1005737. doi:10.1371/journal.ppat.1005737
- Limjindaporn, T., Netsawang, J., Noisakran, S., Thiemmecca, S., Wongwiwat, W., Sudsaward, S., Avirutnan, P., Puttikhunt, C., Kasinrerak, W., Sriburi, R., Sittisombut, N., Yenchitsomanus, P.-T., Malasit, P., 2007. Sensitization to Fas-mediated apoptosis by dengue virus capsid protein. *Biochem. Biophys. Res. Commun.* 362, 334–339. doi:10.1016/j.bbrc.2007.07.194
- Limjindaporn, T., Wongwiwat, W., Noisakran, S., Srisawat, C., Netsawang, J., Puttikhunt, C., Kasinrerak, W., Avirutnan, P., Thiemmecca, S., Sriburi, R., Sittisombut, N., Malasit, P., Yenchitsomanus, P., 2009. Interaction of dengue virus envelope protein with endoplasmic reticulum-resident chaperones facilitates dengue virus production. *Biochemical and Biophysical Research Communications* 379, 196–200. doi:10.1016/j.bbrc.2008.12.070
- Lin, C., Amberg, S.M., Chambers, T.J., Rice, C.M., 1993. Cleavage at a novel site in the NS4A region by the yellow fever virus NS2B-3 proteinase is a prerequisite for processing at the downstream 4A/4B signalase site. *J. Virol.* 67, 2327–2335.
- Lin, R.-J., Chang, B.-L., Yu, H.-P., Liao, C.-L., Lin, Y.-L., 2006. Blocking of interferon-induced Jak-Stat signaling by Japanese encephalitis virus NS5 through a protein tyrosine phosphatase-mediated mechanism. *J. Virol.* 80, 5908–5918. doi:10.1128/JVI.02714-05
- Lindenbach, B.D., Rice, C.M., 2003. Molecular biology of flaviviruses, in: *Advances in Virus Research*. Academic Press, pp. 23–61.
- Lindquist, M.E., Lifland, A.W., Utley, T.J., Santangelo, P.J., Crowe, J.E., 2010. Respiratory Syncytial Virus Induces Host RNA Stress Granules To Facilitate Viral Replication. *J. Virol.* 84, 12274–12284. doi:10.1128/JVI.00260-10
- Liu, B., Zhang, M., Chu, H., Zhang, H., Wu, H., Song, G., Wang, P., Zhao, K., Hou, J., Wang, X., Zhang, L., Gao, C., 2017. The ubiquitin E3 ligase TRIM31 promotes aggregation and activation of the signaling adaptor MAVS through Lys63-linked polyubiquitination. *Nat. Immunol.* 18, 214–224. doi:10.1038/ni.3641
- Liu, L.X., Margottin, F., Gall, S.L., Schwartz, O., Selig, L., Benarous, R., Benichou, S., 1997. Binding of HIV-1 Nef to a Novel Thioesterase Enzyme Correlates with Nef-mediated CD4 Down-regulation. *J. Biol. Chem.* 272, 13779–13785. doi:10.1074/jbc.272.21.13779
- Liu, S., Cai, X., Wu, J., Cong, Q., Chen, X., Li, T., Du, F., Ren, J., Wu, Y.-T., Grishin, N.V., Chen, Z.J., 2015. Phosphorylation of innate immune adaptor proteins MAVS, STING, and TRIF induces IRF3 activation. *Science* 347, aaa2630. doi:10.1126/science.aaa2630

- Liu, W.J., Chen, H.B., Wang, X.J., Huang, H., Khromykh, A.A., 2004. Analysis of adaptive mutations in Kunjin virus replicon RNA reveals a novel role for the flavivirus nonstructural protein NS2A in inhibition of beta interferon promoter-driven transcription. *J. Virol.* 78, 12225–12235. doi:10.1128/JVI.78.22.12225-12235.2004
- Liu, W.J., Wang, X.J., Mokhonov, V.V., Shi, P.-Y., Randall, R., Khromykh, A.A., 2005. Inhibition of interferon signaling by the New York 99 strain and Kunjin subtype of West Nile virus involves blockage of STAT1 and STAT2 activation by nonstructural proteins. *J. Virol.* 79, 1934–1942. doi:10.1128/JVI.79.3.1934-1942.2005
- Lizard, G., Rouaud, O., Demarquoy, J., Cherkaoui-Malki, M., Iuliano, L., 2012. Potential roles of peroxisomes in Alzheimer’s disease and in dementia of the Alzheimer’s type. *J. Alzheimers Dis.* 29, 241–254. doi:10.3233/JAD-2011-111163
- Lobigs, M., Lee, E., 2004. Inefficient Signalase Cleavage Promotes Efficient Nucleocapsid Incorporation into Budding Flavivirus Membranes. *J. Virol.* 78, 178–186. doi:10.1128/JVI.78.1.178-186.2004
- Lorenz, I.C., Allison, S.L., Heinz, F.X., Helenius, A., 2002. Folding and dimerization of tick-borne encephalitis virus envelope proteins prM and E in the endoplasmic reticulum. *J. Virol.* 76, 5480–5491.
- Loschi, M., Leishman, C.C., Berardone, N., Boccaccio, G.L., 2009. Dynein and kinesin regulate stress-granule and P-body dynamics. *J Cell Sci* 122, 3973–3982. doi:10.1242/jcs.051383
- Magalhães, A.C., Ferreira, A.R., Gomes, S., Vieira, M., Gouveia, A., Valença, I., Islinger, M., Nascimento, R., Schrader, M., Kagan, J.C., Ribeiro, D., 2016. Peroxisomes are platforms for cytomegalovirus’ evasion from the cellular immune response. *Scientific Reports* 6, 26028. doi:10.1038/srep26028
- Maidji, E., McDonagh, S., Genbacev, O., Tabata, T., Pereira, L., 2006. Maternal antibodies enhance or prevent cytomegalovirus infection in the placenta by neonatal Fc receptor-mediated transcytosis. *Am. J. Pathol.* 168, 1210–1226. doi:10.2353/ajpath.2006.050482
- Mandl, C.W., Allison, S.L., Holzmann, H., Meixner, T., Heinz, F.X., 2000. Attenuation of tick-borne encephalitis virus by structure-based site-specific mutagenesis of a putative flavivirus receptor binding site. *J. Virol.* 74, 9601–9609.
- Manokaran, G., Finol, E., Wang, C., Gunaratne, J., Bahl, J., Ong, E.Z., Tan, H.C., Sessions, O.M., Ward, A.M., Gubler, D.J., Harris, E., Garcia-Blanco, M.A., Ooi, E.E., 2015. Dengue subgenomic RNA binds TRIM25 to inhibit interferon expression for epidemiological fitness. *Science* 350, 217–221. doi:10.1126/science.aab3369
- Mansfield, K.L., Johnson, N., Cosby, S.L., Solomon, T., Fooks, A.R., 2010. Transcriptional upregulation of SOCS 1 and suppressors of cytokine signaling 3 mRNA in the absence of suppressors of cytokine signaling 2 mRNA after infection with West Nile virus or tick-borne encephalitis virus. *Vector Borne Zoonotic Dis.* 10, 649–653. doi:10.1089/vbz.2009.0259
- Mansuy, J.M., Dutertre, M., Mengelle, C., Fourcade, C., Marchou, B., Delobel, P., Izopet, J., Martin-Blondel, G., 2016a. Zika virus: high infectious viral load in semen, a new sexually transmitted pathogen? *Lancet Infect Dis* 16, 405. doi:10.1016/S1473-3099(16)00138-9
- Mansuy, J.M., Suberbielle, E., Chapuy-Regaud, S., Mengelle, C., Bujan, L., Marchou, B., Delobel, P., Gonzalez-Dunia, D., Malnou, C.E., Izopet, J., Martin-Blondel, G., 2016b. Zika virus in semen and spermatozoa. *Lancet Infect Dis* 16, 1106–1107. doi:10.1016/S1473-3099(16)30336-X

- Marle, G. van, Antony, J., Ostermann, H., Dunham, C., Hunt, T., Halliday, W., Maingat, F., Urbanowski, M.D., Hobman, T., Peeling, J., Power, C., 2007. West Nile Virus-Induced Neuroinflammation: Glial Infection and Capsid Protein-Mediated Neurovirulence. *J. Virol.* 81, 10933–10949. doi:10.1128/JVI.02422-06
- Marmar, W.N., Nungesser, E., Foglia, T.A., 1986. Oxidation of ethyl hexadec-1-enyl ether, a plasmalogen model, in the presence of unsaturated esters. *Lipids* 21, 648–651. doi:10.1007/BF02537215
- Martina, B.E.E., Koraka, P., Osterhaus, A.D.M.E., 2009. Dengue virus pathogenesis: an integrated view. *Clin. Microbiol. Rev.* 22, 564–581. doi:10.1128/CMR.00035-09
- Martins, I.C., Gomes-Neto, F., Faustino, A.F., Carvalho, F.A., Carneiro, F.A., Bozza, P.T., Mohana-Borges, R., Castanho, M.A.R.B., Almeida, F.C.L., Santos, N.C., Da Poian, A.T., 2012. The disordered N-terminal region of dengue virus capsid protein contains a lipid-droplet-binding motif. *Biochemical Journal* 444, 405–415. doi:10.1042/BJ20112219
- Mast, F.D., Jamakhandi, A., Saleem, R.A., Dilworth, D.J., Rogers, R.S., Rachubinski, R.A., Aitchison, J.D., 2016. Peroxisomes Pex30 and Pex29 Dynamically Associate with Reticulons to Regulate Peroxisome Biogenesis from the Endoplasmic Reticulum. *J. Biol. Chem.* 291, 15408–15427. doi:10.1074/jbc.M116.728154
- Mast, F.D., Rachubinski, R.A., Aitchison, J.D., 2015. Signaling dynamics and peroxisomes. *Current opinion in cell biology* 35, 131. doi:10.1016/j.ceb.2015.05.002
- Matsuki, H., Takahashi, M., Higuchi, M., Makokha, G.N., Oie, M., Fujii, M., 2013. Both G3BP1 and G3BP2 contribute to stress granule formation. *Genes Cells* 18, 135–146. doi:10.1111/gtc.12023
- Matsuzaki, T., Fujiki, Y., 2008. The peroxisomal membrane protein import receptor Pex3p is directly transported to peroxisomes by a novel Pex19p- and Pex16p-dependent pathway. *J Cell Biol* 183, 1275–1286. doi:10.1083/jcb.200806062
- Mauracher, C.A., Gillam, S., Shukin, R., Tingle, A.J., 1991. pH-dependent solubility shift of rubella virus capsid protein. *Virology* 181, 773–777.
- Mazroui, R., Sukarieh, R., Bordeleau, M.-E., Kaufman, R.J., Northcote, P., Tanaka, J., Gallouzi, I., Pelletier, J., 2006. Inhibition of ribosome recruitment induces stress granule formation independently of eukaryotic initiation factor 2alpha phosphorylation. *Mol. Biol. Cell* 17, 4212–4219. doi:10.1091/mbc.E06-04-0318
- McEwen, E., Kedersha, N., Song, B., Scheuner, D., Gilks, N., Han, A., Chen, J.-J., Anderson, P., Kaufman, R.J., 2005. Heme-regulated Inhibitor Kinase-mediated Phosphorylation of Eukaryotic Translation Initiation Factor 2 Inhibits Translation, Induces Stress Granule Formation, and Mediates Survival upon Arsenite Exposure. *J. Biol. Chem.* 280, 16925–16933. doi:10.1074/jbc.M412882200
- Medigeshi, G.R., Hirsch, A.J., Brien, J.D., Uhrlaub, J.L., Mason, P.W., Wiley, C., Nikolich-Zugich, J., Nelson, J.A., 2009. West Nile virus capsid degradation of claudin proteins disrupts epithelial barrier function. *J. Virol.* 83, 6125–6134. doi:10.1128/JVI.02617-08
- Meinecke, M., Cizmowski, C., Schliebs, W., Krüger, V., Beck, S., Wagner, R., Erdmann, R., 2010. The peroxisomal importomer constitutes a large and highly dynamic pore. *Nat Cell Biol* 12, 273–277. doi:10.1038/ncb2027
- Mezochow, A.K., Henry, R., Blumberg, E.A., Kotton, C.N., 2015. Transfusion transmitted infections in solid organ transplantation. *Am. J. Transplant.* 15, 547–554. doi:10.1111/ajt.13006

- Miller, S., Kastner, S., Krijnse-Locker, J., Bühler, S., Bartenschlager, R., 2007. The Non-structural Protein 4A of Dengue Virus Is an Integral Membrane Protein Inducing Membrane Alterations in a 2K-regulated Manner. *J. Biol. Chem.* 282, 8873–8882. doi:10.1074/jbc.M609919200
- Miner, J.J., Cao, B., Govero, J., Smith, A.M., Fernandez, E., Cabrera, O.H., Garber, C., Noll, M., Klein, R.S., Noguchi, K.K., Mysorekar, I.U., Diamond, M.S., 2016a. Zika Virus Infection during Pregnancy in Mice Causes Placental Damage and Fetal Demise. *Cell* 165, 1081–1091. doi:10.1016/j.cell.2016.05.008
- Miner, J.J., Sene, A., Richner, J.M., Smith, A.M., Santeford, A., Ban, N., Weger-Lucarelli, J., Manzella, F., Rückert, C., Govero, J., Noguchi, K.K., Ebel, G.D., Diamond, M.S., Apte, R.S., 2016b. Zika Virus Infection in Mice Causes Panuveitis with Shedding of Virus in Tears. *Cell Reports* 16, 3208–3218. doi:10.1016/j.celrep.2016.08.079
- Modhiran, N., Watterson, D., Muller, D.A., Panetta, A.K., Sester, D.P., Liu, L., Hume, D.A., Stacey, K.J., Young, P.R., 2015. Dengue virus NS1 protein activates cells via Toll-like receptor 4 and disrupts endothelial cell monolayer integrity. *Science Translational Medicine* 7, 304ra142–304ra142. doi:10.1126/scitranslmed.aaa3863
- Mohan, K.V.K., Som, I., Atreya, C.D., 2002. Identification of a type 1 peroxisomal targeting signal in a viral protein and demonstration of its targeting to the organelle. *J. Virol.* 76, 2543–2547.
- Mohan, P.M., Padmanabhan, R., 1991. Detection of stable secondary structure at the 3' terminus of dengue virus type 2 RNA. *Gene* 108, 185–191.
- Mongkolsapaya, J., Dejnirattisai, W., Xu, X., Vasanawathana, S., Tangthawornchaikul, N., Chairunsri, A., Sawasdivorn, S., Duangchinda, T., Dong, T., Rowland-Jones, S., Yenichitsomanus, P., McMichael, A., Malasit, P., Screaton, G., 2003. Original antigenic sin and apoptosis in the pathogenesis of dengue hemorrhagic fever. *Nat Med* 9, 921–927. doi:10.1038/nm887
- Mongkolsapaya, J., Duangchinda, T., Dejnirattisai, W., Vasanawathana, S., Avirutnan, P., Jairungsri, A., Khemnu, N., Tangthawornchaikul, N., Chotiyarnwong, P., Sae-Jang, K., Koch, M., Jones, Y., McMichael, A., Xu, X., Malasit, P., Screaton, G., 2006. T Cell Responses in Dengue Hemorrhagic Fever: Are Cross-Reactive T Cells Suboptimal? *The Journal of Immunology* 176, 3821–3829. doi:10.4049/jimmunol.176.6.3821
- Moore, C.B., Bergstralh, D.T., Duncan, J.A., Lei, Y., Morrison, T.E., Zimmermann, A.G., Accavitti-Loper, M.A., Madden, V.J., Sun, L., Ye, Z., Lich, J.D., Heise, M.T., Chen, Z., Ting, J.P.-Y., 2008. NLRX1 is a regulator of mitochondrial antiviral immunity. *Nature* 451, 573–577. doi:10.1038/nature06501
- Moreira, J., Peixoto, T.M., Machado de Siqueira, A., Lamas, C.C., 2017. Sexually acquired Zika virus: a systematic review. *Clin. Microbiol. Infect.* doi:10.1016/j.cmi.2016.12.027
- Mori, Y., Okabayashi, T., Yamashita, T., Zhao, Z., Wakita, T., Yasui, K., Hasebe, F., Tadano, M., Konishi, E., Moriishi, K., Matsuura, Y., 2005. Nuclear Localization of Japanese Encephalitis Virus Core Protein Enhances Viral Replication. *J. Virol.* 79, 3448–3458. doi:10.1128/JVI.79.6.3448-3458.2005
- Morrison, J., Laurent-Rolle, M., Maestre, A.M., Rajsbaum, R., Pisanelli, G., Simon, V., Mulder, L.C.F., Fernandez-Sesma, A., García-Sastre, A., 2013. Dengue Virus Co-opts UBR4 to Degrade STAT2 and Antagonize Type I Interferon Signaling. *PLOS Pathog* 9, e1003265. doi:10.1371/journal.ppat.1003265

- Muñoz-Jordán, J.L., Laurent-Rolle, M., Ashour, J., Martínez-Sobrido, L., Ashok, M., Lipkin, W.I., García-Sastre, A., 2005. Inhibition of alpha/beta interferon signaling by the NS4B protein of flaviviruses. *J. Virol.* 79, 8004–8013. doi:10.1128/JVI.79.13.8004-8013.2005
- Muñoz-Jordán, J.L., Sánchez-Burgos, G.G., Laurent-Rolle, M., García-Sastre, A., 2003. Inhibition of interferon signaling by dengue virus. *Proceedings of the National Academy of Sciences* 100, 14333–14338. doi:10.1073/pnas.2335168100
- Nagila, A., Netsawang, J., Srisawat, C., Noisakran, S., Morchang, A., Yasamut, U., Puttikhunt, C., Kasinrerak, W., Malasit, P., Yenchitsomanus, P., Limjindaporn, T., 2011. Role of CD137 signaling in dengue virus-mediated apoptosis. *Biochem. Biophys. Res. Commun.* 410, 428–433. doi:10.1016/j.bbrc.2011.05.151
- Nain, M., Mukherjee, S., Karmakar, S.P., Paton, A.W., Paton, J.C., Abdin, M.Z., Basu, A., Kalia, M., Vrati, S., 2017. GRP78 Is an Important Host Factor for Japanese Encephalitis Virus Entry and Replication in Mammalian Cells. *J. Virol.* 91, e02274-16. doi:10.1128/JVI.02274-16
- Nair, D.M., Purdue, P.E., Lazarow, P.B., 2004. Pex7p translocates in and out of peroxisomes in *Saccharomyces cerevisiae*. *J. Cell Biol.* 167, 599–604. doi:10.1083/jcb.200407119
- Nash, D., Mostashari, F., Fine, A., Miller, J., O’Leary, D., Murray, K., Huang, A., Rosenberg, A., Greenberg, A., Sherman, M., Wong, S., Layton, M., 1999 West Nile Outbreak Response Working Group, 2001. The outbreak of West Nile virus infection in the New York City area in 1999. *N. Engl. J. Med.* 344, 1807–1814. doi:10.1056/NEJM200106143442401
- Netsawang, J., Noisakran, S., Puttikhunt, C., Kasinrerak, W., Wongwiwat, W., Malasit, P., Yenchitsomanus, P., Limjindaporn, T., 2010. Nuclear localization of dengue virus capsid protein is required for DAXX interaction and apoptosis. *Virus Res.* 147, 275–283. doi:10.1016/j.virusres.2009.11.012
- Netsawang, J., Panaampon, J., Khunchai, S., Kooptiwut, S., Nagila, A., Puttikhunt, C., Yenchitsomanus, P., Limjindaporn, T., 2014. Dengue virus disrupts Daxx and NF-κB interaction to induce CD137-mediated apoptosis. *Biochemical and Biophysical Research Communications* 450, 1485–1491. doi:10.1016/j.bbrc.2014.07.016
- Ng, C.S., Jogi, M., Yoo, J.-S., Onomoto, K., Koike, S., Iwasaki, T., Yoneyama, M., Kato, H., Fujita, T., 2013. Encephalomyocarditis Virus Disrupts Stress Granules, the Critical Platform for Triggering Antiviral Innate Immune Responses. *J. Virol.* 87, 9511–9522. doi:10.1128/JVI.03248-12
- Nordgren, M., Wang, B., Apanasets, O., Fransen, M., 2013. Peroxisome degradation in mammals: mechanisms of action, recent advances, and perspectives. *Front Physiol* 4. doi:10.3389/fphys.2013.00145
- Noronha, L. de, Zanluca, C., Azevedo, M.L.V., Luz, K.G., Santos, C.N.D. dos, Noronha, L. de, Zanluca, C., Azevedo, M.L.V., Luz, K.G., Santos, C.N.D. dos, 2016. Zika virus damages the human placental barrier and presents marked fetal neurotropism. *Memórias do Instituto Oswaldo Cruz* 111, 287–293. doi:10.1590/0074-02760160085
- Nowakowski, T.J., Pollen, A.A., Di Lullo, E., Sandoval-Espinosa, C., Bershteyn, M., Kriegstein, A.R., 2016. Expression Analysis Highlights AXL as a Candidate Zika Virus Entry Receptor in Neural Stem Cells. *Cell Stem Cell* 18, 591–596. doi:10.1016/j.stem.2016.03.012

- Odendall, C., Dixit, E., Stavru, F., Bierne, H., Franz, K.M., Durbin, A.F., Boulant, S., Gehrke, L., Cossart, P., Kagan, J.C., 2014. Diverse intracellular pathogens activate type III interferon expression from peroxisomes. *Nat Immunol* 15, 717–726. doi:10.1038/ni.2915
- Oh, S.-W., Onomoto, K., Wakimoto, M., Onoguchi, K., Ishidate, F., Fujiwara, T., Yoneyama, M., Kato, H., Fujita, T., 2016. Leader-Containing Uncapped Viral Transcript Activates RIG-I in Antiviral Stress Granules. *PLOS Pathog* 12, e1005444. doi:10.1371/journal.ppat.1005444
- Oh, W., Song, J., 2006. Hsp70 functions as a negative regulator of West Nile virus capsid protein through direct interaction. *Biochem. Biophys. Res. Commun.* 347, 994–1000. doi:10.1016/j.bbrc.2006.06.190
- Oh, W., Yang, M.-R., Lee, E.-W., Park, K., Pyo, S., Yang, J., Lee, H.-W., Song, J., 2006. Jab1 Mediates Cytoplasmic Localization and Degradation of West Nile Virus Capsid Protein. *J. Biol. Chem.* 281, 30166–30174. doi:10.1074/jbc.M602651200
- Olagnier, D., Peri, S., Steel, C., Montfoort, N. van, Chiang, C., Beljanski, V., Slifker, M., He, Z., Nichols, C.N., Lin, R., Balachandran, S., Hiscott, J., 2014. Cellular Oxidative Stress Response Controls the Antiviral and Apoptotic Programs in Dengue Virus-Infected Dendritic Cells. *PLOS Pathogens* 10, e1004566. doi:10.1371/journal.ppat.1004566
- Oliveira Melo, A.S., Malinger, G., Ximenes, R., Szejnfeld, P.O., Alves Sampaio, S., Bispo de Filippis, A.M., 2016. Zika virus intrauterine infection causes fetal brain abnormality and microcephaly: tip of the iceberg? *Ultrasound Obstet Gynecol* 47, 6–7. doi:10.1002/uog.15831
- Onomoto, K., Yoneyama, M., Fung, G., Kato, H., Fujita, T., 2014. Antiviral innate immunity and stress granule responses. *Trends in Immunology*. doi:10.1016/j.it.2014.07.006
- Opaliński, Ł., Kiel, J.A.K.W., Williams, C., Veenhuis, M., Klei, I.J. van der, 2011. Membrane curvature during peroxisome fission requires Pex11. *The EMBO Journal* 30, 5–16. doi:10.1038/emboj.2010.299
- Ortega, Á.D., Willers, I.M., Sala, S., Cuezva, J.M., 2010. Human G3BP1 interacts with β -F1-ATPase mRNA and inhibits its translation. *J Cell Sci* 123, 2685–2696. doi:10.1242/jcs.065920
- Överby, A.K., Popov, V.L., Niedrig, M., Weber, F., 2010. Tick-Borne Encephalitis Virus Delays Interferon Induction and Hides Its Double-Stranded RNA in Intracellular Membrane Vesicles. *J. Virol.* 84, 8470–8483. doi:10.1128/JVI.00176-10
- Pan, Y., Li, R., Meng, J.-L., Mao, H.-T., Zhang, Y., Zhang, J., 2014. Smurf2 Negatively Modulates RIG-I-Dependent Antiviral Response by Targeting VISA/MAVS for Ubiquitination and Degradation. *The Journal of Immunology* 192, 4758–4764. doi:10.4049/jimmunol.1302632
- Panavas, T., Hawkins, C.M., Panaviene, Z., Nagy, P.D., 2005. The role of the p33:p33/p92 interaction domain in RNA replication and intracellular localization of p33 and p92 proteins of Cucumber necrosis tomosvirus. *Virology* 338, 81–95. doi:10.1016/j.virol.2005.04.025
- Parquet, M.C., Kumatori, A., Hasebe, F., Morita, K., Igarashi, A., 2001. West Nile virus-induced bax-dependent apoptosis. *FEBS Lett.* 500, 17–24.
- Patkar, C.G., Kuhn, R.J., 2008. Yellow Fever Virus NS3 Plays an Essential Role in Virus Assembly Independent of Its Known Enzymatic Functions. *J. Virol.* 82, 3342–3352. doi:10.1128/JVI.02447-07

- Peña, J., Harris, E., 2011. Dengue virus modulates the unfolded protein response in a time-dependent manner. *J. Biol. Chem.* 286, 14226–14236. doi:10.1074/jbc.M111.222703
- Perera-Lecoin, M., Meertens, L., Carnec, X., Amara, A., 2013. Flavivirus Entry Receptors: An Update. *Viruses* 6, 69–88. doi:10.3390/v6010069
- Petriv, O.I., Tang, L., Titorenko, V.I., Rachubinski, R.A., 2004. A new definition for the consensus sequence of the peroxisome targeting signal type 2. *J. Mol. Biol.* 341, 119–134. doi:10.1016/j.jmb.2004.05.064
- Pham, A.M., Maria, F.G.S., Lahiri, T., Friedman, E., Marié, I.J., Levy, D.E., 2016. PKR Transduces MDA5-Dependent Signals for Type I IFN Induction. *PLOS Pathogens* 12, e1005489. doi:10.1371/journal.ppat.1005489
- Pichlmair, A., Lassnig, C., Eberle, C.-A., Górna, M.W., Baumann, C.L., Burkard, T.R., Bürckstümmer, T., Stefanovic, A., Krieger, S., Bennett, K.L., Rüllicke, T., Weber, F., Colinge, J., Müller, M., Superti-Furga, G., 2011. IFIT1 is an antiviral protein that recognizes 5'-triphosphate RNA. *Nat Immunol* 12, 624–630. doi:10.1038/ni.2048
- Pierson, T.C., Graham, B.S., 2016. Zika Virus: Immunity and Vaccine Development. *Cell* 167, 625–631. doi:10.1016/j.cell.2016.09.020
- Pijlman, G.P., Funk, A., Kondratieva, N., Leung, J., Torres, S., van der Aa, L., Liu, W.J., Palmenberg, A.C., Shi, P.-Y., Hall, R.A., Khromykh, A.A., 2008. A Highly Structured, Nuclease-Resistant, Noncoding RNA Produced by Flaviviruses Is Required for Pathogenicity. *Cell Host & Microbe* 4, 579–591. doi:10.1016/j.chom.2008.10.007
- Piotrowska, J., Hansen, S.J., Park, N., Jamka, K., Sarnow, P., Gustin, K.E., 2010. Stable Formation of Compositionally Unique Stress Granules in Virus-Infected Cells. *J. Virol.* 84, 3654–3665. doi:10.1128/JVI.01320-09
- Platta, H.W., Grunau, S., Rosenkranz, K., Girzalsky, W., Erdmann, R., 2005. Functional role of the AAA peroxins in dislocation of the cycling PTS1 receptor back to the cytosol. *Nat Cell Biol* 7, 817–822. doi:10.1038/ncb1281
- Priyamvada, L., Quicke, K.M., Hudson, W.H., Onlamoon, N., Sewatanon, J., Edupuganti, S., Pattanapanyasat, K., Chokephaibulkit, K., Mulligan, M.J., Wilson, P.C., Ahmed, R., Suthar, M.S., Wrammert, J., 2016. Human antibody responses after dengue virus infection are highly cross-reactive to Zika virus. *PNAS* 113, 7852–7857. doi:10.1073/pnas.1607931113
- Public Health Agency of Canada, 2015. Surveillance of West Nile virus [WWW Document]. Surveillance of West Nile virus. URL <https://www.canada.ca/en/public-health/services/diseases/west-nile-virus/surveillance-west-nile-virus.html> (accessed 3.7.17).
- Quicke, K.M., Bowen, J.R., Johnson, E.L., McDonald, C.E., Ma, H., O'Neal, J.T., Rajakumar, A., Wrammert, J., Rimawi, B.H., Pulendran, B., Schinazi, R.F., Chakraborty, R., Suthar, M.S., 2016. Zika Virus Infects Human Placental Macrophages. *Cell Host & Microbe* 20, 83–90. doi:10.1016/j.chom.2016.05.015
- Raung, S.L., Kuo, M.D., Wang, Y.M., Chen, C.J., 2001. Role of reactive oxygen intermediates in Japanese encephalitis virus infection in murine neuroblastoma cells. *Neurosci. Lett.* 315, 9–12.
- Ray, D., Shah, A., Tilgner, M., Guo, Y., Zhao, Y., Dong, H., Deas, T.S., Zhou, Y., Li, H., Shi, P.-Y., 2006. West Nile virus 5'-cap structure is formed by sequential guanine N-7 and ribose 2'-O methylations by nonstructural protein 5. *J. Virol.* 80, 8362–8370. doi:10.1128/JVI.00814-06

- Reddy, J.K., Krishnakantha, T.P., 1975. Hepatic peroxisome proliferation: induction by two novel compounds structurally unrelated to clofibrate. *Science* 190, 787–789. doi:10.1126/science.1198095
- Reid, C.R., Hobman, T.C., 2017. The nucleolar helicase DDX56 redistributes to West Nile virus assembly sites. *Virology* 500, 169–177. doi:10.1016/j.virol.2016.10.025
- Retallack, H., Lullo, E.D., Arias, C., Knopp, K.A., Laurie, M.T., Sandoval-Espinosa, C., Leon, W.R.M., Krencik, R., Ullian, E.M., Spatazza, J., Pollen, A.A., Mandel-Brehm, C., Nowakowski, T.J., Kriegstein, A.R., DeRisi, J.L., 2016a. Zika virus cell tropism in the developing human brain and inhibition by azithromycin. *PNAS* 113, 14408–14413. doi:10.1073/pnas.1618029113
- Rochon, D., Singh, B., Reade, R., Theilmann, J., Ghoshal, K., Alam, S.B., Maghodia, A., 2014. The p33 auxiliary replicase protein of Cucumber necrosis virus targets peroxisomes and infection induces de novo peroxisome formation from the endoplasmic reticulum. *Virology* 452–453, 133–142. doi:10.1016/j.virol.2013.12.035
- Rodriguez, J.J., Cruz, C.D., Horvath, C.M., 2004. Identification of the Nuclear Export Signal and STAT-Binding Domains of the Nipah Virus V Protein Reveals Mechanisms Underlying Interferon Evasion. *J. Virol.* 78, 5358–5367. doi:10.1128/JVI.78.10.5358-5367.2004
- Rodriguez-Madoz, J.R., Belicha-Villanueva, A., Bernal-Rubio, D., Ashour, J., Ayllon, J., Fernandez-Sesma, A., 2010. Inhibition of the type I interferon response in human dendritic cells by dengue virus infection requires a catalytically active NS2B3 complex. *J. Virol.* 84, 9760–9774. doi:10.1128/JVI.01051-10
- Roe, K., Kumar, M., Lum, S., Orillo, B., Nerurkar, V.R., Verma, S., 2012. West Nile virus-induced disruption of the blood-brain barrier in mice is characterized by the degradation of the junctional complex proteins and increase in multiple matrix metalloproteinases. *J. Gen. Virol.* 93, 1193–1203. doi:10.1099/vir.0.040899-0
- Ron, D., Walter, P., 2007. Signal integration in the endoplasmic reticulum unfolded protein response. *Nat Rev Mol Cell Biol* 8, 519–529. doi:10.1038/nrm2199
- Roosendaal, J., Westaway, E.G., Khromykh, A., Mackenzie, J.M., 2006. Regulated cleavages at the West Nile virus NS4A-2K-NS4B junctions play a major role in rearranging cytoplasmic membranes and Golgi trafficking of the NS4A protein. *J. Virol.* 80, 4623–4632. doi:10.1128/JVI.80.9.4623-4632.2006
- Roth, H., Magg, V., Uch, F., Mutz, P., Klein, P., Haneke, K., Lohmann, V., Bartenschlager, R., Fackler, O.T., Locker, N., Stoecklin, G., Ruggieri, A., 2017. Flavivirus Infection Uncouples Translation Suppression from Cellular Stress Responses. *mBio* 8, e02150-16. doi:10.1128/mBio.02150-16
- Royal Society, 1895. *Proceedings of the Royal Society of London*. Taylor & Francis.
- Rubin, E.J., Greene, M.F., Baden, L.R., 2016. Zika Virus and Microcephaly. *N. Engl. J. Med.* 374, 984–985. doi:10.1056/NEJMe1601862
- Ruggieri, A., Dazert, E., Metz, P., Hofmann, S., Bergeest, J.-P., Mazur, J., Bankhead, P., Hiet, M.-S., Kallis, S., Alvisi, G., Samuel, C.E., Lohmann, V., Kaderali, L., Rohr, K., Frese, M., Stoecklin, G., Bartenschlager, R., 2012. Dynamic Oscillation of Translation and Stress Granule Formation Mark the Cellular Response to Virus Infection. *Cell Host & Microbe* 12, 71–85. doi:10.1016/j.chom.2012.05.013
- Runge, S., Sparrer, K.M.J., Lässig, C., Hembach, K., Baum, A., García-Sastre, A., Söding, J., Conzelmann, K.-K., Hopfner, K.-P., 2014. In Vivo Ligands of MDA5 and RIG-I in

- Measles Virus-Infected Cells. *PLOS Pathogens* 10, e1004081. doi:10.1371/journal.ppat.1004081
- Russo, M., Di Franco, A., Martelli, G.P., 1983. The fine structure of Cymbidium ringspot virus infections in host tissues. III. Role of peroxisomes in the genesis of multivesicular bodies. *J. Ultrastruct. Res.* 82, 52–63.
- Saha, B., Jyothi Prasanna, S., Chandrasekar, B., Nandi, D., 2010. Gene modulation and immunoregulatory roles of interferon gamma. *Cytokine* 50, 1–14. doi:10.1016/j.cyto.2009.11.021
- Samsa, M.M., Mondotte, J.A., Iglesias, N.G., Assunção-Miranda, I., Barbosa-Lima, G., Da Poian, A.T., Bozza, P.T., Gamarnik, A.V., 2009. Dengue virus capsid protein usurps lipid droplets for viral particle formation. *PLoS Pathog.* 5, e1000632. doi:10.1371/journal.ppat.1000632
- Samuel, G.H., Wiley, M.R., Badawi, A., Adelman, Z.N., Myles, K.M., 2016. Yellow fever virus capsid protein is a potent suppressor of RNA silencing that binds double-stranded RNA. *Proc. Natl. Acad. Sci. U.S.A.* 113, 13863–13868. doi:10.1073/pnas.1600544113
- Samuel, M.A., Morrey, J.D., Diamond, M.S., 2007a. Caspase 3-dependent cell death of neurons contributes to the pathogenesis of West Nile virus encephalitis. *J. Virol.* 81, 2614–2623. doi:10.1128/JVI.02311-06
- Samuel, M.A., Wang, H., Siddharthan, V., Morrey, J.D., Diamond, M.S., 2007b. Axonal transport mediates West Nile virus entry into the central nervous system and induces acute flaccid paralysis. *PNAS* 104, 17140–17145. doi:10.1073/pnas.0705837104
- Samuel, M.A., Whitby, K., Keller, B.C., Marri, A., Barchet, W., Williams, B.R.G., Silverman, R.H., Gale, M., Diamond, M.S., 2006. PKR and RNase L Contribute to Protection against Lethal West Nile Virus Infection by Controlling Early Viral Spread in the Periphery and Replication in Neurons. *J. Virol.* 80, 7009–7019. doi:10.1128/JVI.00489-06
- Santos, M.J., Hoefler, S., Moser, A.B., Moser, H.W., Lazarow, P.B., 1992. Peroxisome assembly mutations in humans: Structural heterogeneity in Zellweger syndrome. *J. Cell. Physiol.* 151, 103–112. doi:10.1002/jcp.1041510115
- Scaturro, P., Cortese, M., Chatel-Chaix, L., Fischl, W., Bartenschlager, R., 2015. Dengue Virus Non-structural Protein 1 Modulates Infectious Particle Production via Interaction with the Structural Proteins. *PLOS Pathogens* 11, e1005277. doi:10.1371/journal.ppat.1005277
- Schalich, J., Allison, S.L., Stiasny, K., Mandl, C.W., Kunz, C., Heinz, F.X., 1996. Recombinant subviral particles from tick-borne encephalitis virus are fusogenic and provide a model system for studying flavivirus envelope glycoprotein functions. *J. Virol.* 70, 4549–4557.
- Schmidt, F., Dietrich, D., Eylestein, R., Groemping, Y., Stehle, T., Dodt, G., 2012. The role of conserved PEX3 regions in PEX19-binding and peroxisome biogenesis. *Traffic* 9999, n/a-n/a. doi:10.1111/j.1600-0854.2012.01380.x
- Schmidt, M., Geilenkeuser, W.-J., Sireis, W., Seifried, E., Hourfar, K., 2014. Emerging Pathogens - How Safe is Blood? *TMH* 41, 10–17. doi:10.1159/000358017
- Schoggins, J.W., MacDuff, D.A., Imanaka, N., Gainey, M.D., Shrestha, B., Eitson, J.L., Mar, K.B., Richardson, R.B., Ratushny, A.V., Litvak, V., Dabelic, R., Manicassamy, B., Aitchison, J.D., Aderem, A., Elliott, R.M., García-Sastre, A., Racaniello, V., Snijder, E.J., Yokoyama, W.M., Diamond, M.S., Virgin, H.W., Rice, C.M., 2014. Pan-viral specificity of IFN-induced genes reveals new roles for cGAS in innate immunity. *Nature* 505, 691–695. doi:10.1038/nature12862

- Schoggins, J.W., Wilson, S.J., Panis, M., Murphy, M.Y., Jones, C.T., Bieniasz, P., Rice, C.M., 2011. A diverse range of gene products are effectors of the type I interferon antiviral response. *Nature* 472, 481–485. doi:10.1038/nature09907
- Schreck, R., Rieber, P., Baeuerle, P.A., 1991. Reactive oxygen intermediates as apparently widely used messengers in the activation of the NF-kappa B transcription factor and HIV-1. *The EMBO Journal* 10, 2247.
- Schuberth-Wagner, C., Ludwig, J., Bruder, A.K., Herzner, A.-M., Zillinger, T., Goldeck, M., Schmidt, T., Schmid-Burgk, J.L., Kerber, R., Wolter, S., Stümpel, J.-P., Roth, A., Bartok, E., Drosten, C., Coch, C., Hornung, V., Barchet, W., Kümmerer, B.M., Hartmann, G., Schlee, M., 2015. A Conserved Histidine in the RNA Sensor RIG-I Controls Immune Tolerance to N1-2'O-Methylated Self RNA. *Immunity* 43, 41–51. doi:10.1016/j.immuni.2015.06.015
- Schuessler, A., Funk, A., Lazear, H.M., Cooper, D.A., Torres, S., Daffis, S., Jha, B.K., Kumagai, Y., Takeuchi, O., Hertzog, P., Silverman, R., Akira, S., Barton, D.J., Diamond, M.S., Khromykh, A.A., 2012. West Nile Virus Noncoding Subgenomic RNA Contributes to Viral Evasion of the Type I Interferon-Mediated Antiviral Response. *J. Virol.* 86, 5708–5718. doi:10.1128/JVI.00207-12
- Sehgal, N., Kumawat, K.L., Basu, A., Ravindranath, V., 2012. Fenofibrate Reduces Mortality and Precludes Neurological Deficits in Survivors in Murine Model of Japanese Encephalitis Viral Infection. *PLoS ONE* 7, e35427. doi:10.1371/journal.pone.0035427
- Seth, R.B., Sun, L., Ea, C.-K., Chen, Z.J., 2005. Identification and Characterization of MAVS, a Mitochondrial Antiviral Signaling Protein that Activates NF-κB and IRF3. *Cell* 122, 669–682. doi:10.1016/j.cell.2005.08.012
- Shen, J., Chen, X., Hendershot, L., Prywes, R., 2002. ER Stress Regulation of ATF6 Localization by Dissociation of BiP/GRP78 Binding and Unmasking of Golgi Localization Signals. *Developmental Cell* 3, 99–111. doi:10.1016/S1534-5807(02)00203-4
- Sheth, U., Parker, R., 2003. Decapping and Decay of Messenger RNA Occur in Cytoplasmic Processing Bodies. *Science* 300, 805–808. doi:10.1126/science.1082320
- Smith, J.J., Aitchison, J.D., 2013. Peroxisomes take shape. *Nat Rev Mol Cell Biol* 14, 803–817. doi:10.1038/nrm3700
- Smithburn, K.C., Hughes, T.P., Burke, A.W., Paul, J.H., 1940. A Neurotropic Virus Isolated from the Blood of a Native of Uganda. *American Journal of Tropical Medicine* 20, 471–2.
- Solomon, S., Xu, Y., Wang, B., David, M.D., Schubert, P., Kennedy, D., Schrader, J.W., 2007. Distinct structural features of caprin-1 mediate its interaction with G3BP-1 and its induction of phosphorylation of eukaryotic translation initiation factor 2alpha, entry to cytoplasmic stress granules, and selective interaction with a subset of mRNAs. *Mol. Cell. Biol.* 27, 2324–2342. doi:10.1128/MCB.02300-06
- Sommereyns, C., Paul, S., Staeheli, P., Michiels, T., 2008. IFN-Lambda (IFN-λ) Is Expressed in a Tissue-Dependent Fashion and Primarily Acts on Epithelial Cells In Vivo. *PLoS Pathog* 4, e1000017. doi:10.1371/journal.ppat.1000017
- South, S.T., Gould, S.J., 1999. Peroxisome Synthesis in the Absence of Preexisting Peroxisomes. *The Journal of Cell Biology* 144, 255–266. doi:10.1083/jcb.144.2.255
- Stadler, K., Allison, S.L., Schlich, J., Heinz, F.X., 1997. Proteolytic activation of tick-borne encephalitis virus by furin. *J. Virol.* 71, 8475–8481.

- Stanley, W.A., Filipp, F.V., Kursula, P., Schüller, N., Erdmann, R., Schliebs, W., Sattler, M., Wilmanns, M., 2006. Recognition of a Functional Peroxisome Type 1 Target by the Dynamic Import Receptor Pex5p. *Molecular Cell* 24, 653–663. doi:10.1016/j.molcel.2006.10.024
- Steffens, S., Thiel, H.-J., Behrens, S.-E., 1999. The RNA-dependent RNA polymerases of different members of the family Flaviviridae exhibit similar properties in vitro. *Journal of General Virology* 80, 2583–2590. doi:10.1099/0022-1317-80-10-2583
- Sudhakar, A., Ramachandran, A., Ghosh, S., Hasnain, S.E., Kaufman, R.J., Ramaiah, K.V.A., 2000. Phosphorylation of Serine 51 in Initiation Factor 2 α (eIF2 α) Promotes Complex Formation between eIF2 α (P) and eIF2B and Causes Inhibition in the Guanine Nucleotide Exchange Activity of eIF2B. *Biochemistry* 39, 12929–12938. doi:10.1021/bi0008682
- Suthar, M.S., Diamond, M.S., Gale Jr, M., 2013. West Nile virus infection and immunity. *Nat Rev Micro* 11, 115–128. doi:10.1038/nrmicro2950
- Szilard, R.K., Titorenko, V.I., Veenhuis, M., Rachubinski, R.A., 1995. Pay32p of the yeast *Yarrowia lipolytica* is an intraperoxisomal component of the matrix protein translocation machinery. *The Journal of Cell Biology* 131, 1453–1469. doi:10.1083/jcb.131.6.1453
- Szretter, K.J., Daniels, B.P., Cho, H., Gainey, M.D., Yokoyama, W.M., Gale, M., Jr., Virgin, H.W., Klein, R.S., Sen, G.C., Diamond, M.S., 2012. 2'-O Methylation of the Viral mRNA Cap by West Nile Virus Evades Ifit1-Dependent and -Independent Mechanisms of Host Restriction In Vivo. *PLoS Pathog* 8, e1002698. doi:10.1371/journal.ppat.1002698
- Tabata, T., Petitt, M., Puerta-Guardo, H., Michlmayr, D., Wang, C., Fang-Hoover, J., Harris, E., Pereira, L., 2016. Zika Virus Targets Different Primary Human Placental Cells, Suggesting Two Routes for Vertical Transmission. *Cell Host & Microbe* 20, 155–166. doi:10.1016/j.chom.2016.07.002
- Taguwa, S., Maringer, K., Li, X., Bernal-Rubio, D., Rauch, J.N., Gestwicki, J.E., Andino, R., Fernandez-Sesma, A., Frydman, J., 2015. Defining Hsp70 Subnetworks in Dengue Virus Replication Reveals Key Vulnerability in Flavivirus Infection. *Cell* 163, 1108–1123. doi:10.1016/j.cell.2015.10.046
- Takahashi, M., Higuchi, M., Matsuki, H., Yoshita, M., Ohsawa, T., Oie, M., Fujii, M., 2013. Stress Granules Inhibit Apoptosis by Reducing Reactive Oxygen Species Production. *Mol. Cell. Biol.* 33, 815–829. doi:10.1128/MCB.00763-12
- Takegami, T., Sakamuro, D., Furukawa, T., 1995. Japanese encephalitis virus nonstructural protein NS3 has RNA binding and ATPase activities. *Virus Genes* 9, 105–112. doi:10.1007/BF01702653
- Tal, M.C., Sasai, M., Lee, H.K., Yordy, B., Shadel, G.S., Iwasaki, A., 2009. Absence of autophagy results in reactive oxygen species-dependent amplification of RLR signaling. *PNAS* 106, 2770–2775. doi:10.1073/pnas.0807694106
- Tam, Y.Y.C., Fagarasanu, A., Fagarasanu, M., Rachubinski, R.A., 2005. Pex3p Initiates the Formation of a Preperoxisomal Compartment from a Subdomain of the Endoplasmic Reticulum in *Saccharomyces cerevisiae*. *J. Biol. Chem.* 280, 34933–34939. doi:10.1074/jbc.M506208200
- Tanaka, Y., Chen, Z.J., 2012. STING Specifies IRF3 Phosphorylation by TBK1 in the Cytosolic DNA Signaling Pathway. *Sci. Signal.* 5, ra20-ra20. doi:10.1126/scisignal.2002521
- Tang, E.D., Wang, C.-Y., 2009. MAVS Self-Association Mediates Antiviral Innate Immune Signaling. *J. Virol.* 83, 3420–3428. doi:10.1128/JVI.02623-08

- Tang, W.W., Grewal, R., Shresta, S., 2015. Influence of antibodies and T cells on dengue disease outcome: insights from interferon receptor-deficient mouse models. *Current Opinion in Virology, Animal models for viral diseases / Oncolytic viruses* 13, 61–66. doi:10.1016/j.coviro.2015.04.007
- Tang, W.W., Young, M.P., Mamidi, A., Regla-Nava, J.A., Kim, K., Shresta, S., 2016. A Mouse Model of Zika Virus Sexual Transmission and Vaginal Viral Replication. *Cell Reports* 17, 3091–3098. doi:10.1016/j.celrep.2016.11.070
- Tanner, L.B., Chng, C., Guan, X.L., Lei, Z., Rozen, S.G., Wenk, M.R., 2014. Lipidomics identifies a requirement for peroxisomal function during influenza virus replication. *J. Lipid Res.* 55, 1357–1365. doi:10.1194/jlr.M049148
- Titorenko, V.I., Chan, H., Rachubinski, R.A., 2000. Fusion of small peroxisomal vesicles in vitro reconstructs an early step in the in vivo multistep peroxisome assembly pathway of *Yarrowia lipolytica*. *J. Cell Biol.* 148, 29–44.
- Titorenko, V.I., Rachubinski, R.A., 2001. The life cycle of the peroxisome. *Nat Rev Mol Cell Biol* 2, 357–368. doi:10.1038/35073063
- Toro, A.A., Araya, C.A., Córdova, G.J., Arredondo, C.A., Cárdenas, H.G., Moreno, R.E., Venegas, A., Koenig, C.S., Cancino, J., Gonzalez, A., Santos, M.J., 2009. Pex3p-dependent peroxisomal biogenesis initiates in the endoplasmic reticulum of human fibroblasts. *J. Cell. Biochem.* 107, 1083–1096. doi:10.1002/jcb.22210
- Tourrière, H., Chebli, K., Zekri, L., Courselaud, B., Blanchard, J.M., Bertrand, E., Tazi, J., 2003. The RasGAP-associated endoribonuclease G3BP assembles stress granules. *J Cell Biol* 160, 823–831. doi:10.1083/jcb.200212128
- Tripathi, S., Balasubramaniam, V.R.M.T., Brown, J.A., Mena, I., Grant, A., Bardina, S.V., Maringer, K., Schwarz, M.C., Maestre, A.M., Sourisseau, M., Albrecht, R.A., Krammer, F., Evans, M.J., Fernandez-Sesma, A., Lim, J.K., García-Sastre, A., 2017. A novel Zika virus mouse model reveals strain specific differences in virus pathogenesis and host inflammatory immune responses. *PLOS Pathogens* 13, e1006258. doi:10.1371/journal.ppat.1006258
- Troupin, A., Colpitts, T.M., 2016. Overview of West Nile Virus Transmission and Epidemiology. *Methods Mol. Biol.* 1435, 15–18. doi:10.1007/978-1-4939-3670-0_2
- Tsai, N.-P., Ho, P.-C., Wei, L.-N., 2008. Regulation of stress granule dynamics by Grb7 and FAK signalling pathway. *The EMBO Journal* 27, 715–726. doi:10.1038/emboj.2008.19
- Tsai, T.F., Popovici, F., Cernescu, C., Campbell, G.L., Nedelcu, N.I., 1998. West Nile encephalitis epidemic in southeastern Romania. *Lancet* 352, 767–771.
- Tsai, W.-C., Gayatri, S., Reineke, L.C., Sbardella, G., Bedford, M.T., Lloyd, R.E., 2016. Arginine Demethylation of G3BP1 Promotes Stress Granule Assembly. *J. Biol. Chem.* 291, 22671–22685. doi:10.1074/jbc.M116.739573
- Tsuda, Y., Mori, Y., Abe, T., Yamashita, T., Okamoto, T., Ichimura, T., Moriishi, K., Matsuura, Y., 2006. Nucleolar protein B23 interacts with Japanese encephalitis virus core protein and participates in viral replication. *Microbiol. Immunol.* 50, 225–234.
- Tu, Y.-C., Yu, C.-Y., Liang, J.-J., Lin, E., Liao, C.-L., Lin, Y.-L., 2012. Blocking Double-Stranded RNA-Activated Protein Kinase PKR by Japanese Encephalitis Virus Nonstructural Protein 2A. *J. Virol.* 86, 10347–10358. doi:10.1128/JVI.00525-12
- Tumbarello, D.A., Waxse, B.J., Arden, S.D., Bright, N.A., Kendrick-Jones, J., Buss, F., 2012. Autophagy receptors link myosin VI to autophagosomes to mediate Tom1-dependent

- autophagosome maturation and fusion with the lysosome. *Nat Cell Biol* 14, 1024–1035. doi:10.1038/ncb2589
- Umareddy, I., Pluquet, O., Wang, Q.Y., Vasudevan, S.G., Chevet, E., Gu, F., 2007. Dengue virus serotype infection specifies the activation of the unfolded protein response. *Virology* 367, 91. doi:10.1016/j.virol.2007.08.018
- Urbanowski, M.D., Hobman, T.C., 2013. The West Nile Virus Capsid Protein Blocks Apoptosis through a Phosphatidylinositol 3-Kinase-Dependent Mechanism. *J. Virol.* 87, 872–881. doi:10.1128/JVI.02030-12
- Urbanowski, M.D., Ilkow, C.S., Hobman, T.C., 2008. Modulation of signaling pathways by RNA virus capsid proteins. *Cellular Signalling* 20, 1227–1236. doi:10.1016/j.cellsig.2007.12.018
- van der Zand, A., Gent, J., Braakman, I., Tabak, H.F., 2012. Biochemically Distinct Vesicles from the Endoplasmic Reticulum Fuse to Form Peroxisomes. *Cell* 149, 397–409. doi:10.1016/j.cell.2012.01.054
- Vasquez, R.J., Howell, B., Yvon, A.M., Wadsworth, P., Cassimeris, L., 1997. Nanomolar concentrations of nocodazole alter microtubule dynamic instability in vivo and in vitro. *Mol Biol Cell* 8, 973–985.
- Verma, S., Kumar, M., Gurjav, U., Lum, S., Nerurkar, V.R., 2010. Reversal of West Nile virus-induced blood-brain barrier disruption and tight junction proteins degradation by matrix metalloproteinases inhibitor. *Virology* 397, 130–138. doi:10.1016/j.virol.2009.10.036
- Villar, L., Dayan, G.H., Arredondo-García, J.L., Rivera, D.M., Cunha, R., Deseda, C., Reynales, H., Costa, M.S., Morales-Ramírez, J.O., Carrasquilla, G., Rey, L.C., Dietze, R., Luz, K., Rivas, E., Miranda Montoya, M.C., Cortés Supelano, M., Zambrano, B., Langevin, E., Boaz, M., Tornieporth, N., Saville, M., Noriega, F., CYD15 Study Group, 2015. Efficacy of a tetravalent dengue vaccine in children in Latin America. *N. Engl. J. Med.* 372, 113–123. doi:10.1056/NEJMoa1411037
- Villordo, S.M., Carballeda, J.M., Filomatori, C.V., Gamarnik, A.V., 2016. RNA Structure Duplications and Flavivirus Host Adaptation. *Trends in Microbiology* 24, 270–283. doi:10.1016/j.tim.2016.01.002
- Vivithanaporn, P., Asahchop, E.L., Acharjee, S., Baker, G.B., Power, C., 2016. HIV protease inhibitors disrupt astrocytic glutamate transporter function and neurobehavioral performance. *AIDS* 30, 543–552. doi:10.1097/QAD.0000000000000955
- Wang, C.-C., Huang, Z.-S., Chiang, P.-L., Chen, C.-T., Wu, H.-N., 2009. Analysis of the nucleoside triphosphatase, RNA triphosphatase, and unwinding activities of the helicase domain of dengue virus NS3 protein. *FEBS Lett.* 583, 691–696. doi:10.1016/j.febslet.2009.01.008
- Wang, P., Dai, J., Bai, F., Kong, K.-F., Wong, S.J., Montgomery, R.R., Madri, J.A., Fikrig, E., 2008. Matrix Metalloproteinase 9 Facilitates West Nile Virus Entry into the Brain. *J. Virol.* 82, 8978–8985. doi:10.1128/JVI.00314-08
- Wang, T., Town, T., Alexopoulou, L., Anderson, J.F., Fikrig, E., Flavell, R.A., 2004. Toll-like receptor 3 mediates West Nile virus entry into the brain causing lethal encephalitis. *Nat Med* 10, 1366–1373. doi:10.1038/nm1140
- Wang, X., Hou, L., Du, J., Zhou, L., Ge, X., Guo, X., Yang, H., 2015. Capsid, membrane and NS3 are the major viral proteins involved in autophagy induced by Japanese encephalitis virus. *Vet. Microbiol.* 178, 217–229. doi:10.1016/j.vetmic.2015.05.026

- Watanabe, H., Shiratori, T., Shoji, H., Miyatake, S., Okazaki, Y., Ikuta, K., Sato, T., Saito, T., 1997. A novel acyl-CoA thioesterase enhances its enzymatic activity by direct binding with HIV Nef. *Biochem. Biophys. Res. Commun.* 238, 234–239. doi:10.1006/bbrc.1997.7217
- Waterham, H.R., Ferdinandusse, S., Wanders, R.J.A., 2016. Human disorders of peroxisome metabolism and biogenesis. *Biochimica et Biophysica Acta (BBA) - Molecular Cell Research, Assembly, Maintenance and Dynamics of Peroxisomes* 1863, 922–933. doi:10.1016/j.bbamcr.2015.11.015
- Watters, D., Kedar, P., Spring, K., Bjorkman, J., Chen, P., Gatei, M., Birrell, G., Garrone, B., Srinivasa, P., Crane, D.I., Lavin, M.F., 1999. Localization of a Portion of Extranuclear ATM to Peroxisomes. *J. Biol. Chem.* 274, 34277–34282. doi:10.1074/jbc.274.48.34277
- Welsch, S., Miller, S., Romero-Brey, I., Merz, A., Bleck, C.K.E., Walther, P., Fuller, S.D., Antony, C., Krijnse-Locker, J., Bartenschlager, R., 2009. Composition and Three-Dimensional Architecture of the Dengue Virus Replication and Assembly Sites. *Cell Host & Microbe* 5, 365–375. doi:10.1016/j.chom.2009.03.007
- Wengler, Gerd, Wengler, Gisela, Gross, H.J., 1978. Studies on virus-specific nucleic acids synthesized in vertebrate and mosquito cells infected with flaviviruses. *Virology* 89, 423–437. doi:10.1016/0042-6822(78)90185-X
- Werme, K., Wigerius, M., Johansson, M., 2008. Tick-borne encephalitis virus NS5 associates with membrane protein scribble and impairs interferon-stimulated JAK-STAT signalling. *Cell. Microbiol.* 10, 696–712. doi:10.1111/j.1462-5822.2007.01076.x
- Westaway, E.G., Mackenzie, J.M., Kenney, M.T., Jones, M.K., Khromykh, A.A., 1997. Ultrastructure of Kunjin virus-infected cells: colocalization of NS1 and NS3 with double-stranded RNA, and of NS2B with NS3, in virus-induced membrane structures. *J. Virol.* 71, 6650–6661.
- Whelan, J.N., Tran, K.C., Rossum, D.B. van, Teng, M.N., 2016. Identification of Respiratory Syncytial Virus Nonstructural Protein 2 Residues Essential for Exploitation of the Host Ubiquitin System and Inhibition of Innate Immune Responses. *Journal of Virology* 90, 6453. doi:10.1128/JVI.00423-16
- White, J.P., Cardenas, A.M., Marissen, W.E., Lloyd, R.E., 2007a. Inhibition of Cytoplasmic mRNA Stress Granule Formation by a Viral Proteinase. *Cell Host & Microbe* 2, 295–305. doi:10.1016/j.chom.2007.08.006
- White, J.P., Cardenas, A.M., Marissen, W.E., Lloyd, R.E., 2007b. Inhibition of Cytoplasmic mRNA Stress Granule Formation by a Viral Proteinase. *Cell Host & Microbe* 2, 295–305. doi:10.1016/j.chom.2007.08.006
- White, J.P., Lloyd, R.E., 2012. Regulation of stress granules in virus systems. *Trends Microbiol.* 20, 175–183. doi:10.1016/j.tim.2012.02.001
- White, J.P., Lloyd, R.E., 2011. Poliovirus Unlinks TIA1 Aggregation and mRNA Stress Granule Formation. *J. Virol.* 85, 12442–12454. doi:10.1128/JVI.05888-11
- WHO, 2017. Countries and territories that have reported mosquito-borne Zika virus transmission [WWW Document]. WHO. URL http://www.who.int/emergencies/zika-virus/situation-report/Table1_20012017.PNG?ua=1 (accessed 2.4.17).
- WHO, 2016. Dengue vaccine: WHO position paper – July 2016 [WWW Document]. *Weekly epidemiological record.* URL <http://www.who.int/wer/2016/wer9130.pdf?ua=1> (accessed 12.9.16).

- WHO, 2013. Vaccines and vaccination against yellow fever WHO Position Paper – June 2013 [WWW Document]. Weekly epidemiological record. URL <http://www.who.int/wer/2013/wer8827.pdf?ua=1> (accessed 3.7.17).
- WHO, 2009. Dengue: Guidelines for Diagnosis, Treatment, Prevention and Control: New Edition, WHO Guidelines Approved by the Guidelines Review Committee. World Health Organization, Geneva.
- Williams, C., Opalinski, L., Landgraf, C., Costello, J., Schrader, M., Krikken, A.M., Knoops, K., Kram, A.M., Volkmer, R., Klei, I.J. van der, 2015. The membrane remodeling protein Pex11p activates the GTPase Dnm1p during peroxisomal fission. *PNAS* 112, 6377–6382. doi:10.1073/pnas.1418736112
- Wilson, G.N., Holmes, R.G., Custer, J., Lipkowitz, J.L., Stover, J., Datta, N., Hajra, A., 1986. Zellweger syndrome: diagnostic assays, syndrome delineation, and potential therapy. *Am. J. Med. Genet.* 24, 69–82. doi:10.1002/ajmg.1320240109
- Wilson, J.R., Sessions, P.F. de, Leon, M.A., Scholle, F., 2008. West Nile Virus Nonstructural Protein 1 Inhibits TLR3 Signal Transduction. *J. Virol.* 82, 8262–8271. doi:10.1128/JVI.00226-08
- Winkler, G., Maxwell, S.E., Ruemmler, C., Stollar, V., 1989. Newly synthesized dengue-2 virus nonstructural protein NS1 is a soluble protein but becomes partially hydrophobic and membrane-associated after dimerization. *Virology* 171, 302–305.
- Winston, D.J., Vikram, H.R., Rabe, I.B., Dhillon, G., Mulligan, D., Hong, J.C., Busuttil, R.W., Nowicki, M.J., Mone, T., Civen, R., Tecele, S.A., Trivedi, K.K., Hocevar, S.N., West Nile Virus Transplant-Associated Transmission Investigation Team, 2014. Donor-derived West Nile virus infection in solid organ transplant recipients: report of four additional cases and review of clinical, diagnostic, and therapeutic features. *Transplantation* 97, 881–889. doi:10.1097/TP.0000000000000024
- Wolff, T., O'Neill, R.E., Palese, P., 1996. Interaction cloning of NS1-I, a human protein that binds to the nonstructural NS1 proteins of influenza A and B viruses. *J. Virol.* 70, 5363–5372.
- Wood, C.S., Koepke, J.I., Teng, H., Boucher, K.K., Katz, S., Chang, P., Terlecky, L.J., Papanayotou, I., Walton, P.A., Terlecky, S.R., 2006. Hypocatalasemic Fibroblasts Accumulate Hydrogen Peroxide and Display Age-Associated Pathologies. *Traffic* 7, 97–107. doi:10.1111/j.1600-0854.2005.00358.x
- Wu, Y., Liu, Q., Zhou, J., Xie, W., Chen, C., Wang, Z., Yang, H., Cui, J., 2017. Zika virus evades interferon-mediated antiviral response through the co-operation of multiple nonstructural proteins in vitro. *Cell Discov* 3, 17006. doi:10.1038/celldisc.2017.6
- Xie, X., Zou, J., Puttikhunt, C., Yuan, Z., Shi, P.-Y., 2015. Two distinct sets of NS2A molecules are responsible for dengue virus RNA synthesis and virion assembly. *J. Virol.* 89, 1298–1313. doi:10.1128/JVI.02882-14
- Xu, M., Lee, E.M., Wen, Z., Cheng, Y., Huang, W.-K., Qian, X., Tcw, J., Kouznetsova, J., Ogden, S.C., Hammack, C., Jacob, F., Nguyen, H.N., Itkin, M., Hanna, C., Shinn, P., Allen, C., Michael, S.G., Simeonov, A., Huang, W., Christian, K.M., Goate, A., Brennand, K.J., Huang, R., Xia, M., Ming, G., Zheng, W., Song, H., Tang, H., 2016. Identification of small-molecule inhibitors of Zika virus infection and induced neural cell death via a drug repurposing screen. *Nat Med* 22, 1101–1107. doi:10.1038/nm.4184

- Xu, Z., Anderson, R., Hobman, T.C., 2011. The capsid-binding nucleolar helicase DDX56 is important for infectivity of West Nile virus. *J. Virol.* 85, 5571–5580. doi:10.1128/JVI.01933-10
- Xu, Z., Hobman, T.C., 2012. The helicase activity of DDX56 is required for its role in assembly of infectious West Nile virus particles. *Virology* 433, 226–235. doi:10.1016/j.virol.2012.08.011
- Xu, Z., Waeckerlin, R., Urbanowski, M.D., van Marle, G., Hobman, T.C., 2012. West Nile virus infection causes endocytosis of a specific subset of tight junction membrane proteins. *PLoS ONE* 7, e37886. doi:10.1371/journal.pone.0037886
- Yagita, Y., Hiromasa, T., Fujiki, Y., 2013. Tail-anchored PEX26 targets peroxisomes via a PEX19-dependent and TRC40-independent class I pathway. *J Cell Biol* 200, 651–666. doi:10.1083/jcb.201211077
- Yamada, M., Nakamura, K., Yoshii, M., Kaku, Y., Narita, M., 2009. Brain lesions induced by experimental intranasal infection of Japanese encephalitis virus in piglets. *J. Comp. Pathol.* 141, 156–162. doi:10.1016/j.jcpa.2009.04.006
- Ye, J., Chen, Z., Li, Y., Zhao, Z., He, W., Zohaib, A., Song, Y., Deng, C., Zhang, B., Chen, H., Cao, S., 2017. Japanese Encephalitis Virus NS5 Inhibits Type I Interferon (IFN) Production by Blocking the Nuclear Translocation of IFN Regulatory Factor 3 and NF- κ B. *J. Virol.* 91, e00039-17. doi:10.1128/JVI.00039-17
- Ye, J., Zhu, B., Fu, Z.F., Chen, H., Cao, S., 2013. Immune evasion strategies of flaviviruses. *Vaccine* 31, 461–471. doi:10.1016/j.vaccine.2012.11.015
- Yon, C., Teramoto, T., Mueller, N., Phelan, J., Ganesh, V.K., Murthy, K.H.M., Padmanabhan, R., 2005. Modulation of the nucleoside triphosphatase/RNA helicase and 5'-RNA triphosphatase activities of Dengue virus type 2 nonstructural protein 3 (NS3) by interaction with NS5, the RNA-dependent RNA polymerase. *J. Biol. Chem.* 280, 27412–27419. doi:10.1074/jbc.M501393200
- Yonekawa, S., Furuno, A., Baba, T., Fujiki, Y., Ogasawara, Y., Yamamoto, A., Tagaya, M., Tani, K., 2011. Sec16B is involved in the endoplasmic reticulum export of the peroxisomal membrane biogenesis factor peroxin 16 (Pex16) in mammalian cells. *Proc. Natl. Acad. Sci. U.S.A.* 108, 12746–12751. doi:10.1073/pnas.1103283108
- Yoo, J.-S., Takahashi, K., Ng, C.S., Ouda, R., Onomoto, K., Yoneyama, M., Lai, J.C., Lattmann, S., Nagamine, Y., Matsui, T., Iwabuchi, K., Kato, H., Fujita, T., 2014. DHX36 Enhances RIG-I Signaling by Facilitating PKR-Mediated Antiviral Stress Granule Formation. *PLoS Pathog* 10, e1004012. doi:10.1371/journal.ppat.1004012
- You, J., Hou, S., Malik-Soni, N., Xu, Z., Kumar, A., Rachubinski, R.A., Frappier, L., Hobman, T.C., 2015. Flavivirus Infection Impairs Peroxisome Biogenesis and Early Antiviral Signaling. *J. Virol.* 89, 12349–12361. doi:10.1128/JVI.01365-15
- Youn, S., Li, T., McCune, B.T., Edeling, M.A., Fremont, D.H., Cristea, I.M., Diamond, M.S., 2012. Evidence for a Genetic and Physical Interaction between Nonstructural Proteins NS1 and NS4B That Modulates Replication of West Nile Virus. *J. Virol.* 86, 7360–7371. doi:10.1128/JVI.00157-12
- Young, P.R., Hilditch, P.A., Bletchly, C., Halloran, W., 2000. An antigen capture enzyme-linked immunosorbent assay reveals high levels of the dengue virus protein NS1 in the sera of infected patients. *J. Clin. Microbiol.* 38, 1053–1057.

- Yu, C.-Y., Chang, T.-H., Liang, J.-J., Chiang, R.-L., Lee, Y.-L., Liao, C.-L., Lin, Y.-L., 2012. Dengue virus targets the adaptor protein MITA to subvert host innate immunity. *PLoS Pathog.* 8, e1002780. doi:10.1371/journal.ppat.1002780
- Yu, C.-Y., Hsu, Y.-W., Liao, C.-L., Lin, Y.-L., 2006. Flavivirus Infection Activates the XBP1 Pathway of the Unfolded Protein Response To Cope with Endoplasmic Reticulum Stress. *J. Virol.* 80, 11868–11880. doi:10.1128/JVI.00879-06
- Yu, I.-M., Holdaway, H.A., Chipman, P.R., Kuhn, R.J., Rossmann, M.G., Chen, J., 2009. Association of the pr peptides with dengue virus at acidic pH blocks membrane fusion. *J. Virol.* 83, 12101–12107. doi:10.1128/JVI.01637-09
- Yu, I.-M., Zhang, W., Holdaway, H.A., Li, L., Kostyuchenko, V.A., Chipman, P.R., Kuhn, R.J., Rossmann, M.G., Chen, J., 2008. Structure of the Immature Dengue Virus at Low pH Primes Proteolytic Maturation. *Science* 319, 1834–1837. doi:10.1126/science.1153264
- Yusof, R., Clum, S., Wetzel, M., Murthy, H.M., Padmanabhan, R., 2000. Purified NS2B/NS3 serine protease of dengue virus type 2 exhibits cofactor NS2B dependence for cleavage of substrates with dibasic amino acids in vitro. *J. Biol. Chem.* 275, 9963–9969.
- Zainah, S., Wahab, A.H.A., Mariam, M., Fauziah, M.K., Khairul, A.H., Roslina, I., Sairulakhma, A., Kadimon, S.S., Jais, M.S.M., Chua, K.B., 2009. Performance of a commercial rapid dengue NS1 antigen immunochromatography test with reference to dengue NS1 antigen-capture ELISA. *J. Virol. Methods* 155, 157–160. doi:10.1016/j.jviromet.2008.10.016
- Zand, A. van der, Braakman, I., Tabak, H.F., 2010. Peroxisomal Membrane Proteins Insert into the Endoplasmic Reticulum. *Mol. Biol. Cell* 21, 2057–2065. doi:10.1091/mbc.E10-02-0082
- Zellweger, R.M., Prestwood, T.R., Shresta, S., 2010. Enhanced Infection of Liver Sinusoidal Endothelial Cells in a Mouse Model of Antibody-Induced Severe Dengue Disease. *Cell Host & Microbe* 7, 128–139. doi:10.1016/j.chom.2010.01.004
- Zevini, A., Olganier, D., Hiscott, J., 2017. Crosstalk between Cytoplasmic RIG-I and STING Sensing Pathways. *Trends in Immunology* 38, 194–205. doi:10.1016/j.it.2016.12.004
- Zhang, J., Kim, J., Alexander, A., Cai, S., Tripathi, D.N., Dere, R., Tee, A.R., Tait-Mulder, J., Di Nardo, A., Han, J.M., Kwiatkowski, E., Dunlop, E.A., Dodd, K.M., Folkerth, R.D., Faust, P.L., Kastan, M.B., Sahin, M., Walker, C.L., 2013. A tuberous sclerosis complex signalling node at the peroxisome regulates mTORC1 and autophagy in response to ROS. *Nat Cell Biol* 15, 1186–1196. doi:10.1038/ncb2822
- Zhang, J., Tripathi, D.N., Jing, J., Alexander, A., Kim, J., Powell, R.T., Dere, R., Tait-Mulder, J., Lee, J.-H., Paull, T.T., Pandita, R.K., Charaka, V.K., Pandita, T.K., Kastan, M.B., Walker, C.L., 2015. ATM Functions at the Peroxisome to Induce Pexophagy in Response to ROS. *Nat Cell Biol* 17, 1259–1269. doi:10.1038/ncb3230
- Zhao, B., Yi, G., Du, F., Chuang, Y.-C., Vaughan, R.C., Sankaran, B., Kao, C.C., Li, P., 2017. Structure and function of the Zika virus full-length NS5 protein. *Nature Communications* 8, 14762. doi:10.1038/ncomms14762
- Zhao, Y., Sun, X., Nie, X., Sun, L., Tang, T., Chen, D., Sun, Q., 2012. COX5B Regulates MAVS-mediated Antiviral Signaling through Interaction with ATG5 and Repressing ROS Production. *PLOS Pathogens* 8, e1003086. doi:10.1371/journal.ppat.1003086
- Zhou, M.-T., Qin, Y., Li, M., Chen, C., Chen, X., Shu, H.-B., Guo, L., 2015. Quantitative Proteomics Reveals the Roles of Peroxisome-associated Proteins in Antiviral Innate Immune Responses. *Mol Cell Proteomics* 14, 2535–2549. doi:10.1074/mcp.M115.048413

- Zmurko, J., Marques, R.E., Schols, D., Verbeken, E., Kaptein, S.J.F., Neyts, J., 2016. The Viral Polymerase Inhibitor 7-Deaza-2'-C-Methyladenosine Is a Potent Inhibitor of In Vitro Zika Virus Replication and Delays Disease Progression in a Robust Mouse Infection Model. *PLOS Neglected Tropical Diseases* 10, e0004695. doi:10.1371/journal.pntd.0004695
- Zmurko, J., Neyts, J., Dallmeier, K., 2015. Flaviviral NS4b, chameleon and jack-in-the-box roles in viral replication and pathogenesis, and a molecular target for antiviral intervention. *Reviews in Medical Virology* 25, 205. doi:10.1002/rmv.1835
- Zou, J., Lee, L.T., Wang, Q.Y., Xie, X., Lu, S., Yau, Y.H., Yuan, Z., Geifman Shochat, S., Kang, C., Lescar, J., Shi, P.-Y., 2015. Mapping the Interactions between the NS4B and NS3 proteins of dengue virus. *J. Virol.* 89, 3471–3483. doi:10.1128/JVI.03454-14
- Züst, R., Cervantes-Barragan, L., Habjan, M., Maier, R., Neuman, B.W., Ziebuhr, J., Szretter, K.J., Baker, S.C., Barchet, W., Diamond, M.S., Siddell, S.G., Ludewig, B., Thiel, V., 2011. Ribose 2'-O-methylation provides a molecular signature for the distinction of self and non-self mRNA dependent on the RNA sensor Mda5. *Nat Immunol* 12, 137–143. doi:10.1038/ni.1979